Sheffield Hallam University

A Sheffield Hallam University thesis
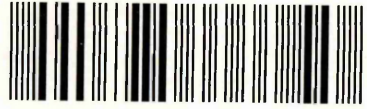
Return to Learning Centre of issue
Fines are charged at 50p per hour

A Statistical Analysis Of The Fatigue Behaviour Of Single And Multi-Spot Welded Joints

Andrew James Clifton

A thesis submitted in partial fulfilment of the requirements of

Sheffield Hallam University for the degree of Doctor of Philosophy

January 2007

Abstract.

Several models exist that can provide predictions for the fatigue properties of a spot welded joint based on geometric data. However, the accuracy of these models tends to diminish as the number of spot welds and complexity of the joint increases. This thesis reports on the findings of an investigative study to assess the applicability of a statistical approach for predicting the fatigue behaviour of a multi-spot welded joint, based on data that can be gathered on single spot welded joints that are geometrically equivalent to the individual spot welds present in the multi-spot welded joint. A series of Staircase and Probit fatigue testing techniques were used to gather extensive data on the fatigue behaviour of a given single spot welded joint geometry. This data was then used, along with the proposed model, to predict the fatigue behaviour of a series of simple multi-spot welded joints consisting of two, four, eight and sixteen nuggets, where all the individual welds present were all ostensibly geometrically identical to the single nugget joints. Actual values for the various multi-spot welded joints were then determined using a series of Staircase fatigue testing techniques and compared to those predicted by the model. The results showed an excellent correlation between predicted and experimental values for the standard deviation of the fatigue strength distribution, and a marginal increase in the experimentally determined mean fatigue strength, when compared to the values predicted by the model. This difference was attributed to a small increase in the width per spot weld in the multi-spot welded joints. Such increases in width have previously been shown to affect the fatigue properties of spot welded joints in this manner. Once this affect was taken into account, the results lend support to the proposed statistical approach for predicting the fatigue behaviour of multi-spot welded joints, based on known data regarding geometrically representative single spot welded joints.

Acknowledgements.

While the following thesis represents the work of an individual, its completion has been aided by the advice and technical assistance of several people, all of whom I would like to extend my gratitude to. In particular I would like to thank my supervisory team leaders, Professor Alan J. Smith and Professor Hans Nordberg, for their technical knowledge and advice, the Outokumpu Stainless Research Foundation and the Engineering and Physical Sciences Research Council, for providing material and financial support, and finally, the technical staff at Sheffield Hallam University, particularly Tim O'Hara and Keith Wright, for their instruction and assistance with regards to fatigue testing, and John Bradshaw and Roger Tingle, for their instrumental instruction and assistance in the workshop.

I would like to extend a special thank you to my wife Patricia, whose relentless love and support throughout this work, gave me the strength each day to perform 'yet another fatigue test'. Finally, I would also like to thank my close friends and family for their understanding and support, and for feigning interest in the intricacies of the fatigue behaviour of spot welded joints, in particular I would like to thank the other members of the Outokumpu Research Group: Emma, Frank, Chris, Jamie, and Tim, whose passionate desires to rise above the 95th percentile and leave all others in their wake, have provided me with both inspiration and amusement throughout the duration of my research.

Nomenclature.

$\Delta\theta_N$:   Angle of nugget rotation.

$\Delta\theta_S$:   Angle of sheet rotation.

AC: Alternating Current.

CTOD: Crack Tip Opening Displacement.

d: Staircase testing step divide level.

DC: Direct Current.

d_n: Proposed Model: Relationship factor equal to the Z value read from the standard normal distribution tables for a probability equal to $\sqrt[n]{0.8413} - \sqrt[n]{0.5}$.

HAZ: Heat Affected Zone.

HCF: High Cycle Fatigue.

HSLA: High Strength Low Alloy steel.

IR: Infrared.

IUT: Item Under Test

K: Stress intensity factor.

ΔK_{TH}:   Threshold stress intensity range.

K_I: Tensional stress intensity factor.

K_{II}:   Shear stress intensity factor.

K_{III}:   Out of plane shear stress intensity factor.

K_{TH}:   Threshold stress intensity factor.

K_{IC}:   Fracture toughness.

K_w: Coefficient of single spot weld standard deviation.

LCF: Low Cycle Fatigue.

LFE: Least Frequent Event.

m_n: Proposed Model: Relationship factor equal to the Z value read from the standard normal distribution tables for a probability equal to $\sqrt[n]{0.5}$.

N: Number of cycles in a fatigue test.

n: Number of nuggets present in a multi-spot welded joint.

o: Staircase testing: Survivor.

P: Fatigue Testing: Applied load.

ΔP: Fatigue Testing: Fatigue load range.

PDF: Probability Density Function.

P(MS): Probability of survival for a multi-spot welded joint.

PSB: Persistent Slip Band.

P(SS):   Probability of survival for a single spot welded joint

R: Fatigue Testing: Stress ratio.

RMS: Root Mean Square.

RSW: Resistance Spot Welding.

S: Fatigue Strength Distribution: Standard Deviation of a single spot welded joint.

S: Fatigue Testing: Fatigue Stress.

ΔS: Fatigue Testing: The range of the stress component of one fatigue stress cycle.

S_m: The standard deviation of the multi-spot welded joint.

S_{max}:   The maximum value of the stress component of one fatigue stress cycle.

S_{min}:   The minimum value of the stress component of one fatigue stress cycle.

TSA: Thermoelastic Stress Analysis.

TSSW: Tensile-Shear Spot Welded.

UTS: Ultimate Tensile Test.

x: Staircase testing: Failure.

X: Fatigue Strength Distribution: Mean fatigue strength of a single spot welded joint.

X_m: Proposed Model: Mean fatigue strength of the multi-spot welded joint.

X_s: Proposed Model: Mean fatigue strength of a proportionally size single nugget joint.

X(Y):   Probit Testing: Derived estimate.

Y: Probit Testing: Transformed per cent survival value identical to Z values found on normal distribution tables.

Table of Contents.

Table of Figures.

17

19

Table of Tables.

Table of Equations.

Table of Equations.

1: Introduction.

Multi-spot welded joints are routinely used in the automotive and other industries to produce structurally critical components. Unfortunately the size and complexity of the joints often limits the practicality of testing their mechanical properties, particularly when long term testing is required, such as in the case of determining fatigue properties.

Conversely, single spot welded joints are easily produced and can be tested on existing equipment with little or no modification. Clearly it would be extremely advantageous to be able to predict the fatigue properties of a multi-spot welded component based on the data obtained from testing single spot welded joints.

Currently there are several models that propose methods for predicting the fatigue life of a given joint of simple geometry, the majority of which are based on a fracture mechanics approach. However, as more spot welds are added and the complexity of the joint increases, these existing models tend to lose their accuracy.

This project intends to determine whether it is possible to divide a complex multi-spot welded joint into its individual welds and determine the overall fatigue properties of the joint as a whole by understanding the fatigue properties of the individual welds. If this process proves successful then the accuracy of the existing fracture mechanics models could still be maintained even for complex joints, provided the joint is first divided into its constituent welds.

1.1: Theoretical Model.

To determine all the factors that should be considered in a model that uses the proposed approach, a baseline must first be established using the simplest situation.

The fatigue strength distribution for a given type of single spot welded joint, for a cycle life of 10^6 cycles, can be assumed to fit a normal distribution. The majority of specimens will be expected to have a particular fatigue strength (the mean fatigue strength), with fewer and fewer specimens exhibiting strengths higher or lower than this value [1].

Fatigue Strength ΔP, kN
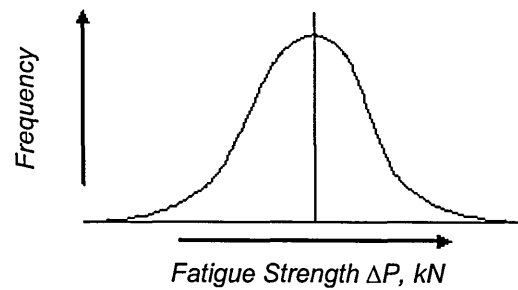
Fig 1.1: Normal distribution of spot weld fatigue strength.

The probability of a particular single spot welded joint surviving a specific fatigue load, A, will be equal to the probability that the joint has a fatigue strength equal to or higher than that load. This is represented by the integral of the area under the normal distribution curve between the specific load, A, and +∞, which is equivalent to the difference between the total area under the curve and the cumulated area up to load A [1].
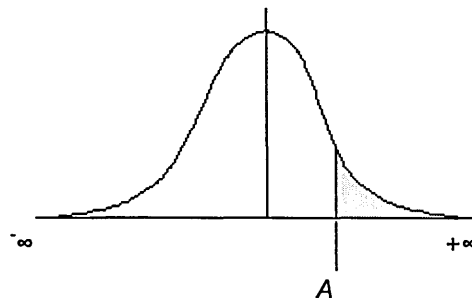
Fig 1.2: Probability of survival at a given fatigue load.

If it is assumed that all the welds present in a multi-spot welded joint have equal properties and the fatigue load is evenly distributed, such that each spot weld is supporting an equal portion of the overall fatigue load at all times, then each spot weld will have an identical probability of survival and the failure or survival of each spot weld can be described as a statistically independent event. If the survival criterion of the multi-spot welded joint is then defined as the survival of 100% of the constituent welds, then the probability of survival for the entire multi-spot welded joint will be equal to the product of the survival probabilities of each individual spot weld, as defined my the multiplication rule of probability [1].
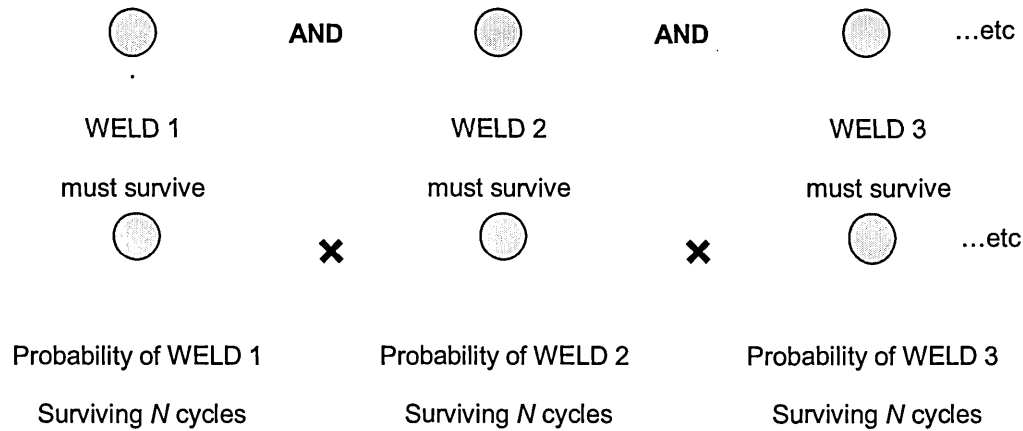
Fig 1.3: Survival conditions for a multi-spot welded joint.

Using these boundary conditions, and the principals of the multiplication rule, a simplified relationship model can be determined, which suggests that the probability of a multi-spot welded joint surviving a fatigue test with a specific fatigue load applied to each individual weld nugget, will be equal to the probability of survival for a single spot welded joint supporting the same fatigue load to the power of *n*, where *n* is the number of weld nuggets present in the joint.

$$P(MS) = P(SS)^n \qquad Eq.\ 1.1$$

Where:

P(MS) = *Probability of survival for a multi-spot weld joint*

P(SS) = *Probability of survival of a single spot weld joint*

n = *Number of weld nuggets that make up the multi-spot weld joint*

By maintaining the premise that the fatigue strength of a given spot welded joint is normally distributed, and if the mean fatigue strength (which is the load that will give a 50% chance of survival), for a cycle life of 10^6, for a single spot welded joint is denoted as X, and the fatigue strength distribution is said to have a standard deviation of S, then the various values for fatigue load can be generalised as the mean strength, X, plus or minus some coefficient, K_w, of the standard deviation, S.

$$X \pm K_w \times S \qquad Eq.\ 1.2$$
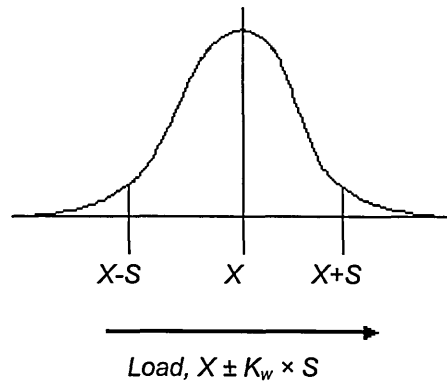
Fig 1.4: Mean and Standard Deviation of a fatigue strength distribution.

If, for convenience, the probability of survival for a single spot welded joint at any given fatigue load is summarised as the total area under the distribution curve, 1, minus a function of the given fatigue load, which represents the cumulated area under the curve up to that fatigue load, then the probability of a joint surviving the 10^6 cycles at any fatigue load can be generalised as:

$$1 - f(X + K_w \times S) \qquad Eq.\ 1.3$$

Where:

1	=	*The total area under the distribution curve.*
X	=	*The mean fatigue load for a single spot weld joint.*
K_w	=	*Any real number.*
S	=	*The standard deviation of the distribution for a single spot weld joint.*
$f(X + K_w \times S)$	=	*The cumulated area up to the load $X + K_w \times S$, which, as discussed, can represent any fatigue load.*

Similarly, the survival probability of a multi-spot welded joint tested under the same conditions, except with the same fatigue load applied to each individual weld nugget, can be generalised as:

$$[1 - f(X + K_w \times S)]^n \qquad Eq.\ 1.4$$

Where:

$1 - f(X + K_w \times S)$	=	*The probability of survival for a single spot weld joint at an applied fatigue load of $X + K_w \times S$*
n	=	*The number of weld nuggets present in the multi-spot weld joint.*

As X and S are constants, survival probability values for various multi-spot weld joints can be determined for various values of K_w using standard normal distribution tables, since the Z values used in these tables reflects the number of standard deviations a variable lies above or below a mean value and therefore corresponds directly to K_w.

K_w	n = 1	n =2	n = 4	n = 8	n = 16
0.0	0.500	0.250	0.062	0.004	0.000
-0.5	0.691	0.478	0.229	0.052	0.003
-1.0	0.841	0.708	0.501	0.251	0.063
-1.5	0.933	0.871	0.758	0.575	0.331
-2.0	0.977	0.955	0.912	0.832	0.692
-2.5	0.994	0.988	0.975	0.951	0.905
-3.0	0.999	0.997	0.995	0.989	0.979

Table 1.1: Probaiblity of survival for various values of n at various levels of K_w.

Plotting this data generates the graph shown in Fig 1.5, which depicts how the probability distribution changes as n increases. From Fig 1.5 the mean fatigue strength and standard deviation of the fatigue strength distribution per nugget of any multi-spot welded joint can be related to the mean fatigue strength and standard deviation of the fatigue strength distribution of a single spot welded joint, in terms of $X + K_w \times S$, by a specific value of K_w, which, for convenience, will be referred to as *Relationship Factors* m_n and d_n for mean fatigue strength and standard deviation respectively.
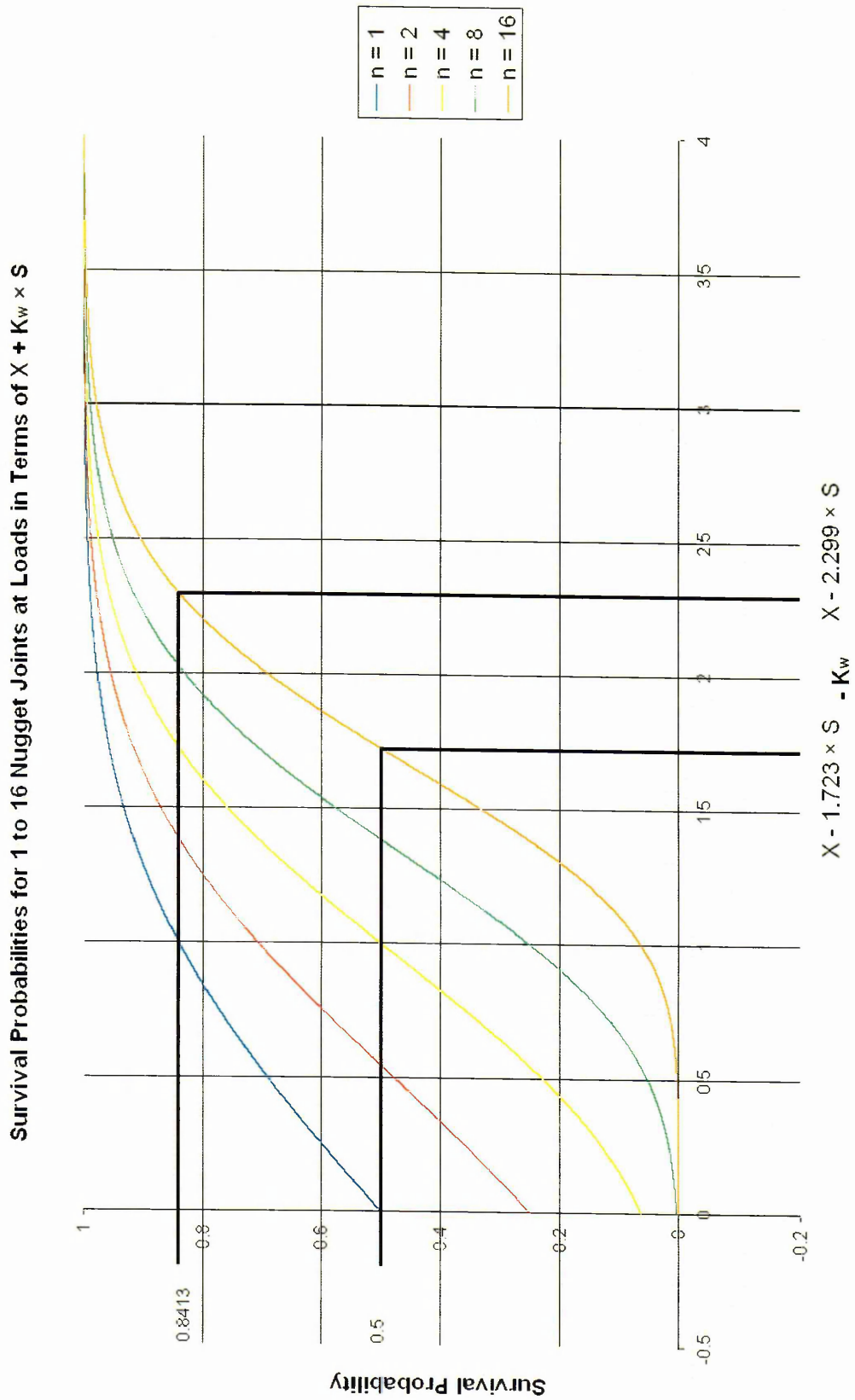
Fig 1.5: Survival probabilities for 1 to 16 nugget joints at loads in terms of X+Kw ×S.

For example the mean fatigue strength per nugget for a sixteen nugget joint can be related to the mean fatigue strength and standard deviation of a single spot welded joint as:

$$X - 1.723 \times S$$

Therefore $m_n = 1.723$

Similarly, the standard deviation per nugget for a sixteen nugget joint can be related to the mean fatigue strength and standard deviation of a single spot welded joint as:

$$(X - 2.299 \times S) - (X - 1.723 \times S) = 0.576 \times S$$

Therefore $d_n = 0.576$

Values for d_n and m_n can be summarised for any multi-spot welded joint by the Z value read from the standard normal distribution tables required to give the following probabilities:

m_n: Z value for a probability of:

$$\sqrt[n]{0.5} \quad \textit{Eq. 1.5}$$

d_n: Z value for a probability of:

$$\sqrt[n]{0.8413} - \sqrt[n]{0.5} \qquad \textit{Eq. 1.6}$$

Where:

n   =   *The number of spot welds present in the multi-spot welded joint.*

Plotting the values of m_n and d_n for increasing values of *n* produces a graphical representation (Fig 1.6) of how mean fatigue strength and standard deviation per nugget changes as the number of weld nuggets in the joint increases. Therefore, according to this basic theory, it should be possible to predict the fatigue properties of a multi-spot welded joint from the experimental data obtained from fatigue testing single spot welded joints.

Fig 1.6: Changes in mean fatigue strength and standard deviation per nugget for joints with

various numbers of nuggets (n)

1.2: Boundary Conditions.

In order to determine if confidence in the suggested theory is justified, certain assumptions and boundary conditions need to be established to control as many of the parameters as possible.

(1)   All welds must have equal properties.

Without equal properties the fatigue strength distribution will be different for each weld, meaning that the probability of survival for each weld, tested using a given set of test parameters, will vary. This will mean that the relationship between the fatigue strength distribution of single and multi-spot welded joints will not fit the simple power relationship explained here.

In order to achieve equal properties it will be necessary to develop a production technique that ensures that the individual nuggets in a multi spot welded joint can be considered to be 'indentical' in both the properties of the nugget and how that section of the joint responds to a given fatigue load.

(2)   Each individual weld in a multi-spot welded speciemen must support an identical portion of the overall fatigue load throughout the test.

If this condition is not fulfilled and maintained then, much like the requirement for equal nugget properties, the survival probability of each nugget in the joint being tested will lie at a different point on the distribution curve and will therefore have a different value. To maintain a balance of fatigue load consideration must be made to the design of the specimens. Attention must also be paid to the fatigue equipment to ensure the load train is rigid enough to distribute and support load evenly across the entire width of all specimens.

(3)   The survival or failure of an individual spot weld in a multi-spot welded joint must be an independent event.

In order for the events to be statistically independent the probability of survival or failure of any individual spot weld must not be dependent on the conditional surival or failure of any other spot weld. If the events are not independent then the simple multiplication rule used to define the probability of survival in a multi-spot welded joint will not apply. The events can be assumed to be independent if an equal portion of the load is support by each spot weld for the duration of the fatigue test and all the welds are identical. Therefore, in order to furfil this criteria, failure must be defined as the instance when one of the welds stops supporting an equal share of the overall load.

(4)   The failure criteria for single and multi-spot welded joints must be the same.

As mentioned, the proposed theory is based on the condition that in order for a multi-spot welded joint to survive, none of the welds present in that joint can fail prior to the completion of the designated cycle life. In orer to maintain the link between the single and multi-spot welded joints, that which defines failure in the single welded specimens must also define failure in any one of the indiividual spot welds that make up the multi-spot joints. Therefore the conditions for failure for a single spot welded joint and the individual welds present in a multi-spot welded joint must be identical.

(5)   The fatigue strength distriubtion for single and multispot welded joints must fit the normal probability function.

This can be assumed as being fulfilled if condition 1 is met.

1.3: Proposed Methodology.

To verify this theory, values for the mean fatigue strength and the standard deviation of the fatigue strength distribution, per nugget, for joints containing one, two, four, eight, and sixteen nuggets, for a cycle life of 10^6 cycles, would need to be determined experimentally. Particular attention would need paying to the values for the single spot welded joints since these values form the basis of the proposed theoretical model.

Once values for the mean fatigue strength and the standard deviation of the fatigue strength distribution per nugget are determined experimentally for the multi-spot welded joints they can be compared to the theoretical values determined from inputting the single nugget values into the proposed theory.

This process of comparison will highlight any possible anomalies associated with increasing the number of weld nuggets within a joint that are not considered in the initially proposed theory. Should any such anomalies become apparent, then the data collected will assist in pinpointing their cause, allowing for the next stage of model development.

In order to define statistically valid values for mean fatigue strength and standard deviation experimentally, a comprehensive series of fatigue tests will need to be carried out that will reveal the probability of survival at various loads for each of the specimen configurations. Since the required data is only concerned with whether the sample survived by completing 10^6 cycles, or whether it failed before completing 10^6 cycles, a response testing approach would be most suitable. There are two types of response test that will be of particular use in this investigation, they are the Staircase and Probit testing methods.

The Staircase testing process is a fatigue response testing approach that can determine a mean value for the fatigue strength of the specimens to be examined in this investigation from a relatively small number of tests [2, 3]. The data collected by the Staircase method can also be used to calculate a value for the standard deviation of the fatigue strength distribution for a given specimen configuration, although this is less accurate than the value calculated for the mean [2, 4].

The Probit method of testing is used to determine the complete Probability Density Function (PDF) of the fatigue strength for a given specimen configuration. The common procedure is to divide the specimens available into several groups and to test one group at a chosen load level, the next group at a second level and so on. The data is then evaluated by considering the number of failures and survivals occurring at each of the load levels and plotting the data as a 'Response Curve'. The response curve will give an accurate representation of the complete PDF for a given specimen configuration, however, the number of specimens required for a Probit testing process is much greater than that required for the Staircase process [2, 3].

Since the data on the single weld specimens will form the basis of the proposed model a more comprehensive analysis needs to be carried out on those specimens. Therefore, the single weld investigation will consist of both a Staircase and Probit testing process. The Staircase process will determine initial values for the mean fatigue strength and standard deviation of the fatigue strength distribution for single spot welded joints. These initial values will then be used to determine load levels for a Probit testing process, which will accurately determine the complete PDF for the fatigue strength of the single welded specimens.

The data taken from the Probit testing of single spot weld specimens will then be used in accordance with the proposed theory to generate estimate values for mean fatigue strength and standard deviation, per nugget, for joints consisting of two , four, eight, and sixteen nuggets.

A Staircase testing process will then be carried out on each of these specimen configurations to determine the actual values for mean fatigue strength and standard deviation per nugget. The experimental result will then be compared to the theoretically determined ones, allowing for a thorough analysis to be carried out.

1.3.1: Summary of Proposed Theoretical Model.

Mathematically the fatigue strength distribution, and therefore the fatigue propoerties, of a multi-spot welded joint consisting of welds that are ostensibly identical, can be shown to be proportional to those of an ostensibly identical single spot welded joint in the following way (taking into account certain boundary conditions):

$$P(MS) = P(SS)^n \qquad Eq. \ 1.1$$

To establish whether confidence in the proposed model is justified a fatigue testing regime comprising of both a Staircase and Probit testing techniques has been suggested.

2: Literature Review.

In order to accurately evaluate the proposed theory, consideration needs to be given to the major process steps in both the manufacture and testing of the various specimen configurations. Understanding the major process steps will allow for appropriate measures to be taken to control the various variables associated with this investigation and assist in the overall compliance with the established boundary conditions. The following section reviews published work and research, which covers the main processes to be used in this project.

2.1: Fundamentals of Resistance spot Welding.

Resistance Spot Welding (RSW) was first introduced by Elihu Thompson more than 100 years ago. The process is most commonly used for the fabrication of sheet metal assemblies up to 5 mm in thickness when the design permits the use of lap joints and airtight seams are not required [5]. Thicker sections can also be welded in this manner, however, the loading of the joint is limited and the extra weight added by the large overlap puts the process at a disadvantage when compared to other processes that do not require a lap, such as laser welding [6, 7, 8, 5].

Joints are made by creating spot welds at intermittent intervals on overlapping sheets of metal. The process is used in preference to mechanical fasteners, such as rivets and screws, when disassembly for maintenance is not required [9]. RSW is also much faster and more economical since a separate fastener is not needed for the assembly.

The process is used extensively for joining low carbon steel sheet metal components for automobiles, cabinets, furniture, ventilation systems, and in the construction sector. Developments in the process have also helped to optimise the process for welding modern materials such as stainless steels and aluminium and copper alloys [6, 7, 8, 10].

2.1.1: Advantages and limitations.

The major advantages of spot welding are its high speed and its adaptability for automation when used in the production of sheet metal assemblies. It can be incorporated into assembly lines with other fabrication operations with relative ease and is also regarded as an economical process in many operations using semiautomatic machines, since it is faster than arc welding or brazing and requires less skill to perform [9].

The process also has some limitations, the three major ones being:

1. The added weight caused by the need for an overlap [9].

2. Spot welded joints are considered to have a low fatigue strength, this is due to the presence of a crack-like notch around the periphery of the nugget, between the joined sheets [9].

3. The full strength of the sheet can not be utilised across the spot welded joint because fusion is intermittent and loading is eccentric due to the overlap [9].

2.1.2: The Welding Process.

Resistance spot welding involves the joining of the faying surfaces of two or more sheets of metal in a localised area by the application of heat and pressure [11, 12].

Force

Electrode

Current

Source

Sheets to be
joined

Force
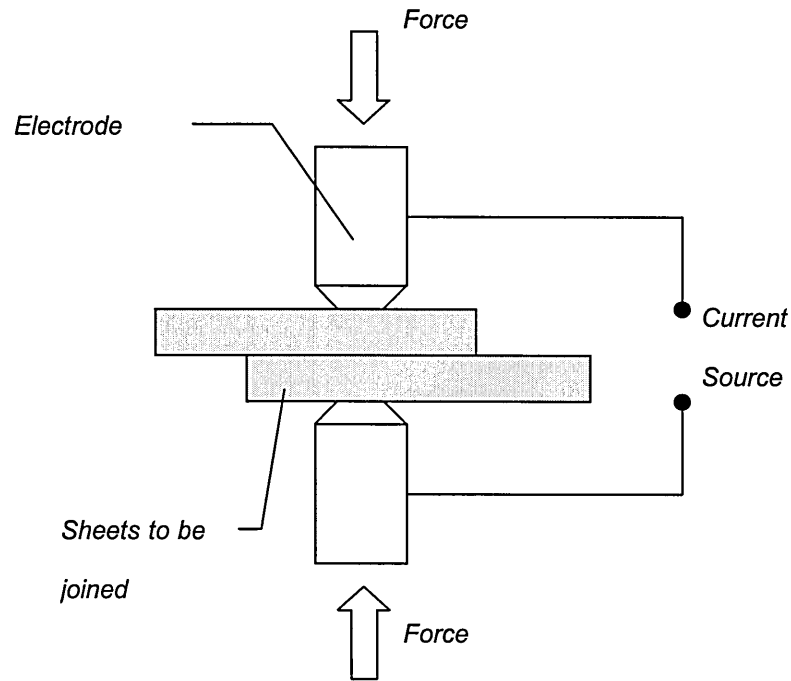
Fig 2.1: The welding process.

The heat is supplied by a short pulse of electric current between two water cooled, copper alloy electrodes, through the workpiece and across the gap separating them, this path is known as the 'secondary circuit' [11]. The electrical resistance in this circuit is at a peak at the join between the two sheets. This means that the transfer of current across this gap generates a tremendous amount of heat in a highly localised area [5, 11, 13, 12].

44

The level of heat generated in this area is so high that the metal of the two sheets melts and runs together creating a molten pool at the sheet interface. At the same time the clamping force applied by the electrodes creates an intimate bond between the two sheets, containing this weld pool in a localised area. Once the current is switched off, the continued application of this force helps to consolidate the weld pool into a weld nugget, with a higher potential for an improved grain structure when compared to other welding processes [6, 11, 14, 13].

Finished
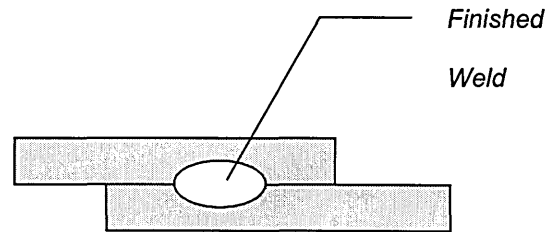
Weld

Fig 2.2: A completed spot weld.

2.1.3: Generating Heat.

The passage of current through a circuit is caused by creating a region of potential difference between two points, in the case of spot welding, this potential difference is found between the two electrodes. By generating a potential difference between two points in a circuit, an electric field is created. This field causes the electrons in the circuit to move in the direction of the voltage drop. These electrons carry a charge across the circuit, therefore generating a current. Inevitably these travelling electrons collide with the stationary ion cores of the material that makes up the circuit. Each of these collisions will involve a degree of friction, which generates a small amount of heat. The amount of friction created by these collisions is a measure of the materials electrical resistance. Higher electrical resistances mean larger amounts of friction, which leads to larger amounts of energy being released in the form of heat when the collisions occur [16, 11]. The amount of heat that is generated when producing a spot weld through resistance heating is therefore a function of the amount of heat energy released by friction between the colliding electrons and ion cores. This is primarily controlled by three factors:

1. The amount of welding current used [6, 5].
2. The duration that this current flows for [6, 5].
3. The electrical resistance at various points in the secondary circuit [6, 5].

The relationship between these three factors, and the amount of heat generated, can be approximated using Joule's Law, which calculates the amount of heat liberated by current travelling through a resistor for a given amount of time [6, 11, 13, 5].

$$Q = I^2 R t \qquad Eq.\ 2.1$$

Where:

Q =   *Heat generated (Joules).*

I =   *Welding current (Amperes).*

R =   *Resistivity (Ohms).*

t =   *Amount of time the current is applied for (Seconds).*

For a more accurate calculation the effect of the following factors would also need to be accounted for [15, 12]:

1. The heat lost through conduction.

2. The heat lost through radiation.

From joules Law it can be seen that heat will be generated at any point in the secondary circuit that offers a resistance to the flow of current. In a joint consisting of two sheets there are at least seven areas of resistance where heat will be generated [5]. These areas are illustrated in Fig 2.3 on the next page.
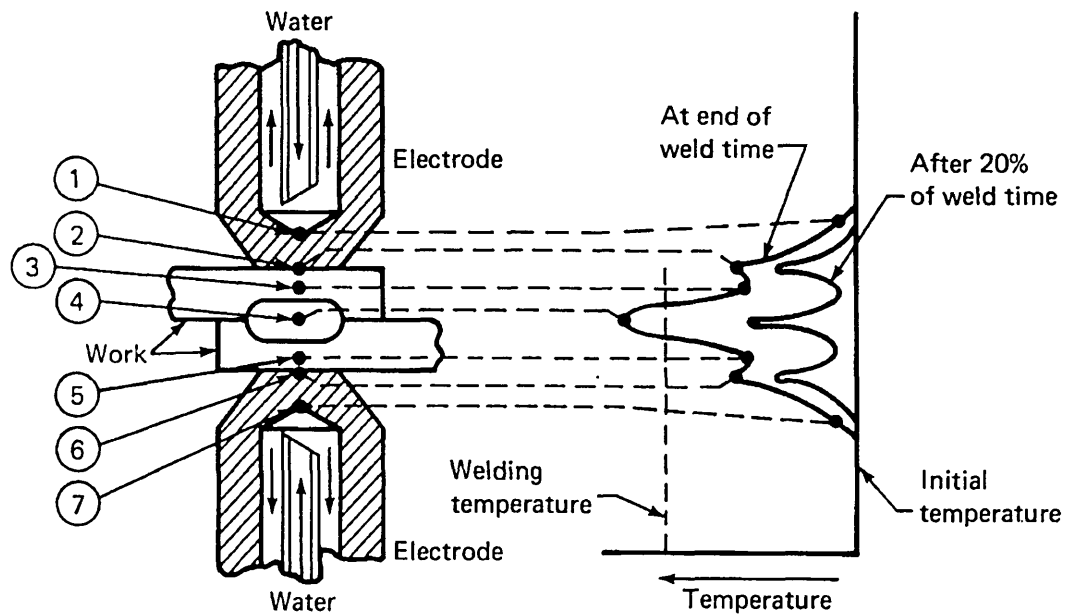
Fig 2.3: Areas of heat generation in spot welding [5].

1 and 7	=	*The electrodes.*
2 and 6	=	*The interface between the electrodes and the workpiece.*
3 and 5	=	*The workpiece itself.*
4	=	*The workpiece interface.*

47

Since the welding current and the time for which it is applied will be constant across all these regions, the amount of heat generated in each of these seven locations will be proportional to their resistance [5, 10, 5, 11]. Welding heat, however, is required only at the workpiece interface, and the heat at all other locations should be minimised. Since the greatest resistance is located at region 4, heat is most rapidly developed at that location [5, 10, 15, 11]. Regions 2 and 6 offer the next highest level of resistance and the temperature also rises rapidly at these locations. However, the heat generated in regions 2 and 6 is rapidly dissipated in the highly conductive, water cooled, copper alloy electrodes [11]. The heat that is maintained in regions 2 and 6 helps maintain the rate of temperature rise in region 4 by retarding the heat lost through conduction into the workpiece, allowing welding temperature to be reached much more quickly [5, 10, 15].
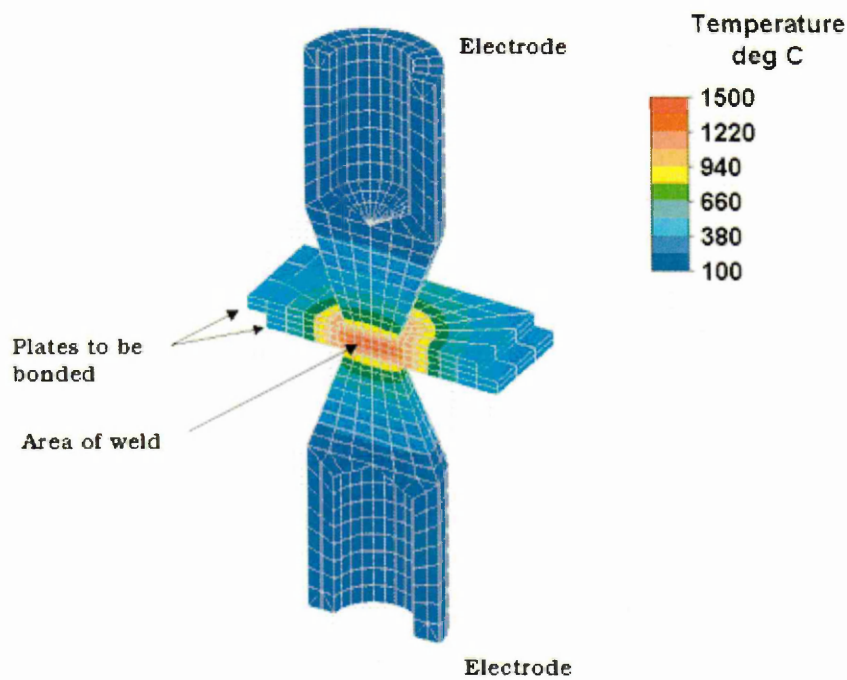
Fig 2.4: Temperature gradients in spot welding [17].

2.1.4: The Welding Cycle.

Despite the speed of RSW, a well defined sequence of events needs to occur during the welding process in order for acceptable results to be achieved. This sequence can be adjusted to maximise the throughput [18].

Every resistance spot weld consists of four major time segments, with each segment taking up a portion of the total weld time. In order to maximise throughput, the four segments need to occur seamlessly in the fraction of a second it takes to make each weld, they occur in the following order [18, 5, 15]:

- Squeeze.
- Weld.
- Hold.
- Off.

Squeeze Time: This is the interval of delay between timer initiation and application of the welding current. It provides time for the welding head to bring the upper electrode into contact with the workpiece and apply the full amount of force. This time should be sufficient to ensure that all the parts of the joint have attained an intimate contact before current is applied [38, 15, 13]. The magnitude of squeeze time should be minimised to maximise throughput but will be ultimately depend upon the distance between the electrodes and the hardness of the material. Typically industry aims for a value around 0.5 seconds [66].

Weld Time: This is the interval during which the welding current flows through the circuit [13, 5, 15]. The magnitude of the weld time is dependent upon the material being welded, but for most stainless steels this value is between 0.3 and 0.6 seconds [66].

Hold Time: This is the interval in which force is maintained on the workpiece after the last impulse of current ceases flow. This interval takes place to ensure that the metal has cooled and solidified, giving the spot weld adequate strength to support itself [14, 5, 15, 13]. Some HSLA materials are hold time sensitive with hold times as great as 0.5 to 1 second. These materials tend to experience interfacial tearing when peel tested [15].

Off Time: This is the interval from the end of the hold time until the beginning of the squeeze time for the next cycle. In an automatic cycle, off time is the time needed to retract the electrodes and to index, remove or reposition the workpiece. In manual operation it is not fixed as a maximum period by the control equipment, but depends on the time taken by the operator to start a new cycle [15, 5, 13].

The four time segments of a welding cycle can be applied in various ways, the simplest welding cycle supplies uniform welding current and electrode force throughout the weld interval [15], as shown below in Fig 2.5.
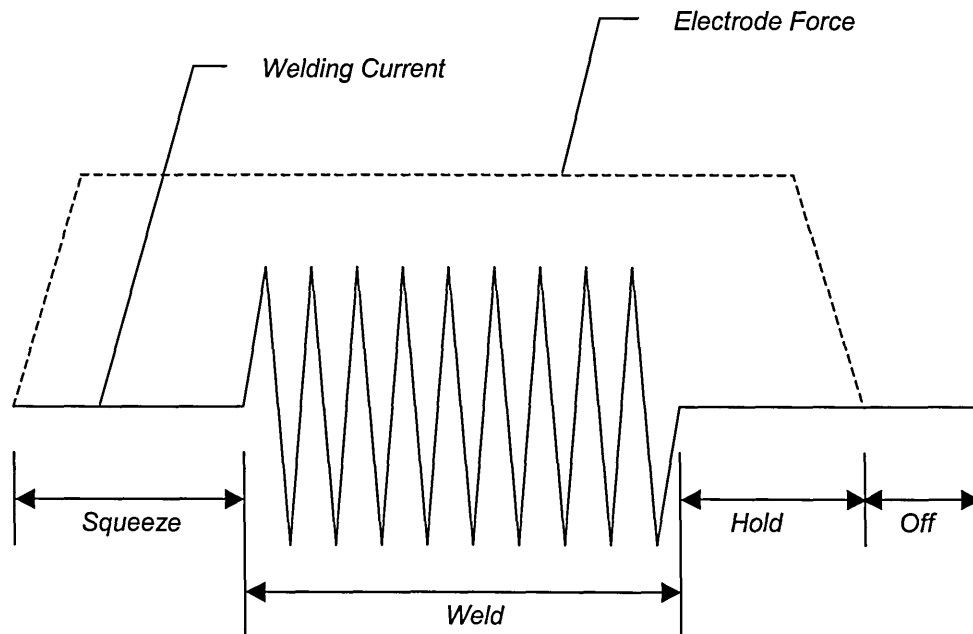
Fig 2.5: A basic welding cycle.

50

In the case of this project, where an Alternating Current (AC) powered spot welder will be used, all of the segments are measured in cycles, where 1 cycle represents one oscillation of the AC power supply. The supply used in this project is a standard UK AC power source, which oscillates at a frequency of 50 Hz, meaning 1 cycle = 0.833 seconds. For Direct Current (DC) powered equipment these segments are measured in milliseconds.

2.1.5: Defects caused by incorrect segment sequencing.

If the welding current is activated too soon after the electrodes are brought into contact with the workpiece, the correct amount of force may not have been achieved before the passage of current commences. This will result in both the sheets and the electrodes not being in intimate contact when the current traverses the workpiece interface, making the electrical resistance at their interfaces much higher than they should be. This increase in resistance will mean that the workpiece will be heated up too quickly and to a much higher temperature than desired, which may cause the outer surfaces to melt. The excessive temperature rise on the surface may also cause the electrodes to stick to the hot surface, copper from the electrodes to be deposited in the weld area, and excessive electrode wear [18]. If the current is applied while the force is still increasing, this could result in weld metal being forced out of the nugget, resulting in severe surface splashing and expulsion, which could lead to the nugget containing an unacceptable amount of porosity [18].

Once the weld is produced, the electrodes need to remain clamped together long enough after the current has finished pulsing for the weld nugget to solidify. If the hold time is too short the nugget may still be too soft to support the join, meaning the joint springs apart, resulting in a weakened weld. If the hold time is too long it will cause unnecessary lengthening of the total weld time [18].

2.1.6: Welding Current.

Both AC and DC are used to produce RSWs. The welding equipment will transform the low current, high voltage line supply to high current, low voltage welding power through the use of a step transformer [5]. A step transformer consists of two coils of wire, each wound around an iron core. The factor by which the current and voltage are stepped up or down is equal to the ratio between the numbers of turns of wire in the coils [19]. Direct current is often used for applications that require high amperage because the load can be balanced on a 3-phase power line; its use in resistance spot welding also reduces the power losses in the secondary circuit [5]. A DC system also allows for more efficient energy conversions by using a physically smaller transformer, this makes DC systems more portable and suited to remote operation [20].
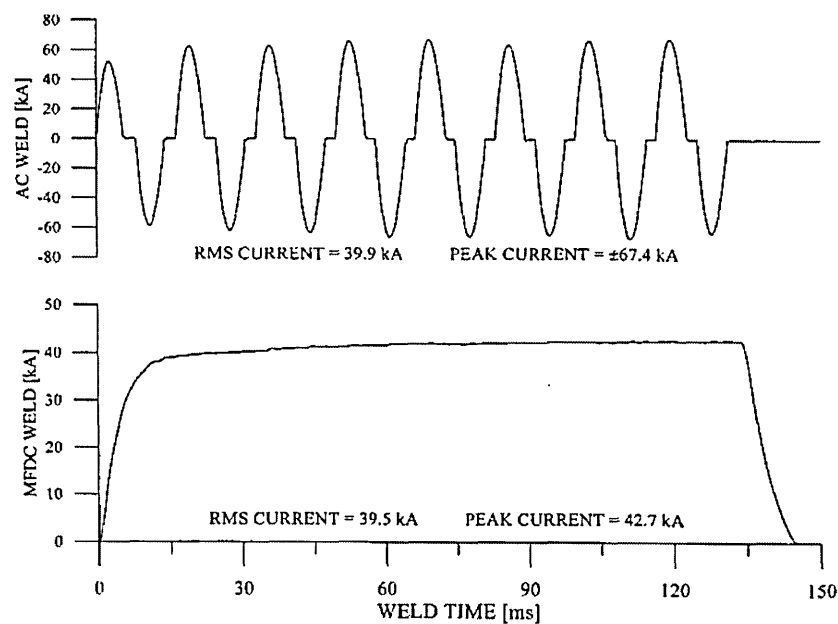
Fig 2.6: AC and DC power supply systems [21].

Another advantage of using a DC system in resistance spot welding is illustrated above in Fig 2.6. They show two current waveforms, each producing the same RMS of current, however, the peak level of the DC system is slightly lower than that of the AC one, which makes the Dc system less susceptible to weld metal expulsion. However, studies have shown that due to the current only flowing in one direction in a DC system, it can lead to uneven electrode wear (between top and bottom), which can also lead to problems with heat balancing [20].

Electric current is a measure of the rate of charge flow past a given point, the higher the current the higher the rate of charge flow [22]. The actual magnitude of current required to produce a resistance spot weld will be inversely proportional to the electrical and thermal resistivities of the workpiece base material [11]. Higher resistance in the material means collisions between the travelling electrons and the stationary ion cores of the workpiece occur more readily and therefore a lower current is required to generate welding temperatures at the workpiece interface [16, 10, 5].

From Joule's law it can be seen that current has a greater affect on the generation of heat than either electrical resistance or time, and while these other two factors do influence the magnitude of heat generated it is current alone that determines the rate of heat development [5, 11]. While the current is passing some of the heat generated is lost, mainly through conduction to the water cooled electrodes. The size to which the nugget will grow, and indeed whether a nugget will form at all, depends on the heat being generated faster than it is lost. Current magnitude is therefore a most critical variable [5, 11].

As well as controlling the magnitude of current in RSW, attention should also be paid to controlling the density of the current passing through the workpiece interface. The current density is the concentration of current passing from the electrode to the workpiece and is calculated by dividing the supplied current magnitude by the contact area between the electrode and the workpiece [11, 19]. Therefore, the size of the contact area of the electrodes is also a critical variable when controlling the amount of current used in producing resistance spot welds. A minimum current density flowing for a finite length of time is required to produce sufficient heat to overcome the losses to the adjacent workpiece and electrodes. Past this point weld nugget size and strength will increase rapidly with increasing current density. However, excessive levels of current density will cause the weakening of the metal surrounding the weld, which may lead to expulsion, cavitations, weld cracking, and lower mechanical strength properties [11, 5, 15].

2.1.7: Welding Time.

Of all the segments of time within a basic welding cycle, weld time is the variable that has the greatest influence on the generation of heat and the production of a spot weld.

As discussed in Section 2.1.6, current determines the rate of heat generation, but the total heat generated is a definite function of weld time [5, 23]. Essentially this is because the amount of weld time determines the length of time current is passed through the circuit and therefore how long heat is generated for. The weld time also determines the rate of heat transfer or loss to the surrounding area, in particular through conduction into the electrodes. These losses increase with increasing weld time and temperature and eventually a weld time will be reached where the heat losses will equal the heat input and the temperatures will plateau [5].

To a certain extent, weld time and current may be complementary, if one of the parameters is lowered the other can be raised and the same amount of heat will be generated [5, 15]. However, since heat transfer is a function of time there is a limit to which welding time can be reduced, regardless of how much welding current is used [5, 15]. This is because if the current is applied in too high a magnitude the rate of heat generation will be too steep and there will not be enough time for sufficient heat to be dissipated at the three surface interfaces. This excessive rate of heat generation will often lead to expulsion and pitting, particularly at the electrode/workpiece interface [15, 23].

The temperature distribution curve in Fig 2.3 shows that for a given current density a minimum length of time has to elapse in order to pass enough current through the circuit and allow the small volume of metal at the workpiece interface to reach its melting temperature [5]. Not allowing current to pass for this length of time will mean insufficient depth of fusion and too little heat being generated at the workpiece interface. If too little heat is generated then the volume of the weld nugget will be smaller than required, which will lead to a reduction in strength and increase the chance of the weld failing prematurely. However, if current flow is continued much after this minimum time, the temperature at the workpiece interface can far exceed the necessary welding temperatures. This can generate gases and metal vapour within the confined space of the weld pool which will increase the internal pressure and may lead to the expulsion of weld metal from the weld nugget [5].

Fig 2.3 also shows that the temperatures at the other six regions of resistance in the secondary circuit increase with time. The inner curve represents the temperature in each region once 20% of the weld time has elapsed, while the outer curve represents the temperature in each region after 100% of the weld time has elapsed. Therefore, longer weld times also increase the risk of overheating in the regions where heat needs to be minimised. This could result in the deterioration of the electrodes and also the extension of the Heat Affected Zone (HAZ) further into the workpiece [5].

2.1.8: Force.

Welding force, or electrode force, is produced by the load exerted on the workpiece by the electrodes. It is usually measured and expressed as a static value, however, electrode force is a dynamic force in operation and is affected by the friction and inertia of the moving parts of the welding equipment [15]. The force is first applied at the start of the squeeze time segment of the welding cycle with its magnitude rapidly increasing so that the full amount of the required force is applied as the welding current is activated at the start of the weld time segment [18]. At this stage of the weld cycle the force is required to bring the various interfaces together and allow the passage of the welding current.

Once the current is activated, the force is maintained to contain the weld pool between the two workpieces and prevent the parting forces of the expanding metal in the weld pool, and the metal fumes released from the weld pool, from separating the workpieces, which would cause weld metal to be expelled [10, 11]. The higher the strength of the steel being welded, the larger the required electrode force will need to be to ensure this intimate contact and prevent the escape of the weld metal [15, 11].

The continued application of a force after the current is deactivated, and while the weld is cooling, allows for consolidation of the weld microstructure under a forgoing force. This leads to a more homogeneous and refined grain structure within the weld nugget, which enhances its mechanical properties [11, 14, 12].

The resulting pressure caused by the application of the welding force directly affects the contact resistance at each of the three material interfaces [11]. At the workpiece interface the surfaces of the two sheets will be a series of peaks and troughs, as shown below in Fig 2.7.
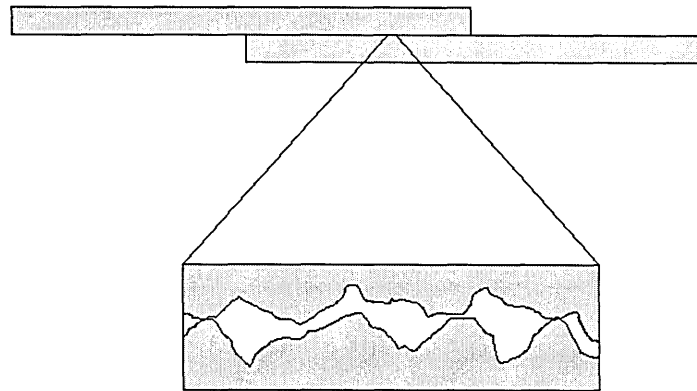
Fig 2.7: Surface asperities on joint overlap.

If the two sheets are simply placed together the actual metal-to-metal contact would be very small, resulting in a high level of contact resistance. When the electrodes apply a force these peaks will be depressed and the metal-to-metal contact area at the workpiece interface will increase, lowering the contact resistance [5].

At first this may seem to be counter productive to the production of spot welds, as it can be seen from Joule's law that, for a given amount of welding current and welding time, a decrease in resistance at the workpiece interface will result in a decrease in the level of heat generated. However, compressing the asperities to increase the contact area at the workpiece interface will allow for the use of higher currents. Due to the dominant influence of welding current over resistance on the generation of heat, decreasing the contact resistance to allow for high welding currents will mean that more heat can be generated, which broadens the scope for producing quality welds [5].

As well as increasing the contact area and lowering contact resistance at the workpiece interface, the application of force will achieve the same effects at the electrode/workpiece interface. Consequently, because the electrode material is often softer than the workpiece, the application of a suitable force will produce a better contact at the electrode/workpiece interface, compared to the interface between the workpiece sheets [5]. This will reduce the amount of heat generated at this location and help prevent defects such as surface spitting and also prevent rapid deterioration of the electrode tips.

For consistent operation it is preferable to use a high electrode force and supplement it with a higher current or weld time. However, particularly when welding low resistivity metals, the contact resistance cannot be reduced too far as there must be some resistance present at the workpiece interface to generate heat [11]. Excessively high forces are also undesirable due to the increase in surface indentation on the sheets and the extra wear caused to the electrode tips [11].

2.1.9: Multi-spot Welding.

Although single welded joints will form an important part of this project the majority of work will be orientated around multi-spot welded joints, it is therefore important to understand the multi-spot welding process and identify any additional variables or problems the process may introduce.

In industry applications the vast majority of joints made using resistance spot welds are produced using more than one spot weld, single spot welded joints are usually only found on test specimens produced to verify the quality of a spot weld made in a material using a given set of spot welding parameters.

The process of multi-spot welding can be done either by producing successive welds with a standard welding gun, with a single pair of electrodes, or, when the production requirements and number of spot welds on the assembly are very large [9], using multi-spot welders. The later consist of a series of hydraulically or air operated upper electrodes and a fixed solid bar or 'mandrel' for the lower electrode [23].
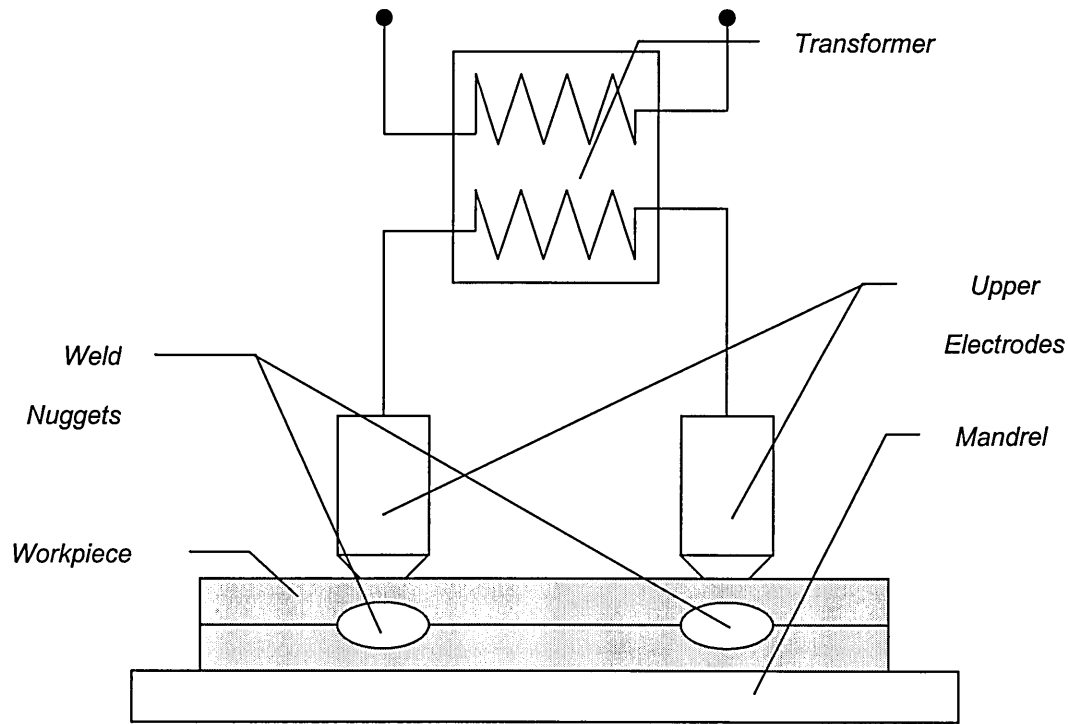
Fig 2.8: A multi-spot welder incorporating a mandrel.

The upper electrodes can be connected by flexible bands to individual transformers or to a common buss bar attached to the transformer [23]. The advantages of the multi-spot welder are that it is designed and configured to produce a specific joint or assembly efficiently and consistently, even with a human operator [9]. The disadvantages are that the system is not very flexible and can not be easily configured to produce complicated joints like those found on an automobile chassis. For this reason it is more common to see single electrode upper arm machines producing successive welds on an automobile manufacturing line.

2.1.10: Current Shunting.

A draw back to producing a successive series of spot welds in a single workpiece or joint is that it can cause an undesirable effect known as Current Shunting, which is sometimes referred to as Current Diversion or Leak Current.
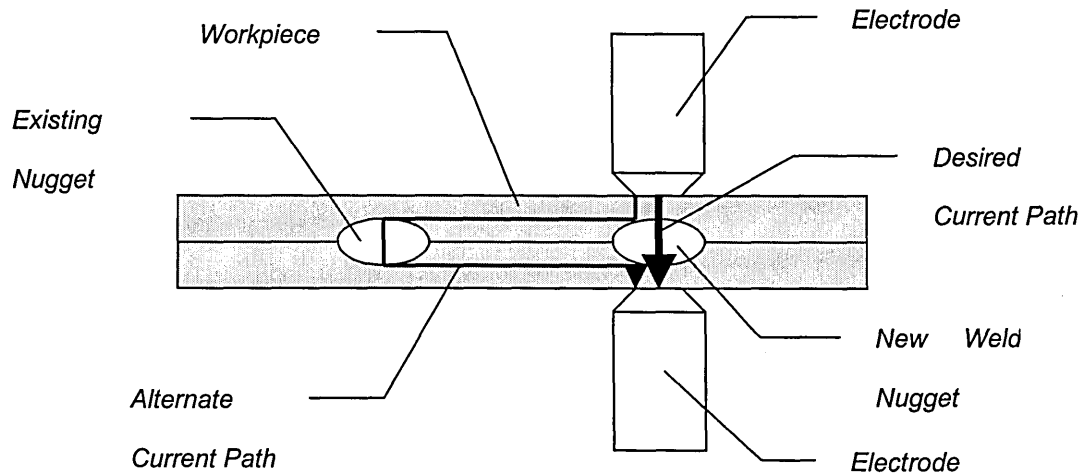
Fig 2.9: Current shunting in series welding.

When a weld is made in close proximity to an existing weld there can sometimes be a low resistance path through the adjacent weld nugget. If this alternative path is of sufficiently low resistance then some of the welding current will by-bass the workpiece interface, between the electrodes, at the new weld nugget location, and travel across the workpiece sheet and through the adjacent nugget. This lowers the amount of active welding current and reduces the amount of heat being generated at the new weld location, which in turn, leads to an undersized weld nugget [14, 9, 11]. As a result, the first weld in a series of welds made in a single piece of metal may be larger than subsequent welds. This means that any single spot weld test specimens, used to verify the quality of welds made with a given set of parameters, could be misrepresentative of a weld made in a series, since the single spot specimen may contain a larger weld than would be obtained in a line of welds made using the same welding parameters [14, 11, 13].

Since current will take the path of least resistance, the amount of current shunting that occurs is dependant upon the ratio of the resistances of any alternate current paths through adjacent welds and the path directly between the two electrodes [9]. The resistance of any alternate current paths through an adjacent weld is a function of the resistivity of the workpiece material, the thickness of the sheet, and the weld spacing. Joints made from thick plate or metals with low resistance will be more prone to current shunting than those made from thinner plate or metals with high resistance, simply because the resistance of the alternate path through an adjacent weld will be lower [14, 9, 11]. The resistance of any alternate path can also be changed by varying the distance between welds, referred to as the pitch distance. As with any electrical circuit the further the current has to travel the higher the overall resistance, by increasing the pitch distance the resistance of the alternate path through any adjacent welds increases and the risk of current shunting is reduced [14, 9, 11].

Since the thickness and resistance of the workpiece sheets are often fixed by design requirements, the best way to limit the amount of current shunting is to choose a pitch distance large enough to make the distance of the alternate path through any adjacent nuggets too long and therefore too resistive. However, the minimum pitch distance needed to prevent current shunting will still be dependant on the conductivity and thickness of the workpiece sheet, the more conductive or thicker the sheet the larger the pitch distance will need to be. For very low resistance metals or when close weld spacing is a design requirement, increasing the pitch distance may not be a viable option. In these instances the welding current used for welds subsequent to the first can be increased to compensate for the amount of current shunting occurring [9, 14, 11].

2.1.11: Summary of the Fundamentals of Resistance Spot Welding.

The resistance spot welding process has many variables, each one affecting the welds that are produced. Although the production of welds that are as mechanically strong as possible is often a requirement in industry, for the purpose of this project the production of consistent welds is paramount.

Control of the welding parameters is therefore the most critical consideration when spot welding the test specimens, however, producing mechanically strong joints should not be dismissed altogether as mechanically strong joints will be more representative of the joints used in industry and will often have more consistent properties when compared with each other.

In order to ensure consistency between the spot welds produced for the test specimens, and therefore help maintain the first boundary condition of the proposed theory, a weldability study is required. This process will assess the welds produced using a given set of welding parameters, with particular attention being paid to repeatability. To understand and account for any possible effect of current shunting when producing the multi-spot welded specimens, an investigation into the effect of pitch distance on the amount of current shunting, and whether an optimum value can be found that limits its affect on spot weld consistency, will also be required.

2.2: Joint Design.

The specimens used in this project are Tensile-Shear Spot Welded (TSSW) joints, since they replicate the most common loading scenarios associated with spot welded joints in industry [24, 25] and their convenient geometry allows for easy testing [26]. The joints consist of two plates of material joined at an overlap by one or more spot welds. A tensile load is then applied in an axial manner, along the length of the specimen, which is transferred through shearing of the weld nugget.
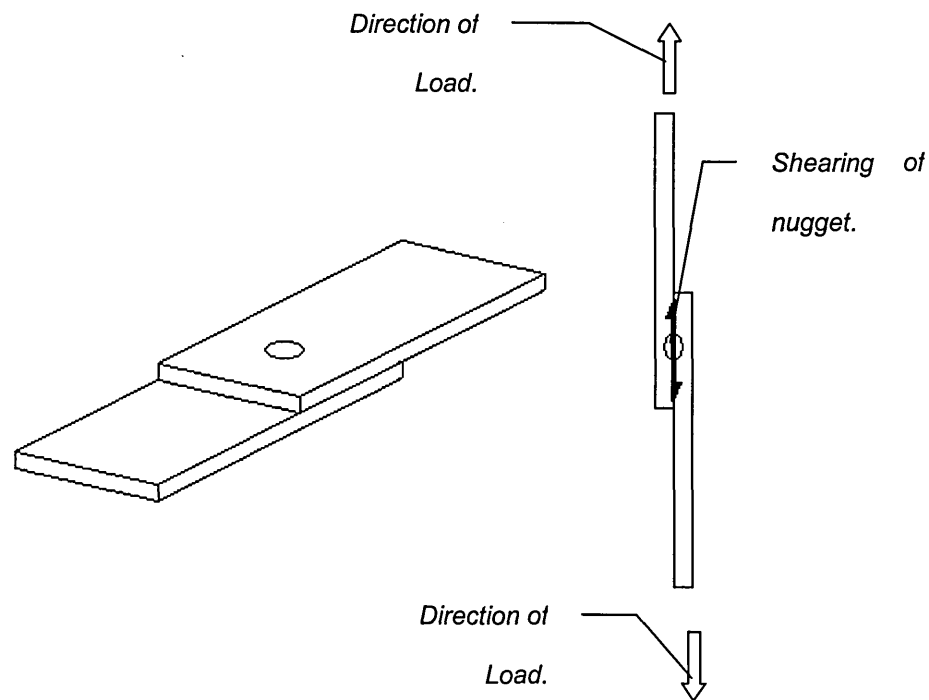
Fig 2.10: The basic single nugget TSSW joint.

When designing TSSW specimen joints there are seven main geometric factors to be considered that will determine the position of any welds and the size of the end specimens, they are:

- Edge Distance.
- Joint Overlap.
- Nugget Size.
- Thickness.
- Width.
- Pitch Distance.
- Free Length.

63

2.2.1: Edge Distance.

The edge distance is the distance from the centre of the last weld nugget in a row of welds to the edge of the sheet. This distance must be large enough to provide a sufficient amount of base material to resist the internal pressure developed in the molten nugget during the welding cycle. If welds are made too close to the edge of any of the sheets to be joined, the base metal at the edge of that sheet will overheat and upset outwards [9, 14, 12].
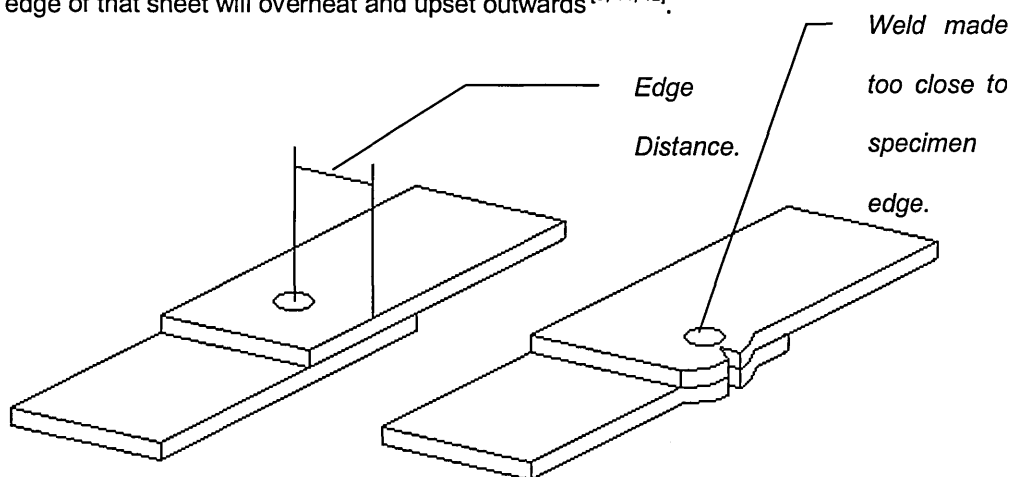
Fig 2.11: Edge distance.

This deformation reduces the restraint on the molten nugget, leading to expulsion of the weld metal. It may also cause excessive electrode indentation and a reduction in the strength of the weld. The minimum edge distance to use is related to the base material properties, the thickness of the sheets being joined, the electrode face contour, and the individual welding cycle [9]. BS 1140: 1993 recommends a minimum edge distance of 1.25d, where d is the diameter of the weld nugget [27].

2.2.2: Joint Overlap.

The joint overlap is the amount of material that overlaps with the other sheet in the joint. It is similar to edge distance in that if the overlap is too small the welds may be made too close to one or more of the edges on the overlap [9, 12], as shown below in Fig 2.12.
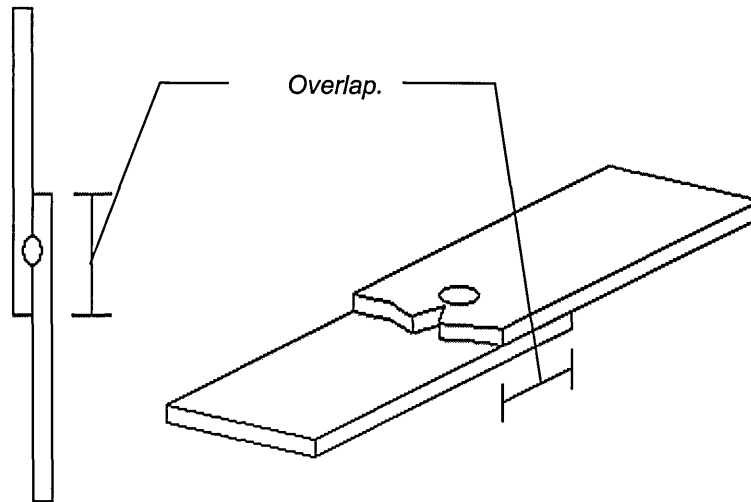
Overlap.

Fig 2.12: Joint overlap.

Generally the minimum permissible overlap is twice the minimum edge distance, however, it should be noted that on joints other than the simple TSSW joints used here, other factors, such as electrode clearance, may necessitate a larger minimum overlap [9].

2.2.3: Nugget Size.

The size of the weld nugget will depend on the thickness of the sheets to be joined. The recommended nugget diameter is related to sheet thickness in the following manner:

$$5\sqrt{t} \qquad Eq.\ 2.2$$

Where t is the thickness of the thinnest sheet to be joined [24, 27, 28].
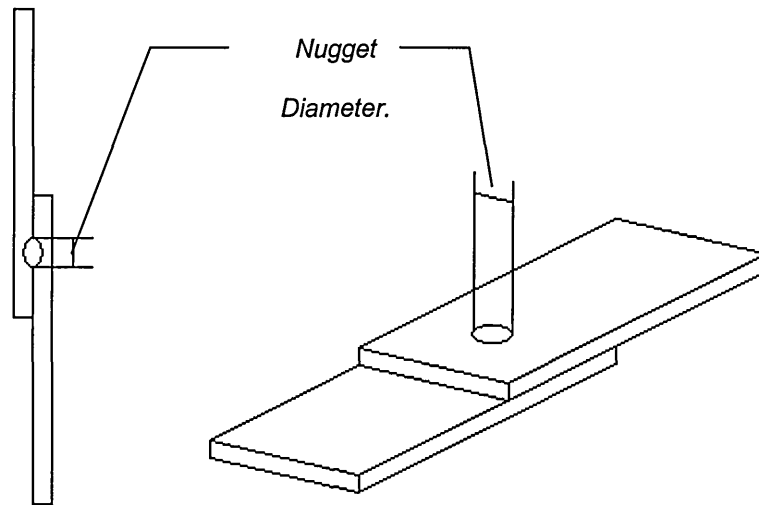
Fig 2.13: Nugget size.

Nugget size is primarily controlled by altering the diameter of the electrode tip, i.e. increasing its size will result in an increase in the nugget diameter [11]. It should be pointed out that increasing the electrode tip diameter will lead to a reduction in the current density and the force exerted by the electrodes. Therefore, it is advisable that increases in electrode tip diameter be accompanied by a corresponding increase in the welding current and the applied load.

2.2.4: Thickness.

The thickness of the sheets to be joined will normally be determined by the end application of the joint or assembly and is therefore less easy to vary. Thicker sheets require more heat to produce the welds due to increases in the amount of heat lost through conduction in the bulk of the base metal. They also require a larger weld nugget to support the extra loads associated with using thicker sections of material. There is a limit to the thickness of the sheet that can be joined using spot welds due to the extra weight added to the assembly by the large overlap [6].
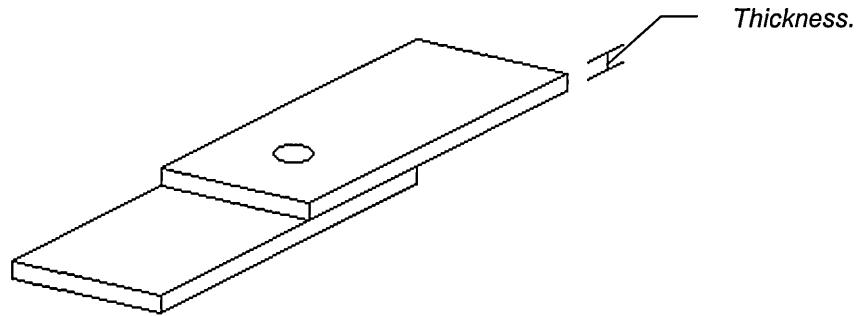
Fig 2.14: Sheet thickness.

2.2.5: Width.

The width of the joint will be a factor of both the minimum edge distance and the number of welds that make up the joint. In multi-spot welded joints, consisting of rows of spot welds, each nugget will be spaced apart from the next by the pitch distance. Therefore the sample width chosen will need to be large enough to account for the spacing between each of the required welds and the minimum edge distance required for the particular type of alloy and process being used.
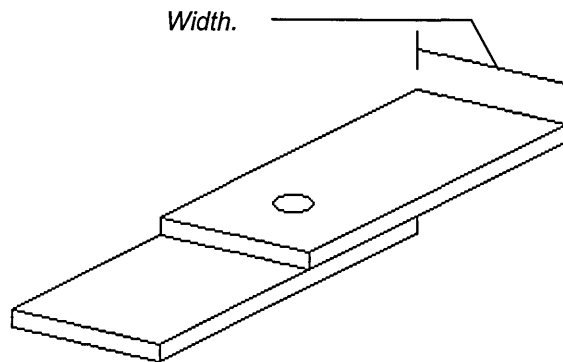
Fig 2.15: Width of TSSW joints.

67

2.2.6: Pitch Distance.

As mentioned previously in Section 2.1.9, the pitch distance is the distance separating adjacent welds in a multi-spot welded joint, measured from the centre of one weld to the next [14, 9].
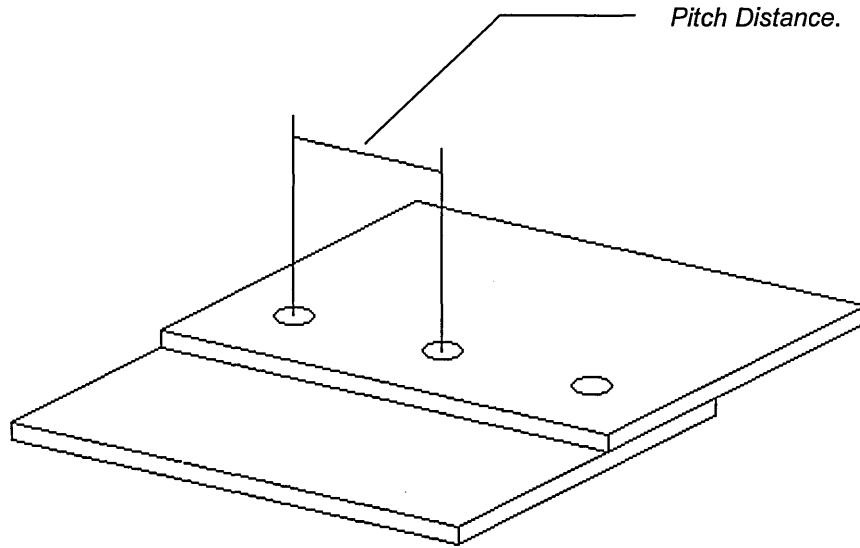
Fig 2.16: Pitch distance.

Altering the pitch distance will affect the number of welds that can be made in a joint of a given width, it will also affect the degree of current shunting occurring in the welding process, particularly when welding materials with higher electrical conductivity, such as plain carbon steels [14, 9]. For normal purposes the pitch distance should not be less than 3d, where d is the diameter of the nugget [11].

2.2.7: Free Length.

The free length of a specimen is the actual length that will be transmitting load during testing. The free length will comprise of a portion of the length of the individual metal sheets being joined and the joint overlap being used. The amount of free length required will depend on the type of testing being carried out, in which case appropriate standards should be consulted, and whether free length is a factor being investigated. It should be noted that sufficient material should be left over at each end of the joint to allow for any fastening that may be required by the test equipment.
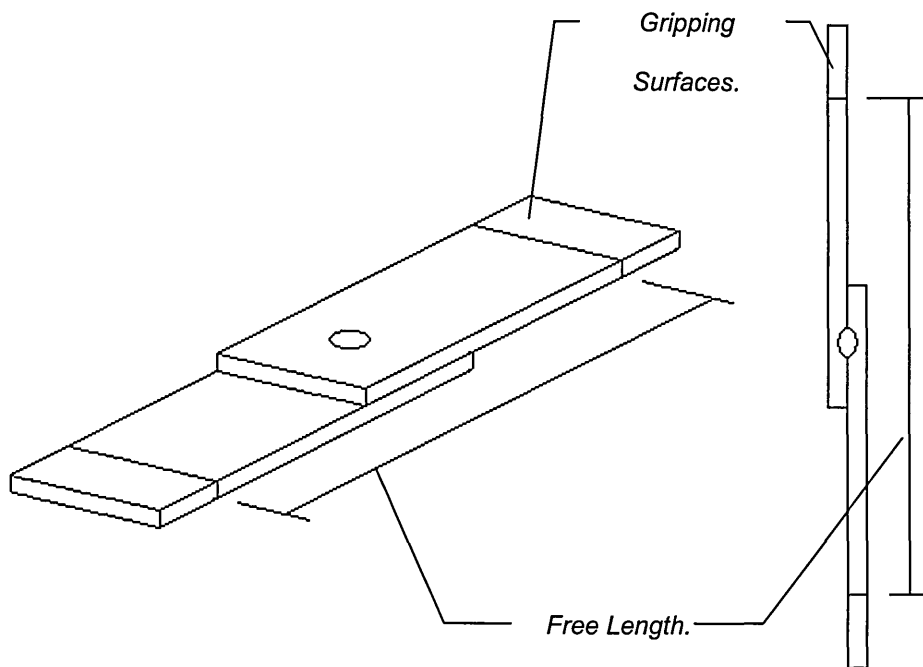
Fig 2.17: Free length of TSSW joints.

In addition there is also the matter of positioning the spot welds. Normally these will be positioned in the centre of the overlap, midway along the free length. When multi-spot welds are used they should be aligned uniformly about the centre line of the direction of the applied load to ensure a balanced load distribution.

2.2.8: Summary of Joint Design.

As mentioned, the use of TSSW joints in this project reflects the most common loading scenarios of spot welded joints in industry [24, 25], however, by using this type of joint it should also be easier to maintain a balanced fatigue load whilst testing, which will assist in maintaining the second and third boundary condition of the proposed theory. To take advantage of this the nuggets of the multi-spot welded joints need to be made in a single straight line across the centre of the overlap. Control over the values of the various joint dimensions explained in this section will also be an important factor in maintaining a uniform distribution of fatigue load and fatigue properties; this is explained in more detail in Section 2.3.6, Fatigue Testing of TSSW Joints.

2.3: Fatigue.

The applications of constructional and structural alloys involve a wide variety of operating conditions, but very seldom do these conditions solely involve the application of a constant static load. Instead, the majority of these alloys will experience fluctuating or 'cyclic' loading conditions resulting from their service application or environment [29, 30].

Basic considerations taken in the early design stages of an assembly mean that the single application of a static load is rarely responsible for material failure in an engineering assembly. Conversely, the repeated application of small loads, which from a static load design perspective would be considered safe, has the potential to cause the sudden and catastrophic failure of an engineering alloy or component. Such failures are the result of fatigue and are referred to as fatigue failure [29].

In its broadest sense, the term fatigue failure refers to failures that are the result of recurring cyclic stresses, nominally at levels below the yield strength of the material. It is this relatively low level of stress required that makes fatigue a particularly dangerous failure mechanism and difficult to prevent by only regarding the physical strength of materials [29, 30, 31].

2.3.1: Fatigue Testing.

It is estimated that at least 75% of all mechanical and structural failures have been caused by some form of fatigue, therefore a high level of importance is placed on understanding and preventing fatigue failure [32, 33]. Understanding is achieved through fatigue testing, which constitutes an important section of the qualification procedure for engineering alloys and components for their service applications.

There are many considerations to take into account when planning a fatigue test and the decision for which approach to use is dependant on the specimen and the information required. Typically, there are two main testing parameters for consideration, namely the stress cycle and the stress ratio.

2.3.1.1: Stress Cycle.

The stress cycle is the smallest section of the stress-time function, which is repeated periodically and identically. It is defined by the stress components (load, displacement or strain etc), the shape, and the frequency [34].
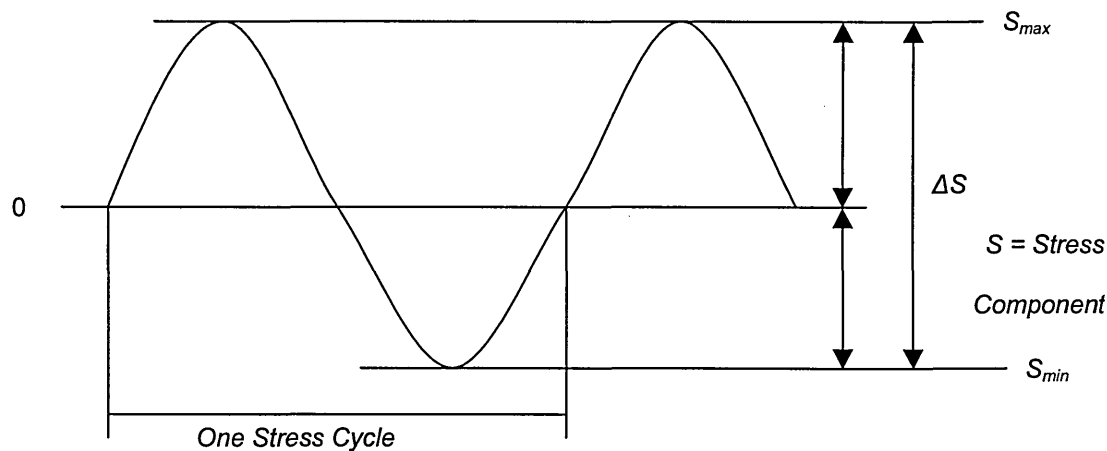
Fig 2.18: The fatigue stress cycle.

2.3.1.2. Stress Ratio (R).

The stress ratio is the ratio between the maximum value (S_{max}) and minimum value (S_{min}) of the stress component used in one stress cycle [34].

72

2.3.1.3: SN Curves.

August Wöhler was the first to study fatigue and propose an empirical approach [33]. Between 1852 and 1870 Wöhler investigated the progressive failure of railway axles at loads bellow that which was thought to be safe [33, 31]. During his investigation, Wöhler constructed a test rig that subjected 2 railway axles, simultaneously, to a rotating bending test. Wöhler plotted the nominal stress, *S*, versus the number of cycles to failure, *N*, for a series of tests to produce what is now known as an *S-N* curve [33]. Modern *S-N* curves are the most readily available data on fatigue testing and typically plot stress on the y-axis against Log *N* on the x-axis. The curves are used to express properties such as a materials endurance, which is defined as the number of cycles to failure at a given stress [32, 30, 31, 33].
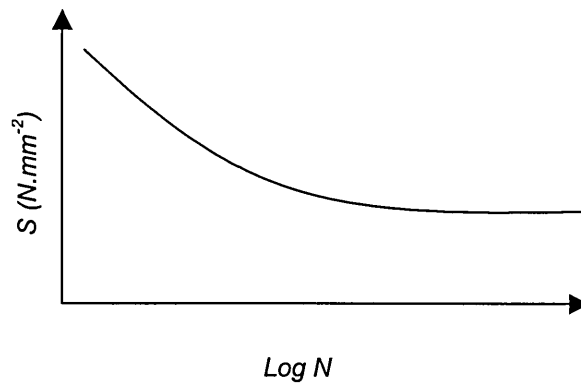
Fig 2.19: A typical S-N curve.

2.3.2: Types of Fatigue Test.

Fatigue testing can take many forms, depending on the type of information that is sought. However, the majority of tests can be divided into three categories.

1. Fatigue of cracked specimens.

The component or specimen contains a pre-existing crack, this is typical of almost any large structure, particularly those containing welds. Final fracture life is governed by the propagation rate of the crack, therefore this area of testing is mostly used to establish data on crack propagation rates to determine the service lifetime of engineering alloys and components before the cracks reach a critical size [35].

2. Fatigue of uncracked specimens.

The components or specimens used in this type of testing are typically smooth and polished, although notches or changes in cross section can be present in some components. The fatigue life of uncracked specimens is often concerned with the time taken to initiate a fatigue crack. Fatigue testing of uncracked specimens can be subcategorised into two further areas of study, high and low cycle fatigue [32, 35].

- High Cycle Fatigue (HCF).

High cycle fatigue typically involves stresses far below the yield point of the alloy being tested and relates to endurances from 10^4 cycles to infinity, which is usually classed as 50×10^6 cycles in terms of a laboratory test. The data collected is usually plotted in the form of an *S-N* curve so as to determine whether the alloy under test displays either a fatigue limit or an endurance limit. Fatigue limits are categorised as the stress, below which, the material cannot be fractured by fatigue. It is define by the point on the *S-N* graph where the curve becomes parallel with the x-axis. Most steels and ferrous alloys exhibit a fatigue limit, as does titanium. [35, 32, 30, 31].
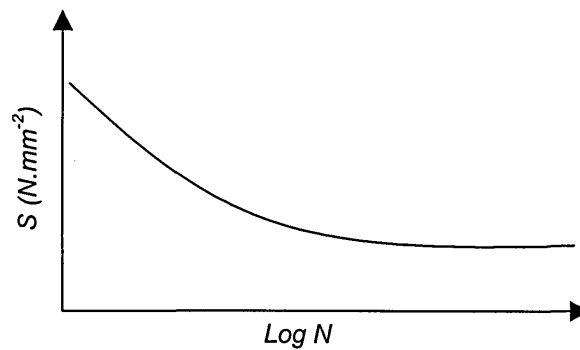
Fig 2.20: An S-N curve displaying a fatigue limit.

S-N curves for materials that display a steadily decreasing slope, instead of a parallel section, indicate that fractures can still occur even at very low loads, after several hundred million stress cycles. In such materials it is usual to quote what is termed the 'endurance limit', which is the maximum stress range required to give a large, specific number of cycles, usually 50×10^6 cycles. Endurance limits are typically found in non ferrous metals [35, 32, 30, 31].
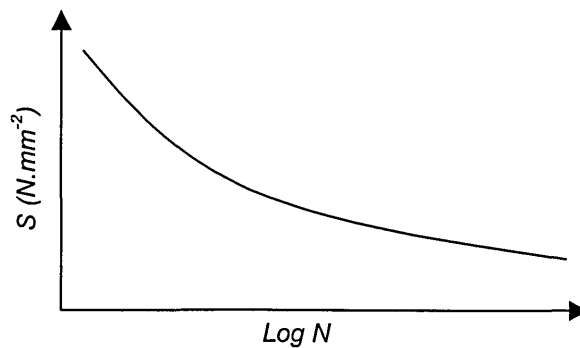
Fig 2.21: An S-N curve displaying an endurance limit.

- Low Cycle Fatigue (LCF).

Failure from low cycle fatigue usually results from applications of high strains or stresses that, in the vicinity of any flaws or defects, can be elevated to levels in excess of the yield point of the alloy. This causes marked plastic deformation, which assists in crack initiation. The cycle lives covered by low cycle fatigue are typically $\leq 10^4$ cycles [35, 32]. For a long time the low cycle region of fatigue was ignored, as the majority of engineering structures exposed to fatigue where expected to have a working life ranging from several million cycles to infinity before finally failing. Efforts where therefore concentrated on the low stress, high cycle life of testing. However, a low cycle life does not necessarily indicate a short lifetime, since lifetime is a function of the cyclic frequency at which the stress cycle is repeated. Structures, such as an aircraft fuselage, are only pressurised once every flight and so may take some time to complete 1000 cycles of stress [32].

3. Tests designed to replicate service life conditions.

These tests often use simplified versions of the actual assemblies to reduce the complexity and cost of the testing process, however, they sometimes necessitate the application of more than one type of stressing. This can be mechanical, thermal, corrosive, or a combination of the three. The data gathered from these types of fatigue tests enables designers and engineers to understand the cause of a particular in service problem or determine the useful service life of a component and therefore help establish suitable maintenance schedules.

2.3.3: Basic Elements of a Fatigue Test System.

The complexity of a fatigue testing system varies depending on the type of testing carried out on them. Basic fatigue testing of engineering alloys can be done using a fairly simple setup, however, systems designed to test the fatigue behaviour of whole assemblies during service conditions can sometimes be highly complex as they often need to reproduce several stressing situations that are akin to what the component might see in service. Regardless of the complexity of the type of test, a fatigue test system has four basic elements; the load train, the control system, the sensors, and the communication system [29].

2.3.3.1: The Load Train.

The load train consists of a frame, grips, specimen, and drive system [29].
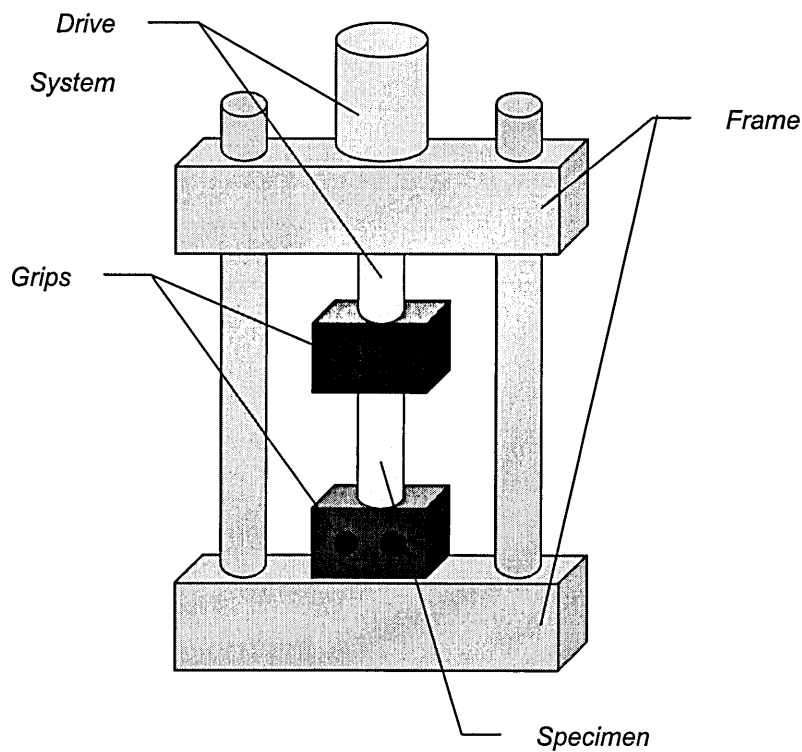
Fig 2.22: The load train of a fatigue testing machine.

77

2.3.3.2: Frame.

The purpose of the frame is to support the specimen, and any sensors associate with the test, and to react the forces applied to the specimen by the drive system. The structural stiffness of the frame is very important as it affects the cyclic frequency of load applications, with a stiffer frame allowing for a higher permitted testing frequency. The frame also forms part of the feedback loop and, as such, must remain a passive element. If the loading of the specimen causes resonance in the frame the actual testing process would be disrupted, possibly causing undesired damage to the specimen [29].

2.3.3.3: Grips.

The choice of grips is governed by the specimen design and the loading requirements of the given test. For the purposes of this investigation the grips will need to be wide enough to secure specimens up to, and including, sixteen nuggets wide. The grips must also be rigid enough to support and distribute load evenly across the entire width of the specimens.

2.3.3.4: Specimen.

The specimen design is controlled by the information sought from the testing process. However, with all specimens care must be taken to ensure that they are manufactured in a manner that limits the possibility of undesired defects, in particular notches, from appearing in the specimen. Care must also be taken in their storage and handling so as to prevent exposure to corrosive environments or substances and also reduce the risk of mechanical damage [29].

2.3.3.5: Drive System.

The drive system is the keystone of the load train and the entire system. Its primary function is to receive a time dependant signal (the program) from the control system, convert that signal to a load-time, or displacement-time, excitation (the stress cycle) and faithfully transfer that excitation to the specimen to be fatigue tested. It should be capable of responding to not only simple sinusoidal input signals, but also to very complex signals characteristic of, or simulating, actual service loads or displacement conditions. Modern drive systems are hydraulically operated and use an actuator to transmit the required load or displacement [29].

2.3.3.6: Control System.

The purpose of the control system is to continuously command the test system to follow a set of programmed test parameters that define the stress cycle. In general a control system needs to include:

- A means of inputting the test parameters of the stress cycle and initiating the test. [29].

- A means of adjusting and maintaining the test parameters in response to information supplied by the monitoring elements (sensors) [29].

- A means of terminating the test upon the achievement of some status. For example, the completion of a predetermined number of cycles or the exceedance of a specified deflection limit. It also requires the means to react accordingly to a malfunction transmitted through a signal from safety cut-offs or fail-safe devices [29].

2.3.3.7: Sensors.

A sensor contains a transducer, which is a device that converts a physical quantity or measureand, such as load or displacement, into an electrical, pneumatic or hydraulic signal. The transducer output signal is fed back to the control system, where it is either acted upon automatically in the form of automated maintenance of the test program, or it is sent to a read out device for continuous communication with the test engineer [29].

A piece of fatigue test equipment will contain sensors for various parameters, depending on the requirements of the test. The most common sensor used is the load cell, which is used to regulate the applied forces with a high degree of accuracy [29].

2.3.3.8: Communication System.

The communication of the data received by the sensors to the test engineer is important as it provides the engineer with information on the state of the current test and also assists in the recording of pertinent data. The majority of modern test systems incorporate a selection of read-out devices in the control system software. However, additional devices, such as oscilloscopes, are still used for some tailored tests [29].

2.3.4: Fatigue Failure Mechanism.

The failure process for fatigue occurs within the atomic structure of the alloy being tested and begins on the application of the first stress cycle. The process has two distinct phases, crack initiation and crack propagation.

2.3.4.1: Crack Initiation.

When a material is fatigue tested above its fatigue limit the atoms within the grains of the material slide and shear against each other along their closest packed, or slip, planes by a process known as slip. The mechanism of slip results in the movement of the inherent dislocations, found in the atomic structure of the material, towards the material surface. After several cycles the movement of dislocations in this manner inevitably causes a dislocation pile up, which results in the formation of a structure known as a Persistent Slip Band (PSB). The PSB is a region at the material surface where the constant movement of material along its slip planes results in areas that rise above (extrusions) or fall below (intrusions) the surface of the component. Under the repeated cyclic loading conditions of fatigue, these PSBs broaden and intensify until a point is reached where separation occurs between the individual slip planes and a crack is formed, this is known as a stage 1 crack [32, 35, 36, 31, 33].

(Suresh 1991)
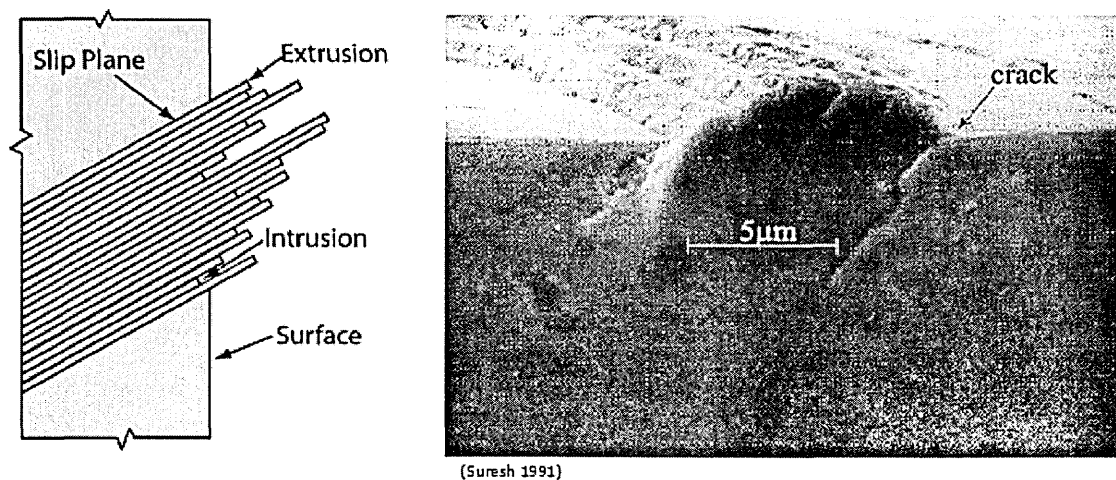
Fig 2.23: Fatigue crack initiation [36].

2.3.4.2: Crack Propagation.

The initiation of a crack forms a substantial discontinuity in the material and will therefore have a considerable affect on the local stress at the tip of the crack. Even if the applied fatigue stress is below the yield strength of the material, the stress concentrating effect of the crack will cause a local area of elevated stress at the crack tip, known as the plastic zone, which can be above the yield strength. On the application of a tensile stress the material in the plastic zone stretches open by an amount, δ, creating new surfaces (Fig 2.24). When the stress is removed the plastic zone relaxes and the crack closes causing this new surface to fold forward, extending the crack by approximately δ (Fig 2.24). This process continues with the cyclic application of the stress cycle, propagating the crack in a slow but predictable manner up to the point where the critical crack size for the applied stress is reached and fast fracture occurs [32, 35].
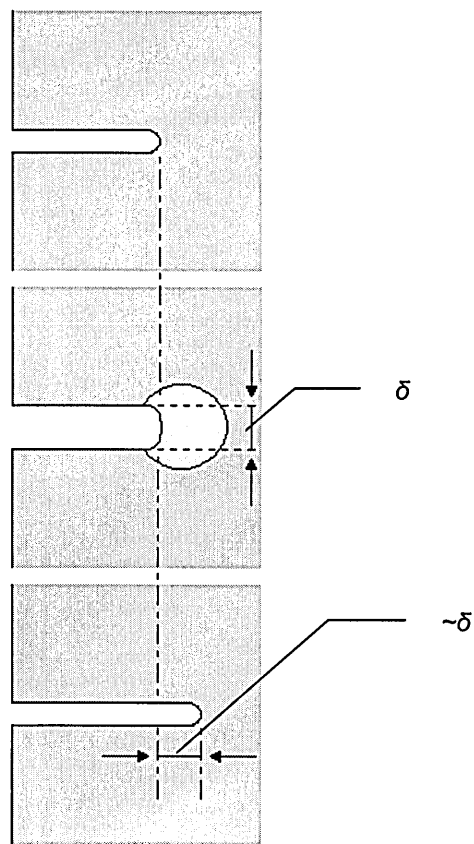
Fig 2.24: Fatigue crack propagation.

Most engineering alloys contain microscopic defects and inclusions within their microstructure. The presence of these defects means that on the application of a stress to a pre-cracked specimen, voids will form around the defects that fall within the plastic zone at the tip of the crack. These voids will link up with each other and with the crack tip, assisting the propagation rate of the crack [32, 35].
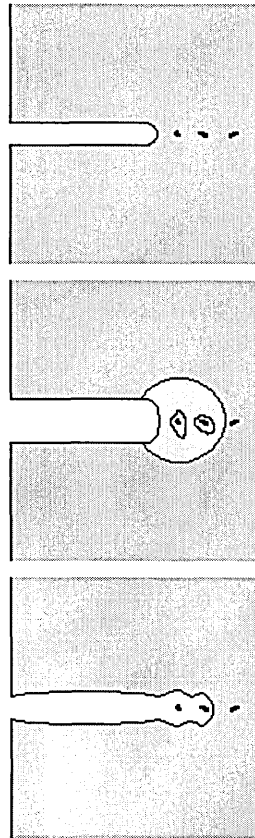
Fig 2.25: Fatigue crack propagation in engineering materials.

The extent to which the processes of crack initiation and crack propagation contributes to the overall fatigue life of a component is mostly down to the components design, particularly its geometry. If the component is relatively smooth and free from notches, or other stress raisers, then a significant proportion of the life is spent initiating the crack. If the component contains a crack or a geometric feature, which is severe enough to create a significant discontinuity in the load supporting ability of the component, then the time spent initiating a crack is negligible and the majority of the fatigue life is spent propagating the crack.

2.3.5: Factors affecting Fatigue Properties.

Many factors can affect the fatigue characteristics of an engineering alloy or component, the majority are linked by their effect on the surface or sub-surface condition of the material [37]. The following section lists and describes the most common factors.

2.3.5.1: Geometrical Factors.

The most important factor that can influence the fatigue properties of an engineering alloy or component is the presence of any cracks, notches or sharp changes in cross section. These discontinuities are often the result of a specific design requirement, but can be more subtly featured in the form of tool and machining marks, scratches, or identification and inspection marks. They can also be caused by damage sustained during manufacture and service life [38, 30]. The presence of a discontinuity, like those described above, can result in the formation of an unbalanced stress field when the component is loaded in a uniform manner. The gap produced by the discontinuities prevents load from being transmitted evenly, this produces regions of elevated stress in the areas adjacent to the discontinuities, which are much greater than the average and nominal stresses across the entire cross section of the component. Therefore, even if the applied stress is far below the yield strength of the material, the presence of a sufficiently severe discontinuity can elevate the stress in a localised area to a level high enough to cause plastic deformation. Such discontinuities are referred to as stress raisers or stress concentrators and they are the most likely origins for fatigue failures [29, 38, 30].
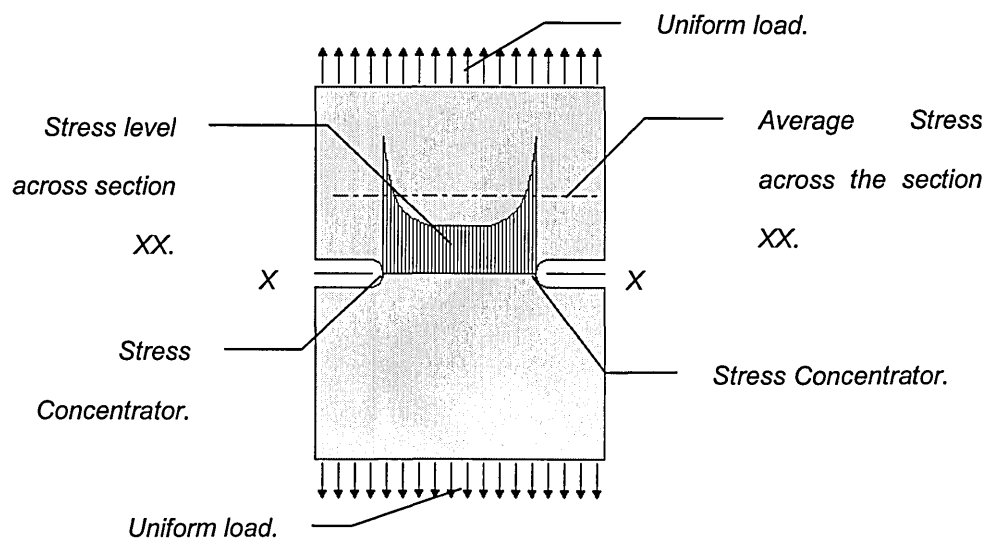
Fig 2.26: The effect of geometric factors on stress levels.

84

2.3.5.2: Environmental Factors: Temperature.

Many engineering components are exposed to extremes of temperature during their service lives, therefore the effect of temperature on the fatigue properties of engineering alloys is of considerable importance. Experiments carried out on various aluminium and steel alloys show that at low temperatures (-50°C) fatigue strengths are as good as, or better than, those achieved at room temperatures (+20°C). High temperatures have little effect up to ~300°C, after which point fatigue strength increases up to a maximum level. Past this point fatigue strength falls rapidly to levels well below that seen at room temperature. At high temperatures materials that previously displayed a fatigue limit at room temperature also tend to lose this attribute. Creep can also become a factor at very high temperatures and often overrides fatigue as the cause of failure [32].

2.3.5.3: Environmental Factors: Corrosion.

The majority of fatigue tests are carried out in air as a reference condition, however, service conditions often involve a corrosive environment that can have an effect on fatigue. Under static loading conditions a corrosive environment does not pose any additional problem if the oxide film present on the material surface prevents further corrosion. During fatigue, the application of a cyclic stress continuously ruptures this film exposing fresh material to the corrosive environment. The presence of an oxide film also assists in the initiation of a crack due to its effect on surface topography and microstructure. Once initiated the resulting stress concentration at the tip of the crack breaks the oxide film, exposing fresh surfaces to the corrosive environment. Once the corrosive medium enters the crack it can also act as a form of electrolyte, with the crack tip becoming an anode from which material is removed. This assists in the propagation rate of the crack, shortening the fatigue life at a given stress [32].

2.3.5.4: Surface Finish and Treatment.

As discussed, the presence of stress concentrators, even those created by minor machining marks, poses the biggest problem to fatigue properties in engineering alloys. Vast improvements can therefore be achieved by polishing any machined surfaces to remove any of these potential crack initiation sites. The introduction of residual compressive stresses on the surface of a metal will also have beneficial effects on fatigue properties, since they will have the effect of closing any cracks that may initiate, meaning larger stresses are required to propagate them. Common methods for achieving this are induction hardening, carburising and nitriding. Residual compressive stresses can also be introduced by physical processes such as shot peening, which also has the added benefit of removing any stress concentrators left by machining marks [32, 30, 33].

2.3.6: Fatigue of Tensile-Shear Spot Welded Joints.

In order to fatigue test TSSW joints, it is appropriate to consider load range, ΔP, rather than a stress range, ΔS. This is because of the difficultly in accurately determining the nugget dimensions without damaging the nuggets.

From a microstructural perspective, the application of a tensile fatigue load, in an axial manner, to a TSSW joint, results in a unique pattern of crack development and growth, leading to either sheet or shear failure, although both failure modes can occur concurrently [25]. Sheet failure begins on the application of the first stress cycle, cracks initiate between the joined sheets at the edge of the diffusion bonded zone, at an angle of 70° to 80° with respect to the direction of applied load [24, 39, 40, 30].
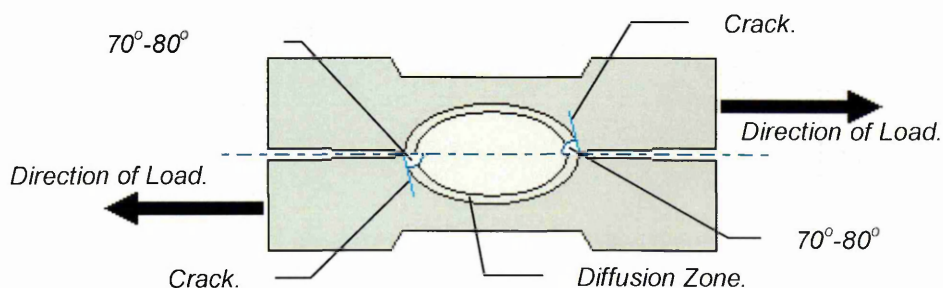
Fig 2.27: Sheet crack initiation.

86

The continued cyclic application of the stress cycle propagates these cracks at a continued angle of 70° to 80°, with respect to the direction of applied load, along the edge of the Heat Affected Zone (HAZ), through the thickness of the sheet, until the cracks breach the external surfaces of the plates [24, 41, 40, 30, 42, 43].
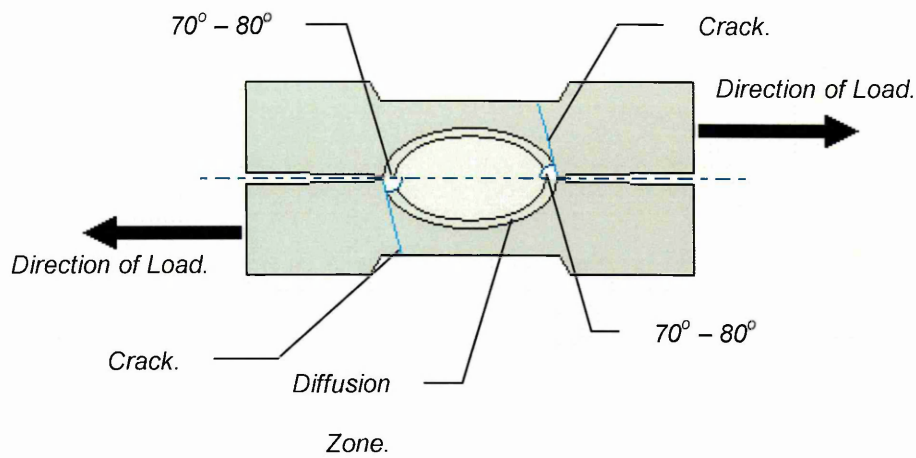
Fig 2.28: Sheet crack through thickness growth.

Once on the surface, subsequent applications of the stress cycle results in lateral propagation of the fatigue cracks across the width of the joint, forming what is known as an 'eye brow' crack [30, 42, 43].
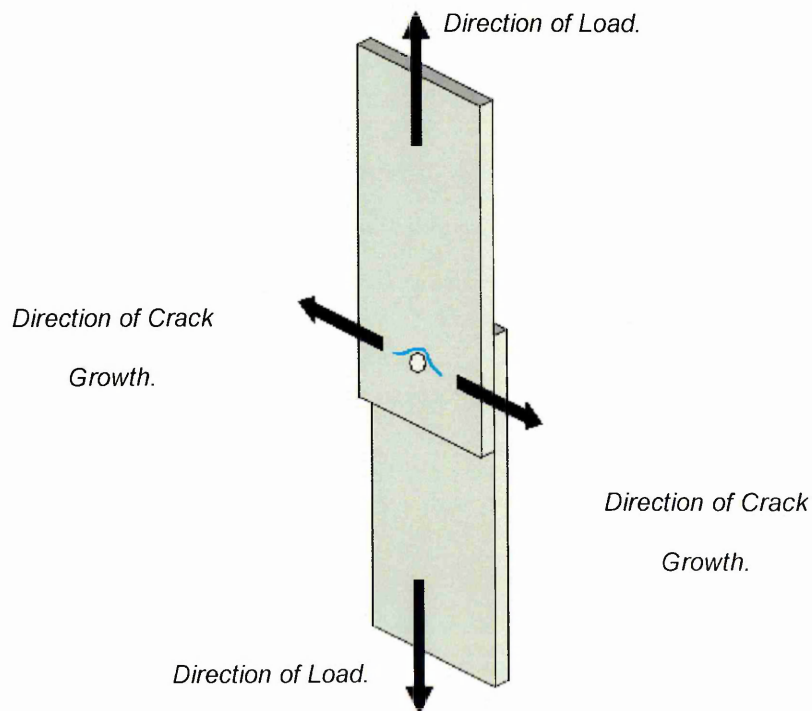
Fig 2.29: Lateral fatigue crack growth.

Crack growth continues in this manner until complete failure occurs when, depending on the width of the specimen, either the crack spans the entire width of the specimen or when the remaining intact material is no longer sufficient to support the applied load and fast fracture occurs by longitudinal tears that originate from the tips of the fatigue cracks.

Shear failure has been shown to compete with sheet cracking and is caused by cracks that initiate at the sides of the spot welds. The cracks advance from both sides of the nugget, perpendicular to the direction of applied load, towards the centre of the nugget. Failure finally occurs by shear overload of the remaining ligaments of the nugget [25].

Direction of Load.

Direction of Crack Growth.

Direction of Crack Growth.

Direction of Load.
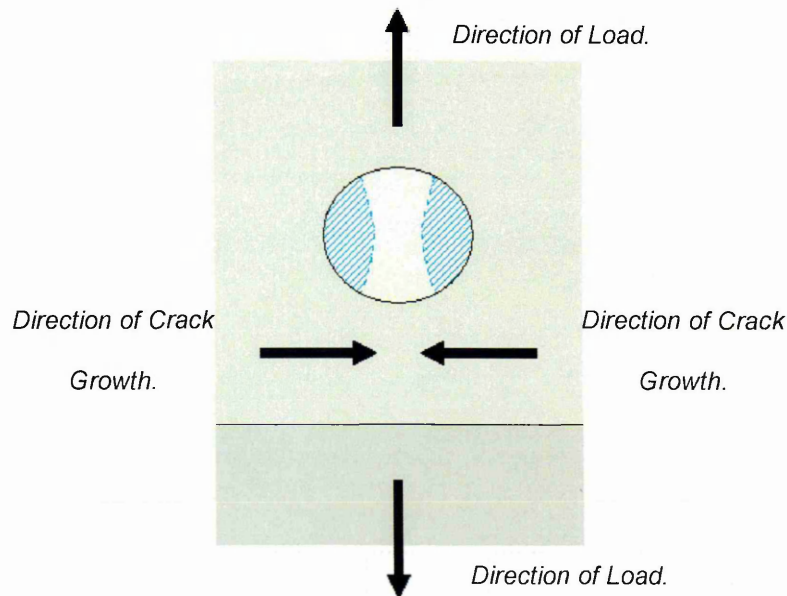
Fig 2.30: Shear fatigue failure.

As mentioned, these cracking modes occur concurrently and compete with one another for dominance [25]; the overriding cracking behaviour that causes final failure is dependant on the dominant mode of loading, which in turn is dependant on the degree of joint rotation.

2.3.6.1: Joint Rotation.

The geometry of a lap joint is such that, when a tensile load is applied, the joint tends to rotate about the weld nugget. This is a result of the eccentric load path, which is caused by the inherent misalignment of the sheets present in a lap joint. When a tensile load is applied, the eccentricity of the load path causes the sheets to separate in an attempt to align themselves and the load path, the higher the load, the more the sheets separate, and the greater the degree of rotation, although, for normal combinations of load and sheet thickness, the rotation rarely exceeds $3°$. In terms of a fatigue test carried out on a given sample, the application of the tensile portion of the stress cycle will result in a degree of joint rotation proportional to the magnitude of the applied tensile load and the ability of the joint to resist rotation[44].
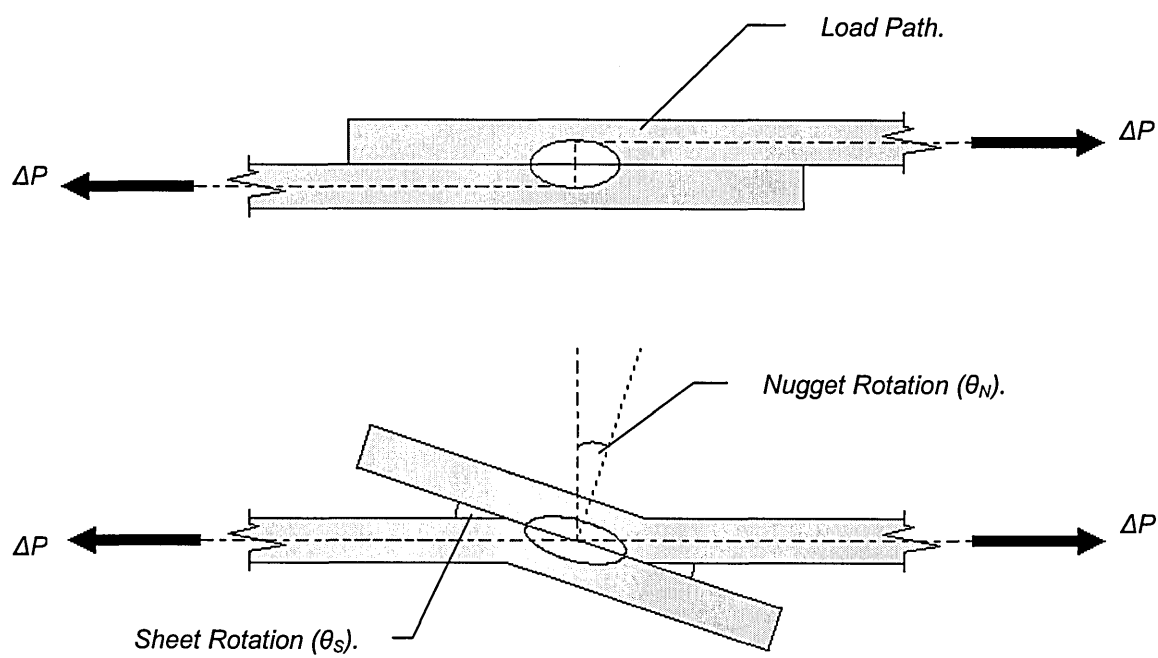
Fig 2.31: Joint rotation in spot welded joints.

2.3.6.2: Loading Modes and Stress Intensity.

As can be seen in Fig 2.31, rotation in this manner changes the mode of loading on the nugget from in plane shear (mode II) to tensile (mode I), hence, joints of this configuration are called Tensile-Shear Spot Welded (TSSW) joints. However, in doing this, the rotation of the joint also results in the application of an out of plane shear stress (mode III). This creates a complex loading regime in which all three modes of loading are acting upon the nugget at various points of each stress cycle.
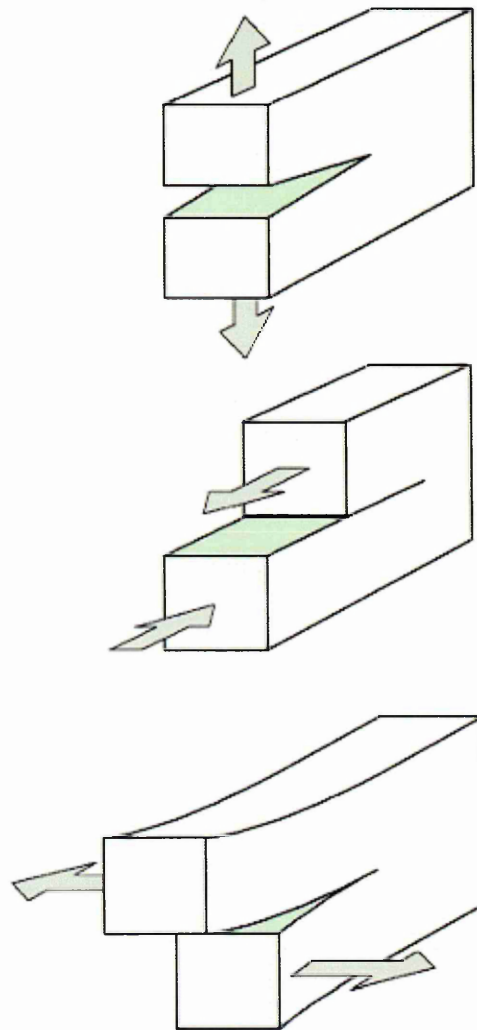
Fig 2.32: The three modes of loading [48].

Due to the geometrical changes in the cross section of a spot welded joint, a crack-like notch is created at the edge of the diffusion bonded zone of the weld nugget [24, 41, 39]. The location and severity of this notch results in a significant discontinuity when a tensile load is applied, which is sufficient to cause rotation of the joint. This results in regions of concentrated stress, which can be summarised in terms of the stress intensity factor, K.

On the application of a tensile load that is just below the minimum magnitude required to cause rotation, the shear stress intensity factor, K_{II}, reaches a maximum value at point A of the weld nugget, as shown in Fig 2.32 below. Once the load is high enough to cause rotation, the separation of the sheets increases the tensional stress intensity factor, K_{I}, at point A of the weld nugget, until maximum rotation for the applied load is achieved, at which point K_{I} also reaches a maximum value at point A. During this transition from zero rotation to full rotation the out of plane shear stress intensity factor, K_{III}, reaches a maximum value at point C of the weld nugget, which is also shown in Fig 2.33.

(reverse side of joint).

(reverse side of joint).
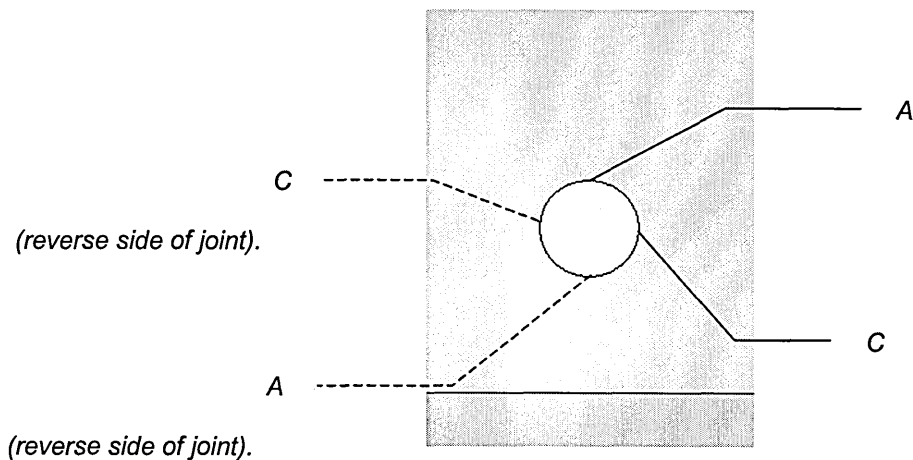
Fig 2.33: Sheet and Shear failure initiation sites.

As would be expected, sheet cracking is governed predominantly by the tensile mode of stress and therefore initiates where K_I attains a maximum value. Shear cracking however, is governed by the out of plane shear mode of stress and so initiates at the point where K_{III} reaches a maximum value [25, 45]. Cracking in a given mode can only occur if the stress intensity factor for that mode exceeds a minimum value, known as the threshold stress intensity factor, K_{TH}. The speed at which a crack then propagates is dependant upon how much the stress intensity factor, for that mode, exceeds the value for K_{TH}. Therefore, the dominant mode of failure is dependant on the dominant mode of stress intensity. Since the magnitude of K_I is a product of the amount of joint rotation, joints that rotate easily tend to fail through sheet cracking. However, in joints that are more resistant to rotation, K_I is unable to attain such a high value, which leaves K_{III} as the dominant stress intensity factor. Therefore stiffer joints tend to fail by shear cracking. [25, 45].

In joints that exhibit a small amount of joint rotation, both types of cracking can occur simultaneously [46], since both of these stress intensity factors attain maximum values at different points in the stress cycle. The propagation of a crack by one of the modes also aids in increasing the level of stress intensity in that mode. Hence, in joints where both modes of cracking occur concurrently, they compete with one another for dominance.

92

2.3.6.3: Fatigue Testing of Multi-Spot Welded Joints.

In this investigation the multi-spot welded joints tested are arranged into a single row of welds, made perpendicular to the direction of applied load, with each spot weld supporting an equal portion of the overall applied load. In this arrangement the fatigue crack behaviour of multi-spot welded joints is nearly identical to that of single welded joints. Linder and Larsson [47] demonstrated this by testing ten nugget multi-spot welded 'H' specimens, which are illustrated below.
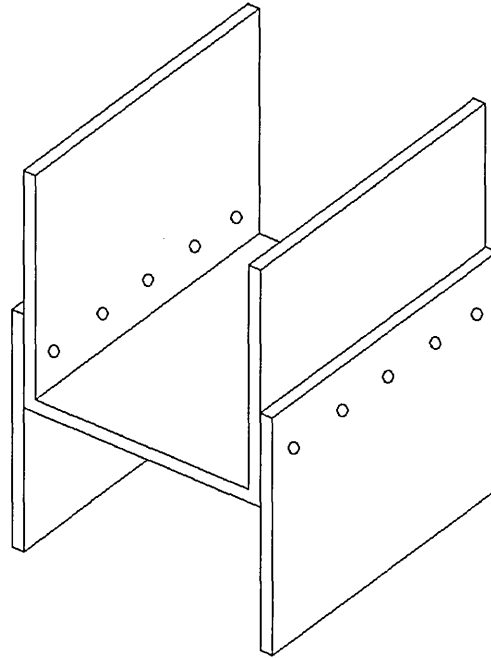
Fig 2.34: Multi-spot welded 'H' specimens.

The specimens tested in the Linder and Larsson study displayed welds with cracks that all started at the edge of the diffusion bonded zone, before propagating at an angle of ~70° through the sheet thickness, towards the outside surface. Once on the surface each of these cracks grew laterally, away from the spot welds, in exactly the same manner as described earlier for single welded joints. The only difference with multi-spot welded joints is that complete fracture occurs when all the lateral cracks have reached a sufficient size to coalesce into one single crack that spans the entire specimen width.

Since these cracks were observed in all the welds it can be assumed that each spot weld supported an equal portion of the overall load. Furthermore, examination of the supplied images, which are shown below in Fig 2.35, indicates that when fracture finally did occur, the individual cracks above each of the spot welds where of a similar size, suggesting that the equal loading conditions were maintained for the entire duration of the test.
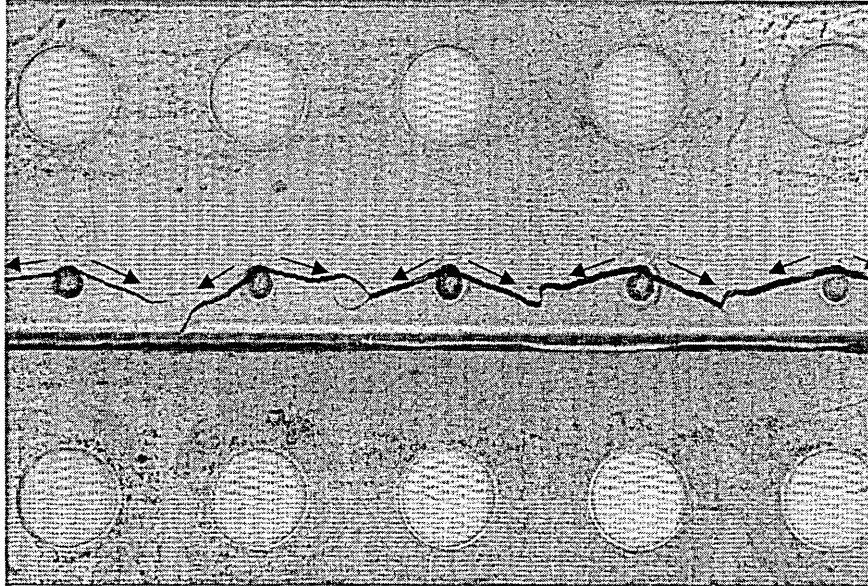
Fig 2.35: Final crack size and direction of propagation in multi-spot welded H specimens.

Although the geometry and arrangement of these specimens differs from those used in this investigation, the principles are the same, in that the welds were arranged in a single 'effective' row, perpendicular to the load path, with each one supporting an equal portion of the overall load. The failure characteristics of the tests carried out in the Linder Larsson study can therefore be expected to be very similar to those displayed in this study.

2.3.7: Models for Predicating Fatigue Behaviour in Spot Welded Joints.

As discussed in Section 2.3.2, components that contain existing cracks, or severe defects, such as TSSW joints, have fatigue lives that are governed by the propagation rate of the crack. In this type of situation a fracture mechanics approach can be used to predict the subsequent growth rate of the crack. Since the time taken for crack initiation in such components is negligible, the predictions for the growth rate of the crack will also reflect on the total fatigue life of the component at a given level of cyclic stress [32].

As mentioned, the state of stress in the vicinity of a crack can be expressed in terms of the stress intensity factor, K, which is a function of the size of the crack, the stress acting upon it and a geometric correction factor [35, 32, 48].

$$K = Y\sigma\sqrt{(\pi a)} \quad \textit{Eq. 2.3}$$

Where:

K = *Stress intensity factor.*

Y = *The geometric correction factor.*

σ = *The applied stress.*

a = *The length of the crack.*

However, in fatigue, K varies over a stress intensity range, ΔK, between S_{min} and S_{max}.

$$\Delta K = K_{max} - K_{min} \quad \textit{Eq. 2.4}$$

$$\Delta K = Y(S_{max} - S_{min})\sqrt{(\pi a)} \quad \textit{Eq. 2.5}$$

The calculated value for ΔK can be related to the crack growth rate during a given set of cyclic loading conditions by several different expressions. The most common of these is the Paris-Erdogan equation, which stipulates [32, 31, 49, 50]:

$$\frac{da}{dN} = C(\Delta K)^m \quad Eq.\ 2.6$$

Where:

$\frac{da}{dN}$ =   *The crack growth rate represented as the change in crack length, a, over the change in the number of cycles, N.*

C =   *Material constant.*

m =   *Material constant.*

ΔK =   *Stress intensity range.*

Of course, as the crack increases in size the value of ΔK will also increase, so the crack growth rate will vary throughout the fatigue process. This variation is illustrated below in Fig 2.36 [32].
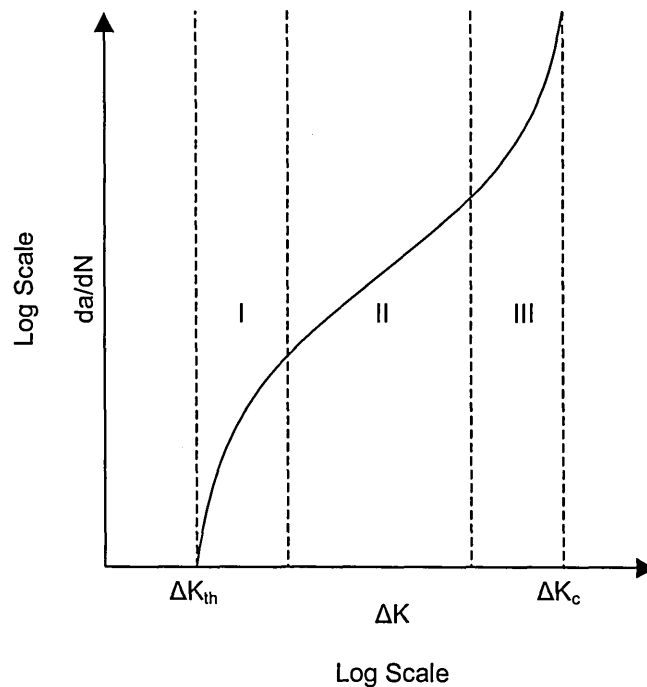
Fig 2.36: Variation in fatigue crack growth rate.

From Fig 2.36, three distinct regions of crack growth can be seen. The first region, Region I, begins at the threshold value of stress intensity, ΔK_{TH}, below which crack propagation does not occur, and continues until the slope of the curve becomes constant [51, 32].

The steep gradient seen in Region I is also exhibited in the third region, Region III, where the crack growth rate tends towards an infinitely large value, increasing the values for K_{min} and K_{max}. Failure finally occurs by fast fracture either when the value for K_{max} exceeds the fracture toughness of the material, K_{IC}, or when the remaining ligament of material, ahead of the crack, fails by plastic collapse [51, 32].

The second region of crack growth, Region II, represents the zone in which the growth rate is effectively linear and fatigue crack growth can be represented by the Paris-Erdogan equation. The fatigue life of most engineering components may be considered solely in this range, once allowance has been made for the minimum crack length employed, which is normally related to the limitations of a particular inspection technique or design code requirement [51, 49].

Since the Paris-Erdogan equation expresses the rate at which a fatigue crack will grow under a set of given cyclic stress conditions, it can be used to determine the fatigue life before the crack reaches such a size that failure will occur on the next applied stress cycle [32, 51].

If the initial size of the crack is denoted a_o, then the number of cycles, N_f, until the crack reaches a critical size, a_f, such that failure occurs on the application of the next stress cycle, can be obtained by substituting Equation 2.3 into the Paris-Erdogan equation and integrating the resulting equation [32, 51, 49].

$$\frac{da}{dN} = C\left[Y\Delta S\sqrt{(\pi a)}\right]^m \qquad Eq.\ 2.7$$

Integrated:

$$N_f = \frac{2}{C(Y\Delta S)^m \pi^{m/2}(2-m)}\left(a_f^{1-m/2} - a_o^{1-m/2}\right) \qquad E.q.\ 2.8$$

In practice it has been found that the mean stress intensity also affects the growth rate of the crack. High mean stress intensity indicates raised levels of S_{min} and S_{max}, leading to levels of S_{max} that approach the yield strength of the material, which inevitably increases the crack growth rate [32, 51].

As mentioned, the geometry of a TSSW joint lends itself well to a typical pre-cracked, or notched, fatigue specimen, meaning a negligible amount of time is spent initiating a crack. Therefore, a fracture mechanics approach, similar to that already described, can be used to predict the fatigue life of TSSW joints [26]. However, the cracking behaviour of a TSSW joint is not as straight forward as a typical notched fatigue specimen and determining values for stress intensity factors can be difficult, therefore little work has been done in this area [52].

The majority of work has been carried out by Pook, who derived expressions to describe the stress intensity factors in TSSW joints using relationships developed by Paris, Sih and Kassir. Pook arrived at the following expressions for circular connections between sheets [52, 45]:

$$K_I = \frac{P}{\left(\frac{d}{2}\right)^{3/2}} \left(0.341 \cdot \left(\frac{d}{t}\right)^{0.397} \right) \qquad \text{when: } \frac{d}{t} \leq 10 \quad Eq.\ 2.9$$

$$K_{II} = \frac{P}{\left(\frac{d}{2}\right)^{3/2}} \left(0.282 + 0.162 \cdot \left(\frac{d}{t}\right)^{0.710} \right) \quad \text{when: } 1.92 \leq \frac{d}{t} \leq 10 \quad Eq.\ 2.10$$

$$K_{III} = \frac{P}{\left(\frac{d}{2}\right)^{3/2}} \left(0.282 + 0.162 \cdot \left(\frac{d}{t}\right)^{0.710} \right) \quad Eq.\ 2.11$$

Where:

P   =   *The applied load per spot weld.*

d   =   *The diameter of the weld nugget.*

t   =   *The thickness of the sheets to be joined.*

These expressions apply to single spot welded joints or joints containing a single row of spot welds, arranged perpendicular to the direction of applied load [52].

For connections comprising of single spot welded joints or joints containing a single row of spot welds, arranged perpendicular to the direction of applied load, values for K_I, K_{II}, and K_{III} can also be expressed in terms of the average shear stress on the connection at the points where the stress intensity factors peak (point A, Fig 2.32, for K_I and K_{II} and point C, Fig 2.32, for K_{III}) [52].

$$K_I = \tau \left(\frac{\pi d}{2}\right)^{\frac{1}{2}} \left(0.605\left(\frac{d}{t}\right)^{0.397}\right) \quad Eq.\ 2.12$$

$$K_{II} = \tau \left(\frac{\pi d}{2}\right)^{\frac{1}{2}} \left(0.5 + 0.287\left(\frac{d}{t}\right)^{0.710}\right) \quad Eq.\ 2.13$$

$$K_{III} = \tau \left(\frac{\pi d}{2}\right)^{\frac{1}{2}} \left(0.5 + 0.287\left(\frac{d}{t}\right)^{0.71}\right) f\left(\frac{d}{w}\right) \quad Eq.\ 2.14$$

Where:

τ = *The average shear stress.*

d = *The diameter of the weld nugget.*

t = *The thickness of the sheets to be joined.*

$f\left(\dfrac{d}{w}\right)$ = *Equation 2.16:* $\dfrac{\pi d}{4w}\tan\left[\left(\dfrac{\pi}{2}\left(1-\dfrac{d}{2w}\right)\right)\right]^{\frac{1}{2}}$

w = *Half the specimen width for single spot welded joints or the pitch distance for multi-spot welded joints.*

However, in deriving these expressions two assumptions are made, namely:

- Stress intensity ratios for elliptical connections between half spaces also apply to circular connections between sheets.

- No rotation of the joint occurs as the load is increased.

These expressions are therefore very restrictive, both in the type of joint they cover and in that they do not take account of the changes in the stress intensity factor occurring due to rotation of the joint when the load is increased [52, 45].

To overcome this, and the difficulties of determining stress intensity factors that take account of all the geometric factors of a spot welded joints Davidson proposed a relationship between the fatigue properties and the stiffness of the joint. Davidson suggests that the separation between the sheet surfaces, caused by the rotation of the joint, when a static load, proportional to the fatigue load, ΔP, is exerted upon the joint, can be correlated to the Crack Tip Opening Displacement (CTOD) of the growing fatigue crack, which in turn can be correlated to ΔK [45, 52].

This is done by assuming that the angle of nugget rotation, $\Delta\theta_N$, is proportional to the CTOD, and since ΔK is proportional to $\sqrt{\text{CTOD}}$, ΔK is also proportional to $\sqrt{\Delta\theta_N}$. The resulting model is shown below [45, 52]:

$$N_f = A(\Delta E)^{-3} \quad Eq.\ 2.15$$

Where:

N_f =   *The fatigue life [cycles].*

A =   *Constant, 1.84×10^{15} [cycles.$(N.deg^{1/2}/mm)^3$].*

ΔE =   *A quantity referred to as the cyclic energy, which is calculated as follows:*

$$\Delta E = \frac{\Delta P \Delta\theta_N^{1/2}}{t} \qquad Eq.\ 2.16$$

Where:

ΔP =   *The fatigue load [N].*

$\Delta\theta_N$ =   *The angle of rotation at ΔP [deg].*

t =   *The sheet thickness [mm].*

The limitations of attempting to analytically determine the stress intensity factor in order to predict fatigue properties can therefore be circumvented by experimentally determining $\Delta\theta_N$ [45, 52].

Davidson's model works well with TSSW joints as they rotate about the region of highest stress concentration when a tensile load is applied. However, in reality, spot welded joints are produced in a variety of configurations which have different loading arrangements, only a fraction of which are subject to rotation.

A more general model that uses a fracture mechanics approach is proposed by Linder, Larsson and Bergengren. Their model takes account of all three stress intensity modes that can act upon a spot welded joint during fatigue, depending on its geometry and the direction in which the load is applied. The resulting model is based on the summation of the three stress intensity factors to produce an effective stress intensity factor, based on the most dominant mode of stress. This model is therefore applicable to a variety of joint configurations that use different loading arrangements and can therefore be used to describe the fatigue strength of a spot welded joint, regardless of its geometry or loading mode [53, 43].

2.3.8: Factors Effecting Fatigue Properties of TSSW Joints.

Studies have shown that for a given fatigue test procedure, load and cycle life, the fatigue properties of as-welded TSSW joints are dependant on joint design rather than the strength of the base material [41, 54, 55, 56]. Several investigations have been carried out examining the effect of increasing the tensile strength of the base material on the fatigue properties of TSSW joints. The consensus is that increasing the base material strength results in improved fatigue life only for short cycle lives ($<10^4$). This would support the opinion that fatigue life is mainly occupied by crack propagation rather than crack initiation [24, 41, 30, 55, 43]. However, this would be expected since a sharp crack-like notch is already present in the most highly stressed region at the edge of the diffusion zone [24, 30, 43].

Generally it has been found that varying a parameter such that the fatigue life of a TSSW joint increases also brings about a reduction in the amount of joint rotation, and vice versa [24, 30, 54, 55]. This has led to the acceptance of a joint parameter, which is a measure of the resistance of the joint to rotate under load. This parameter is simply defined as the amount of joint rotation (either sheet, $\Delta\theta_S$, or nugget, $\Delta\theta_N$,) per unit of fatigue load, ΔP, and is referred to as joint stiffness.

The parameters that have been found to have the greatest influence on the stiffness of a TSSW joint, and hence fatigue properties, are all related to joint design or joint geometry [24, 41, 54, 55]. The following sections give details of the most common parameters:

2.3.8.1: Sheet Thickness.

Normally, as the thickness of the sheet increases, the size of the spot weld required to satisfactorily join the sheets increases proportionally. As such examining the effect of only altering sheet thickness can be difficult as there are limits on the sheet thickness that can be satisfactorily welded with a given weld diameter. After this point the nugget becomes too small to support the joint. However, experiments examining the effect of increasing only the thickness of the sheet on the fatigue life of a joint have shown that increasing the thickness of the sheets in a TSSW joint increases the joint stiffness, and hence, the fatigue life at a given fatigue load [24, 55, 44].

inches
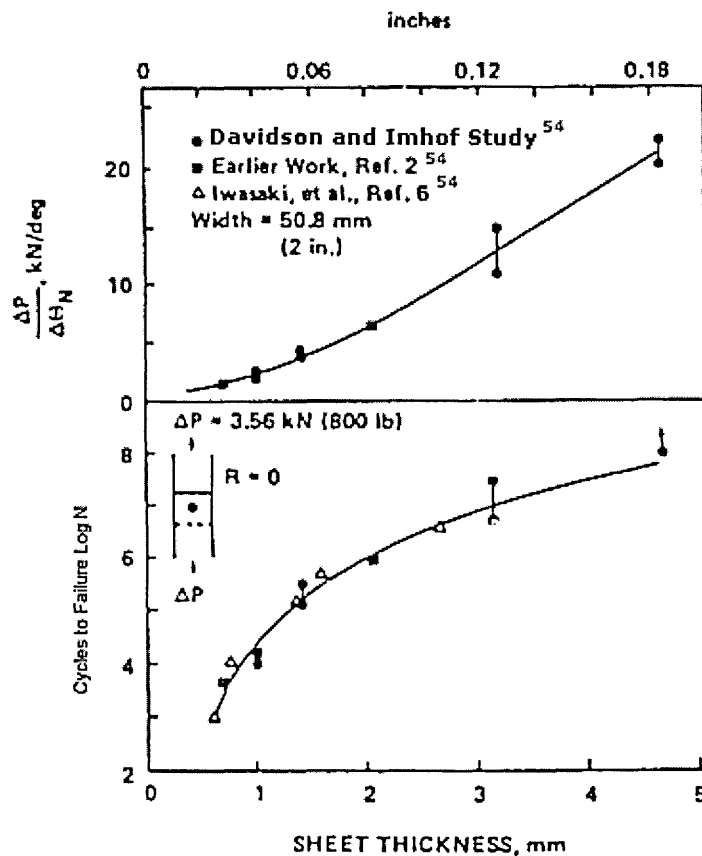
Fig 2.37a: The effect of sheet thickness on joint stiffness (top) [55].

Fig 2.37b: The effect of sheet thickness on fatigue life (bottom) [55].

2.3.8.2: Weld Nugget Size.

Increases in weld nugget diameter have been demonstrated to give an increase in the stiffness of a TSSW joint, and hence, an increase in the fatigue properties [25, 56], although the effect is not as prominent as the effect of increasing sheet thickness [55]. There is some evidence to suggest that the effect of increasing weld diameter can only be seen in the short life regime, in the longer life regime (cycles >10^6) the effect of increasing weld diameter can diminish [24].
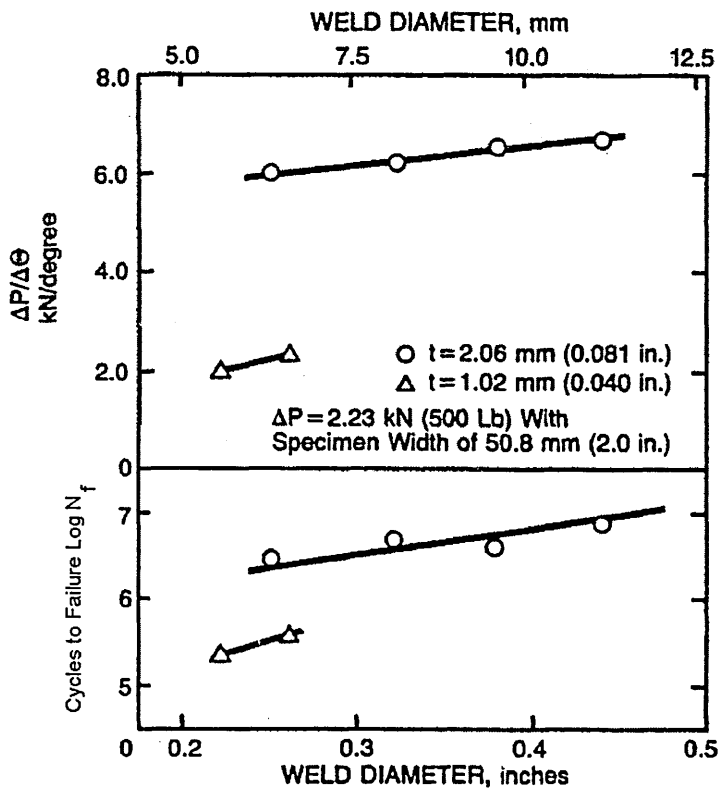
Fig 2.38a: The effect of spot weld diameter on the joint stiffness (top) [25].

Fig 2.38b: The effect of spot weld diameter on Fatigue life (bottom) [25].

It has also been shown that the combined effects of increasing the sheet thickness and spot weld size on the fatigue properties of a TSSW joint are greater than the sum of their individual benefits [24].

105

2.3.8.3: Specimen Width.

Orts [54] has reported that a reduction in sample width will have a detrimental effect on the fatigue properties of TSSW joints, particularly in the high cycle regime.
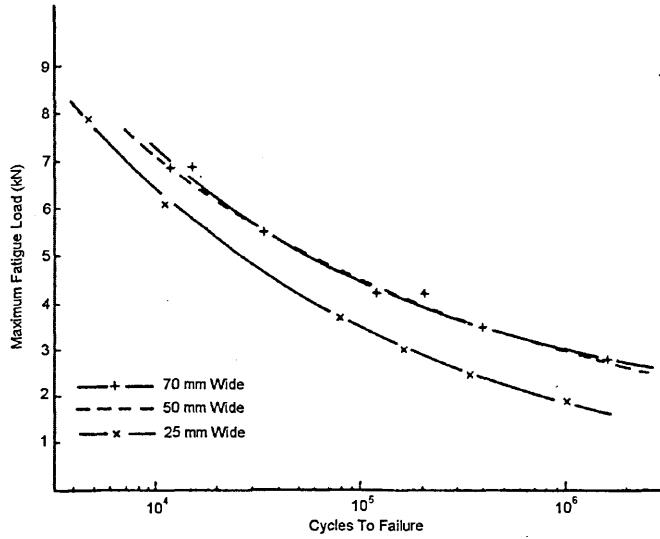
Fig 2.39: Effect of sample width on fatigue strength.

Davidson [25] also reports a similar effect with regards to joint width and fatigue properties, but also noted the corresponding increase in joint stiffness with increased joint width.
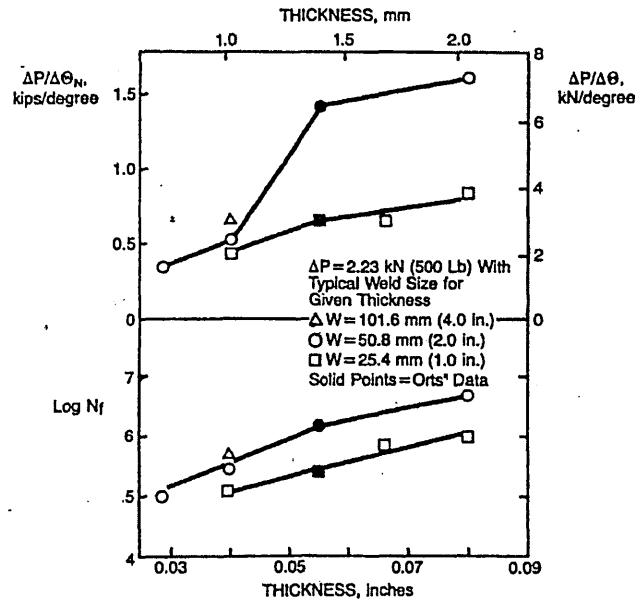
Fig 2.40: Effect of sample width on joint stiffness (top) and fatigue life (bottom).

The improvement in fatigue performance obtained through increasing the specimen width is also reported by British Steel Technical [43].

2.3.8.4: Edge Distance.

Davidson [25] reported that as the edge distance of single, double, and triple weld joints decreases, the fatigue life per weld also decreases. Davidson reported that this decrease in fatigue performance is related to a complex interaction between an increase in rotation, due to a decrease in stiffness, and a decrease in the torsional stress intensity factor, K_{III}, as the edge distance decreases [25]. With respect to the single weld specimen, the decrease in edge distance would also mean a decrease in the specimen width, which has already been confirmed by other sources [54], to reduce joint stiffness, and hence, fatigue properties.

2.3.8.5: Pitch Distance.

There is some evidence to suggest that the spacing between individual welds has an effect on the fatigue properties of a multi-spot welded joint made with a single row of welds at right angles to the direction of applied load. Davison, Soto et al. [25] have each performed experiments recording the fatigue performance of various multi-spot welded joints made using a single row of welds at different pitch distances. The results suggest that as the pitch distance increases the fatigue performance of the joint increased. However, although both compared joints containing the same number of welds they also kept the width of the joint constant. This would mean that as the pitch distance increased the edge distance would decrease. Therefore it could be that the results of these experiments are affected by the drop in edge distance at increased pitch distances. This is acknowledged by Davidson in the discussion of his results [25].

2.3.8.6: Non Geometric Factors.

In addition to the geometric factors that affect the fatigue performance of a joint for a given fatigue test, load, and cycle life, other parameters can be altered to manipulate the response of a TSSW joint. For example, if the stress ratio or R value is lowered to below $R = 0$, then it would mean that the joint was being exposed to compressive loads on the lower portion of the stress cycle. Since fatigue life of TSSW joints is purported to be governed by crack growth, exposing the joint to a compressive load may lead to crack closure, which will prolong the fatigue life. Experiments have shown that if two joints are exposed to the same fatigue load range, ΔP, but one was tested with a negative R value and one with a positive R value, comparison of these two joints would suggest superior properties in the joint tested using a negative R value, since crack closure would have retarded crack growth [24].

A second factor worth considering is that of the state of any residual stress indicative of any welding process. Tests carried out by Overbeeke and Draisma [24] showed that in joints that had undergone a stress relieving process the R value could be as high as $R = 0.1$ before crack closure no longer occurred. However, joints that were in the "as welded" condition still contained enough tensile residual stresses to maintain an open crack even at R values as low as $R = -1.0$.

2.3.9: Defining Fatigue Failure in TSSW Joints.

It was established in Section 1.2 that in order to test the proposed theory the definition of a fatigue failure had to be constant for both single and multi-spot welded joints and that failure had to be defined as the point where an individual spot weld was no longer supporting an equal portion of the overall load. Due to the sheet thickness and simplicity of the joints used in this project, a significant amount of joint rotation occurs under the application of a tensile load. For this reason sheet cracking is the dominant failure mechanism for both the single and multi-spot specimens. It is therefore necessary to consider failure in terms of the various stages of sheet cracking rather than shear cracking.

Many ways currently exist for defining the fatigue failure of a TSSW joint by the mechanism of sheet cracking, most of which centre around the different stages of growth of the lateral crack seen in the later stages of the fatigue life of TSSW joints. It would therefore seem logical to examine these existing methods and use or adapt one so that it can be easily applied to testing multi-spot welded joints.

Generally, manufacturers prefer a conservative definition of fatigue failure in TSSW joints, by defining it as the point where the crack has penetrated the external surface of the joint and is about to commence lateral propagation. Davidson and Imhof used this approach and defined fatigue failure as the point at which a 'thumb nail' crack was observable on the exterior of the specimen[26].

Conversely, Orts, Wilson and Fine defined failure as a certain increase in the displacement, or stroke, of the fatigue testing equipment, which corresponded to the presence of a surface crack which stretched almost the entire width of the specimen. Cooper and Smith also defined failure as the point when the lateral crack had caused the virtual separation of the two sheets comprising the TSSW joint[26].

The conservative approach, although more widely recognised by industry, is difficult to determine and is open to the biases of the operator. However, since the equipment is operating in load control, defining failure as a surface crack, which almost stretches to a length of one spot pitch, allows for the use of automatic machine trips, which are monitoring the stroke of the actuator. Once the crack reached a certain length the corresponding decrease in specimen stiffness would cause an increase in machine stroke, which could be set to automatically stop the machine. Defining fatigue failure as the point when a surface crack reaches 1 spot pitch in size is also a more practical approach to apply to multi-spot welded joints as it allows for easier monitoring. Initial testing of example multi-spot welded joints of the configuration used in this study showed that the growth rate of the all the cracks was reasonably constant up until the instant before complete fracture. This would suggest that categorising a fatigue failure as the point when a single fatigue crack spanned a length equal to one pitch distance would stop the test before the load supporting ability of the individual spot welds present in the joint became unbalanced. This would maintain the required condition of keeping the survival probability of the individual spot welds in a multi-spot welded joint as statistically independent events.

2.3.10: Summary of Fatigue of TSSW Joints.

Control of the fatigue testing process will be an important factor in this investigation. Accurate measurement and communication of the loads being applied to the specimen will improve the accuracy of the resulting data and help identify previously unaccounted factors. With respect to the testing equipment, the jaws will be a critical component in helping to maintain the second and therefore third boundary condition. They need to be able to maintain rigidity in the load train, especially for the larger multi-spot welded joints. They also need to support and distribute load evenly across the entire specimen width throughout the test if the second and third boundary conditions are to be maintained.

As mentioned, the requirements of the fourth boundary condition regarding fatigue failure can best be met by defining fatigue failure as a surface crack of a critical size. Such a condition will be easy to monitor for the single spot welded joints and the most practical with respect to the multi-spot welded joints.

Through past studies, the criticality of joint geometry and its affect on the fatigue behaviour of joints similar to those used in this study has been thoroughly explored. Therefore, in order to maintain the first boundary condition it is critical that single spot weld joints are geometrically identical to the individual spot welds in the multi-spot weld specimens, thus ensuring a proportional effect on joint stiffness and therefore fatigue properties.

2.4: EN AISI 301 Austenitic Stainless Steel.

As discussed in Section 2.3.8, the base sheet properties has little effect on the behaviour of a TSSW joint in terms of fatigue, however, an understanding of the material is required in order to produce a reliable and consistent welding schedule for producing welds of adequate mechanical strength.

The material chosen for this project is 1mm thick, quarter hardened, EN AISI 301 austenitic stainless steel sheets. AISI 301 is a high strength steel, available in strip and wire form with a tensile strength of up to 1800 MPa [57]. It has excellent heat and corrosion resistance and is commonly used for decorative features, such as automotive trim and finishes on kitchen equipment [58], although its ability to retain ductility in up to the half hardened condition make it a choice material to be rolled or brake formed into aircraft, architectural, and rail car structural components [57].

C	S	Mn	Cr	Si	Ni	P
0.15 Max	0.030 Max	2.00 Max	16.00 -18.00	0.1 Max	6.00 - 8.00	0.040 Max

Table 2.1: AISI 301 ¼ Hardened Chemical Data [58, 59].

Tensile Strength (MPa) min	860
Yield Strength 0.2% Proof (MPa) min	515
Elongation (% in 50mm) (thick.>0.76mm) min	25

Table 2.2: AISI 301 ¼ Hardened Mechanical Data [57].

Density (kg.m^{-3})	8000
Elastic Modulus (GPa)	193
Mean Coefficient of Thermal Expansion 0 - 538 C^{o} (μm.m^{-1}.C^{o-1})	18.2
Thermal Conductivity @ 500 C^{o} (W.m^{-1}.K)	21.5
Electrical Resistivity (nΩ.m)	720

Table 2.3: AISI 301 ¼ Hardened Physical Data [57].

2.4.1: Resistance Weldability of AISI 301.

Welding of austenitic stainless steels is relatively simple, and in most cases the welding procedure for various resistance welding processes is comparable to that used for welding mild steels. However, there are several areas of importance that the operator should be aware of when optimising the welding process [61].

The optimum electrode force will be considerably higher than that required for resistance spot welding mild steels. This is due to the overall higher strength and hardness of austenitic stainless steel and its tendency to retain their strength at elevated temperatures. These higher mechanical properties mean that more force is required to maintain an intimate contact between the faying surfaces at the location of the weld. It is recommended that in order to obtain good results the electrode force should be 2 to 3 times higher than that used for welding similar thicknesses of mild steel [61, 60].

The higher electrical resistance of austenitic stainless steel, compared to mild steels, means that more heat can be generated for a given magnitude of current. Therefore, the optimum welding current for spot welding austenitic stainless steels will generally be slightly lower than that required for welding similar thicknesses of mild steel [61, 50, 60].

The thermal conductivity of stainless steel is much lower than that of mild steel and when localised heating occurs, such as that found when producing a spot weld, the thermal gradient of the weld zone and surrounding material is very steep. As a result the quality of the welds produced in stainless steel is very sensitive to variations in the welding parameters and conditions. Therefore the operator needs to be mindful of the control and consistency of the welding process, particularly when multi-spot welded joints are being produced [61].

The coefficient of thermal expansion of austenitic stainless steels is considerably higher than that of mild steel, this combined with the poor thermal conductivity, and therefore highly localised heating around the individual spot welds, can lead to large amounts of distortion and stress as a result of weld shrinkage on cooling. To minimise these stresses, allowances must be made in the initial joint design to compensate for any shrinkage by limiting the size of the individual nuggets. Generally, the upper safe limit for the nugget diameter is 4 to 5 times the thickness of the thinnest sheet to be welded, and if necessary the use of many smaller sized spot welds is preferred to a few larger sized ones [61, 60].

2.4.2: Weld Quality.

The appearance of spot welds made in austenitic stainless steel is normally of a high standard. However, discolouration of the base material in the HAZ can be unsightly for some applications. If discolouration is occurring, it can be prevented by maintaining the electrode force until the weld has cooled to below the oxidisation temperature. If slight discolouration still persists it can be removed by cleaning with powdered pumice, scrubbing with alkali cleansers, or by brief immersion in a room temperature solution of 10% nitric acid and 2% hydrofluoric acid or 50% hydrochloric acid [62].

The consistency of the welds produced is most easily measured by analysing the internal structure of the nugget and measuring the depth of fusion and nugget diameter. The weld nugget diameter and depth of fusion can be measured by cutting through the centre of the weld, mounting the specimen, and after sufficient grinding and polishing, etching in a hot solution of 20% nitric acid plus 5% hydrofluoric acid. This process will clearly outline the edge of the nugget, allowing the diameter and depth of fusion to be measured when examined under a microscope. Alternatively an electrolytic etch using a 10% solution of oxalic acid has shown to have a similar effect. This process will also reveal the presence of any blow holes or cracks, indicative of a poor weld. Ideally the weld nuggets should be free from any form of cracking and porosity, although generally, a small amount of porosity can be tolerated [62].

2.4.3: Summary of EN AISI 301 Austenitic Stainless Steel.

Although the properties of the base material will have little effect on the fatigue properties of the joints used in this investigation it will have a significant affect on the properties of the welds produced. Particular attention will therefore need to be paid to the control of the welding parameters and conditions to help minimise variation and maintain the first boundary condition. The poor electrical conductivity of EN AISI 301 austenitic stainless steel will go some way to help minimise the effect of current shunting on nugget consistency by limiting any viable alternate current paths through any existing welds when producing the multi-spot welded specimens.

The distortion that is likely to be caused, particularly when producing the multi-spot specimens, is of concern as it will vary depending on the number of welds present and the size of the joint. This will introduce differing amounts of residual stresses into each of the different sized joints produced in this investigation, which could result in an unbalanced fatigue load, particularly in the larger multi-spot welded specimens, which contravenes the first boundary condition. Procedures for limiting residual stress, or at least maintaining a balance of residual stress across all specimens, will therefore be required.

3. Methodology.

It has been established that the main tasks for confirming the proposed theory, discussed in Section 1.1, will be accomplished by using a comprehensive fatigue testing schedule comprising of Staircase and Probit testing processes. However, in order to establish a baseline, and to ensure that the specimens comply with the boundary conditions set out at the start of the project, it is also necessary to carry out a basic mechanical properties check on the supplied material as well as a weldability study and an optimum pitch distance investigation first.

Since weld consistency is of paramount importance in this investigation, a weldability study into the quality and repeatability of welds produced using various values of spot welding variables was carried out in order to find optimum parameter levels that would produce both consistent and strong welds. The need for consistency between welds made in the multi-spot welded joints also prompted an investigation into the effect of current shunting on weld consistency. If the effects of current shunting are not accounted for then the consistency of welds made in the multi-spot welded joints would be jeopardised, which would disassociate any of the data collected from supporting or disproving the proposed theory.

3.1: Experimental Techniques.

Throughout this project several key experimental techniques have been employed, the details of these techniques are discussed in the following sub-sections.

3.1.1: Lap-Shear Tests.

Lap-shear tests are static tensile tests carried out on TSSW joints to determine the shear load that the joint as a whole can sustain [28]. The magnitude of the maximum sustainable shear load is dependant upon the surrounding base material, the geometry of the specimen, and the properties of the weld nugget itself. During the test, values for applied load and extension are recorded and presented in the form of a load-extension graph, similar to that shown below in Fig 3.1. Load is typically monitored as opposed to stress as an accurate measurement for the cross sectional area of the weld nugget is difficult to determine in a non destructive manner, making measurements of stress impractical. The recorded data gives an indication of the strength of the joint for a given arrangement of parameters.
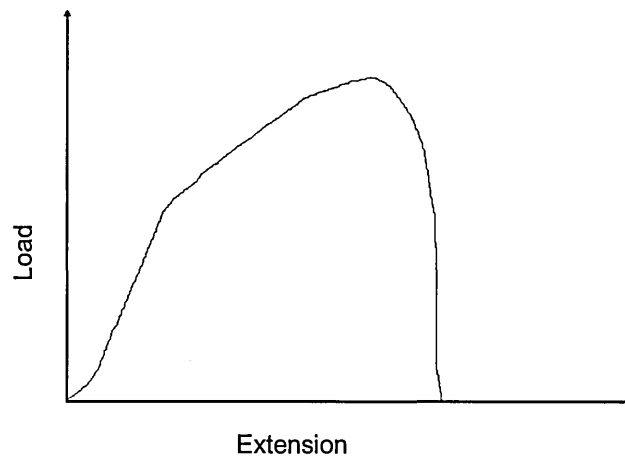
Fig 3.1: Typical load-extension graph obtained from a lap-shear test.

119

There are two types of failure mode that can be observed during the lap-shear testing process. The first is the weld pull-out or "button" failure (Fig 3.2), which is the preferred failure mode as it shows that the join is stronger than the base material [11]. The second type of failure is known as an interface failure or weld shear (Fig 3.3). This type of failure is associated with joints where the weld nugget is weaker than the base material and is therefore often considered to be evidence of a poor quality weld. However, weld shear can also occur when the joint stiffness is high enough to prevent sufficient joint rotation from occurring during the lap-shear test, for a through thickness crack to develop [24, 30].
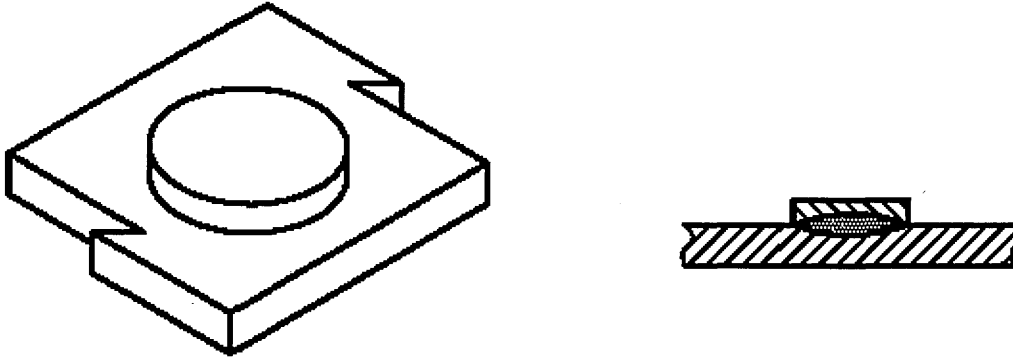
Fig 3.2: Weld pull-out or "button" failure mode.
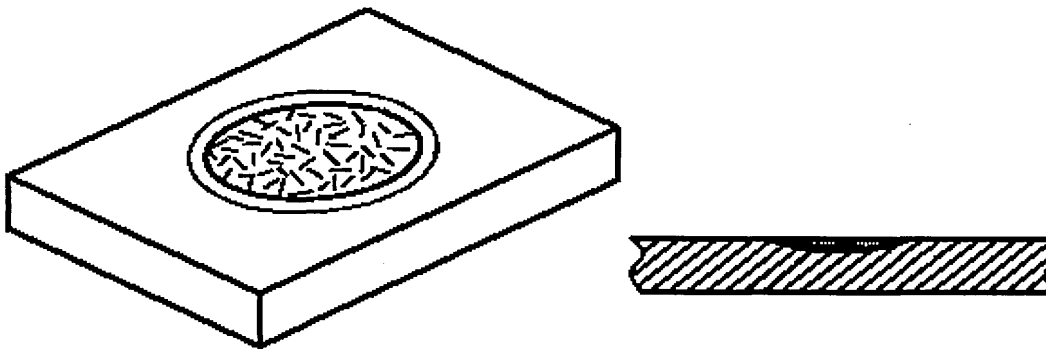
Fig 3.3: Interface or weld shear failure mode.

In industry the gathered data is ultimately used to quantifying the quality of a welded joint produced using a particular set of spot welding parameters, but it can also be used as a means for comparison when determining the effect of changing a given welding variable. In addition, the process can be used to compare the consistency of welds made using the same conditions and parameter levels. This makes the process of particular use when quantifying the quality and consistency of welds made as part of the Weldability study and the Optimum Pitch Distance investigation in this project.

For this project all the lap-shear tests were carried out on an Instron 4206 uniaxial tensile testing machine, fitted with a 150 kN load cell, and using a cross head speed of 10 mm.min^{-1}. For every test the clamping jaws were manually aligned to maintain the eccentric loading pattern of the TSSW joints throughout the test. This feature of the equipment negated the need to use shim plates to align the specimens with the jaws, as recommended in BS EN ISO 14273:2001. The dimensions for the specimens are given in the corresponding sections where the test was used.

3.1.2: Staircase Fatigue Testing.

The Staircase method is a fatigue response testing approach that can be used to determine median values for the fatigue strength of a given specimen configuration from a relatively small number of tests [2, 3, 63].

To begin carrying out the procedure correctly estimates for the mean fatigue strength and the standard deviation of the fatigue strength distribution for the Item Under Test (IUT) must be made. The first specimen is then tested at a load level equal to the estimate for the mean fatigue strength. If a failure occurs prior to the pre-assigned cycle life, the load level for the next specimen is decreased by a step divide value equal to the estimate for the standard deviation; if the specimen does not fail within the pre-assigned number of cycles, the load level for the next specimen is increased by a step divide value equal to the estimate for the standard deviation [2, 3].

The testing continues in this manner, with the load level of each succeeding test being increased or decreased depending on the preceding result. This procedure results in the testing being concentrated mainly on three load levels, centred on the mean level. For this reason, this method is a very efficient way for determination of the mean value [2, 3, 63].

The estimates for mean fatigue strength and standard deviation are best made by referring to similar items where values for mean fatigue strength and standard deviation have already been determined through experimentation [2, 3]. Alternatively a series of 'preliminary' tests can be carried out to determine an estimate for the mean fatigue strength. Preliminary testing starts at a well chosen, but otherwise arbitrary, load amplitude and continues in the same manner as the actual staircase process, but using a step divide that is larger than what the final step size is predicted to be. The preliminary testing then ends when the initial sequence of failures or survivals changes, indicating the first 'turnaround'. Actual Staircase testing then begins, starting at the turnaround load level and using the chosen final step size as a load interval. If preliminary testing is employed the results up to and including the first turnaround are commonly omitted from the analysis [63].

The final step size, *d*, between the load levels should be very close to the actual standard deviation of the fatigue strength distribution for the IUT. Accuracy between the estimated and actual values for the standard deviation is therefore preferred, but this is not a strict condition. The interval should not, however, be larger than twice the actual standard deviation [2, 3].

The collected data is recorded as shown below, the specimens that fail before the completion of the pre-assigned cycles are represented by x's and those that do not fail (survive) are represented by o's. The chart allows for quick and easy determination of the load level for the next test.

Load Level																			
Mean Estimate + 2d						X													
Mean Estimate + d		X				O		X						X				X	
Mean Estimate	O		X		O			X					O		X		O		X
Mean Estimate - d				O						X		O				O			
Mean Estimate - 2d											O								

Fig 3.4: Example of a staircase chart.

To ensure an adequate level of accuracy and to limit the number of unnecessary tests, the optimum number of specimens required when carrying out a Staircase process is between 20 and 50 specimens [64].

3.1.2.1: Analysis of Staircase Results.

The analysis of data collected from Staircase tests is simple and reliable on the condition that the distribution is normal and the interval between the load levels is approximately equal to the standard deviation [3, 65].

The first stage of the analysis is to determine which event, out of failures and survivals, accounted for the least number of occurrences during the test, since the analysis is carried out using only the Less Frequent Event (LFE) [2, 63].

Once the LFE is established, the individual load levels that were used in the testing process are labelled, starting with 0 (zero) for the lowest level at which there was a recorded occurrence of the LFE and finishing at the highest load level that recorded an occurrence of the LFE. All other load levels outside these boundaries are discounted.

The collected data is then arranged in the form of a table, as shown below.

Load, L_i	i	N_i	iN_i	i^2N_i
...	...	...	...	...
...	...	...	...	...
...	...	...	...	...
L_2	2	N_2	$2N_2$	$4N_i$
L_1	1	N_1	N_1	$1N_i$
L_0	0	N_0	0	0
Sum		N	A	B

Table 3.1: Example of data collected from a typical Staircase test.

Where:

L_i =   Load used at corresponding level.

i =   Load level label, 0 is assigned to the lowest load, L_0, on which the least frequent event occurs. 1 is assigned to the next highest level, etc.

N_i =   The number of least frequent events at the corresponding levels.

iN_i =   The product of i and N_i at each level.

i^2Ni =   The product of i^2 and N_i at each level.

N = $\sum N_i$

A = $\sum iN_i$

B = $\sum i^2 N_i$

The resulting data created from the analysis carried out in Table 3.1 is then used to calculate values for the mean fatigue strength using the following equation [2, 4, 63].

$$E\mu = L_0 + d\left(\frac{A}{N} \pm \frac{1}{2}\right) \qquad Eq. \; 3.1$$

Where:

μ =   *Mean failure load.*

L_0 =   *The load at level i=0*

d =   *The chosen interval between load spacing.*

A = $\sum iN_i$

N = $\sum N_i$

$+\frac{1}{2}$ is used if the LFE is survivals, $-\frac{1}{2}$ is used if the LFE is failures or if the occurrences of events are equally split.

It has been suggested that the accuracy of the mean fatigue strength calculated using the protocols of the Staircase process is unaffected by the underlying distribution or its relative skewness [63]. Therefore, even if the distribution is not normal the Staircase process can still produce an accurate mean value [63].

The data collected by the Staircase method can also be used to calculate a value for the standard deviation, of the fatigue strength distribution, using the following equation. However, the results are less accurate than the method used to calculate a value for the mean fatigue strength [2, 4, 63].

$$s = 1.620d\left(\frac{BN - A^2}{N^2} + 0.029\right) \quad Eq.\ 3.2$$

Where:

s	=	*The standard deviation of the fatigue strength.*
d	=	*The chosen interval between load spacing.*
B	=	$\sum i^2 N_i$
N	=	$\sum N_i$
A	=	$\sum i N_i$

If the final step size chosen for the Staircase tests is significantly higher than the actual standard deviation, then the resulting test data will have insufficient spread to use the previous equation to calculate a value for the standard deviation with a reasonable level of accuracy and an alternate equation should be used. The occurrence of this situation is represented by the value of the convergence factor, which is calculated using the method described below [63]:

$$Convergence\ Factor = \frac{BN - A^2}{N^2} \quad Eq.\ 3.3$$

Where:

$B \quad = \quad \sum i^2 N_i$

$N \quad = \quad \sum N_i$

$A \quad = \quad \sum i N_i$

If the convergence factor is less than 0.3, the alternate equation, which is shown below, should be used to calculate a value for the standard deviation [63].

$$s = 0.53d \quad\quad Eq.\ 3.4$$

Where:

$s \quad = \quad$ *The standard deviation of the fatigue strength.*

$d \quad = \quad$ *The chosen interval between load spacing.*

If the convergence factor is greater than 1.2, then neither equation will be able to produce a sufficiently accurate value for the standard deviation. [2, 4, 63].

3.1.2.2: Applying 95% Confidence Limits to Staircase Results.

The standard deviation of a sample mean can normally be given by the standard deviation of the population divided by the square of the sample size, as shown below in Equation 3.5 [65, 64].

$$\sigma_m = \frac{\sigma}{\sqrt{N}} \qquad Eq.\ 3.5$$

Where:

σ_m =   *Standard deviation of the mean.*

σ =   *Standard deviation of the population.*

N =   *Sample size.*

For the situation presented by the results generated using a Staircase approach, this expression must be multiplied by a factor, *G*, which is dependant upon the ratio *d/s* and the position of the mean relative to the testing levels. In practice the true value of *σ* is unknown and instead the standard deviation calculated from the results, *s*, must be used in its place [65, 64].

$$s_m = \frac{Gs}{\sqrt{N}} \qquad Eq.\ 3.6$$

Where:

s_m =   *Standard deviation of the mean.*

G =   *Correction factor.*

s =   *Calculated standard deviation of the population.*

N =   *Sample size.*

Once s_m is calculated the 95% confidence interval on the mean can be estimated using Equation 3.7 below [65, 64].

$$m \pm k s_m \qquad Eq.\ 3.7$$

Where:

m   =   *Mean.*

s_m =   *Standard deviation of the mean.*

k   =   *A factor chosen from tables of the normal deviate to give the desired percentage point. For upper and lower 2.5% points k = 1.96.*

The standard error of the standard deviation of a population can ordinarily be expressed as the standard deviation divided by the square of twice the sample size, as shown below in Equation 3.8 [65, 64].

$$\sigma_s = \frac{\sigma}{\sqrt{2N}} \qquad Eq.\ 3.8$$

Where:

σ_s =   *Standard error of the standard deviation.*

σ =   *Standard deviation of the population.*

N   =   *Sample size.*

However, the situation presented by the Staircase process requires that this expression be multiplied by an additional factor, *H*, which, as with the calculation for the standard deviation of the mean, is dependant upon the ratio *d/s* and the position of the mean relative to the testing levels. In practice the true value of *σ* is unknown and instead the standard deviation calculated from the results, *s*, must be used in its place [65, 64].

$$s_s = \frac{Hs}{\sqrt{N}} \qquad Eq.\ 3.9$$

Where:

S_s =   *Standard error of the standard deviation.*

H   =   *Correction factor.*

s   =   *Calculated standard deviation of the population.*

N   =   *Sample size.*

It should be noted that the additional factor, *H*, incorporates the *1/√2* seen in Equation 3.8.

Once s_s is calculated, the 95% confidence interval on the standard deviation can be estimated using Equation 3.10 below [65, 64]:

$$s \pm ks_s \qquad Eq.\ 3.10$$

Where:

s   =   *Standard deviation.*

s_s =   *Standard error of the standard deviation.*

k   =   *A factor chosen from tables of the normal deviate to give the desired percentage point. For upper and lower 2.5% points k = 1.96.*

Various values for G and H are plotted below in Fig 3.5 as a function of d/s. The solid branch of each line represents the value of G or H when the mean falls on one of the testing levels, while the dashed branch gives the value when the mean falls midway between two levels. Curves for other positions of the mean would fall between the two branches [65, 64].
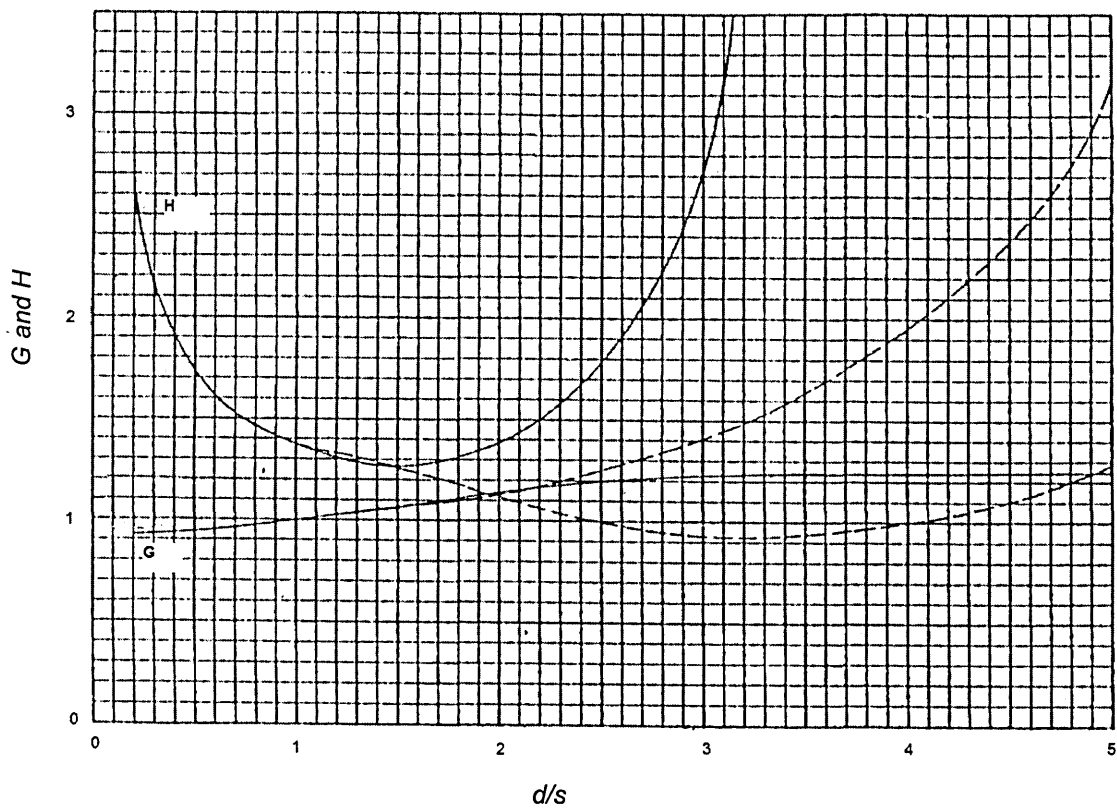
Fig 3.5: Values for in G and H as a function of d/s [65].

3.1.3: Probit Fatigue Testing.

The Probit method of testing allows for the determination of the complete PDF for any IUT, based on a success or failure criteria. The process is not restricted to fatigue testing and has been commonly used in the medical profession to determine effective concentrations of antibiotics to treat common infections.

In terms of a Probit fatigue test, the common procedure is to divide the specimens available into several groups and to test one group at a chosen load level, the next group at a second level, and so on. The data is then evaluated by considering the number of failures (specimens that do not complete the designated number of cycles) and survivals (specimens that do complete the designated number of cycles) occurring at each of the load levels and plotting the data on a graph of load versus probability of survival. The trend of the data is then evaluated in the form of a fitted line known as a 'Response Curve'. For an accurate representation of the full distribution it is recommended that there should be a minimum of two load level groups tested above, and two load level groups tested below, the mean level [2, 3].

3.1.3.1: Determining Load Levels.

When determining load levels previous data for the same component or material should be used as a guide. If no existing data is available a preliminary test, such as the Staircase method, may be required. [2]

3.1.3.2: Group Weighting.

The analysis of the data collected in a Probit test may be made graphically or analytically. In either case, if equal sized groups of specimens have been used at each load level, a weighting procedure will be required. This complication can be eliminated by allocating more tests to percentage points corresponding to larger variances of the observations. If the distribution is assumed to be normal then the following table gives appropriate sizes for the groups. [2, 3]

Expected Percentage Survival	Relative Group Size
25 to 75	1
15 to 20	1.5
80 to 85	1.5
10	2
90	2
5	3
95	3
2	5
98	5

Table 3.2: Relative group sizes based on expected survival per cent.

Appropriate group size allocation is necessary for fitting the response curve by the usual analytical method of least squares and would also facilitate the computation of any confidence limits. Each group should not consist of less than 5 specimens and the total tested at all load levels should be at least 50 for an accurate representation of the complete distribution. [2, 3]

3.1.3.3: Analysis of Response Curves [2].

The analysis of Probit test results is carried out by plotting the per cent survivals, *p,* at each of the load levels tested and fitting a trend line, referred to as a response curve, to the data points. While a response curve may be drawn on any type of graph paper, experience has shown that the per cent survival values tend to lie along a straight line when plotted on Normal probability paper.

If the observed per cent survival values lie along a straight line when plotted on Normal probability paper a straight line may be fitted to the points by eye or by the method of least squares. The later method is more precise and not subject to the biases that may be introduced by a person fitting a line by eye. The equations for the slope and intercept of a line fitted by the method of least squares to per cent survival values having equal weights are shown below.

$$Slope, b = \frac{\sum (XY) - k\overline{X}\overline{Y}}{\sum X^2 - k\overline{X}^2} \qquad Eq.\ 3.11$$

$$intercept, a = \overline{Y} \qquad Eq.\ 3.12$$

Where:

X	=	*Applied load value.*
Y	=	*Transformed value of the stated per cent survival value.*
p	=	*per cent survival in each group of specimens tested.*
$\overline{X}$	=	$\sum X/k$ = *average of X values.*
$\overline{Y}$	=	$\sum Y/k$ = *average of Y values.*
k	=	*Total number of groups tested.*

The equation for the fitted line is:

$$Y_f = a + b(X - \overline{X}) \qquad Eq.\ 3.13$$

To draw in the line fitted to the observed values by the method of least squares at least two values of applied load, and the corresponding values of p_f, should be selected and connected with a straight line.

3.1.3.4: Response Curve Example.

During a hypothetical Probit fatigue test performed for a cycle life of N cycles, the following results where obtained

Applied Load, X, (kN)	Number of Specimens in Group	No. Specimens Surviving 10^6 Cycles	Per cent Survival, p
40	15	14	93.33
41.5	8	6	75
43	5	3	60
44.5	8	2	25
46	15	1	6.67

Table 3.3: Hypothetical Probit fatigue test results.

The per cent survival values are transformed into corresponding Y values (also referred to as Z values) found in any Normal probability table.

Per cent Survival, p	Transformed Value, Y
93.33	-1.5
75	-0.67
60	-0.27
25	+0.67
6.67	+1.5

Table 3.4: Hypothetical transformed Y values.

Fitted Y_f values can now be calculated for each value of applied load tested and a response curve can be fitted to the data.

Applied Load, X, (kN)	X^2	Observed Per Cent Survival, p	Observed Transformed Values, Y	XY	Fitted Values	
					Y_f	p_f
40.0	1600	93.33	-1.50	-60	-1.51	93.4
41.5	1722.3	75	-0.67	-27.81	-0.78	78.2
43.0	1849	60	-0.27	-11.61	+0.05	52.0
44.5	1980.3	25	+0.67	29.815	+0.68	24.8
46.0	2116	6.67	+1.50	69	+1.41	7.9
Sum	215	9267.5		-0.27	-0.6	
Average	$\overline{X} = 43$			$\overline{Y} = -0.054$		

Table 3.5: Response curve for hypothetical Probit fatigue test data.

136

Fitted line intercept, *a*:

Intercept, $a = \overline{Y}$

a = -0.054

Slope of fitted line, *b*:

$$\text{Slope, } b = \frac{\sum(XY) - k\overline{XY}}{\sum X^2 - k\overline{X}^2} \qquad b = \frac{-0.6 - 5 \times 43 \times -0.054}{9267.5 - 5 \times 43^2}$$

b = 0.49
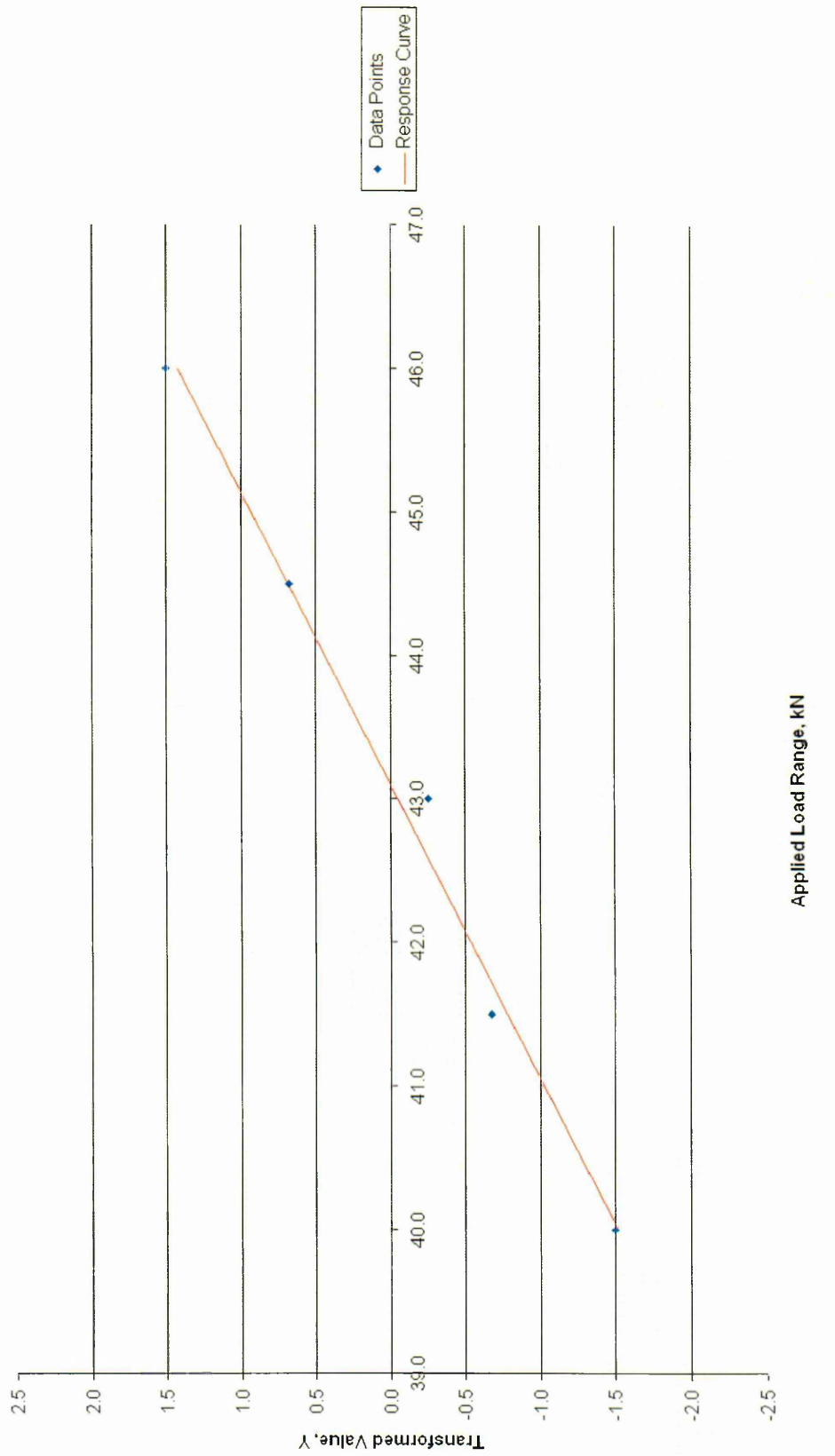
Fig 3.6: Example response curve plotted using least squares method.

3.1.3.5: Derived Estimate *X(Y)* [2].

The derived estimate, known as *X*, a function of *Y*, is the process used to determine an estimate of the load required for a stated value of p or *Y* and is calculated using the method shown below.

$$X(Y) = \overline{X} + \frac{Y - a}{b} \qquad Eq.\ 3.14$$

Where:

X(Y)　　=　　*The Derived estimate.*

$\overline{X}$　　=　　*Average of X values (applied load values)* $\left(\sum X / k \right)$.

Y　　=　　*Transformed value of the stated per cent value.*

a　　=　　*Intercept point of the fitted line.*

b　　=　　*Slope of the fitted line.*

3.1.3.6: Derived Estimate Example.

Using the results from the hypothetical Probit test in the response curve example:

The slope of the fitted line, $b = 0.49$

The intercept of the fitted line, $a = -0.054$

The average applied load, $\overline{X} = 43$

Stated Per Cent Survival	Transformed Value, Y	Derived Estimate, $X(Y)$
90	-1.28	41.6
75	-0.67	42.4
50	0	42.9
25	+0.67	43.8
10	+1.28	44.6

Table 3.6: Derived estimates for hypothetical Probit fatigue test data.

3.2: Experimental Procedure.

The following sub-sections explain the experimental process used to establish the data required to achieve the goals set out at the start of this project.

3.2.1: Base Material Characterisation.

To check the consistency of the supplied material, and to determine a baseline, a series of basic mechanical examination tests were carried out on four randomly selected sheets of the supplied AISI 301.

3.2.2: Tensile Tests.

Five flat sided tensile test specimens were produced from each of the four randomly selected sheets. The dimensions of each specimen were in accordance with BS EN 10002-1:2001 and are shown below.
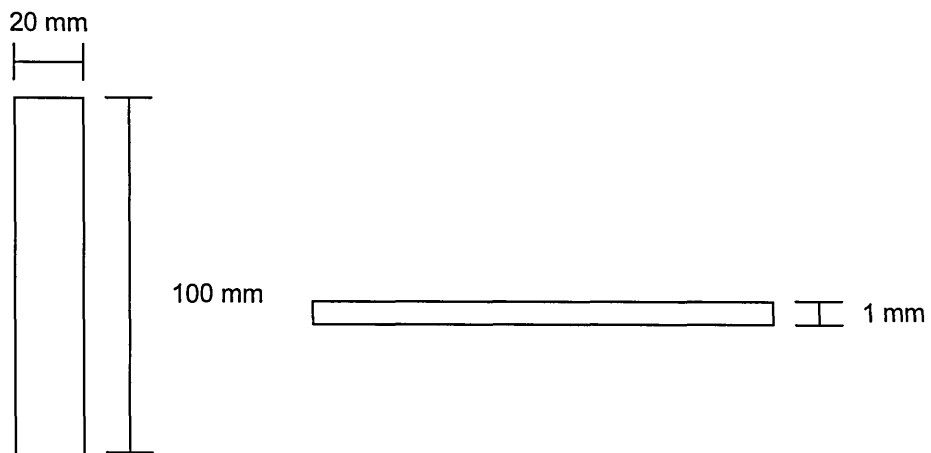
Fig 3.7: Dimensions for flat tensile test specimens.

Each specimen was then tensile tested on an Instron 4206 uniaxial tensile testing machine, fitted with a 150 kN load cell and using a cross head speed of 10 mm.min^{-1}. For each specimen the Ultimate Tensile Strength (UTS) was recorded in MPa. The values for each of the five tests carried out on each sheet were then averaged to produce an average UTS for each sheet.

3.2.3: Hardness Tests.

A sample of material was taken from each of the same four sheets used to carry out the tensile tests. Each sample of material was mounted in bakelite and ground and polished to a 1 μm finish. Five measurements for hardness were then taken from each sample using a Vickers Hardness testing machine with a 20 kg load. The five values taken from each of the four sheets were then averaged to produce an average hardness for each of the four sheets.

3.2.4: Weldability Study.

To determine the optimum spot welding parameters and process for producing consistent quality welds, a weldability study was carried out. This involved producing single welds in TSSW joints using various combinations of spot welding variables. The geometry of the joints was in accordance with BS EN ISO 14273:2001 and are shown below. For each combination of parameters five specimens were produced, all of which were tested in lap-shear as described previously in Section 3.1.1. This gave an indication of which particular combination of variables produced the strongest and most consistent welds.
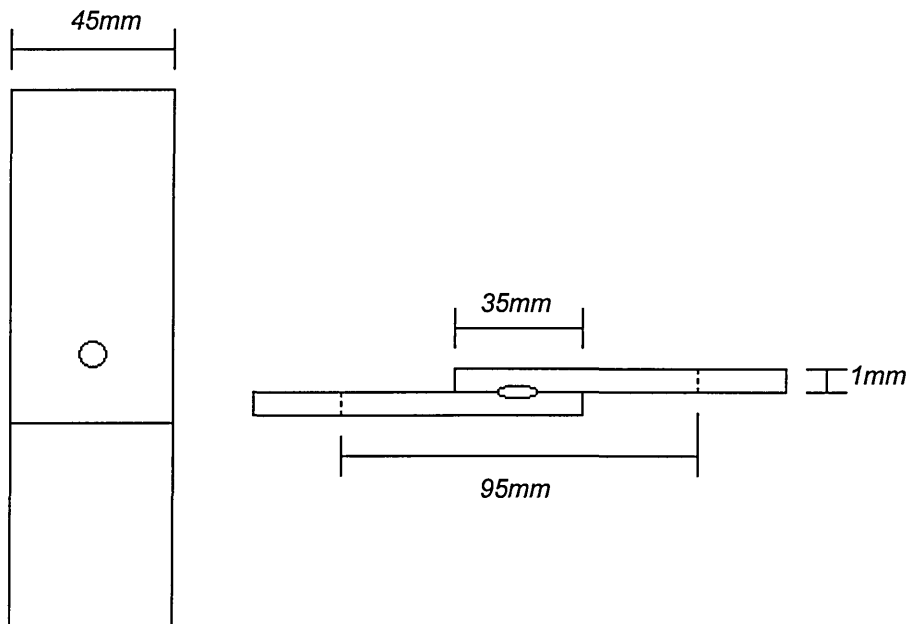
Fig 3.8: Specimen geometry of TSSW joints for weldability study.

As this project deals with only one grade and thickness of stainless steel many of the variables normally found in a weldability study can be eliminated. In addition, to simplify the study further, the welding schedule was kept simple by excluding pre-heat, current ramping, current pulsation, and post weld heating from the welding cycle. Instead a simple squeeze, weld, hold, and off cycle was used, with squeeze and hold times fixed at 25 cycles (0.5 seconds).
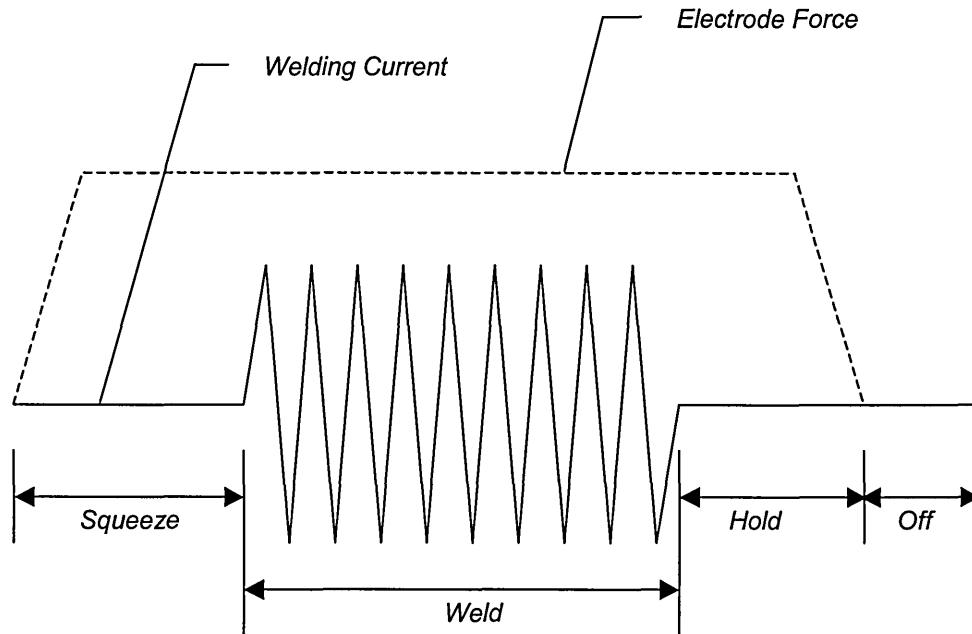
Fig 3.9: A basic welding cycle.

For the purpose of this study it was also decided to maintain the electrode force at a maximum value of 3.25 kN. This was because lower amounts of electrode force had displayed a tendency for expulsion, therefore producing a higher risk for poor consistency between welds. Furthermore, the electrode tip diameter was kept constant at 6 mm, since this size electrode had shown to produce welds with diameters between $4\sqrt{t}$ and $5\sqrt{t}$ (where t is the plate thickness). Although the diameter of the welds produced was not consistently up to the recommended size of $5\sqrt{t}$, larger electrodes could not be used, since this would reduce the load per unit area at the electrode tip as the maximum amount of force available was already being applied. As the material being welded in this project was very strong and hard, lowering the load per unit area in this manner would produce lower quality welds. Limiting the variables in this manner allowed for a very simple weldability study to be developed, which would only focus on the effects of welding current and welding time on weld quality and consistency.

143

Preliminary testing indicated that welding currents below 3.6 kAmps would not generate the amount of heat required to produce welds of an acceptable level of strength, while currents above 4.6 kAmps showed a tendency to cause the electrodes to stick to the workpiece. It was also found that welding times below 10 cycles would not allow enough time for the current to overcome the resistances of the secondary circuit, therefore making resistance spot welding impossible. As with the use of excessive currents, welding times in excess of 30 cycles also showed a tendency to cause the electrodes to stick to the workpiece due to an excess amount of heat being generated. For these reasons, the welding currents that were investigated started at 3.6 kAmps and increased in increments of 0.2 kAmps to 4.6 kAmps. Likewise, the welding times that were investigated in this study started at 10 cycles and increased in increments of 5 cycles up to 30 cycles.

For each combination of variables five TSSW joints were produced, allowing for an average weld strength to be determined for each parameter set and also to give an indication of consistency and repeatability. The average failure load in kN for each combination of parameters was plotted on a 3D contour map along with the welding current and welding time. This contour map gave a good indication of the change in weld strength with variations in welding time and current, allowing for an optimum set of welding parameters to be identified based on weld strength. The range of values obtained from the five specimens produced at each parameter set were also plotted on a 3D contour map in the same manner as the average strength results. This contour map gave a good indication of the consistency of welds produced at each parameter set and allowed for optimum values based on weld consistency to be identified.

To ensure consistency between specimens, the following precautions were taken:

- The electrode tips were re-dressed every 30 welds. The newly redressed electrodes were then 'bedded' in by producing 6 welds in an off-cut of the material to be welded.

- When the equipment was first activated the coolant was allowed to circulate for 5 minutes to allow the temperature of the electrodes and connecting parts of the spot welder to stabilise.

- A TSSW jig was machined from a block of wood to ensure all lap-shear specimens were produced to the same dimensions. The geometry and application of the jig is shown below.
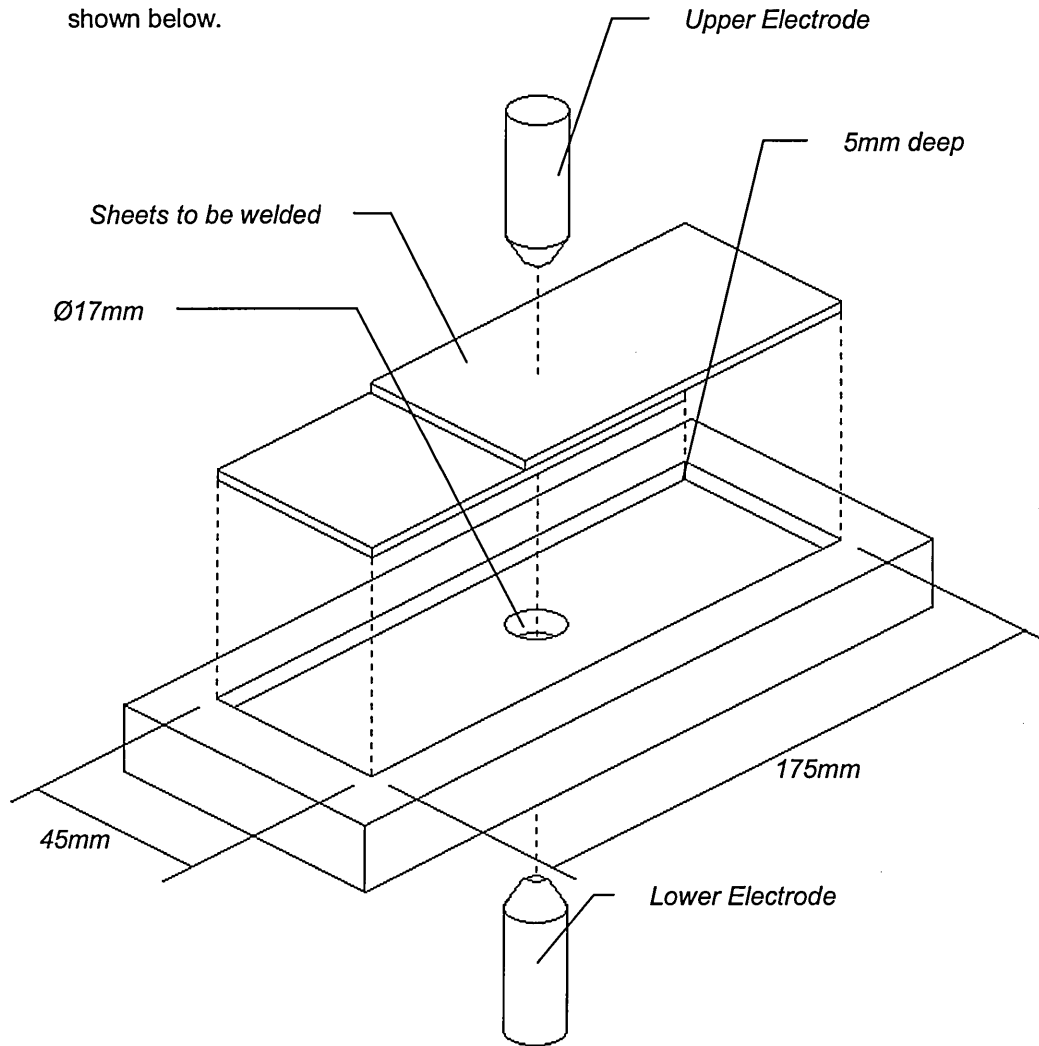
Fig 3.10: Geometry and application of TSSW jig.

3.3.5: Optimum Pitch Distance Study.

To investigate the effect of pitch distance on the consistency of welds made in a single row, multi-spot welded samples were produced with pitch distances of 12.5 mm, 15 mm, 17.5 mm, 20 mm, 30 mm, 40 mm, and 50 mm, using the optimum welding values found in the Weldability Study. Each sample consisted of a single row of five consecutively made welds, separated by the specified pitch distance. The centres of the first and last welds on every sample were situated half a pitch distance from the sample edge.
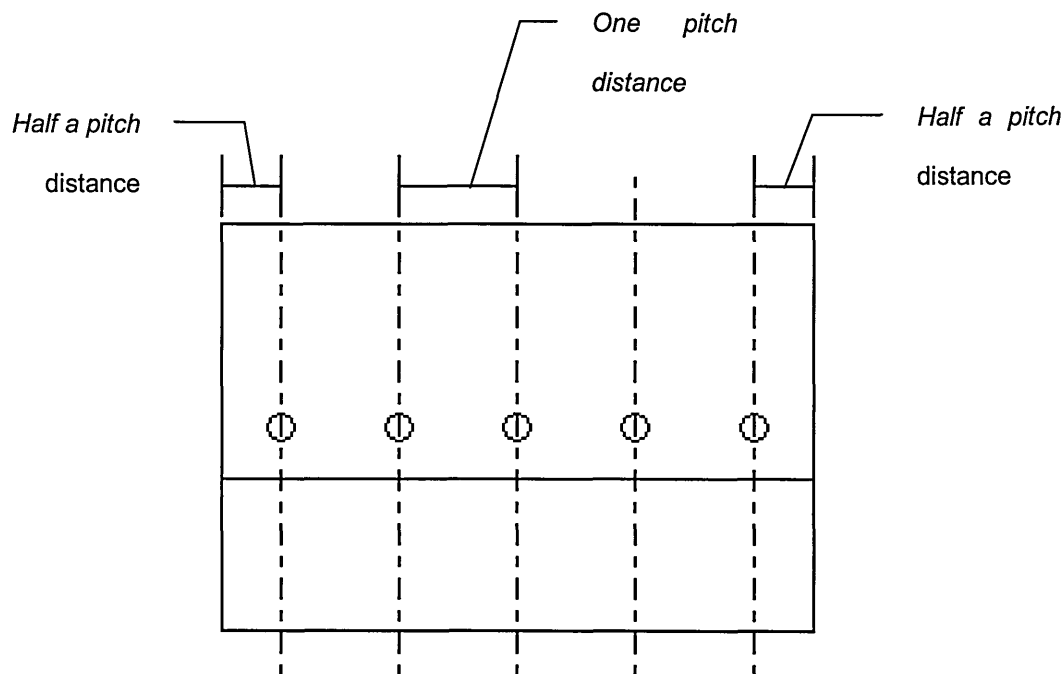
Fig 3.11: Geometry of 5 nugget multi-spot samples for optimum pitch study.

The free length and overlap of all the multi-spot joints were the same as those used in the Weldability Study, and are shown below.
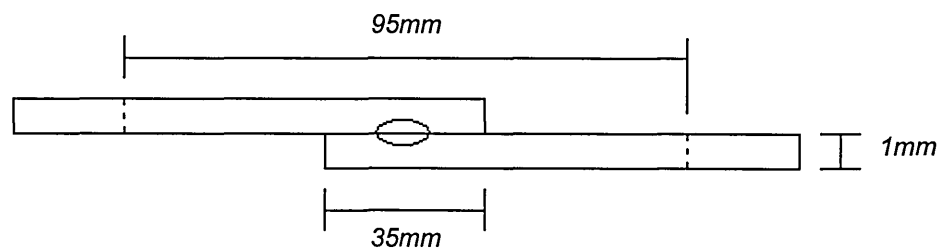
Fig 3.12: Free length and overlap of multi-spot samples for optimum pitch study.

146

To maintain consistency when producing the samples, a wooden jig was machined for each of the pitch distances to be investigated. An example jig and its operation are illustrated below in Fig 3.13.

Sample

Upper
electrode

Wooden jig incorporating five
holes separated at their centres
by the specified pitch distance

Lower
electrode
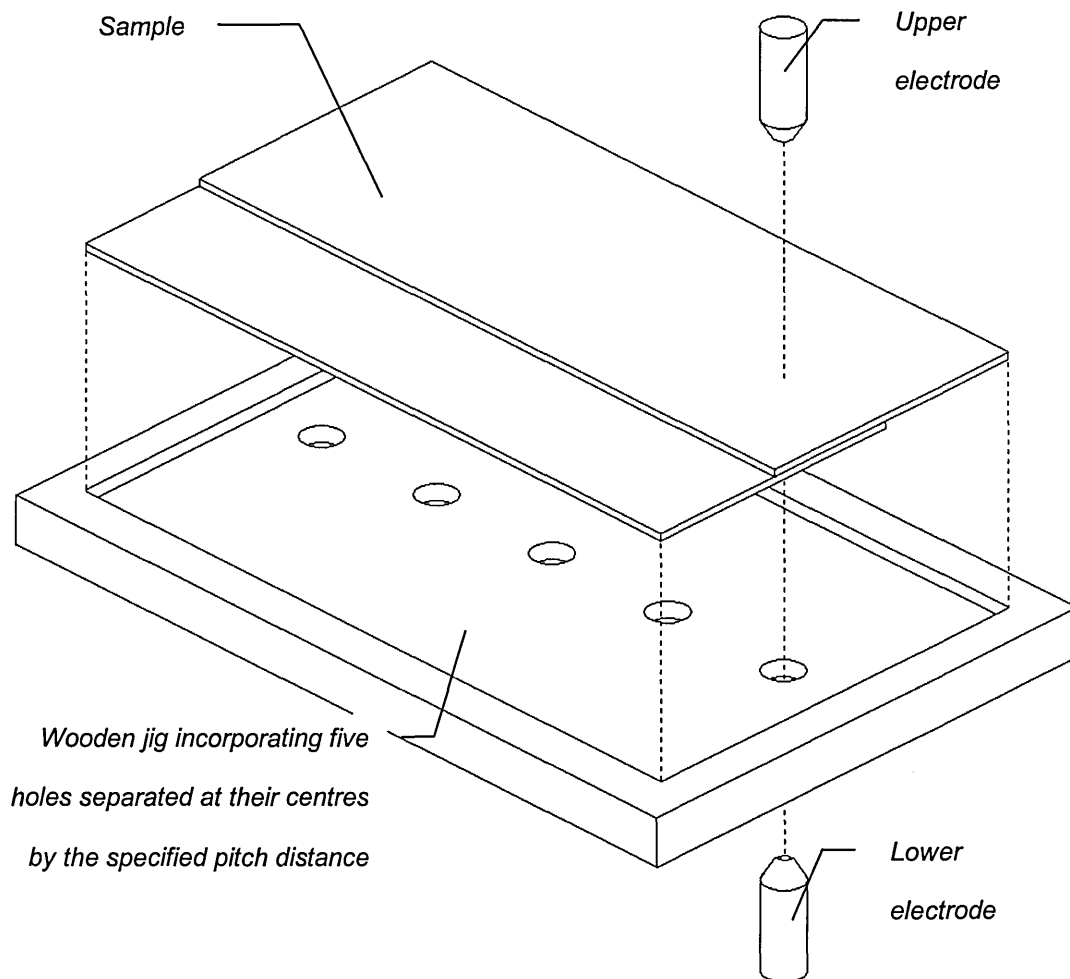
Fig 3.13: Example multi-spot welding jig for optimum pitch distance study.

As with the weldability study, care was taken to maintain the consistency of the electrodes by redressing the tips every 30 welds. Time was also allowed for the temperature of the equipment to stabilise on first activation of the coolant.

The consistency of the spot welds made at each of the stated pitch distances was then examined by measuring variations in the strength of the individual spot welds and also by measuring variations in the diameters of the nuggets of the individual spot welds made at a given pitch distance.

3.3.5.1: Variation in Nugget Strength.

Three samples produced at the seven pitch distances under investigation were each cut into five individual specimens of equal dimensions, as shown below in Fig 3.14, each one containing a single weld in the centre of the specimen.
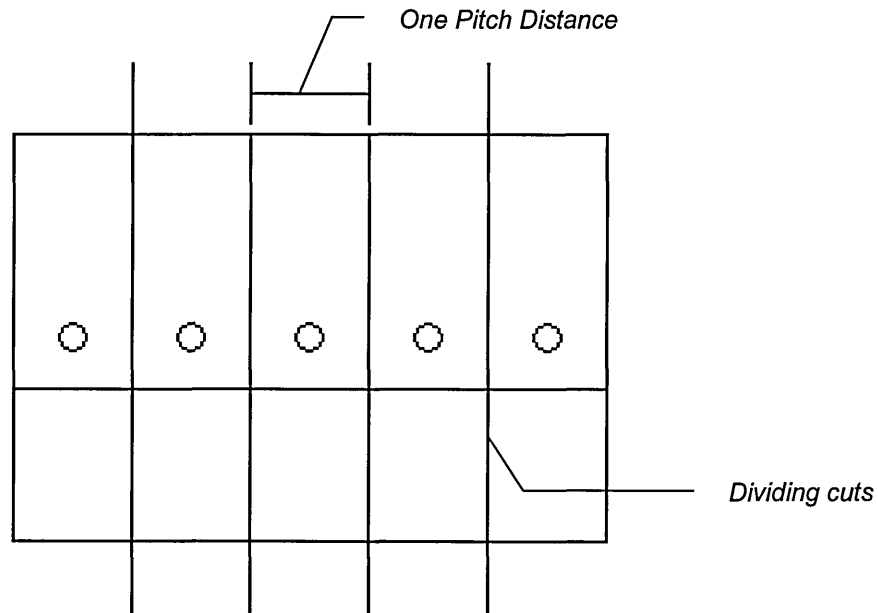
Fig 3.14: Dividing the samples into five individual specimens.

The width of each of the single weld specimens was equal to the pitch distance of the sample they were taken from.

Each single weld specimen was tested using the lap-shear testing process described in Section 3.1.1. The results of the work carried out in the Weldability Study suggested that the individual weld specimens would fail by interface failure rather than by pull out failure, indicating failure of the weld nugget rather than the parent material. This suggests that the load recorded at failure is a measurable representation of the mechanical strength of the individual weld.

For each of the pitch distances under investigation the failure loads for each of the five welds, taken from each of the three samples, was recorded and averaged for each weld position. The averaged values were then plotted on a graph of failure load versus weld position and a trend line was applied. This produced a graph that depicted the variation in average failure load, between single weld nuggets, at each of the pitch distances under investigation. The range of results and trend was then analysed allowing for an appropriate pitch distance and methodology for producing multi-spot welded joints with consistent mechanical properties to be found.

3.3.5.2: Variation in Nugget Diameter.

One sample produced from each of the seven pitch distances under investigation was separated into individual weld specimens in the same way as was described previously in Section 3.3.5.1. The single weld specimens taken from each of the different pitch distance samples were then sectioned across the centre line of each nugget.

The sectioned nuggets were then mounted in conductive bakelite and were ground and polished to remove any surface marks. They were then electrolytically etched in a 10% Oxalic solution, so as to highlight the nugget boundary. The diameter of each nugget was then measured using an optical microscope and digital image analyser.

The measurements for each nugget taken from a given pitch distance sample were then plotted on a graph of nugget diameter versus weld position. The trend of the results for each pitch distance were then analysed, allowing for an appropriate pitch distance and methodology for producing multi-spot welded joints with consistent nugget dimensions to be found.

In order to section the nuggets so that the portion of the nugget viewed under the microscope was as close to the centre as possible, the sectioning cut was made slightly off-centre. This was to take account of the material that would be lost through the thickness of the saw blade and through the grinding and polishing process.

In terms of accuracy, since the saw blade was 1.5 mm thick it was reasonable to assume that the sectioning cut could be made with an accuracy of ± 0.75 mm off the required position. If it were assumed that every sectioning cut was made at the limits of this tolerance then the measurements taken for nugget diameter would be a minimum value in terms of a confidence range. Based on this assumption, and using the established level of tolerance for the sectioning cut, an upper limit for the actual size of the nugget diameter of each of the nuggets could be determined.

Using Fig 3.15 below, if the measurement taken for each nugget diameter, *y*, is assumed to have been taken at a distance of 0.75 mm from the centre line of the nugget, then the actual nugget diameter can be determined by solving the hypotenuse of triangle *i* in Fig 3.15 below, since the hypotenuse is equal to the radius of the nugget and is therefore directly proportional to the diameter.
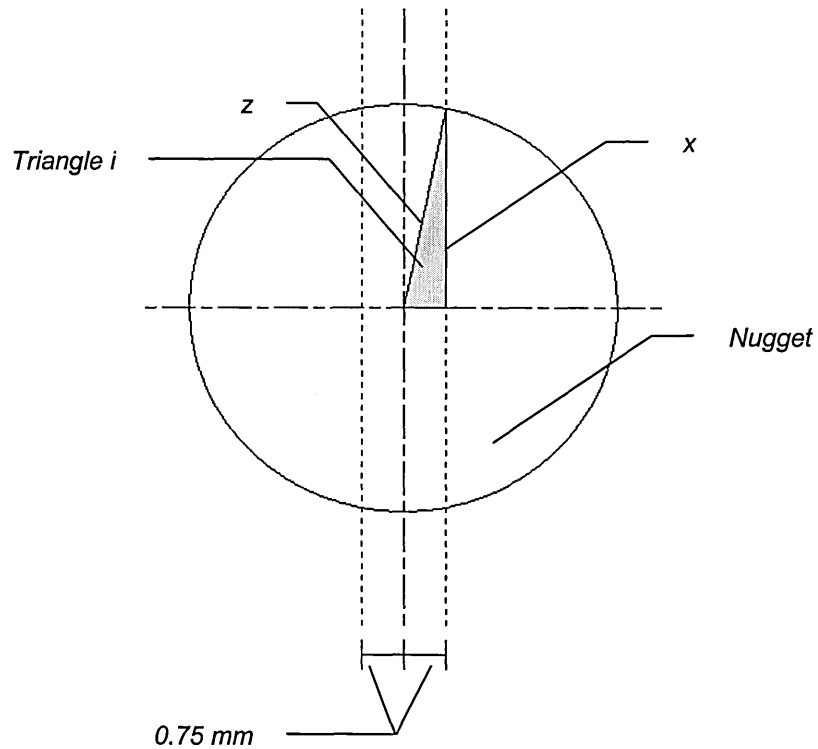
Fig 3.15: Cutting accuracy for nugget diameter investigation.

$$z^2 = x^2 + 0.75 \ mm^2$$

Since $x = y/2$

$$z^2 = (y/2)^2 + 0.75 \ mm^2$$

Assuming the sectioning cut was made at the maximum permissible error, the nugget diameter would be equal to:

$$2 \times \sqrt{\left(\frac{y}{2}\right)^2 + 0.75mm^2}$$

Eq. 3.15

151

3.3.6: Variation in Nugget Diameter at Extremely Close Pitch Distances.

To clarify the results for the investigation into the effect of pitch distance on nugget diameter, a second study was carried out that would examine the effect of current shunting on nugget diameter at the very extremes of close pitch distances.

Five joints were produced, each consisting of two welds separated by a pitch distance of 6 mm, the dimensions for these joints are shown below in Fig 3.16. The two nuggets were then sectioned across their centre line and measurements for their respective diameters were taken.
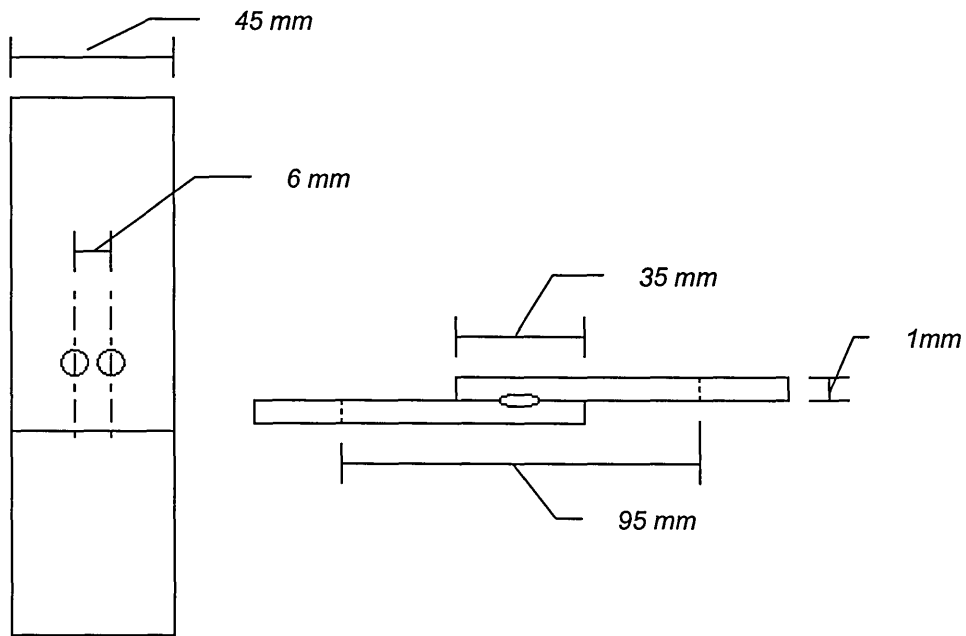
Fig 3.16: Dimensions of extreme pitch distance specimens.

Since it appeared that the weld nuggets produced using the chosen set of welding parameters were in the region of 4 – 5 mm in diameter, using a pitch distance of 6 mm was effectively the smallest distance that could separate two consecutive welds before they started to overlap. Any difference in weld diameter caused by current shunting will be most prolific in the first and second welds made in a given series of spot welds, since the first weld would not have experienced any current shunting. By producing samples consisting of two welds separated by such a close pitch distance and comparing their diameters, the effect of current shunting on nugget diameter should be at its most severe. Analysis of the nugget diameter of these welds provides a greater perspective of the effect of current shunting on nugget diameter by providing a worse case scenario.

To minimise any error that could be introduced by comparing the diameter of two nuggets that were not sectioned precisely down the centre of the weld, a unique procedure was adopted. A jig, similar to those used in the previous welding feasibility studies, was machined with a single, off centre hole for producing each weld. Each specimen was placed into the jig and, once the hole was aligned with the electrodes, the first weld was made.
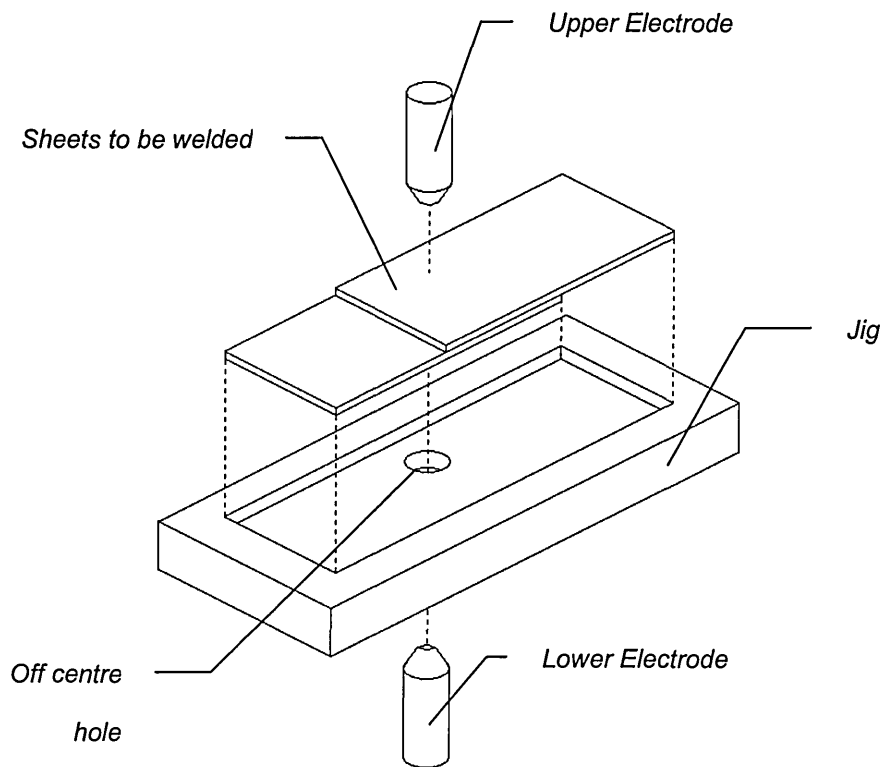
Fig 3.17: Operation of extreme pitch distance specimen jig for first weld.

153

The specimen was then flipped through 180° as shown below in Fig 3.18.
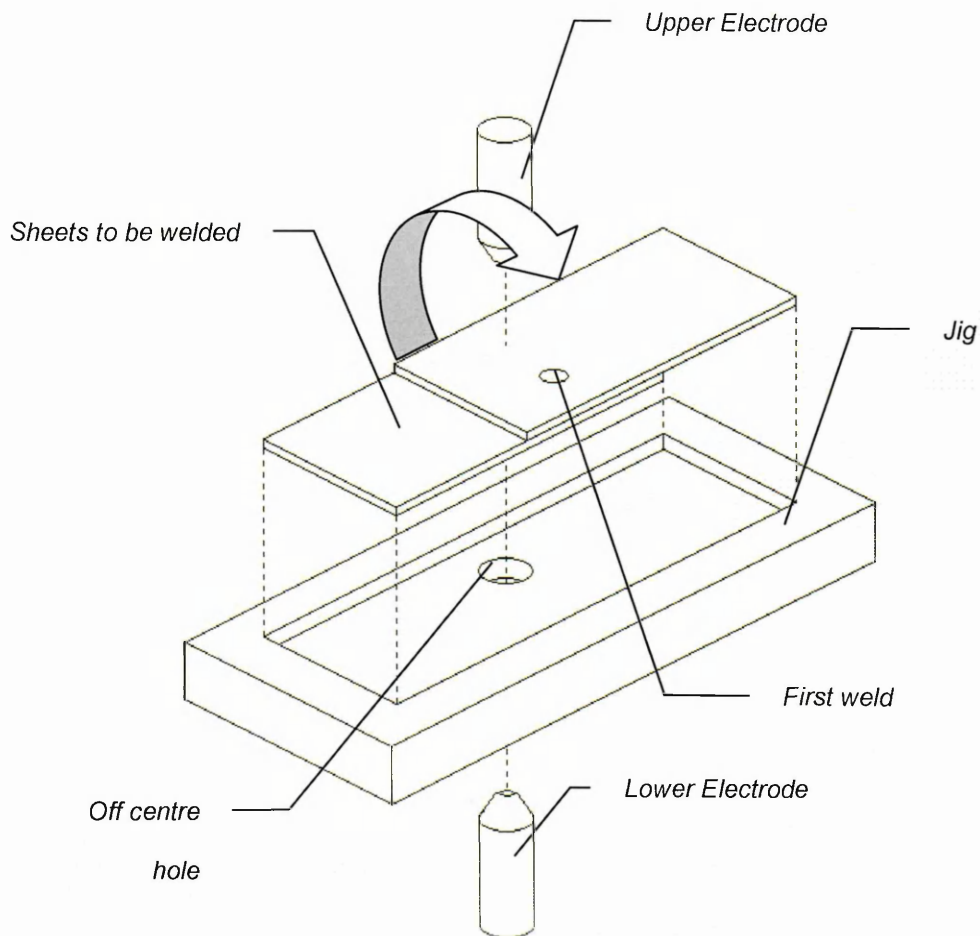
Fig 3.18: Operation of extreme pitch distance specimen jig for second weld.

This situated the specimen so that the centre of the second weld would be sited directly in line with, and along the same perpendicular plane as, the centre of the first weld.
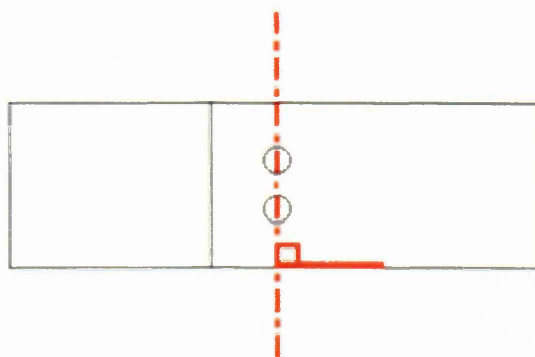
Fig 3.19: positioning of first and second welds.

Producing the welds in this manner meant that both nuggets could be sectioned with a single cut made perpendicular to the side of the specimen. Due to the positioning of the two welds, this cut would section both nuggets in exactly the same position, relative to one another. Therefore, even if the cut is made off-centre, any difference in diameter between the two nuggets will be apparent and representative of the true difference. However, the further away the cut is made from the centre of the two nuggets, the more exaggerated the diameter difference becomes.
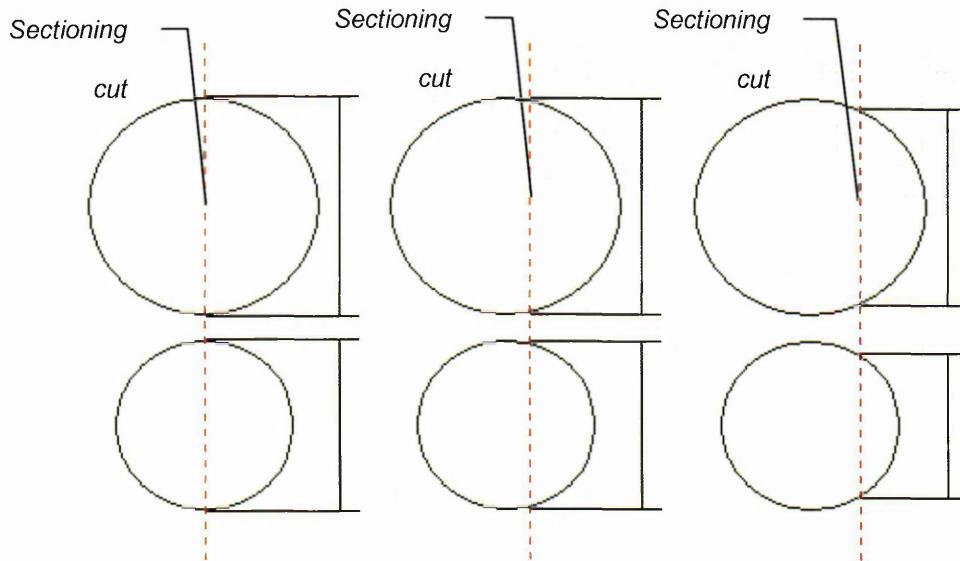
Fig 3.20: Difference in nugget diameters is always apparent, regardless of positioning of the sectioning cut.

Using the same principles for the accuracy of the sectioning cut discussed in the Variation in Nugget Diameter Study, an upper limit on the actual difference in diameter between the two nuggets from each specimen was determined.

The sectioned nuggets were mounted in conductive bakelite and electrolytically etched in a 10% Oxalic solution to highlight the nugget boundaries. The sectioned faces of the nuggets were then viewed under an optical microscope and measurements for the diameter of the first and second nugget on each specimen were taken using a digital image analyser. The gathered data was then used to calculate the change in nugget diameter occurring between the first weld and the second weld made in a series using the smallest feasible pitch distance. The calculations for change in nugget diameter were then analysed to determine the 'worst case' effect of current shunting on nugget diameter using this grade of stainless steel.

155

3.3.7: Production of Fatigue Test Specimens.

Based on the optimum data found in the Weldability Study and the Optimum Pitch Distance Study, all fatigue specimens were produced from multi-spot welded samples consisting of nineteen consecutive welds made in a single row, the dimensions for which are shown below.
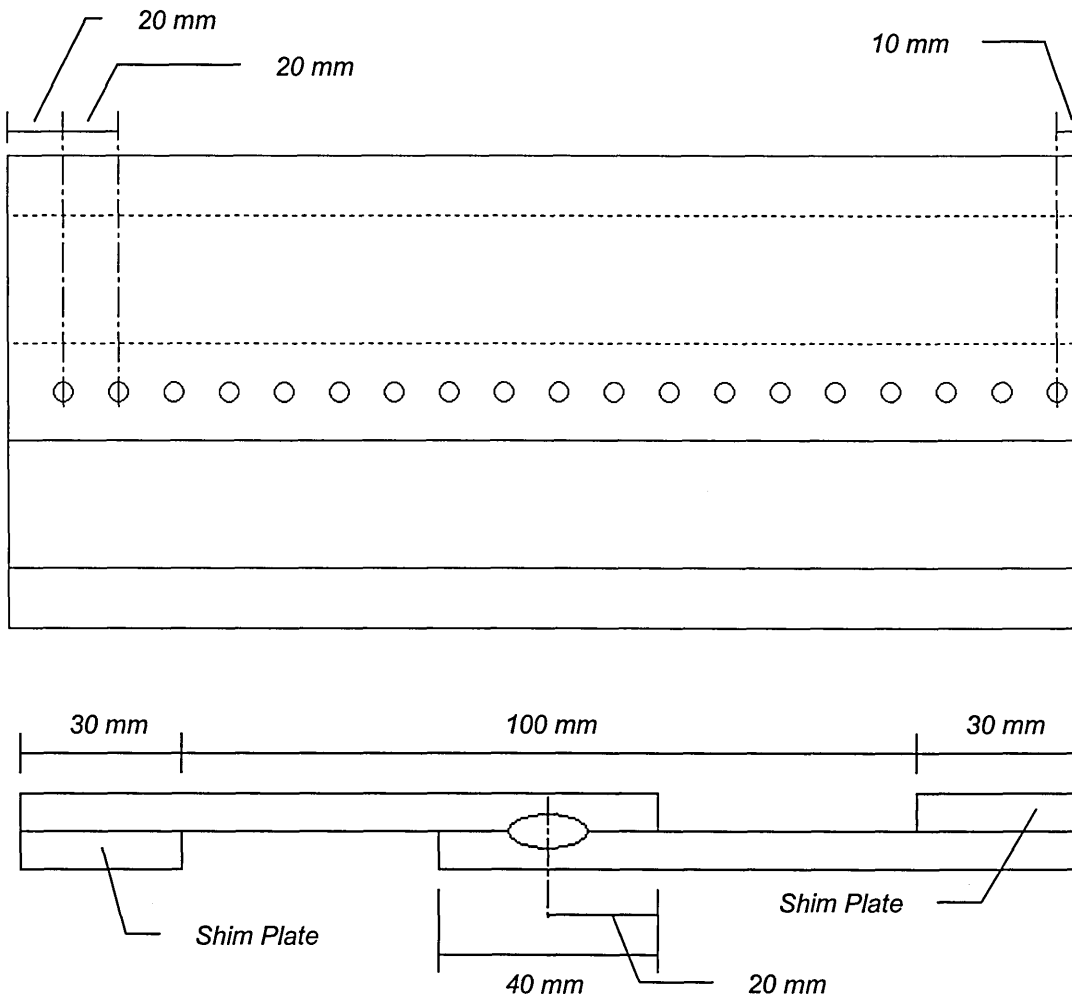
Fig 3.21: Geometry of 19 nugget TSSW fatigue specimens.

As the jaws available on the fatigue testing equipment were not manually adjustable all the samples had shim plates welded to each end of the joint. These plates where positioned such that they did not overlap with the free length of the specimen when it was being tested. Using the plates in this manner would maintain the eccentric loading regime associated with TSSW joints throughout the testing process.

The first two welds on each multi-spot welded sample were removed and discarded, since these were found to have a tendency to display properties that were different to the remaining welds (discussed in more detail in Sections 5.3 to 5.4), leaving each sample with seventeen spot welds and the following dimensions.
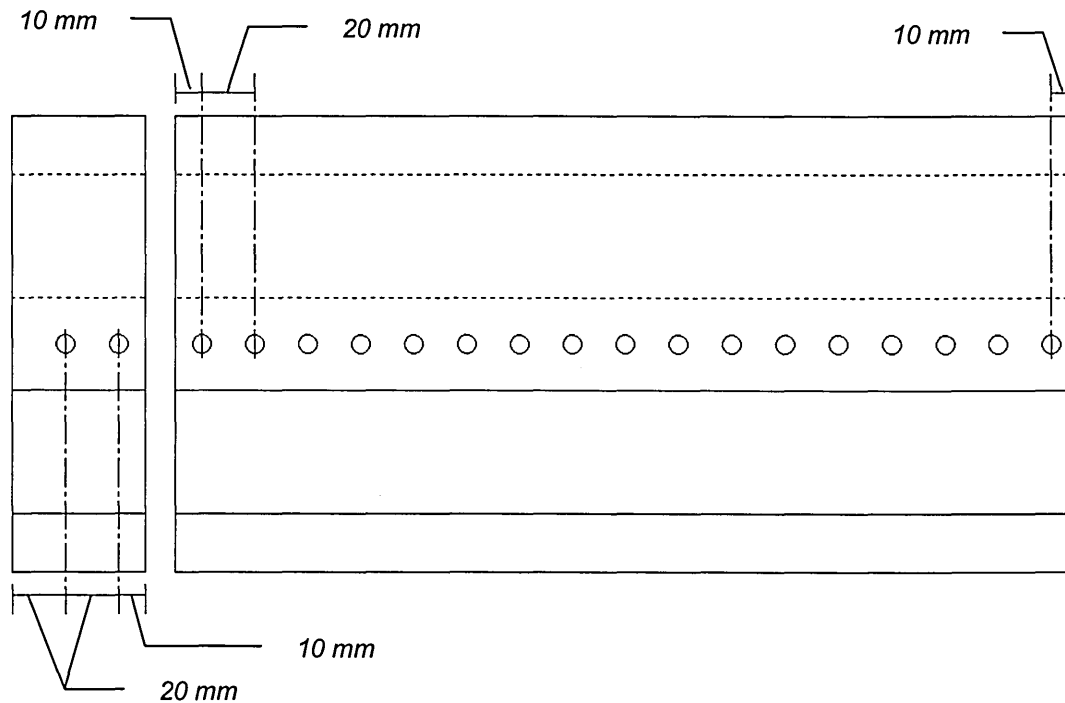
Fig 3.22: Geometry of seventeen nugget TSSW fatigue specimens.

The seventeen nugget samples where then cut into specimens consisting of one, two, four, eight, or sixteen nuggets, for the purposes of fatigue testing. The dimensions for each of these samples are shown in Figs 3.23 through 3.27.

Producing the samples in this manner ensured that all the weld nuggets in the one, two, four, eight, and sixteen nugget specimen joints would have gone through the same manufacturing process. This reduced the risk of variations being introduced between the single spot welded joints and any of the multi-spot welded joints and also helped to maintain the same levels of residual stresses, caused by distortion in the specimen, throughout the different types of joint.
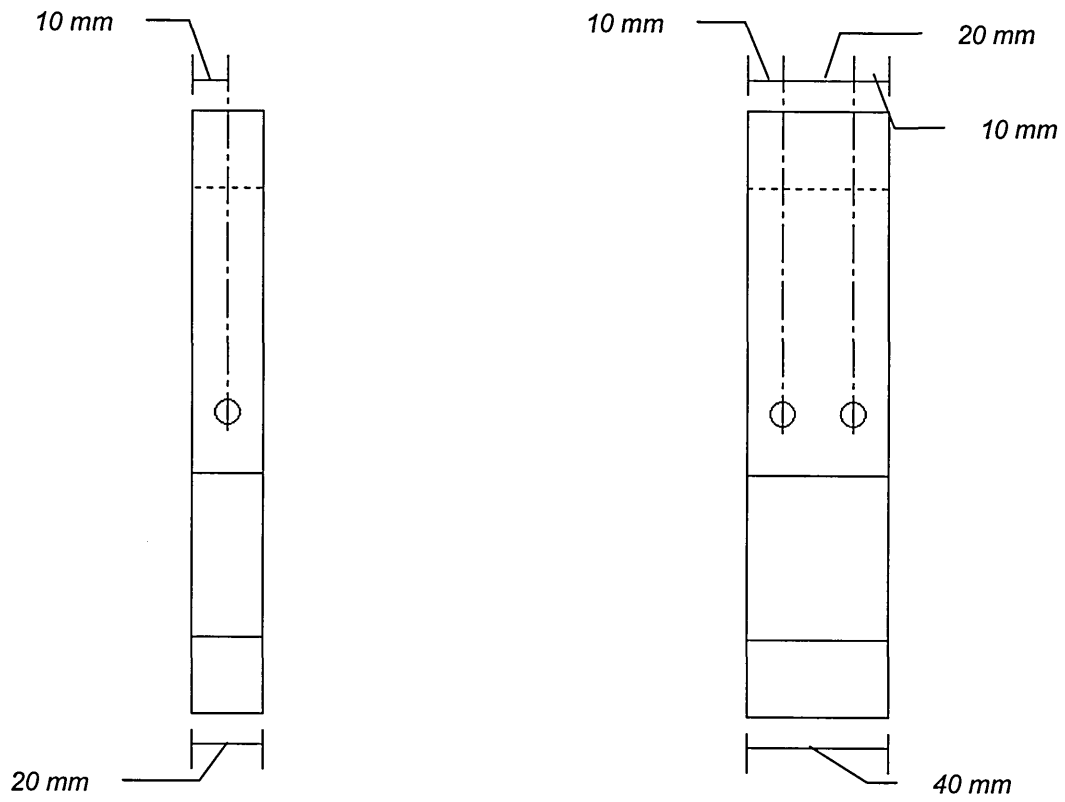
Fig 3.23: [LEFT] Geometry of single nugget TSSW fatigue specimens.

Fig 3.24: [RIGHT] Geometry of double nugget TSSW fatigue specimens.
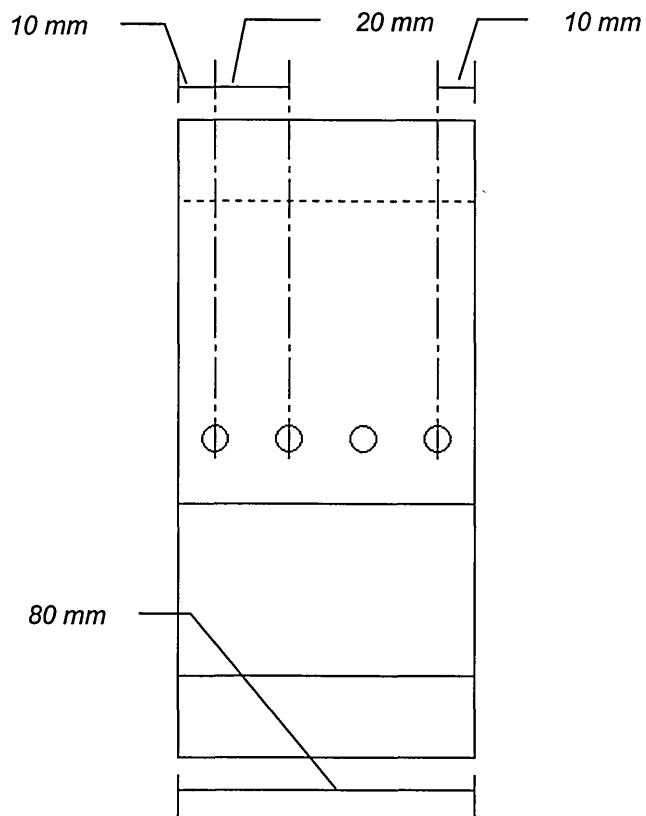
Fig 3.25: Geometry of four nugget TSSW fatigue specimens.
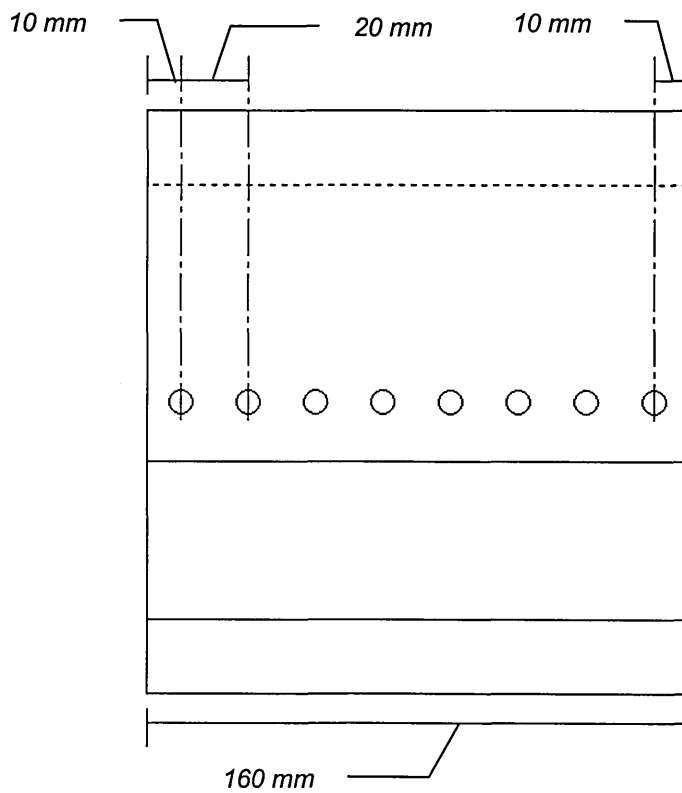
Fig 3.26: Geometry eight nugget TSSW fatigue specimens.
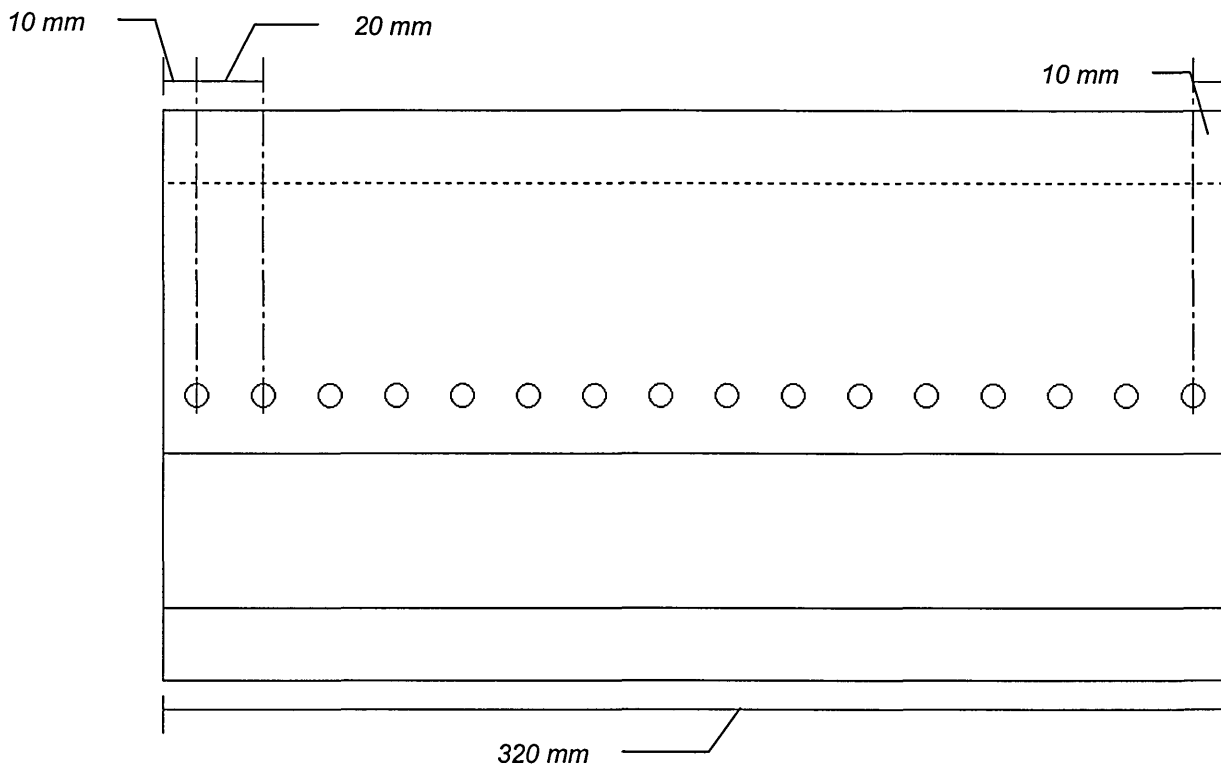
Fig 3.27: Geometry of sixteen nugget TSSW fatigue specimens.

3.3.8: Fatigue Testing.

The following sub-sections explain the specific procedures used when Staircase and Probit testing the single and multi-spot welded joints. In all the fatigue tests carried out in this project the preservation of consistency is of paramount importance. To limit any variation that might be caused, all the fatigue tests were carried out on the same piece of equipment. This consisted of a Dartec load train with a 50 kN dynamic load cell and a Rubicon control system. All tests were carried out using a repeating sinusoidal stress cycle with a frequency of 25 Hz and an R value of 0.1.

3.3.8.1: Staircase Fatigue Testing of Single Nugget Joints.

Twenty five single nugget spot welded specimens where subjected to a Staircase fatigue test programme, which was carried out as described in Section 3.1.2, to determine preliminary values for the mean fatigue strength and the standard deviation of the fatigue strength distribution for single spot welded joints. Due to the low loads that would be used in these tests, the load cell was set to a lower operational load range of ± 5 kN.

An estimate for the mean fatigue strength and starting load range of 0.756 kN, along with an estimate for the standard deviation and step division of 0.027 kN was made based on experimental data obtained from testing similar joints [21]. As set out in the project specification the cycle life was fixed at 10^6 cycles, specimens that failed prior to completing 10^6 cycles where counted as a failure and specimens that reached or surpassed 10^6 cycles were deemed to be survivals.

As described in Section 2.3.9 the definition of a fatigue failure was when any surface crack spanned a distance of 1 pitch distance across the specimen width. In the case of a single spot welded joint this was found to coincide with an increase in the testing stroke of 1 mm, therefore automatic trips were set at a ± 1 mm deviation from the maximum and minimum displacement values during normal cycling.

3.3.8.2: Probit Testing of Single Nugget Joints.

The values for mean fatigue strength and standard deviation calculated from the single nugget Staircase results were used to produce a preliminary version of the complete PDF for single spot welded joints, which is shown below in Fig 3.28. Using the preliminary PDF, magnitudes for the load ranges were determined that would theoretically produce per cent survival probabilities of 10, 30, 50, 70 and 90%. To maintain consistency between the Staircase and Probit results the same equipment and settings that were used in the Staircase study were also employed in the Probit study.

Staircase PDF Estimate
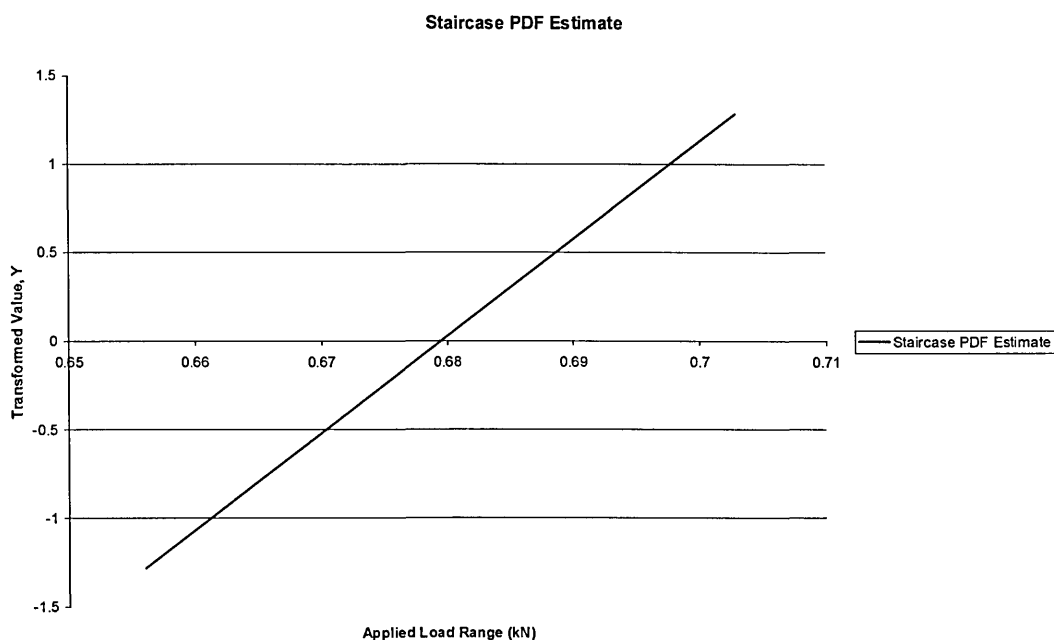
Fig 3.28: PDF estimate derived from Staircase data.

The process began by testing twenty specimens at the load range believed to produce 50% survivals. The number of surviving and failing specimens were recorded, therefore establishing an accurate per cent survival probability at the given load range. The actual per cent survival at this load range was then calculated and, based on its conformity to the expected 50% value, minor adjustments to the calculated load levels were made. Specimens were then apportioned to the remaining load range levels and tested in accordance with the procedures set out in Section   3.1.3.

The values for mean fatigue strength and standard deviation determined by the Staircase study indicated that a single nugget specimen, fatigue tested at an applied fatigue load range of 0.6795 kN, should have a 50% chance of completing 10^6 cycles before failure. To confirm this information, twenty single nugget specimens were to be tested at this applied fatigue load range and the actual per cent probability of survival calculated. However, the control system for the fatigue equipment used in this investigation required the operator to input a peak and trough load, rather than a load range. For an R value of 0.1 the required fatigue load range transcribes to a peak and trough load of 0.755 kN and 0.0755 kN respectively. Unfortunately, due to limits on the resolution of the achievable loads, these values had to be rounded up to 0.76 kN and 0.076 kN for the peak and trough load respectively, which transcribes to a fatigue load range of 0.684 kN.

As the start load had to be adjusted to fit the constraints of the testing equipment, it was important to re-calculate the expected per cent survival probability. Using the estimate of the PDF generated by the Staircase results, a single nugget specimen fatigue tested at a load range of 0.684 kN should have a 40.3% probability of surviving the designated 10^6 cycles. Of the twenty specimens that were tested at this adjusted load range only three survived past 10^6 cycles, this corresponded to a per cent survival probability of 15%, which is significantly lower than the expected value. Due to the variance at such an extreme per cent survival probability, extra specimens needed to be tested at this load range to ensure sufficient levels of confidence. In accordance with the guidelines for sample weighting set out in Table 3.2 from Section 3.1.3, since twenty specimens were to be tested for the mean values, a per cent survival probability of 15% would require the testing of thirty specimens to achieve an acceptable level of confidence. Of the additional ten specimens that were tested at this load range only one survived past 10^6 cycles. This meant that the actual per cent survival probability at a load range of 0.684 kN was 13.3%.

Due to the significant difference between the expected and actual per cent survival probabilities, it was decided to re-calculate the estimate of the PDF for the fatigue strength of single nugget specimens based on the new data gathered from this first Probit test, but keeping the standard deviation the same as that which was calculated in the Staircase study.
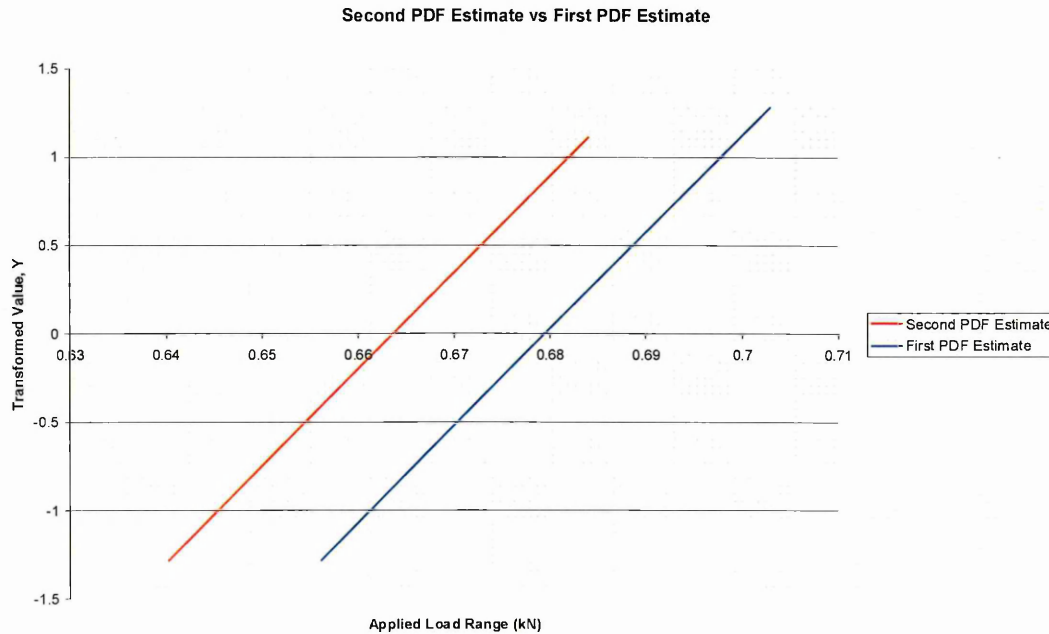
Fig 3.29: Second PDF estimate vs. first estimate.

This produced a new estimate PDF, which had an expected mean fatigue strength value of 0.6637 kN and a standard deviation of 0.0183 kN. As before, the mean fatigue strength value predicted by this adjusted estimate of the PDF was to be confirmed by testing twenty single nugget specimens at the predicted mean fatigue strength load range and determining the actual per cent survival probability through the number of specimens that survived past 10^6 cycles. However, as with the previous load value, due to the constraints of the testing equipment this value had to be adjusted to 0.6660 kN, which corresponded to a per cent survival probability of 45.6%. Of the twenty specimens tested at this load range level nine survived past the designated 10^6 cycles, meaning a per cent survival probability of 45%. This confirmed that the second PDF estimate for the fatigue strength of single nugget joints was more accurate and could therefore be used to determine the remaining load levels needed to generate enough data points to produce an accurate response curve.

Using the adjusted estimate of the PDF for the fatigue strength of single nugget specimens, load range levels were calculated that corresponded to per cent survival probabilities of 30, 70 and 90%, the exact load levels are shown below in Table 3.7.

Load Range (kN)	Per Cent Survival Probability
0.6733	30
0.6541	70
0.6403	90

Table 3.7: Initial load range levels and group sizes chosen for Probit tests.

As with the previous tests, the constraints of the fatigue testing equipment prevented the use of these exact load ranges and adjusted values had to be used. Table 3.8 below lists the initial and adjusted load range levels with their respective expected per cent survival probabilities. The table also lists the number of specimens tested at each load level, which were weighted in accordance with Table 3.2 in Section 3.1.3.

Initial Load Range (kN)	Initial Per Cent Survival Probability	Adjusted Load Range (kN)	Adjusted Per Cent Survival Probability	No. Tested
0.6733	30	0.6750	27.4	20
0.6541	70	0.6570	64.9	20
0.6403	90	0.6390	91.4	40

Table 3.8: Adjusted load range levels and group sizes chosen for Probit tests.

The resulting per cent survival probabilities at the adjusted load range levels were then plotted on a graph of transformed *Y* values versus applied load range. The plotted data points were then analysed with a response curve in the manner explained in Section 3.1.3.3. The resulting response curve (Fig 4.86) gave an accurate representation of the complete survival PDF for single spot welded joints.

3.3.8.3: Staircase Testing of Multi-Spot Welded Joints.

In order to maintain consistency, the multi-spot welded Staircase study was carried out on the same Dartec fatigue equipment as the single nugget fatigue investigation. Due to the larger load levels used in this investigation the load cell was set to a load range of ± 10 kN for the four and eight nugget specimens and ± 20 kN for the sixteen nugget specimens.

The values for the mean fatigue strength and standard deviation of single nugget joints were calculated from the single nugget response curve using the derived estimate calculations described in Section 3.1.3.5.

Derived Estimate for mean: 0.664 kN

Derived Estimate for standard deviation: 0.020 kN

These values were then used in accordance with the theory suggested in Section 1.1 to determine estimate values for the mean fatigue strength and the standard deviation per spot weld for two, four, eight, and sixteen nugget specimens. Thirty multi-spot welded specimens of each joint configuration were then Staircase tested in accordance with the procedures explained in Section 3.1.2, using the estimated mean fatigue strength, multiplied by the number of spot welds, as a starting load range and the estimated standard deviation, multiplied by the number of spot welds, as the step division. The values calculated for the starting load and step division for each of the multi-spot welded joints to be tested in this project are given and explained over the following three pages.

Predicted Mean Fatigue Strength per Spot Weld of a Multi-spot Welded Joint:

$$X_m = X_s - m_n \times S \qquad Eq.\ 3.16$$

Predicted Standard Deviation per Spot Weld of a Multi-spot Welded Joint:

$$S_m = d_n \times S \qquad Eq.\ 3.17$$

Where:

X_m = *Mean fatigue strength per nugget of the multi-spot welded joint.*

X_s = *Mean fatigue strength of a proportionally size single nugget joint.*

m_n = *Mean fatigue strength relationship factor equal to the Z value read from the standard normal distribution tables for a probability equal to $\sqrt[n]{0.5}$.*

S_m = *Standard deviation per nugget of the multi-spot welded joint.*

d_n = *Standard Deviation relationship factor equal to the Z value read from the standard normal distribution tables for a probability equal to $\sqrt[n]{0.8413} - \sqrt[n]{0.5}$.*

S = *Standard deviation of a proportionally size single nugget joint.*

No. Nuggets in Joint	m_n	d_n	X_m (kN)	S_m (kN)	Mean Fatigue Strength per Joint (kN)	Standard Deviation per Joint (kN)
2	0.544	0.842	0.653	0.017	1.306	0.034
4	0.988	0.726	0.644	0.015	2.575	0.059
8	1.385	0.641	0.636	0.013	5.087	0.104
16	1.723	0.576	0.629	0.012	10.063	0.187

Table 3.9: Mean fatigue strength and standard deviation of the fatigue strength distribution values for whole multi-spot welded joints.

167

As with the calculated load levels used in the Probit tests, restrictions in the testing equipment did not allow for the use of the exact load levels shown in Table 3.9. The starting load and step divide had to be changed slightly for each joint configuration from the predicted values for mean fatigue strength and standard deviation, in order for the Staircase tests to be carried out as specified. The adjusted loads are shown below in Table 3.10.

No. Nuggets in Joint	Mean Fatigue Strength per Joint (kN)	Standard Deviation per Joint (kN)	Adjusted start load (kN)	Adjusted Step Divide (kN)
2	1.306	0.034	1.306	0.036
4	2.575	0.059	2.574	0.054
8	5.087	0.104	5.087	0.099
16	10.063	0.187	10.063	0.189

Table 3.10: Adjusted mean fatigue strength and standard deviation of the fatigue strength distribution values for whole multi-spot welded joints.

The experimentally obtained results for mean fatigue strength and standard deviation per spot weld, for each of the multi-spot welded joints tested, were then plotted as data points (Figures 4.91 and Figs 4.92) along with the theoretical values shown below in Figs 3.30 and 3.31, allowing for a comparison of the theoretical and experimental data.

Theoretical Mean Fatigue Strenth per Nugget
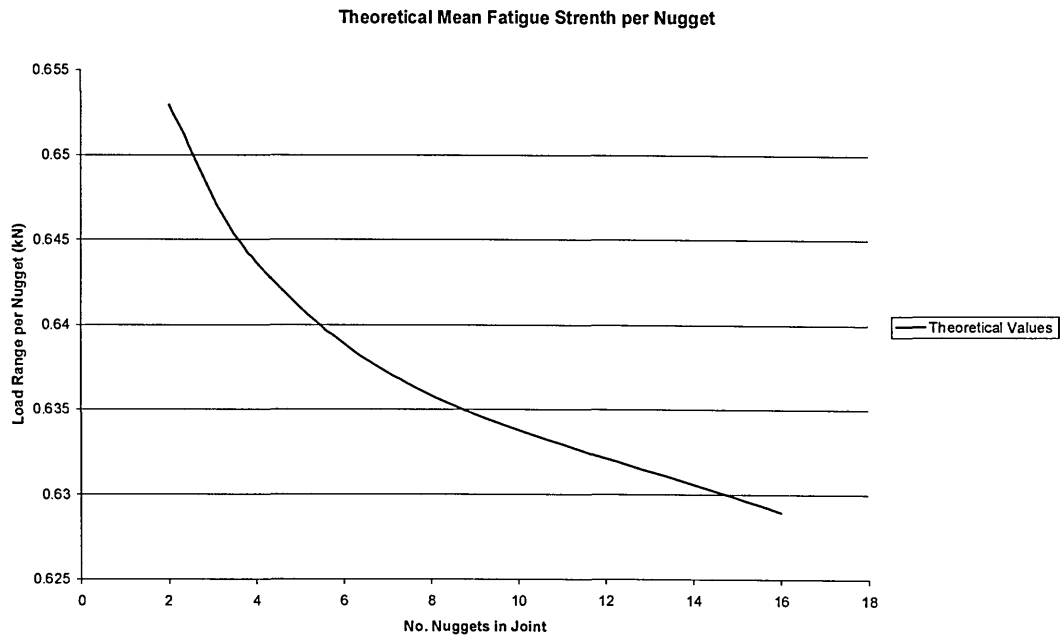
Fig 3.30: Changes in theoretical mean fatigue strength per spot weld as the number of welds increases.

Theoretical Standard Deviaiton per Nugget
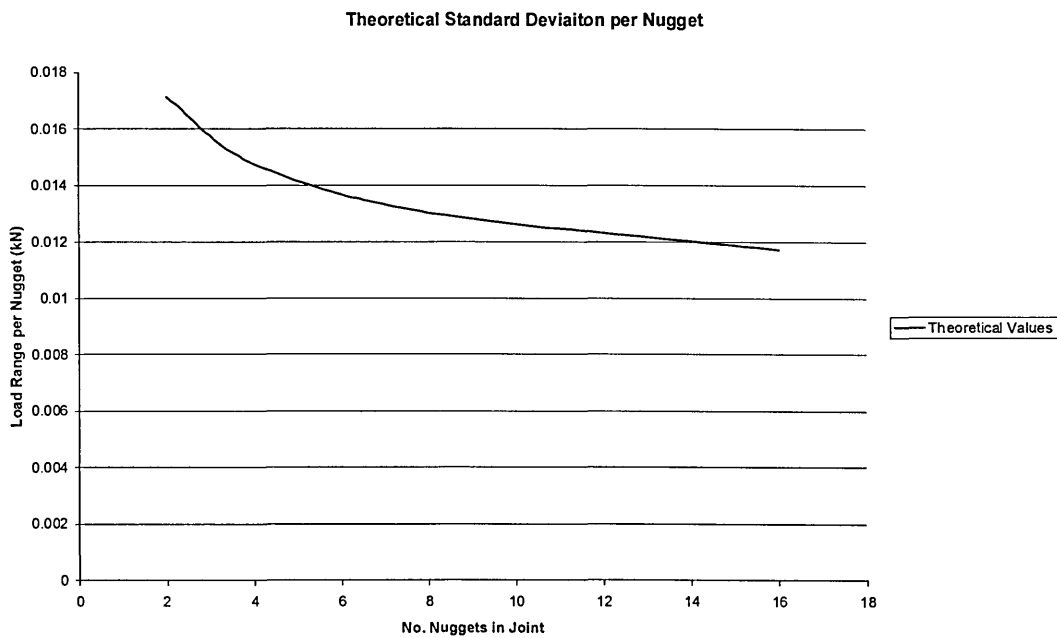
Fig 3.31: Changes in theoretical standard deviation of the fatigue strength distribution per spot weld as the number of welds increases.

3.3.8.4: Defining Failure in Multi-Spot Welded Joints.

As discussed in Section 2.3.9, fatigue failure of all the joints to be tested in this project is defined as the point when a single surface crack spans a distance equal to one pitch distance. With the single spot welded specimens this condition was easily monitored by observing the extremes of displacement achieved by the actuator during normal cycling and activating automatic trips when these increased by 1 mm, since this corresponded to a crack size equal to one pitch distance and would therefore stop the test the instant failure had occurred. However, since the multi-spot welded joints contained more than one weld nugget, a crack equal to one pitch distance over one of the weld nuggets would not necessarily cause any measurable change in displacement since the remaining spot welds would still offer a significant amount of support to the joint.

To monitor the size of any surface cracks in the multi-spot welded specimens, and determine when they had reached a large enough size to be categorised as failures, a new and unique monitoring system was developed. The system comprised of two banks of digital cameras (one for each side of the specimen) that were monitored by a computer using video monitoring software. The exact start time of every fatigue test was noted from the computers internal clock and recorded, the cameras were then positioned and the video monitoring software was activated.
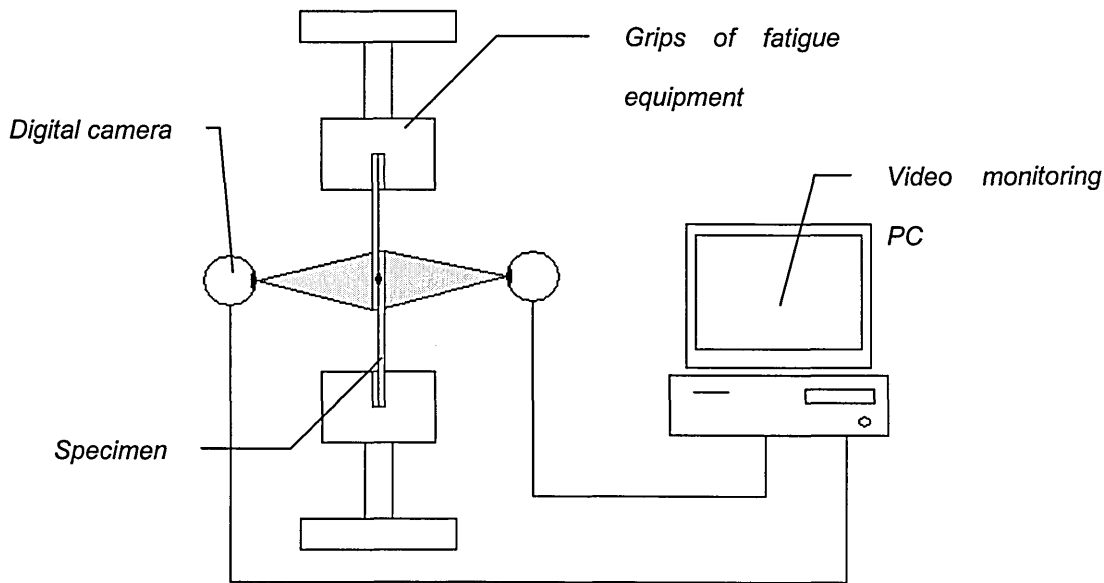
Fig 3.32: Schematic of the multi-spot welded joint monitoring system.

170

After each test the video footage was reviewed to determine the exact time when the conditions for failure had been met. Using this time, and the frequency of the testing process, the cycle life at failure could be easily calculated. If this cycle life was below the designed 10^6 cycles, then the specimen was classified as a failure, if it was above, the specimen was classified as a survivor.

Fig 3.33: Photograph of the computer display showing the camera views for a sixteen nugget

Staircase fatigue test.
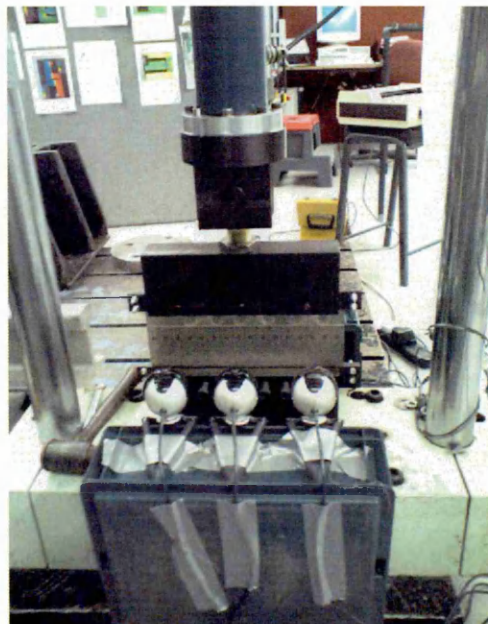
Fig 3.34: Photograph showing the three cameras that monitor one side of a sixteen nugget

Staircase fatigue test.
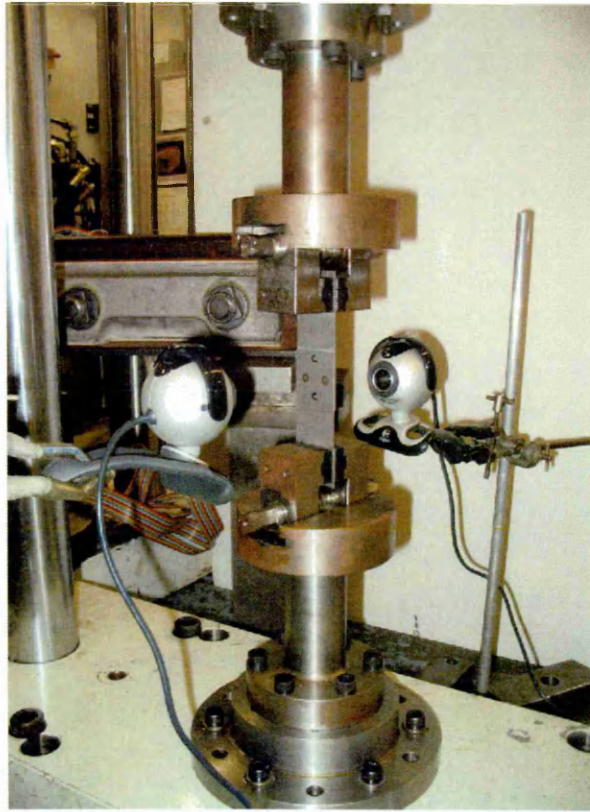
Fig 3.35: Photograph showing the two cameras used to monitor both sides of a double weld

Staircase fatigue test.

Fig 3.36: Photograph showing the video monitor equipment for a sixteen nugget fatigue test.

172

3.3.9: Additional Experiments.

The uniform distribution of load across each of the individual spot welds in the multi-spot welded joints was critical to having confidence in the proposed theory. It was believed that due to the slightly uneven cracking that was observed in some of the multi-spot welded joints that the load may not be balanced throughout each fatigue test and that, at some point, the load was possibly being redistributed unevenly, which would cast doubt on the independent nature of each welds survival probability. To obtain data that proved that the load distribution of the multi-spot welded joints was even across the entire width of each specimen for the duration of a fatigue test, a series of additional experiments were carried out using Thermoelastic Stress Analysis (TSA).

3.3.9.1: Thermoelastic Stress Analysis (TSA) [66].

When a substance is forced to change volume by the application of an external force it causes a change in temperature. This phenomenon, known as the 'thermoelastic effect' can be induced by either a compressive stress, which heats the substance, or a tensile stress, which cools the substance. Once the load is released, and assuming the substance has not been taken past its elastic limit, it returns to its original shape and temperature. The variation in temperature that occurs during a loading cycle can be used to identify and measure the intensity of stress fields for an Item Under Test (IUT).

For the process to work there must be no appreciable conduction of heat between the loading and unloading of the IUT. This is easily done by ensuring that the applied load is changed rapidly enough to minimise the time available for conduction to occur

The variations in temperature that occur during a loading cycle are in the order of $\pm 0.001^{\circ}C$ and so can only be detected by the most modern and sensitive infrared (IR) detectors. TSA uses a highly sensitive IR camera to record the thermal variations and generate an image of an IUT while it is subjected to an externally applied cyclic load. The image map is comprised of different colour intensities, which correspond to different amounts of thermal change and, hence, to the location and varying intensities of stresses. The downside of TSA is that it can only measure temperature change, and therefore stress intensity, on the surface of an IUT.

In order to determine if and when load redistribution was occurring, a TSA was carried out on 3 of the eight nugget specimens. Each of the specimens was subject to a fatigue test for 10^6 cycles, at an applied load range of 5.584 kN, which is equal to the mean fatigue strength plus one standard deviation of the fatigue strength distribution, according to the eight nugget Staircase results. This load was chosen as each specimen should theoretically have an 83.14% chance of failing before it reaches 10^6 cycles. This would mean a high chance of failure, but still ensured a long enough cycle life so that adequate data could be gathered. To ensure consistency with the experiments carried out earlier the testing was carried using the same equipment and settings as used before.

During each fatigue test a DeltaTherm 1000 TSA camera was used to monitor the stress fields present during the loading cycle. Once each test was started, the camera would record data for 10 minutes, after which point it would produce an imaged, based on the thermal data and loading signal from the fatigue equipment, which would indicate the average position and intensity of the stress fields over the last 10 minutes. An image was produced and recorded in this manner every 100,000 cycles, starting at 100,000 cycles, until the specimen failed by complete fracture.

The objectives of this experiment were to ensure that each of the nuggets was equally loaded at the beginning of each test. This would be done by analysing the size and position of each of the stress fields that should be present above each of the spot welds in the first image produced by the DeltaTherm. If each of the weld nuggets is supporting an equal portion of the overall load, then each of the stress fields should be equal in size to one another and should be emanating from a point directly adjacent to the boundary of the HAZ.

The second objective was to determine if, and when, the load was being redistributed. This was done by analysing the size and shape of the stress fields present on each of the images taken at the 100,000 cycle intervals. Variations in the size or shape of the stress fields, when compared to one another, could indicate a redistribution of load. If the load was being redistributed, then it could indicate that the survival of one weld was a conditional event, subject on there being other welds present to redistribute the load to, rather than being an independent event that was unaffected by the number of welds around it.

4: Results.

4.1: Base Material Characterisation.

The following two tables contain the results for the tensile testing and hardness testing that was carried out on four randomly selected sheets of the supplied AISI 301 in order to establish the base material mechanical properties.

		Sheet			
		1	2	3	4
		UTS (MPa)			
Specimen	1	1023.41	1016.34	1024.58	1008.95
	2	1020.83	1008.43	1012.36	1010.91
	3	994.04	1005.91	1003.46	1013.85
	4	1028.23	1020.83	1011.41	1006.98
	5	1019.43	1024.08	1022.85	1015.35
	Mean	*1017.19*	*1015.12*	*1014.93*	*1011.21*

Table 4.1: Tensile test results of the supplied AISI 301.

		Sheet			
		1	2	3	4
		HV_{20}			
Measurement	1	275	278	275	277
	2	275	274	272	269
	3	277	274	271	271
	4	272	269	275	274
	5	272	275	268	267
	Mean	*274.2*	*274*	*272.2*	*271.6*

Table 4.2: Vickers hardness test results for the supplied AISI 301.

175

4.2: Weldability Study.

The following table displays the individual lap-shear failure loads obtained from the five joints welded using each set of the different parameter values used in the weldability study. The values for group mean, minimum failure load, maximum failure load, and range determined from the five specimens tested at each parameter set are also shown.

			Welding Time (Cycles)				
			10	15	20	25	30
			Failure Load (kN)				
Welding Current (kAmps)	3.6	Specimen 1	6.616	6.483	5.939	5.903	5.774
		Specimen 2	6.737	6.467	6.270	6.092	5.911
		Specimen 3	6.853	6.467	6.193	6.052	5.976
		Specimen 4	6.793	6.419	6.193	5.907	5.710
		Specimen 5	6.704	6.640	6.133	5.931	5.613
		Mean Value	*6.741*	*6.495*	*6.146*	*5.977*	*5.797*
		Min Value	6.616	6.419	5.939	5.903	5.613
		Max Value	6.853	6.640	6.270	6.092	5.976
		Range	0.237	0.221	0.331	0.189	0.363
		Range (% of Mean)	3.52	3.40	5.39	3.16	6.26
	3.8	Specimen 1	7.240	7.099	6.584	6.451	6.511
		Specimen 2	7.457	7.107	6.725	6.495	6.237
		Specimen 3	7.212	6.970	6.833	6.487	6.290
		Specimen 4	7.494	6.902	6.636	6.487	6.213
		Specimen 5	7.361	6.922	6.797	6.564	6.390
		Mean Value	*7.353*	*7.000*	*6.715*	*6.497*	*6.328*
		Min Value	7.212	6.902	6.584	6.451	6.213
		Max Value	7.494	7.107	6.833	6.564	6.511
		Range	0.282	0.205	0.249	0.113	0.298
		Range (% of Mean)	3.84	2.93	3.71	1.74	4.71
	4.0	Specimen 1	8.448	7.377	7.002	7.224	6.692
		Specimen 2	8.380	7.433	7.127	7.184	6.853
		Specimen 3	8.372	7.357	7.228	7.027	6.833
		Specimen 4	7.933	7.333	7.236	6.974	6.914
		Specimen 5	7.977	7.425	7.119	7.208	6.717
		Mean Value	*8.222*	*7.385*	*7.142*	*7.123*	*6.802*
		Min Value	7.933	7.333	7.002	6.974	6.692
		Max Value	8.448	7.433	7.236	7.224	6.914
		Range	0.515	0.100	0.234	0.250	0.222
		Range (% of Mean)	6.26	1.35	3.28	3.51	3.26

Table 4.3: Lap-shear results for weldability study.

			Welding Time (Cycles)				
			10	15	20	25	30
			Failure Load (kN)				
Welding Current (kAmps)	4.2	Specimen 1	8.468	8.037	7.586	7.474	7.337
		Specimen 2	7.470	8.049	7.731	7.635	7.292
		Specimen 3	8.464	7.981	7.619	7.554	7.284
		Specimen 4	8.690	7.892	7.764	7.627	7.309
		Specimen 5	8.806	8.013	7.953	7.566	7.401
		Mean Value	*8.380*	*7.994*	*7.731*	*7.571*	*7.325*
		Min Value	7.470	7.892	7.586	7.474	7.284
		Max Value	8.806	8.049	7.953	7.635	7.401
		Range	1.336	0.157	0.367	0.161	0.117
		Range (% of Mean)	15.94	1.96	4.75	2.13	1.60
	4.4	Specimen 1	7.063	8.440	8.255	8.335	7.808
		Specimen 2	9.431	8.718	8.448	8.271	8.227
		Specimen 3	9.213	8.484	8.311	8.291	7.953
		Specimen 4	7.333	8.376	8.408	8.090	7.981
		Specimen 5	7.635	8.694	8.484	8.231	8.134
		Mean Value	*8.135*	*8.542*	*8.381*	*8.244*	*8.021*
		Min Value	7.063	8.376	8.255	8.090	7.808
		Max Value	9.431	8.718	8.484	8.335	8.227
		Range	2.368	0.342	0.229	0.245	0.419
		Range (% of Mean)	29.11	4.00	2.73	2.97	5.22
	4.6	Specimen 1	7.309	9.261	9.040	8.951	8.609
		Specimen 2	7.691	9.044	9.076	8.754	8.649
		Specimen 3	8.098	9.084	8.931	8.968	8.714
		Specimen 4	7.651	9.036	9.137	8.851	8.738
		Specimen 5	7.204	9.247	9.004	8.859	8.557
		Mean Value	*7.591*	*9.134*	*9.038*	*8.877*	*8.653*
		Min Value	7.204	9.036	8.931	8.754	8.557
		Max Value	8.098	9.261	9.137	8.968	8.738
		Range	0.894	0.225	0.206	0.214	0.181
		Range (% of Mean)	11.78	2.46	2.28	2.41	2.09

Table 4.4: Lap-shear results for weldability study continued.

Fig 4.1 below shows the variation in the mean lap-shear failure load for joints welded at each of the different parameter values investigated in the weldability study.

3D Contour Map of Failure Load versus Welding Parameter Values
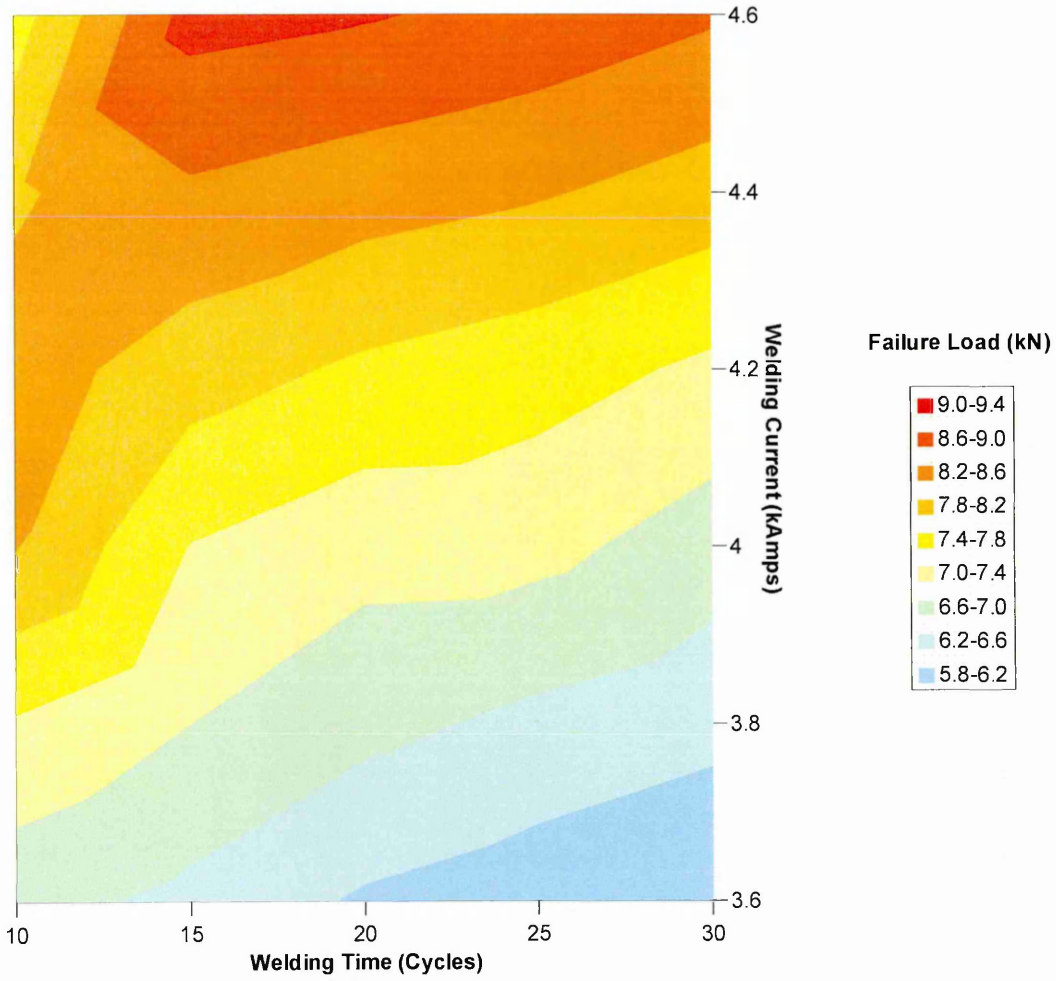
Fig 4.1: Variation in Weld strength with changes to spot welding parameters.

Fig 4.2 below shows the variation in the range of values obtained from the five specimen joints welded at each of the different parameter value sets investigated in the weldability study.

Varitation in Range for Different Welding Parameter Values
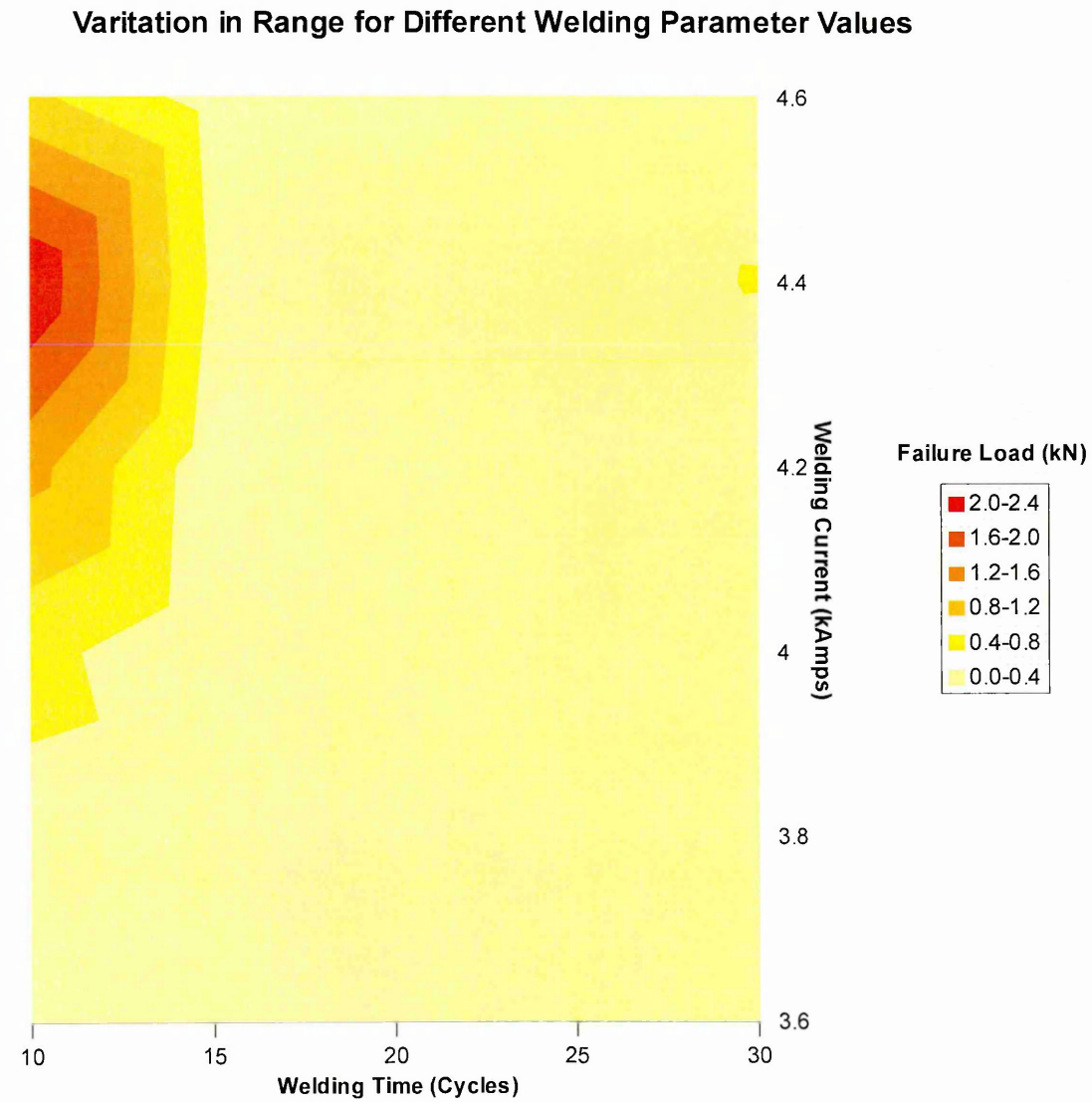
Fig 4.2: Consistency of weld strength with changes to spot welding parameters.

4.3: Optimum Pitch Distance Study.

4.3.1: Variation in Nugget Strength.

The following two tables display the lap-shear failure loads obtained from the individual spot welds taken from each of the three joints welded at each of the different pitch distances under investigation. The values for group mean, minimum failure load, maximum failure load, and range, determined for each of the welds taken from the three samples tested, are also shown.

			Weld Position				
			1	2	3	4	5
Pitch Distance (mm)	12.5	Specimen 1	7.623	7.107	8.033	8.15	8.21
		Specimen 2	8.504	8.082	8.311	8.017	7.639
		Specimen 3	8.029	8.279	8.029	8.335	7.908
		Mean	*8.052*	*7.823*	*8.124*	*8.167*	*7.919*
		Min Value	7.623	7.107	8.029	8.017	7.639
		Max Value	8.504	8.279	8.311	8.335	8.210
		Range	0.881	1.172	0.282	0.318	0.571
		Range (% of Mean)	10.94	14.98	3.47	3.89	7.21
	15	Specimen 1	8.657	8.517	8.315	8.315	8.186
		Specimen 2	8.303	8.263	8.368	8.392	8.166
		Specimen 3	8.601	8.364	8.376	8.017	8.372
		Mean	*8.520*	*8.381*	*8.353*	*8.241*	*8.241*
		Min Value	8.303	8.263	8.315	8.017	8.166
		Max Value	8.657	8.517	8.376	8.392	8.372
		Range	0.354	0.254	0.061	0.375	0.206
		Range (% of Mean)	4.15	3.03	0.73	4.55	2.50

Table 4.5: Lap-shear results for variation in weld strength study for pitch distances of 12.5 mm and 15 mm.

180

			Weld Position				
			1	2	3	4	5
Pitch Distance (mm)	17.5	Specimen 1	8.400	8.118	8.271	8.504	8.504
		Specimen 2	8.802	8.629	8.621	8.605	8.633
		Specimen 3	8.778	8.239	8.557	8.448	8.283
		Mean	*8.660*	*8.329*	*8.483*	*8.519*	*8.473*
		Min Value	8.400	8.118	8.271	8.448	8.283
		Max Value	8.802	8.629	8.621	8.605	8.633
		Range	0.402	0.511	0.350	0.157	0.350
		Range (% of Mean)	4.64	6.14	4.13	1.84	4.13
	20	Specimen 1	8.702	8.408	8.053	8.210	8.335
		Specimen 2	8.645	8.154	7.989	8.098	8.001
		Specimen 3	8.907	8.593	8.573	8.476	8.440
		Mean	*8.751*	*8.385*	*8.205*	*8.261*	*8.259*
		Min Value	8.645	8.154	7.989	8.098	8.001
		Max Value	8.907	8.593	8.573	8.476	8.440
		Range	0.262	0.439	0.584	0.378	0.439
		Range (% of Mean)	2.99	5.24	7.12	4.58	5.32
	30	Specimen 1	8.605	8.283	8.343	8.315	8.202
		Specimen 2	8.682	8.283	8.492	8.396	8.247
		Specimen 3	8.553	8.247	8.263	8.130	8.283
		Mean	*8.613*	*8.271*	*8.366*	*8.280*	*8.244*
		Min Value	8.553	8.247	8.263	8.130	8.202
		Max Value	8.682	8.283	8.492	8.396	8.283
		Range	0.129	0.036	0.229	0.266	0.081
		Range (% of Mean)	1.50	0.44	2.74	3.21	0.98
	40	Specimen 1	8.545	8.335	8.545	8.202	8.239
		Specimen 2	8.702	8.492	8.452	8.376	8.339
		Specimen 3	8.432	8.488	8.376	8.714	8.388
		Mean	*8.560*	*8.438*	*8.458*	*8.431*	*8.322*
		Min Value	8.432	8.335	8.376	8.202	8.239
		Max Value	8.702	8.492	8.545	8.714	8.388
		Range	0.270	0.157	0.169	0.512	0.149
		Range (% of Mean)	3.15	1.86	2.00	6.07	1.79
	50	Specimen 1	8.653	8.549	8.331	8.327	8.706
		Specimen 2	8.867	8.456	8.327	8.396	8.174
		Specimen 3	8.581	8.215	8.436	8.291	8.331
		Mean	*8.700*	*8.407*	*8.365*	*8.338*	*8.404*
		Min Value	8.581	8.215	8.327	8.291	8.174
		Max Value	8.867	8.549	8.436	8.396	8.706
		Range	0.286	0.334	0.109	0.105	0.532
		Range (% of Mean)	3.29	3.97	1.30	1.26	6.33

Table 4.6: Lap-shear results for variation in weld strength study for pitch distances of 17.5 mm, 20 mm, 30 mm, 40 mm and 50 mm.

The following sections display images of the lap-shear failures for each of the individual welds taken from the three samples tested at each pitch distance being investigated. The mean lap-shear values for each weld from the three samples are also presented in a graph, which shows the change in strength between welds made in the same series.

4.3.1: 12.5 mm Pitch Specimens.
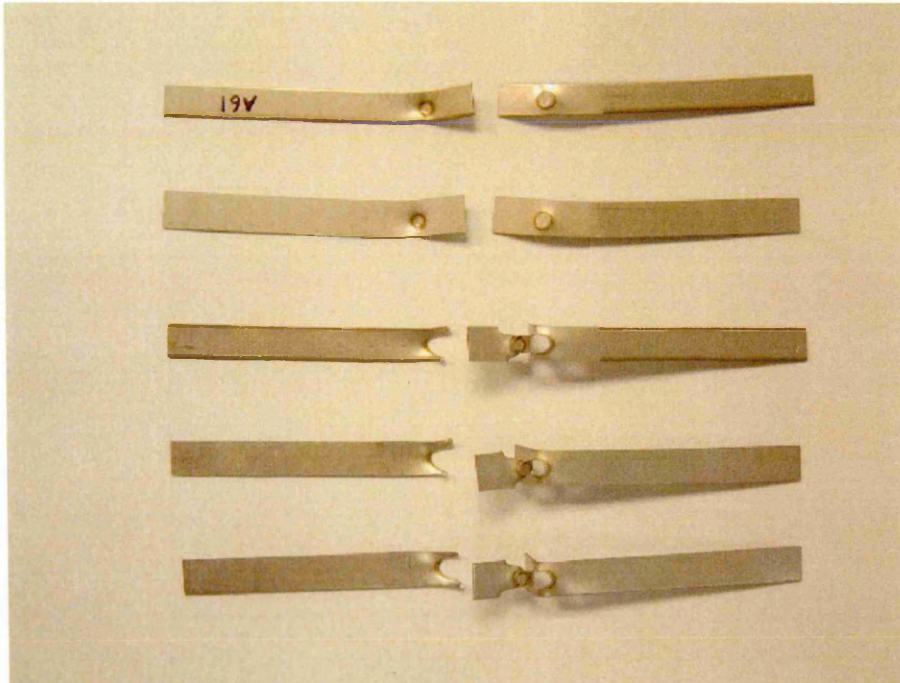
Fig 4.3: Sample 1 with weld positions running in sequence from top to bottom.
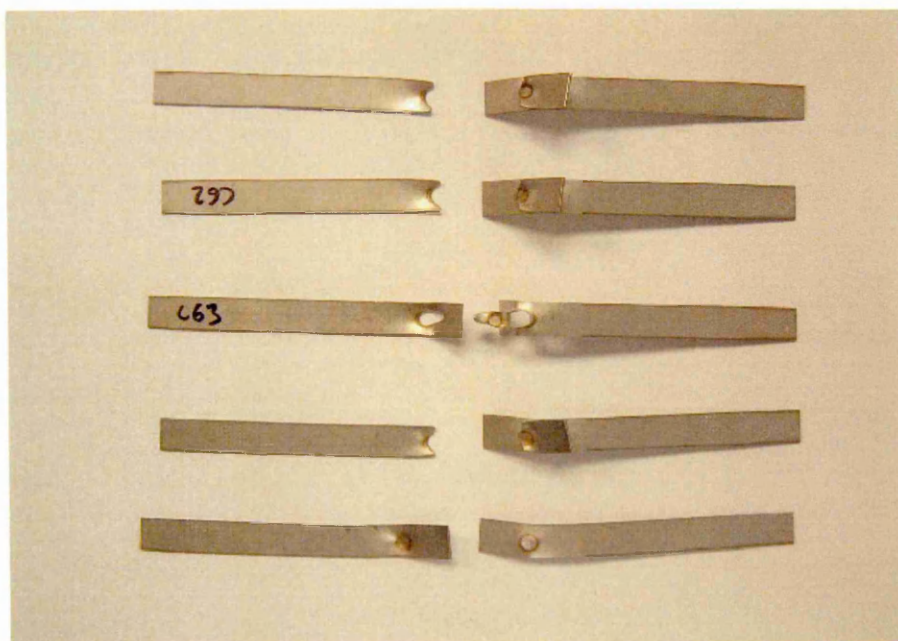
Fig 4.4: Sample 2 with weld positions running in sequence from top to bottom.
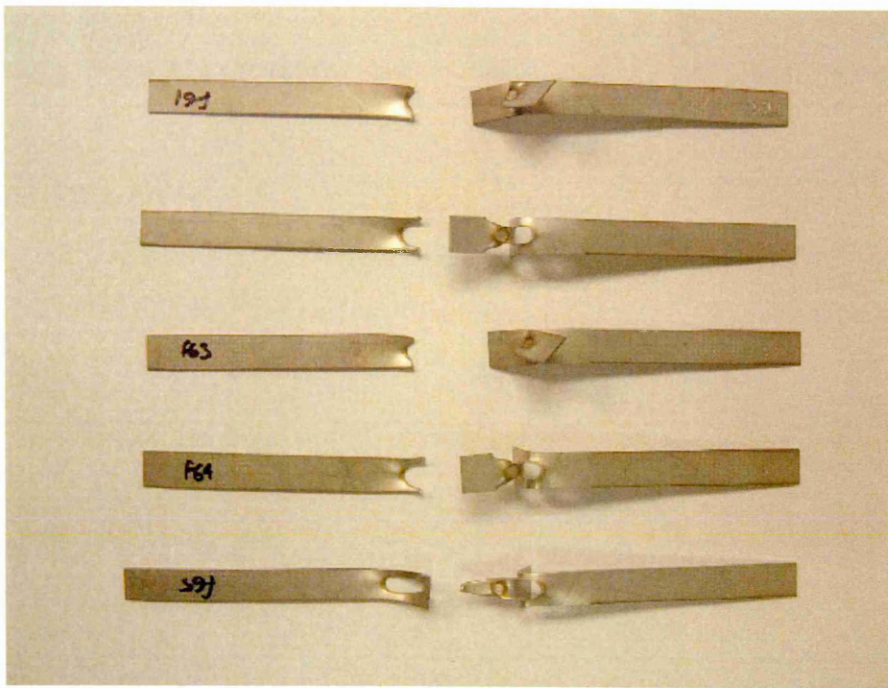
182

Fig 4.5: Sample 3 with weld positions running in sequence from top to bottom.

Variation in Nugget Strength at 12.5mm Pitch
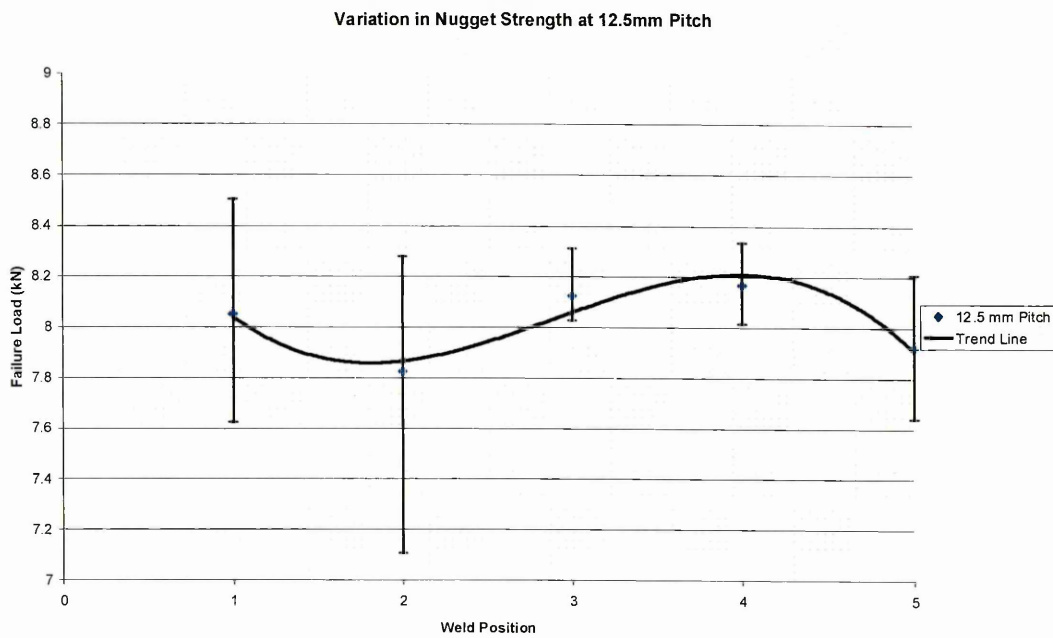
Fig 4.6: Variation in nugget strength at 12.5 mm pitch.

4.3.1.2: 15 mm Pitch Specimens.
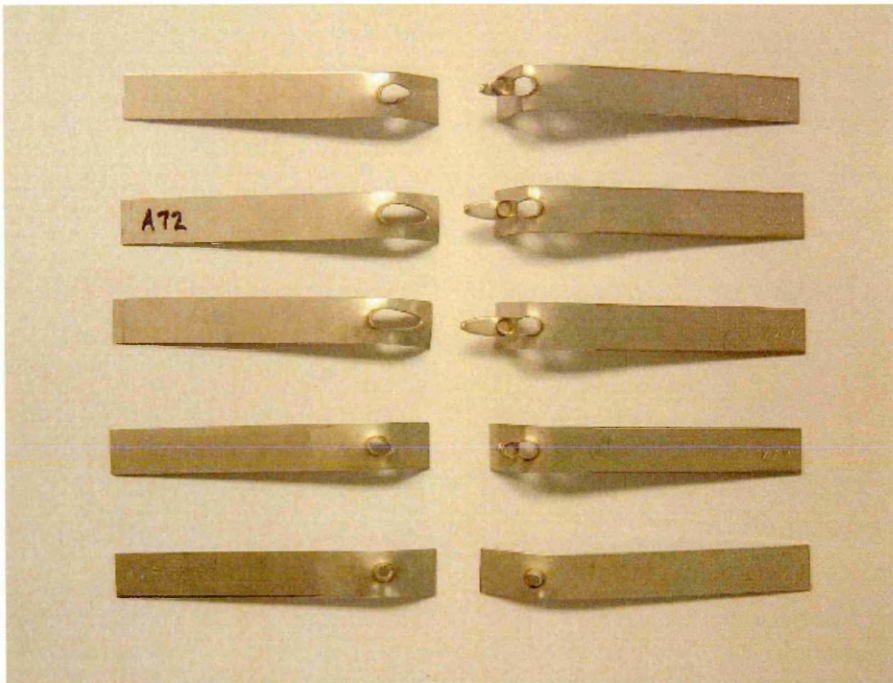
Fig 4.7: Sample 1 with weld positions running in sequence from top to bottom.
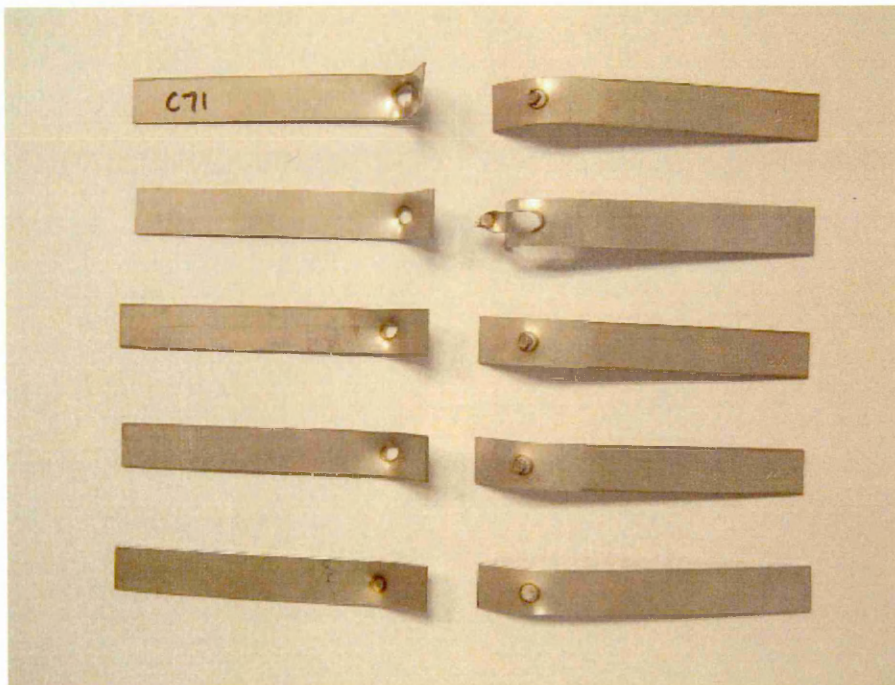
Fig 4.8: Sample 2 with weld positions running in sequence from top to bottom.

184
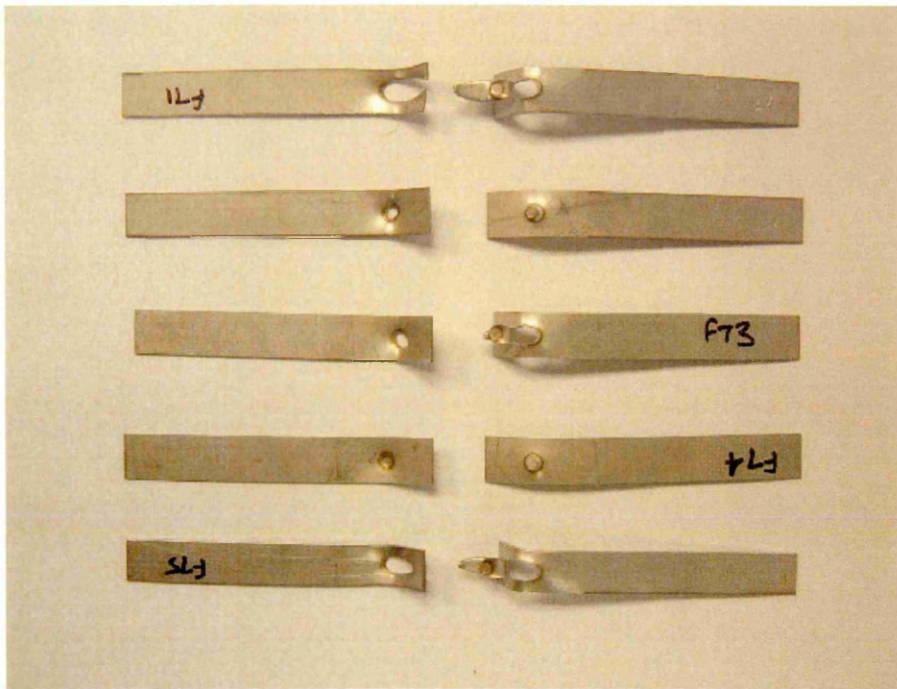
Fig 4.9: Sample 3 with weld positions running in sequence from top to bottom.
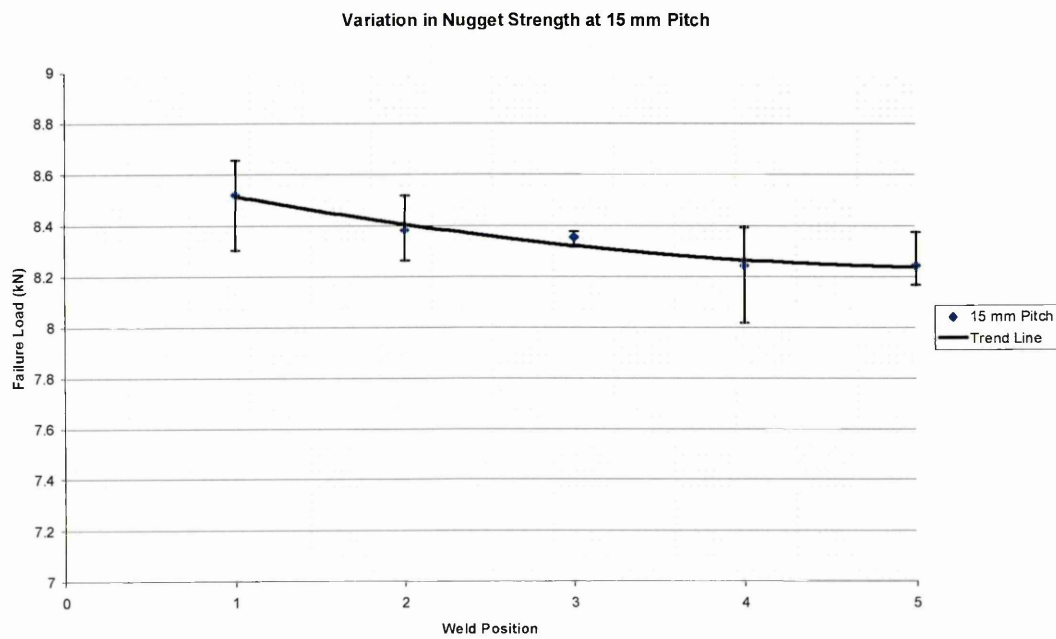
Fig 4.10: Variation in nugget strength at 15 mm pitch.

4.3.1.3: 17.5 mm Pitch Specimens.
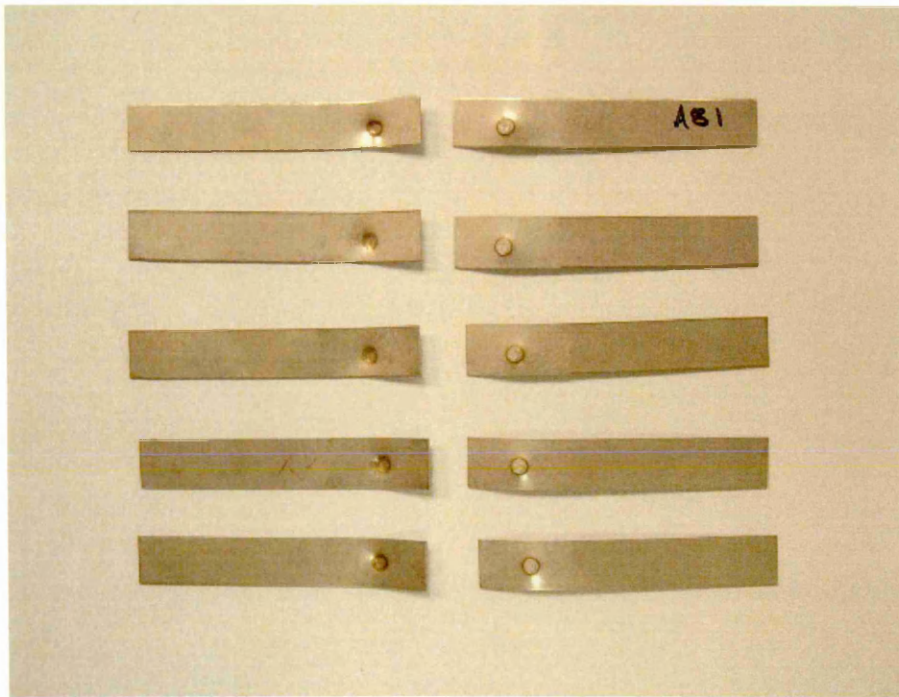
Fig 4.11: Sample 1 with weld positions running in sequence from top to bottom.
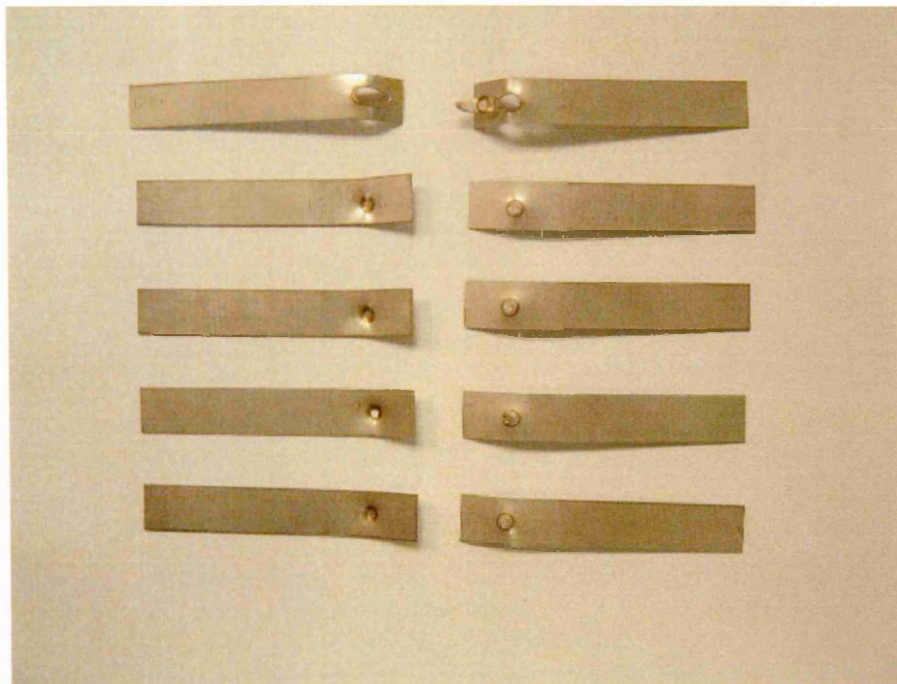
Fig 4.12: Sample 2 with weld positions running in sequence from top to bottom.
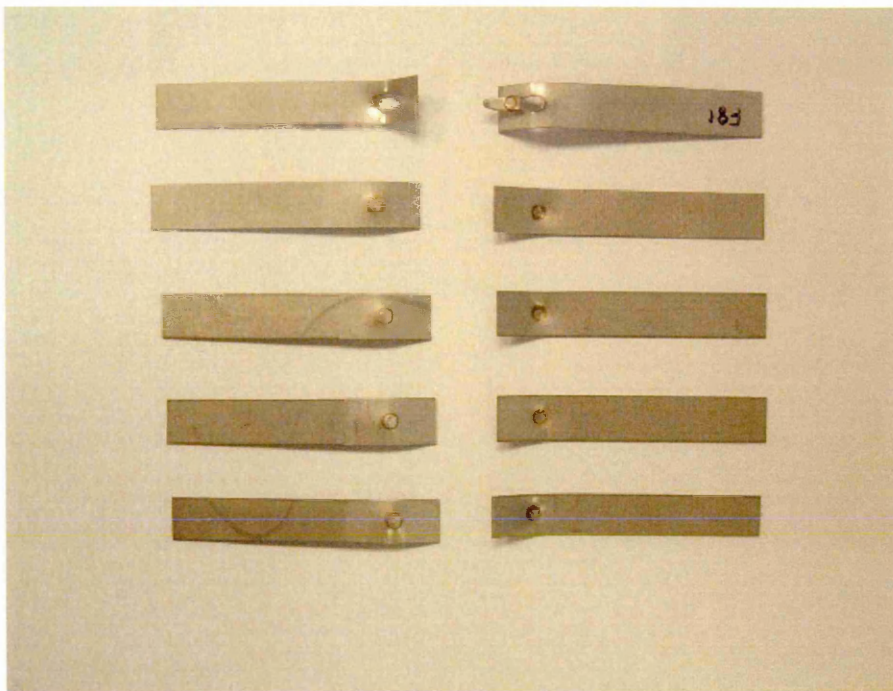
Fig 4.13: Sample 3 with weld positions running in sequence from top to bottom.

Variation in Nugget Strength at 17.5 mm Pitch
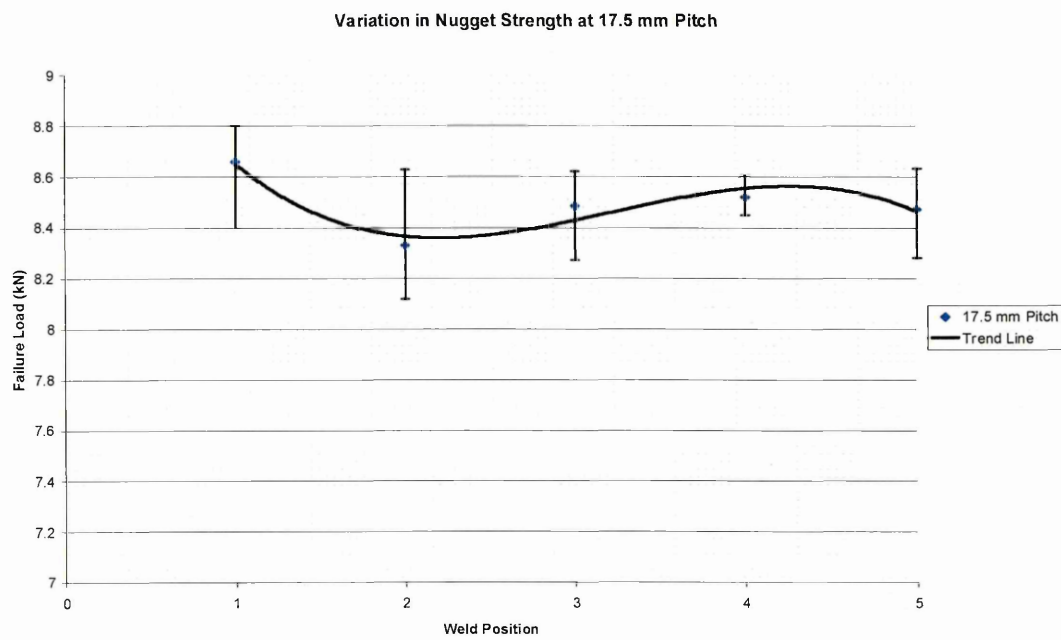
Fig 4.14: Variation in nugget strength at 17.5 mm pitch.

187

4.3.1.4: 20 mm Pitch Specimens.
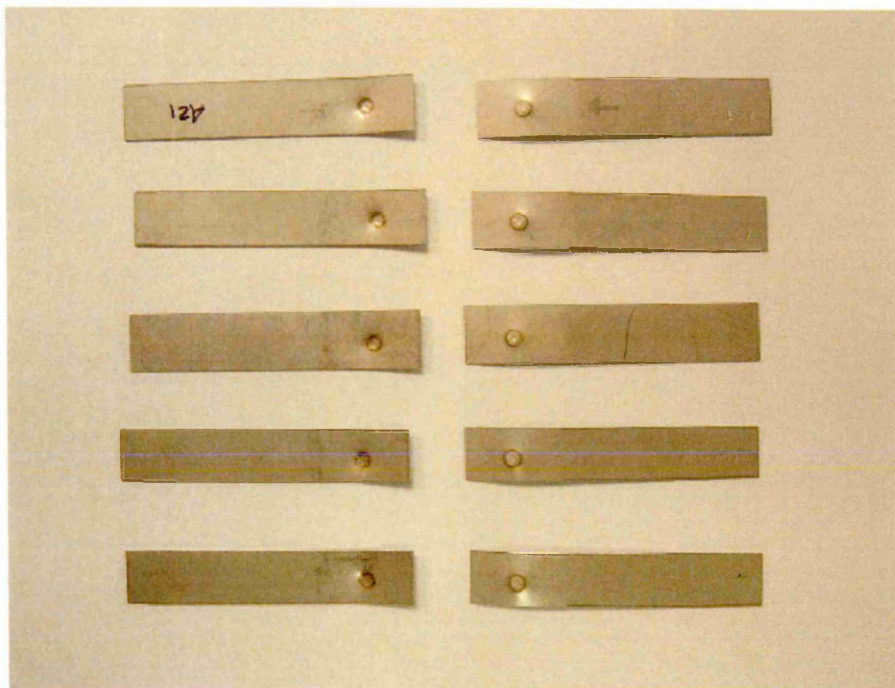
Fig 4.15: Sample 1 with weld positions running in sequence from top to bottom.
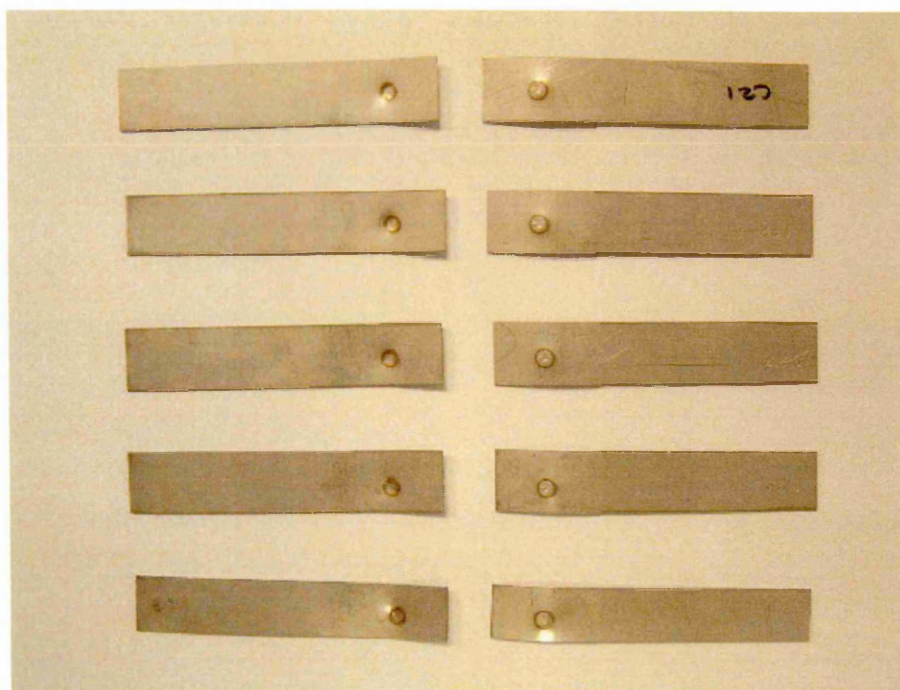
Fig 4.16: Sample 2 with weld positions running in sequence from top to bottom.

188
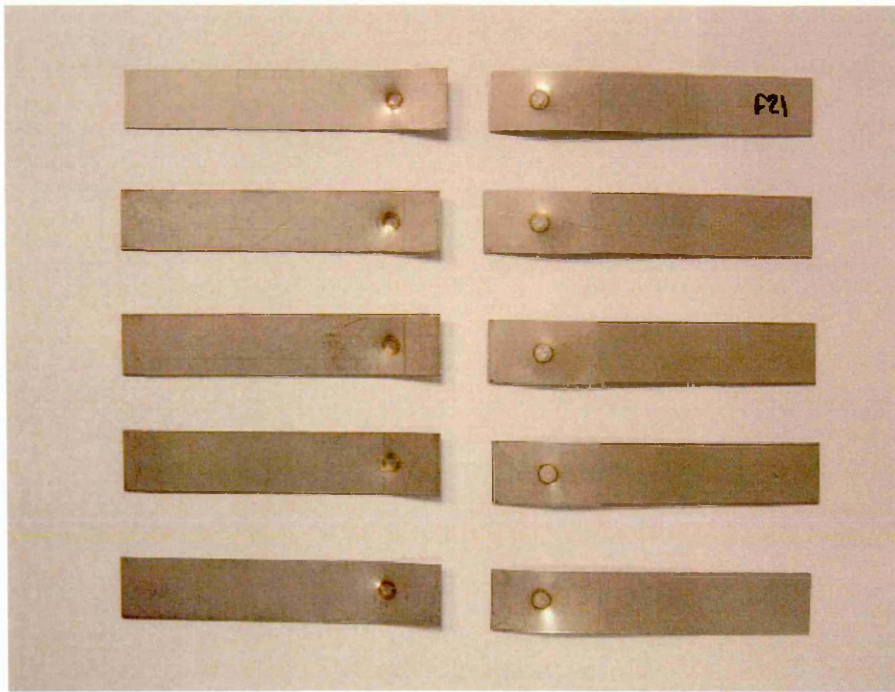
Fig 4.17: Sample 3 with weld positions running in sequence from top to bottom.
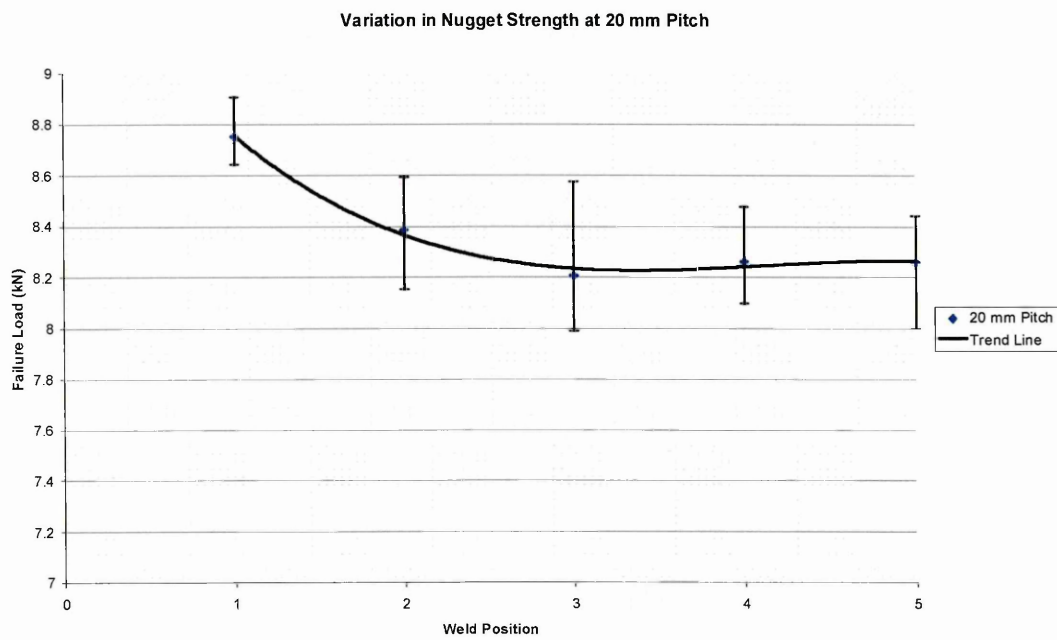
Fig 4.18: Variation in nugget strength at 20 mm pitch.

4.3.1.5: 30 mm Pitch Specimens.
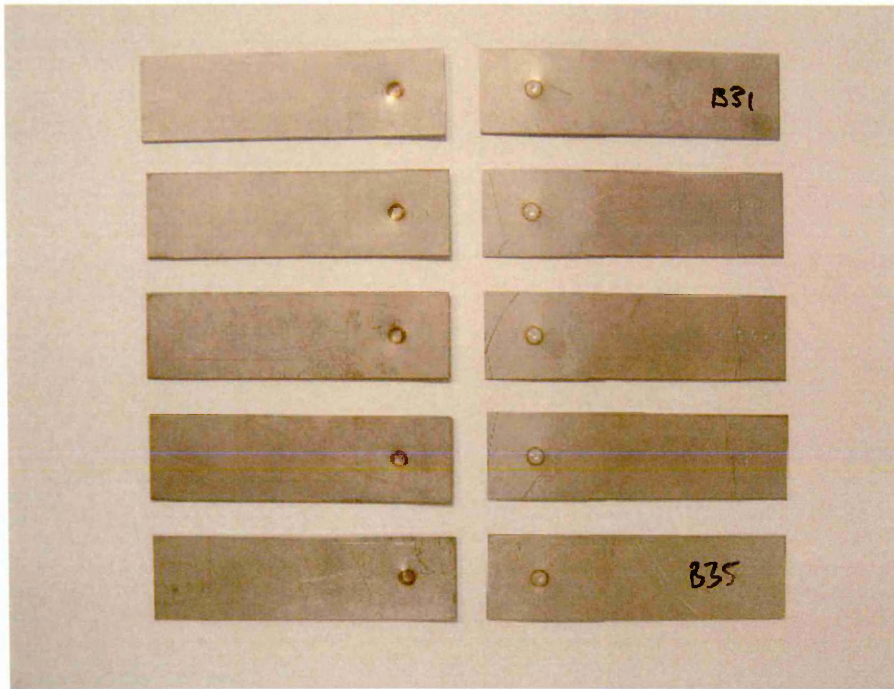
Fig 4.19: Sample 1 with weld positions running in sequence from top to bottom.
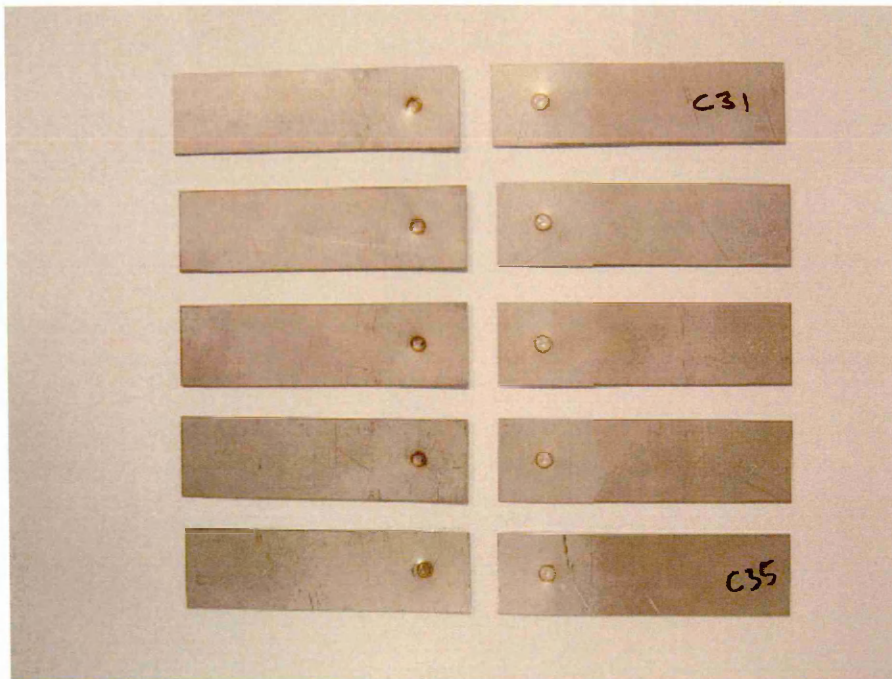
Fig 4.20: Sample 2 with weld positions running in sequence from top to bottom.
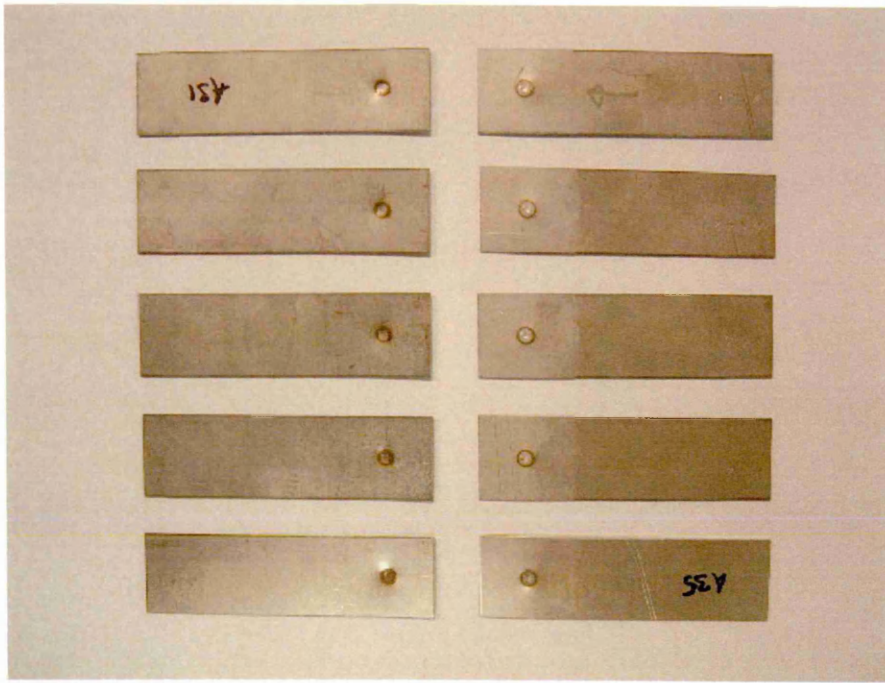
Fig 4.21: Sample 3 with weld positions running in sequence from top to bottom.
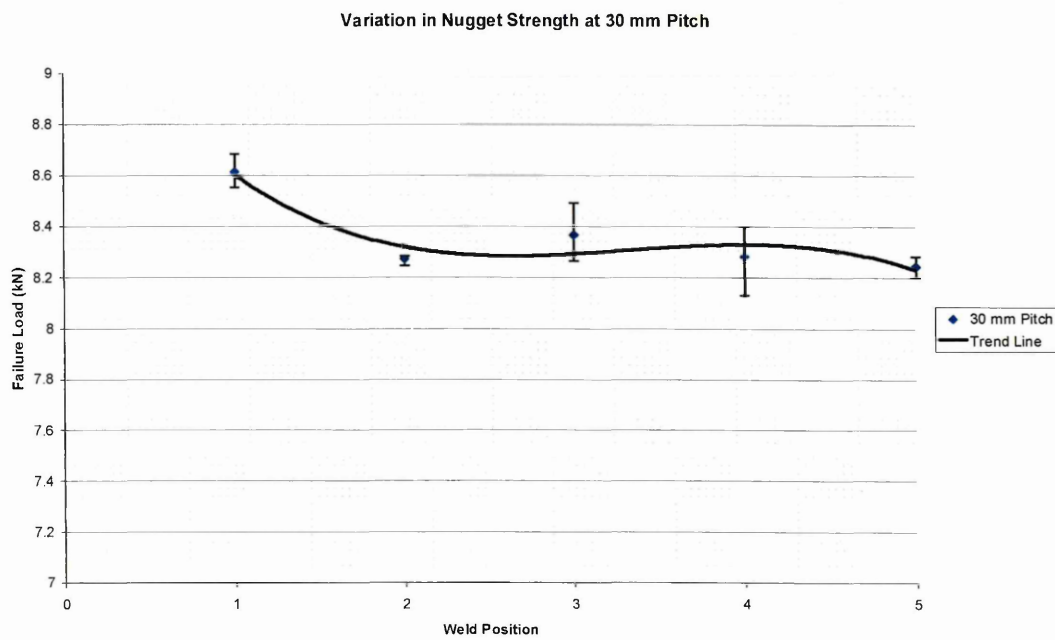
Fig 4.22: Variation in nugget strength at 30 mm pitch.

4.3.1.6: 40 mm Pitch Specimens.
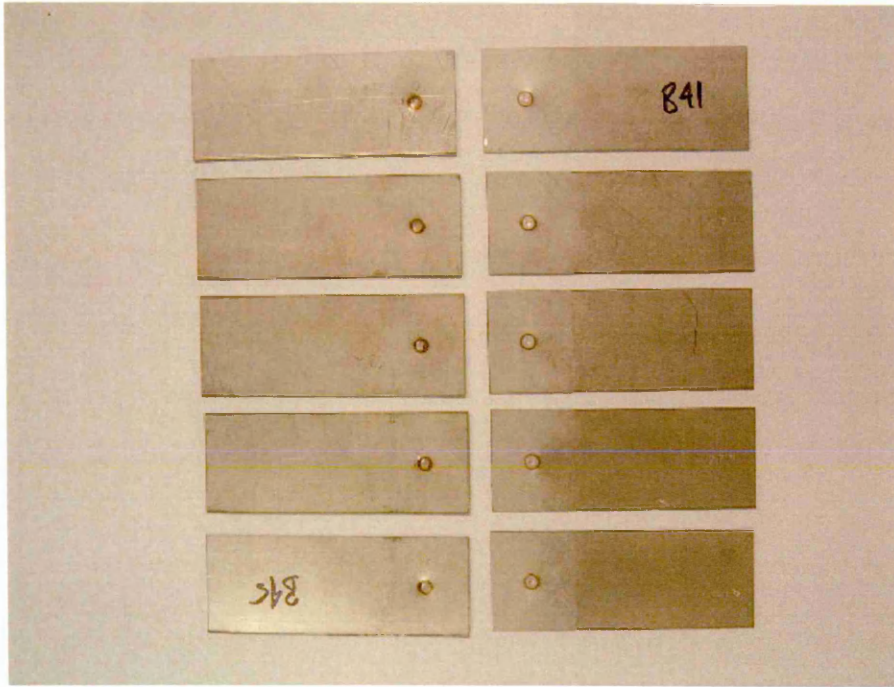
Fig 4.23: Sample 1 with weld positions running in sequence from top to bottom.
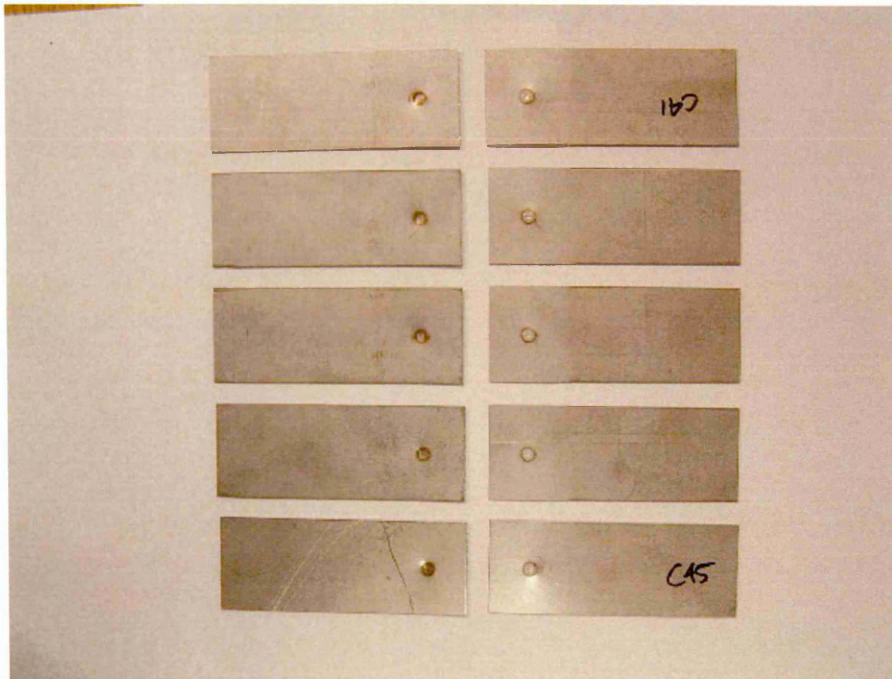
Fig 4.24: Sample 2 with weld positions running in sequence from top to bottom.
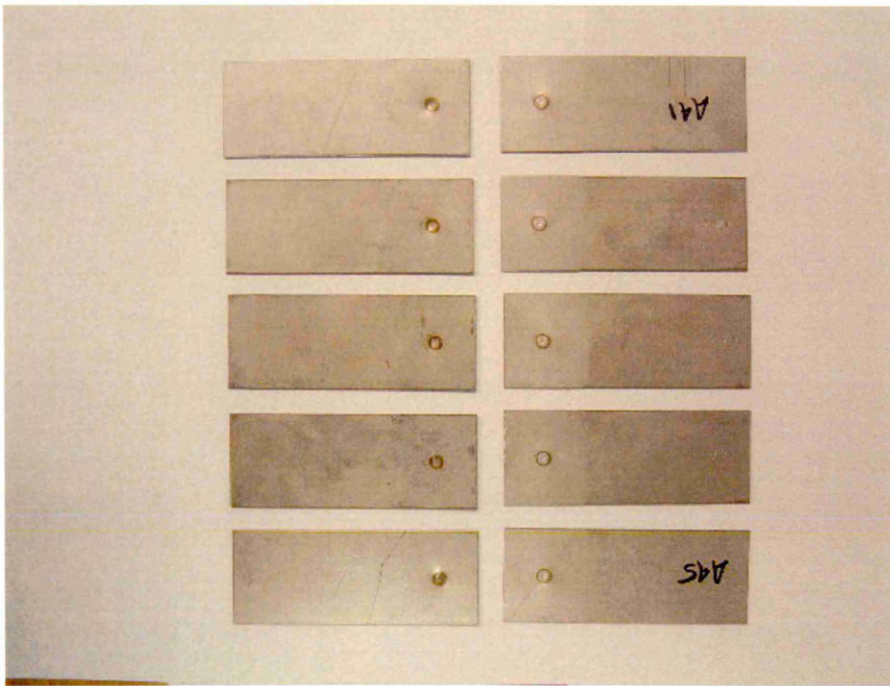
Fig 4.25: Sample 3 with weld positions running in sequence from top to bottom.
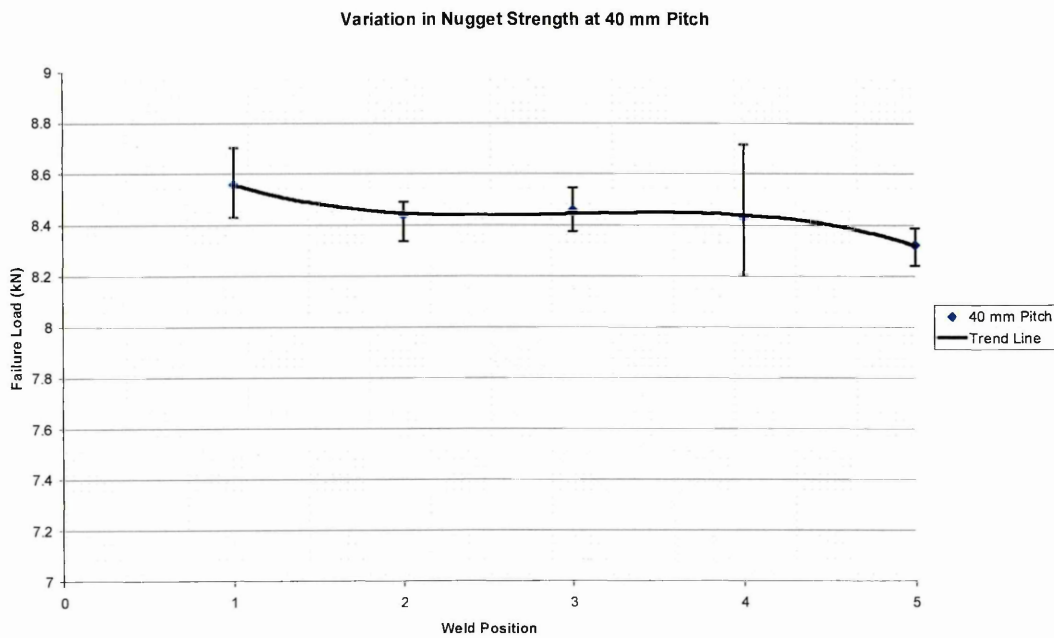
Fig 4.26: Variation in nugget strength at 40 mm pitch.

4.3.1.7: 50 mm Pitch Specimens.
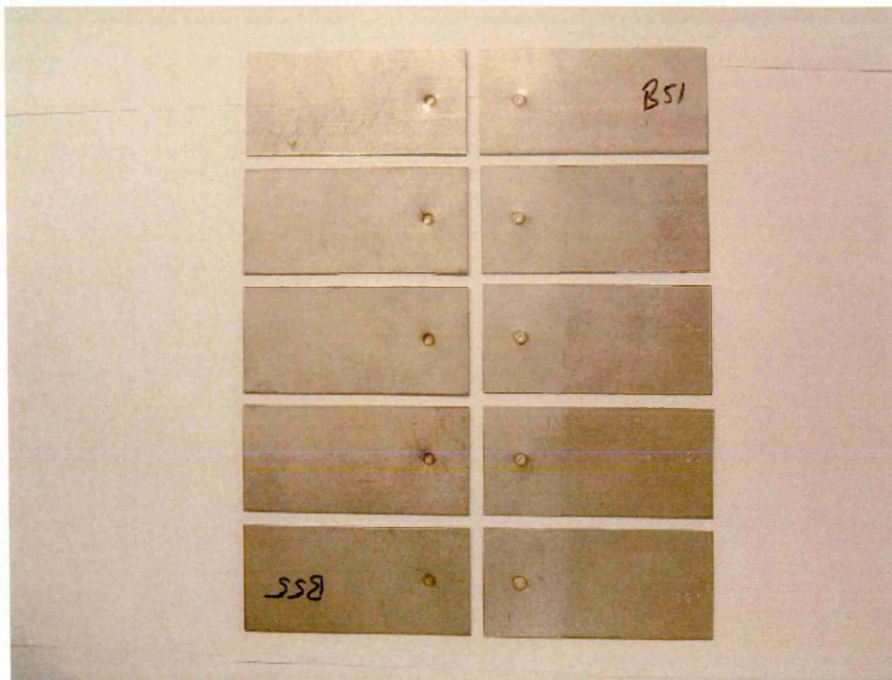
Fig 4.27: Sample 1 with weld positions running in sequence from top to bottom.
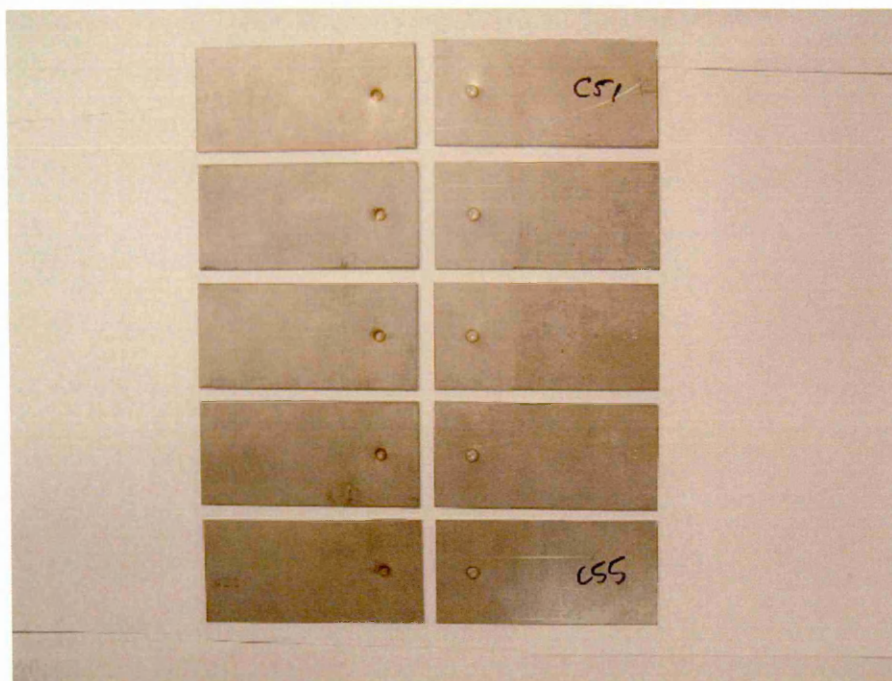
Fig 4.28: Sample 2 with weld positions running in sequence from top to bottom.
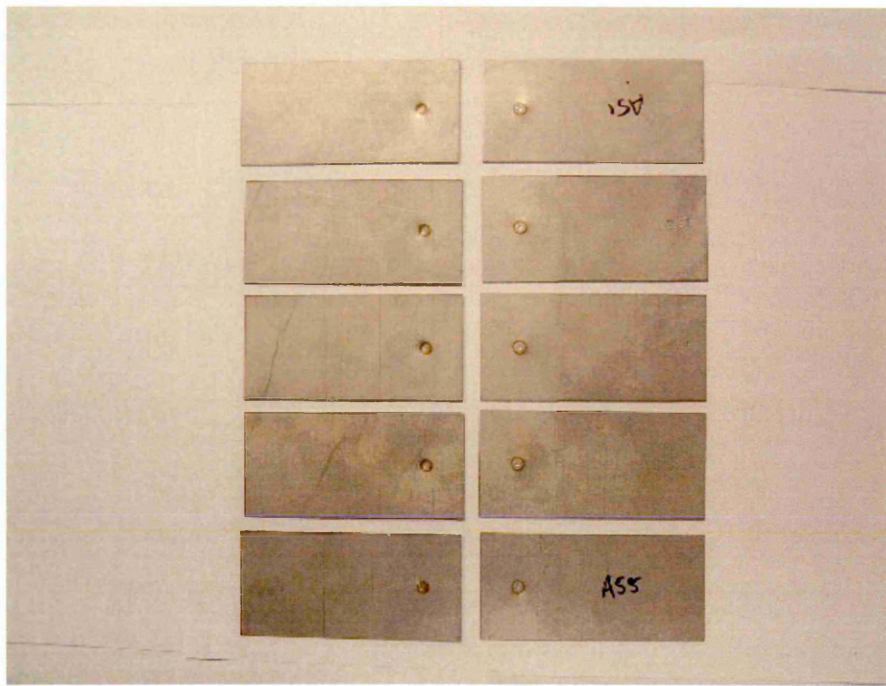
Fig 4.29: Sample 3 with weld positions running in sequence from top to bottom.
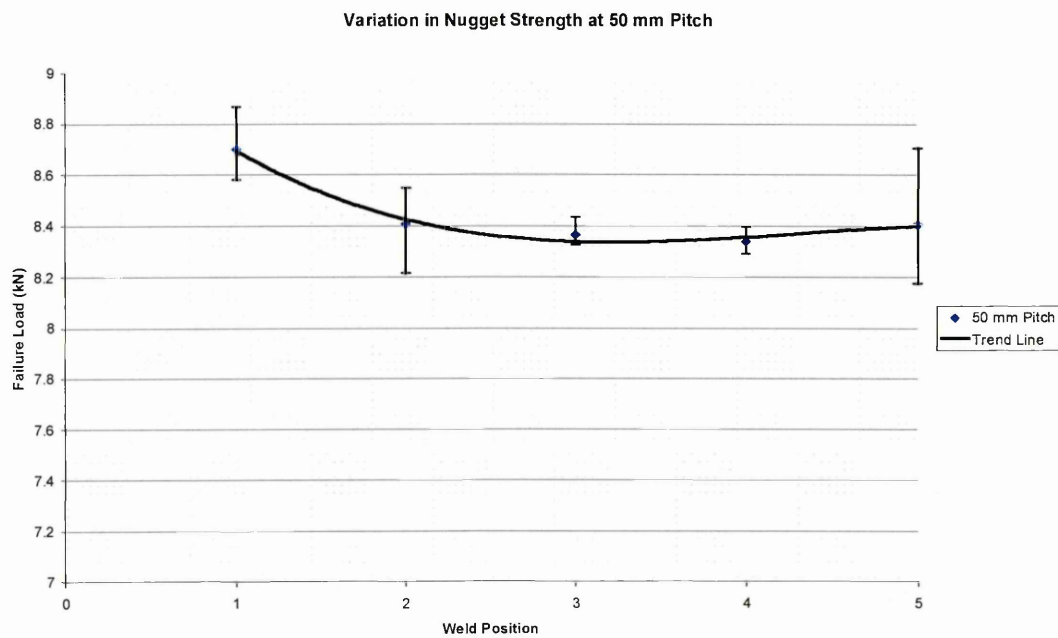
Fig 4.30: Variation in nugget strength at 50 mm pitch.

195

4.3.2: Variation in Nugget Diameter.

The table below shows the measured diameter of each weld taken from one of the samples welded at each of the pitch distances being investigated.

		Pitch Distance (mm)						
		12.5	15	17.5	20	30	40	50
		Nugget Diameter (mm)						
Weld Position	1	4.56	4.39	4.48	4.38	4.28	4.44	4.37
	2	4.46	4.42	4.48	4.4	4.53	4.31	4.4
	3	4.41	4.4	4.43	4.37	4.37	4.42	4.45
	4	4.39	4.41	4.53	4.28	4.51	4.53	4.35
	5	4.54	4.33	4.52	4.4	4.44	3.93	4.56

Table 4.7: Variation in nugget diameter at various pitch distances.

The following images are those taken by the optical microscope and used to determine the diameter of each of the welds tested. Each group of images concludes with a graph which shows the variation in weld diameter between welds made in the same series at a given pitch distance.

4.3.2.1: 12.5 mm Pitch Specimens.

Fig 4.31: Weld 1.

Fig 4.32: Weld 2.
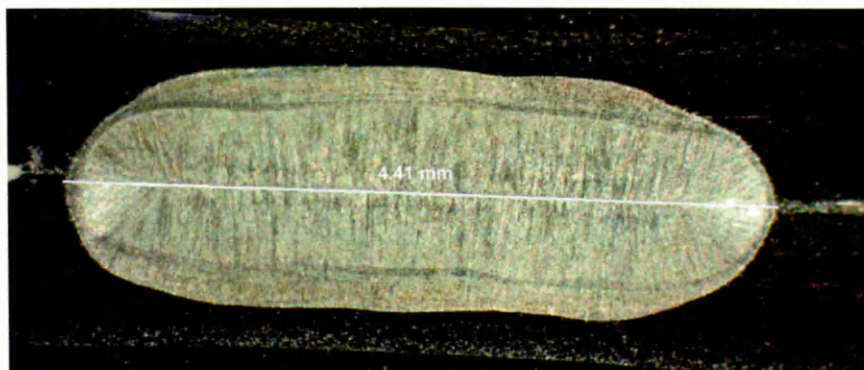
Fig 4.33: Weld 3.
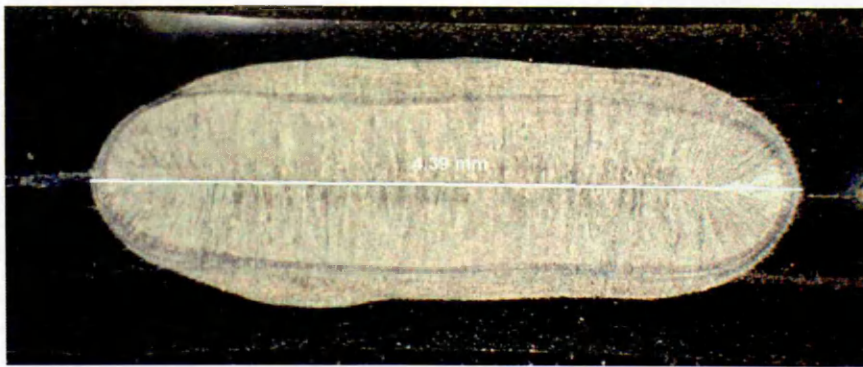
Fig 4.34: Weld 4.

Fig 4.35: Weld 5.

Variation in Nugget Diamter at 12.5mm Pitch
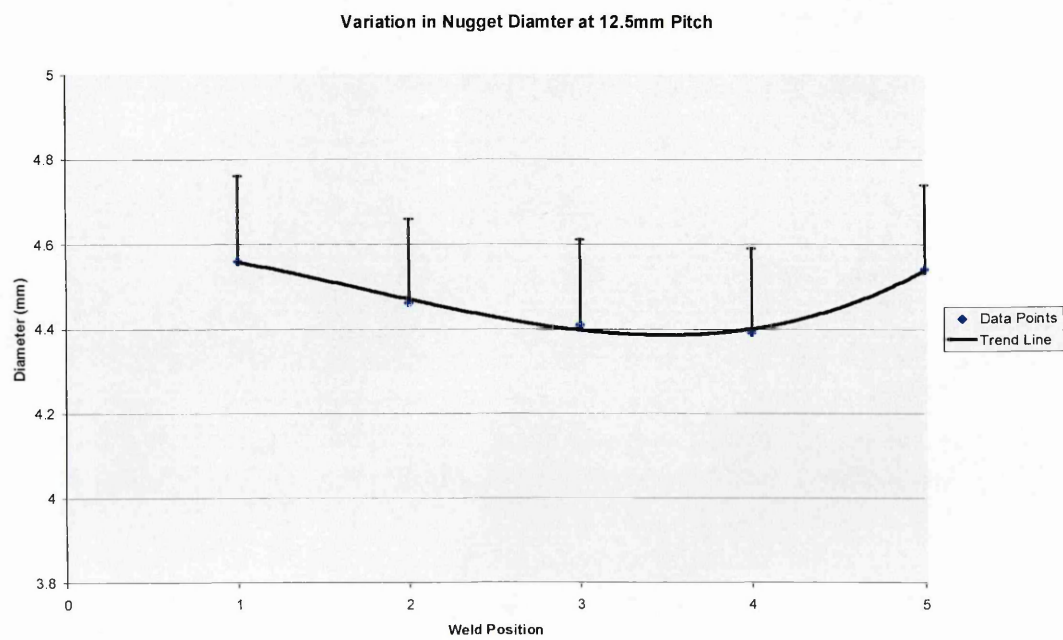
Fig 4.36: Variation in nugget diameter at 12.5 mm pitch.

4.3.2.2: 15 mm Pitch Specimens.
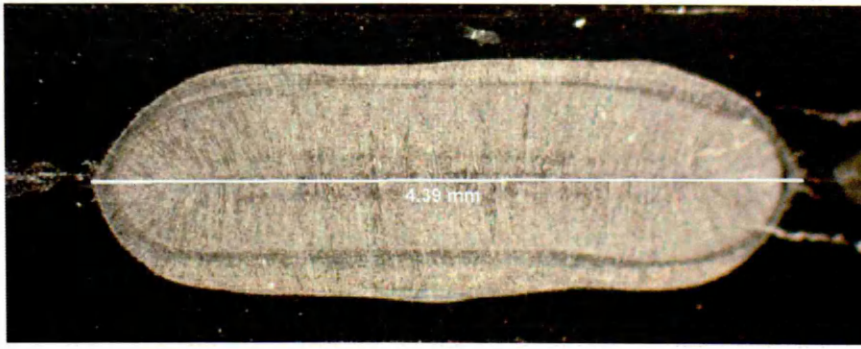
Fig 4.37: Weld 1.
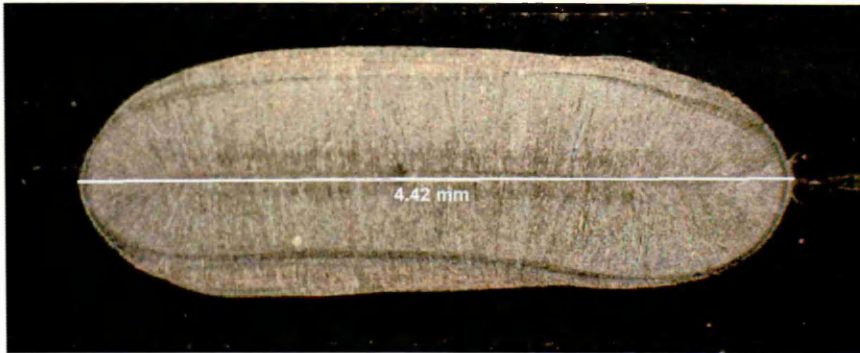
Fig 4.38: Weld 2.
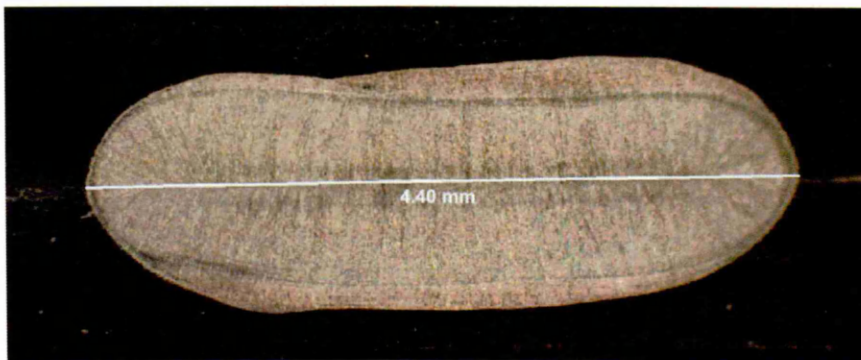
Fig 4.39: Weld 3.

Fig 4.40: Weld 4.

Fig 4.41: Weld 5.

Variation in Nugget Diamter at 15mm Pitch
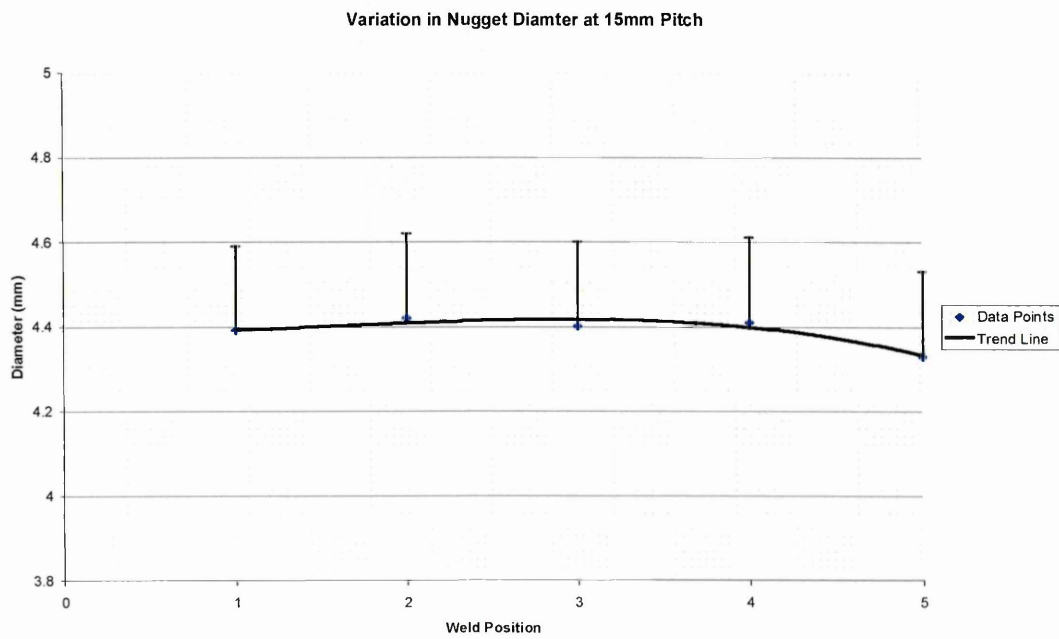
Fig 4.42: Variation in nugget diameter at 15 mm pitch.

200

4.3.2.3: 17.5 mm Pitch Specimens.

Fig 4.43: Weld 1.

Fig 4.44: Weld 2.
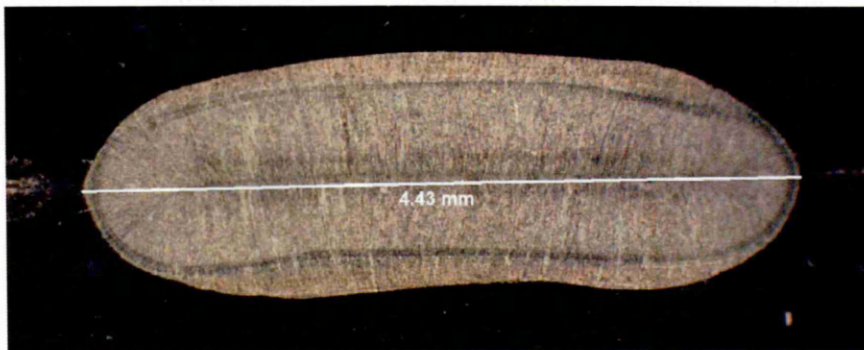
Fig 4.45: Weld 3.
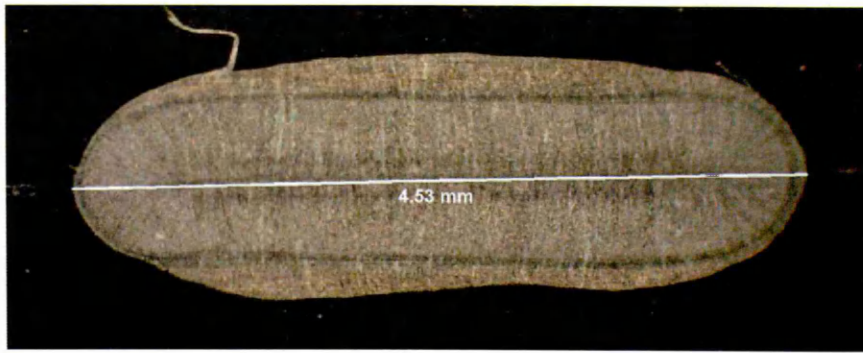
Fig 4.46: Weld 4.

Fig 4.47: Weld 5.
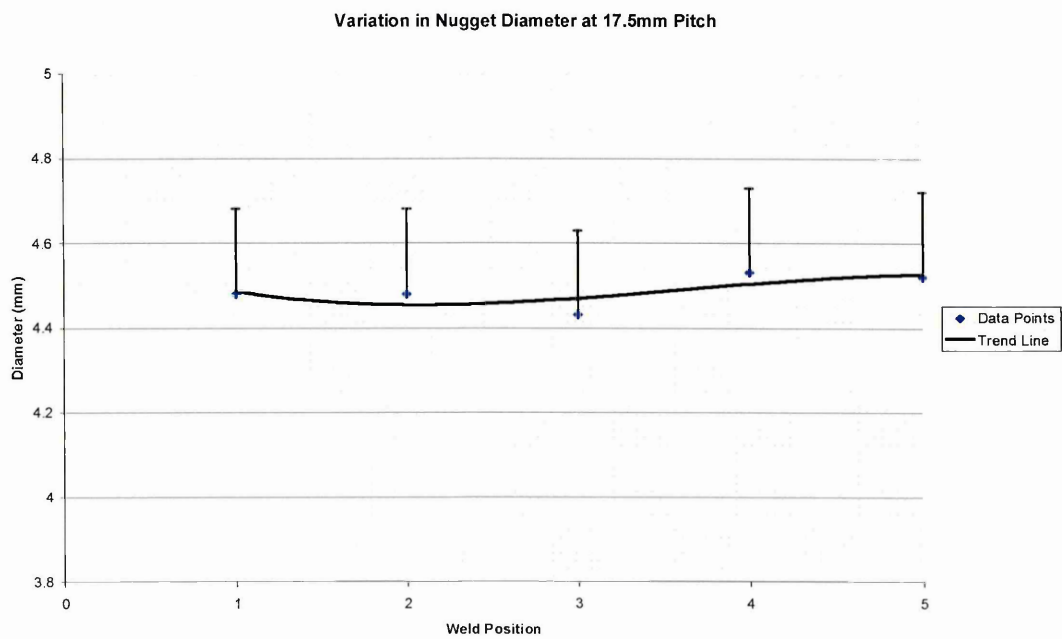
Fig 4.48: Variation in nugget diameter at 17.5 mm pitch.

202

4.3.2.4: 20 mm Pitch Specimens.
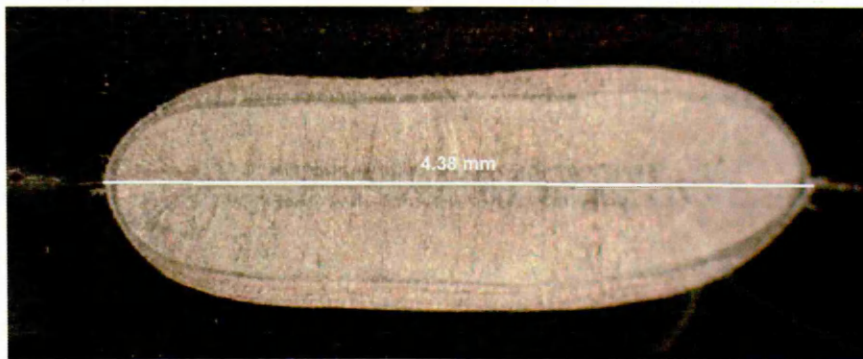
Fig 4.49: Weld 1.
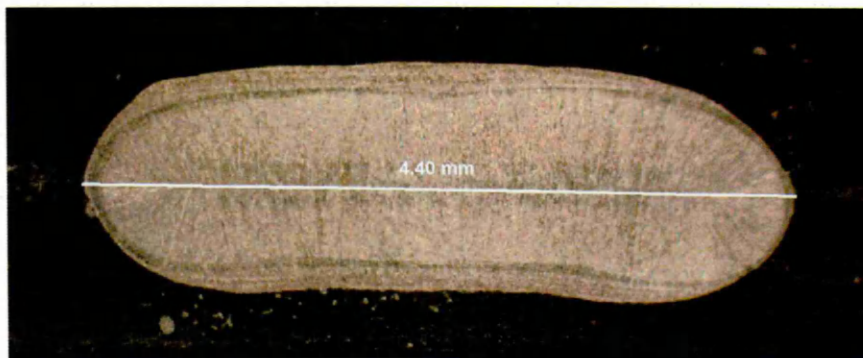
Fig 4.50: Weld 2.
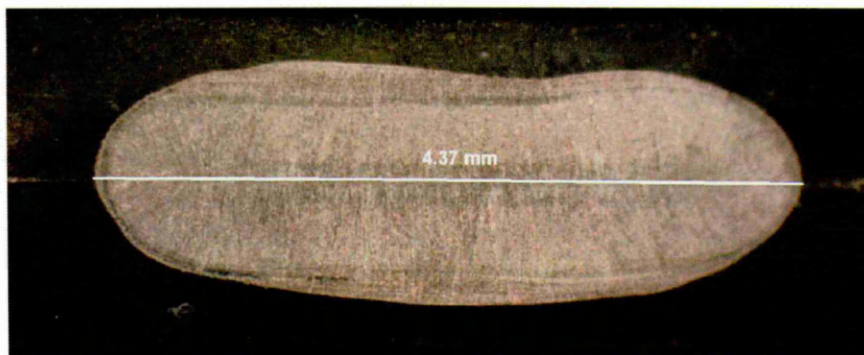
Fig 4.51: Weld 3.
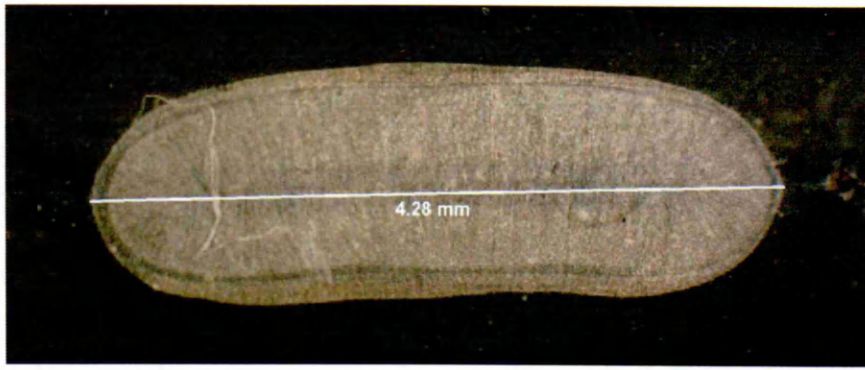
Fig 4.52: Weld 4.
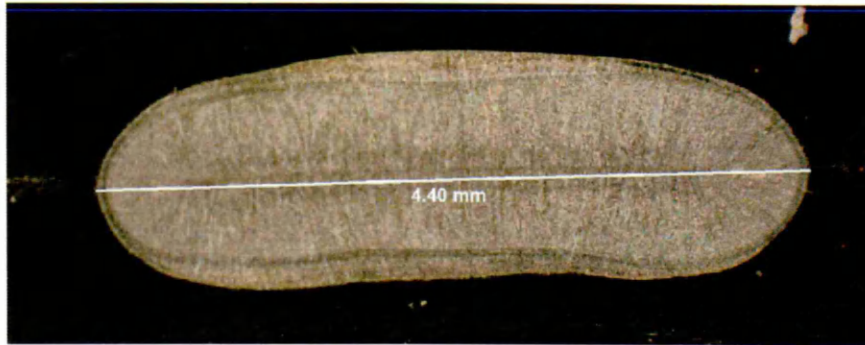
Fig 4.53: Weld 5.
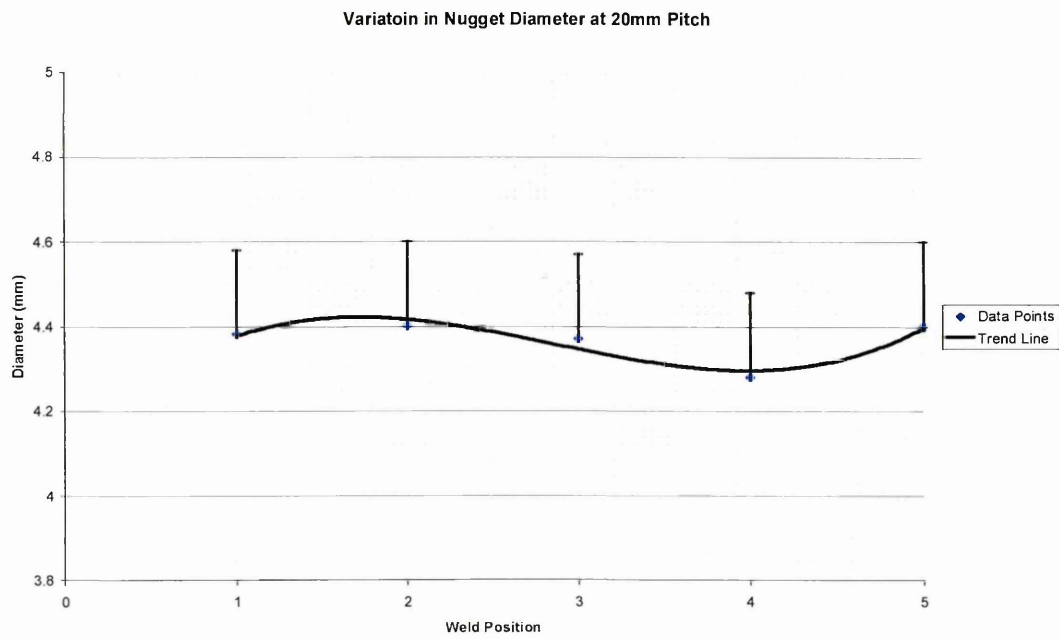
Fig 4.54: Variation in nugget diameter at 20 mm pitch.

204

4.3.2.5: 30 mm Pitch Specimens.
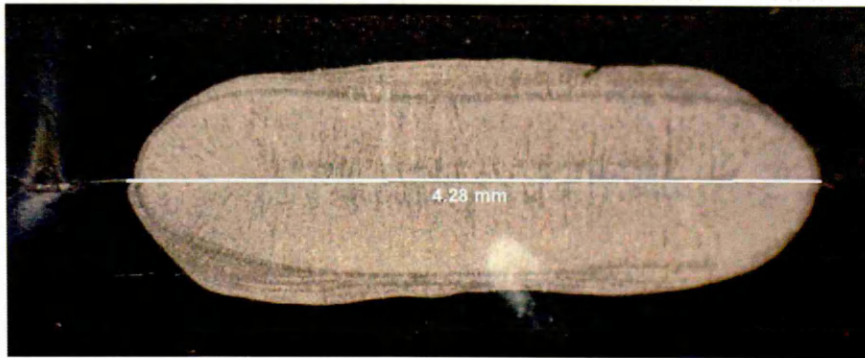
Fig 4.55: Weld 1.
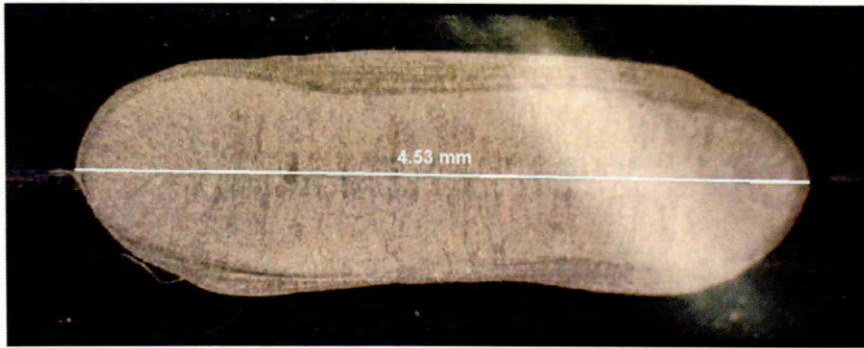
Fig 4.56: Weld 2.

Fig 4.57: Weld 3.
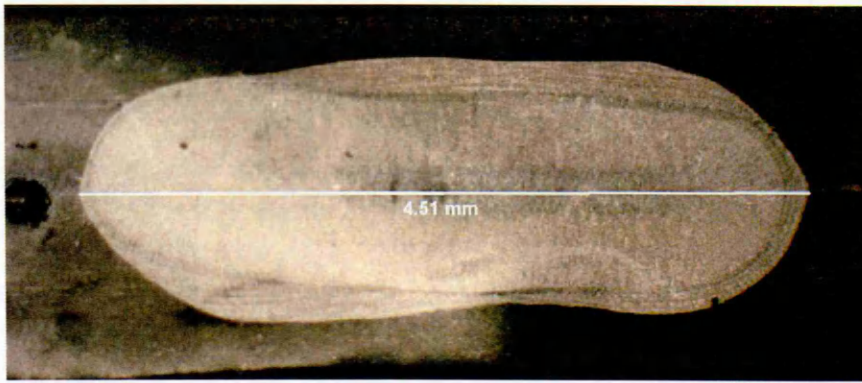
Fig 4.58: Weld 4.

Fig 4.59: Weld 5.

Variation in Nugget Diameter at 30mm Pitch
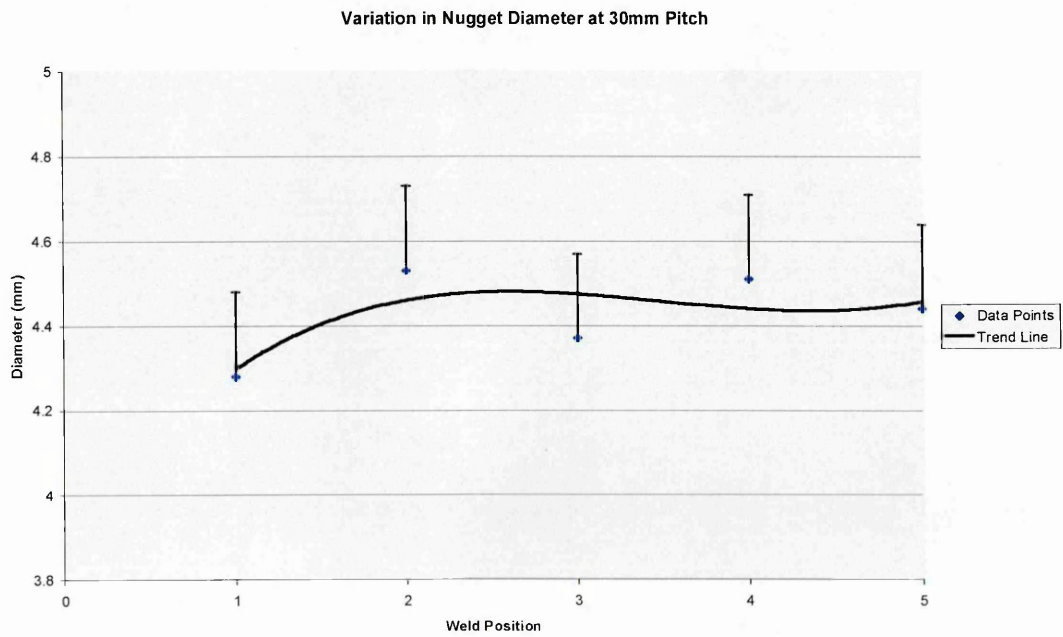
Fig 4.60: Variation in nugget diameter at 30 mm pitch.

206

4.3.2.6: 40 mm Pitch Specimens.

Fig 4.61: Weld 1.
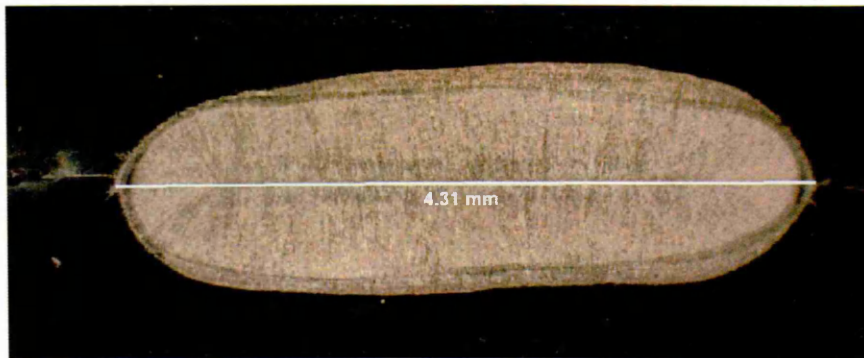
Fig 4.62: Weld 2.

Fig 4.63: Weld 3.
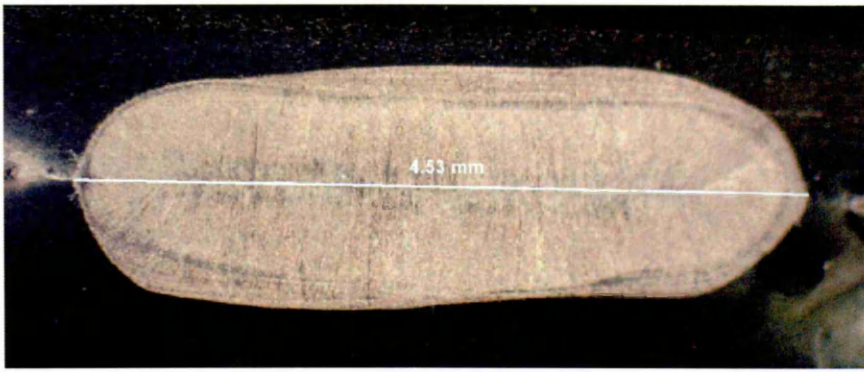
Fig 4.64: Weld 4.

Fig 4.65: Weld 5.
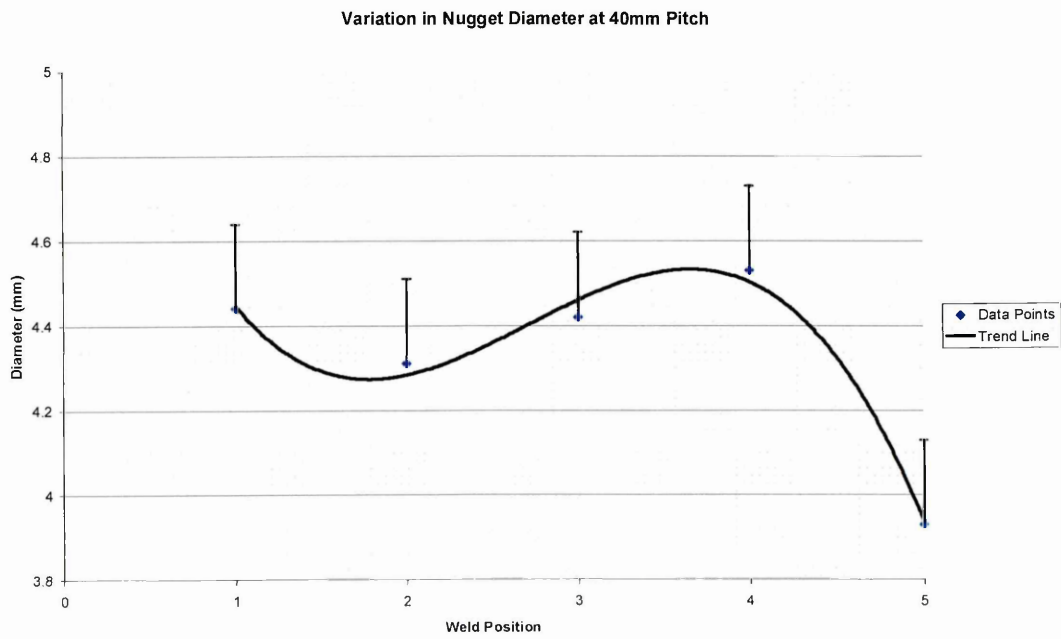
Fig 4.66: Variation in nugget diameter at 40 mm pitch.

208

4.3.2.7: 50 mm Pitch Specimens.

Fig 4.67: Weld 1.
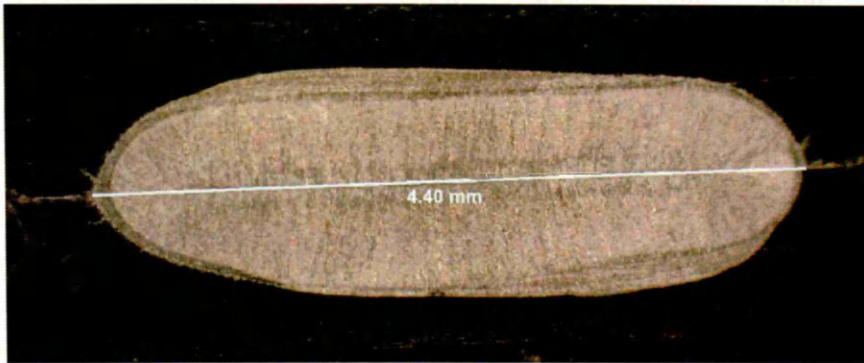
Fig 4.68: Weld 2.
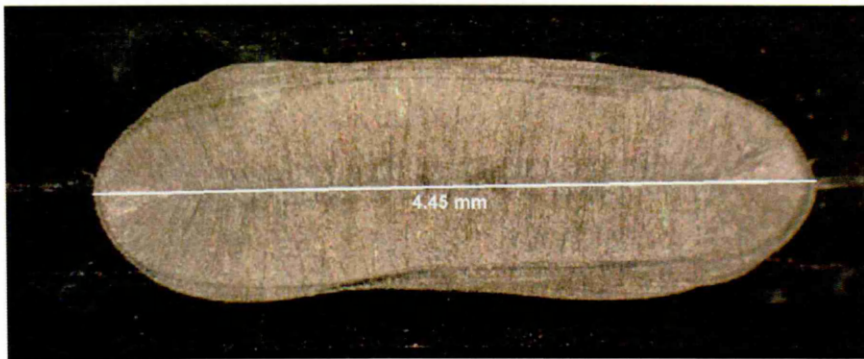
Fig 4.69: Weld 3.
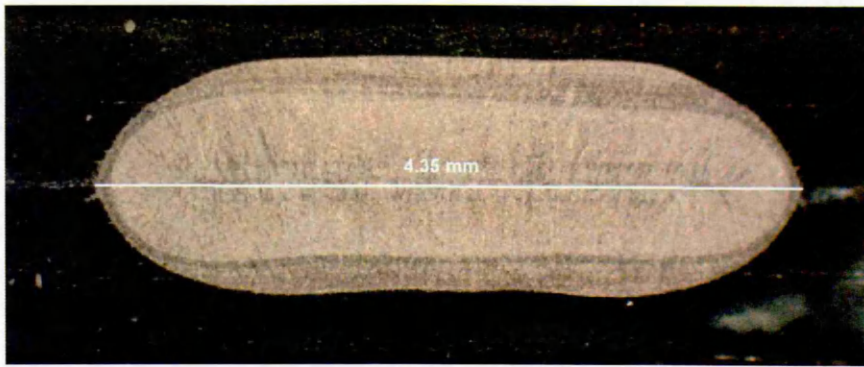
Fig 4.70: Weld 4.

Fig 4.71: Weld 5.

Variation in Nugget Diameter at 50mm Pitch
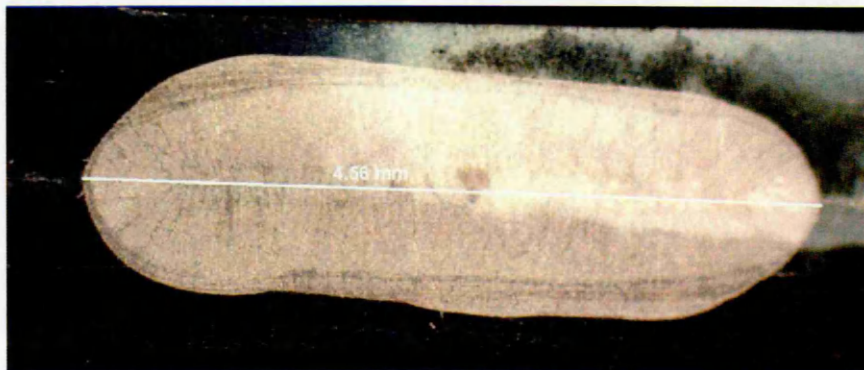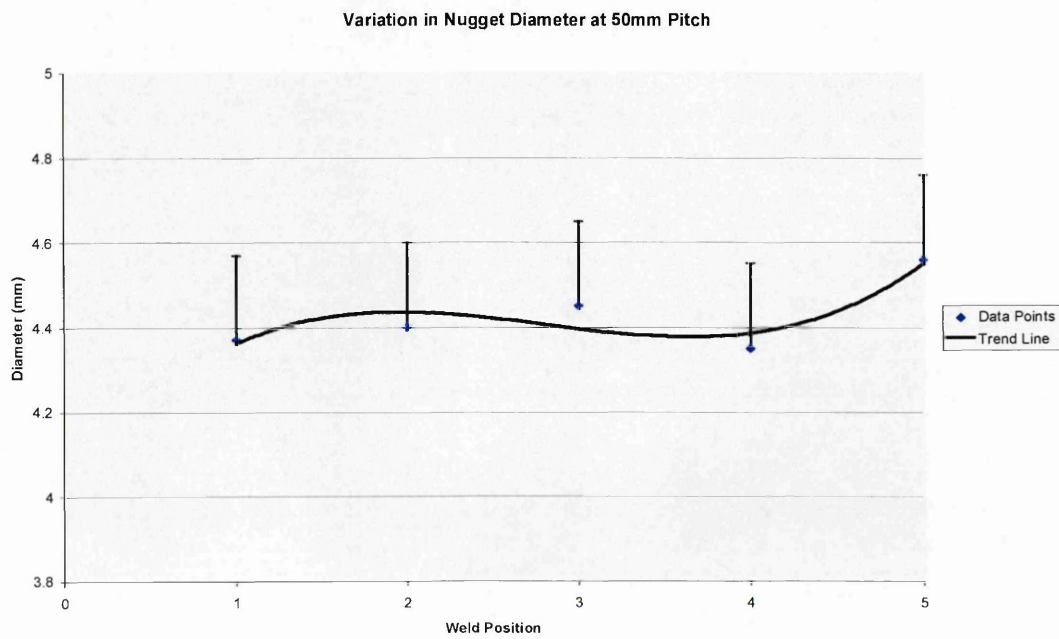
Fig 4.72: Variation in nugget diameter at 50 mm pitch.

210

4.3.3: Variation in Nugget Diameter at Extremely Close Pitch Distances.

The table below shows the measured diameter of each of the two welds taken from each of the five extreme pitch distance specimens produced in the Extremely Close Pitch Distance Study. In addition, the upper limit on diameter, based on the accuracy of the measuring process, is also given for each of the measurements made. These values are then presented in a graph which displays the measured value as a data point and the upper diameter limits as an error bar. Following the table and graph are the images of each of the welds taken by the optical microscope that were used to determine diameter.

Specimen	Measured Diameters (mm)			Upper Limit Diameters (mm)		
	Weld 1	Weld 2	Difference	Weld 1	Weld 2	Difference
1	4.34	4.29	0.05	4.592	4.545	0.047
2	4.13	4.04	0.09	4.394	4.309	0.084
3	4.27	4.28	-0.01	4.526	4.535	-0.009
4	4.27	4.27	0.00	4.526	4.526	0.000
5	4.47	4.45	0.02	4.715	4.696	0.019

Table 4.8: Variation in nugget diameter at 6 mm pitch distances.
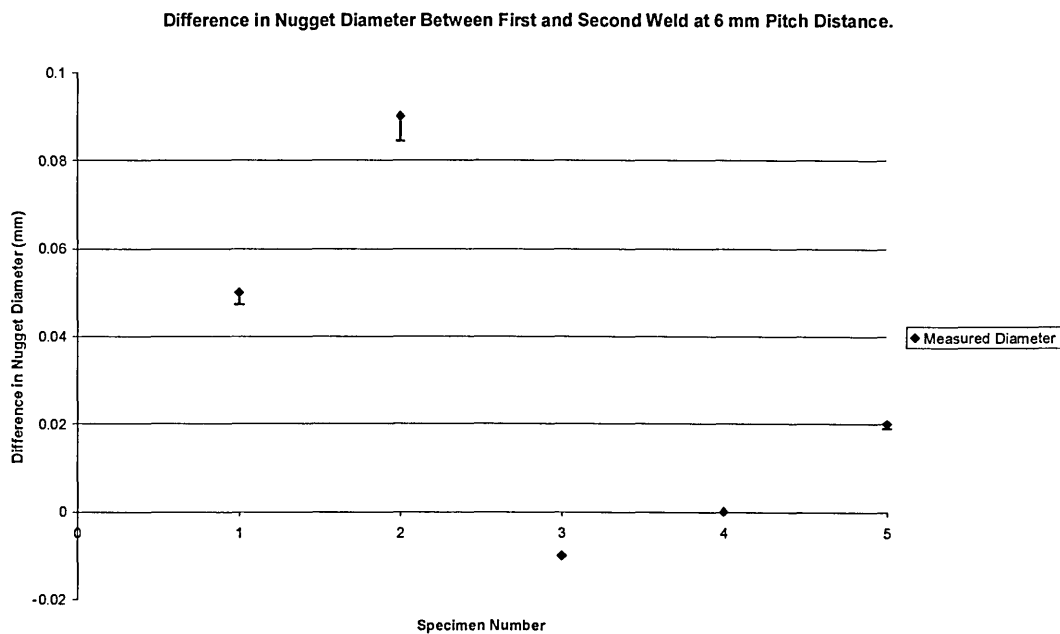
Fig 4.73: Different in nugget diameter between two welds made at 6 mm pitch distances.

211
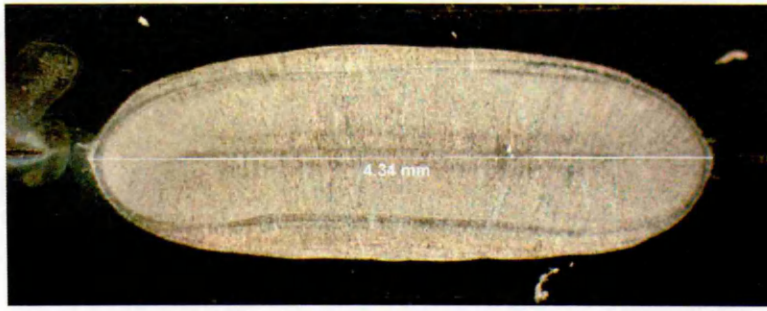
Fig 4.74: Specimen 1 Weld 1.
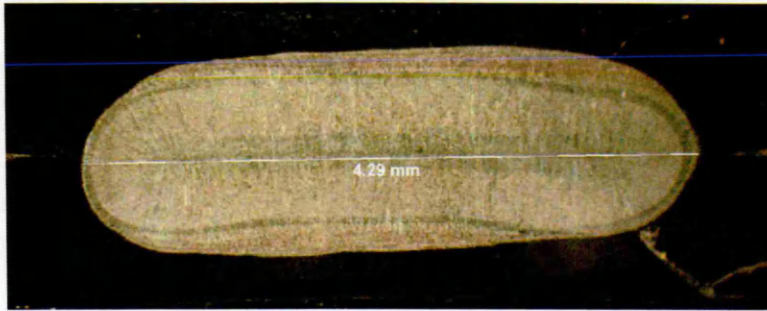
Fig 4.75: Specimen 1 Weld 2.
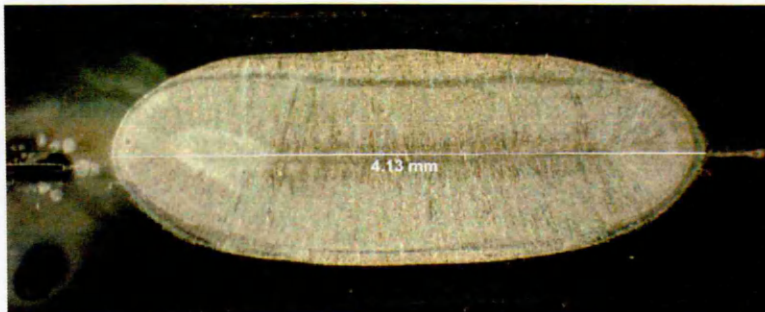
Fig 4.76: Specimen 2 Weld 1.

Fig 4.77: Specimen 2 Weld 2.
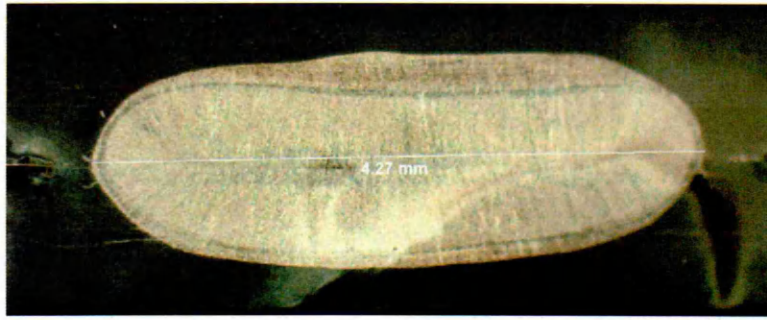
Fig 4.78: Specimen 3 Weld 1.
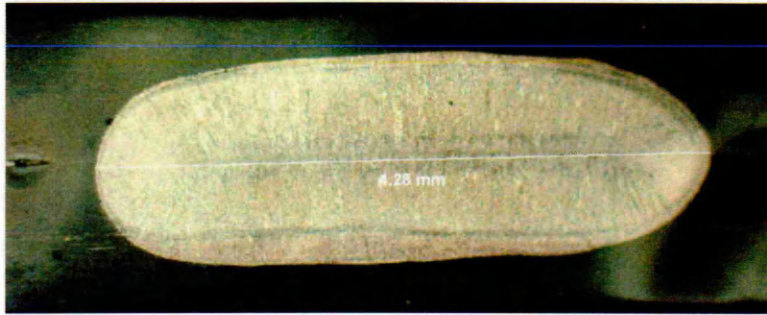
Fig 4.79: Specimen 3 Weld 2.
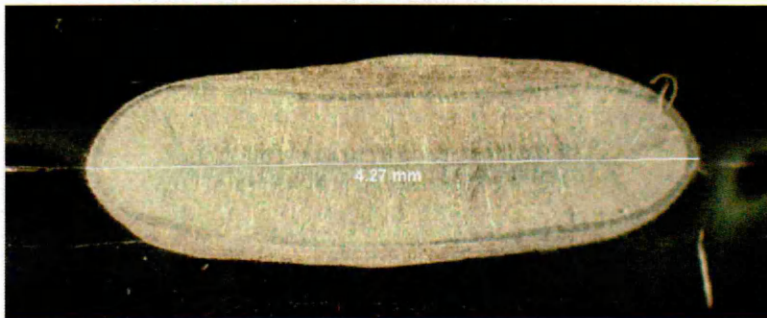
Fig 4.80: Specimen 4 Weld 1.
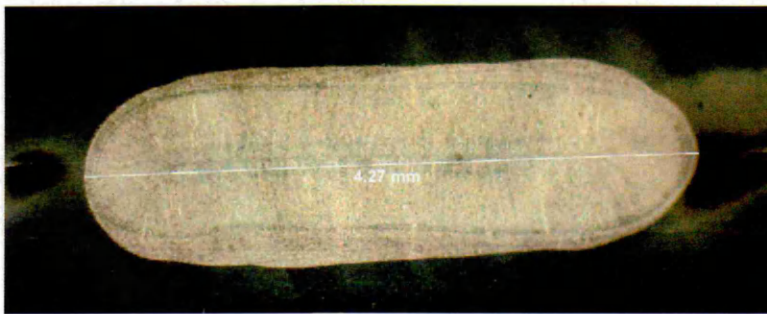
Fig 4.81: Specimen 4 Weld 2.
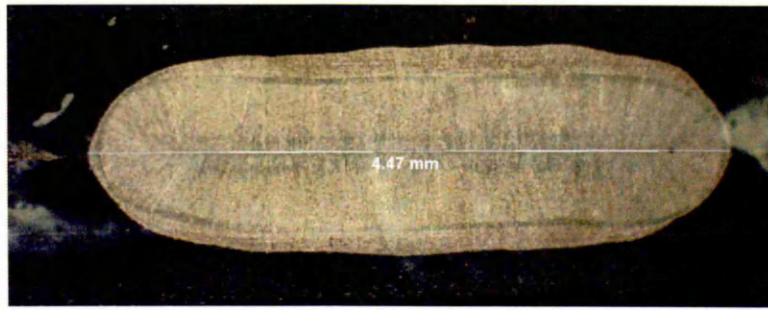
Fig 4.82: Specimen 5 Weld 1.

Fig 4.83: Specimen 5 Weld 2.

4.4: Fatigue Study.

The following section contains the results from all the fatigue tests carried out on the single nugget specimens.

4.4.1: Staircase Fatigue Testing of Single Nugget Joints.

Below are the tabulated results for the single nugget staircase tests.

Load Range, kN	Step No. i	1	2	3	4	5	6	7	8	9	10	11	12	13	14	15	16	17	18	19	20	21	22	23	24	25	Survivals, r	Failures, f
0.729								×																			0	1
0.702	2		×		×		○		×						×		×				×						1	6
0.675	1	○		○		○				×		×		○		○		×		○		×		×		×	6	6
0.648	0										○		○						○				○		○		5	0
																											Σr = 12	Σf = 13

Fig 4.84: Single nugget Staircase results.

215

The data gathered from the tabulated Staircase results were then used in accordance with the procedures detailed in Section 3.1.2.1 to determine calculated values for the mean fatigue strength and the standard deviation of the fatigue strength distribution for single nugget joints. Upper and lower 95% confidence limits were also determined for the calculated values for both the mean and standard deviation.

Step divide used: 0.027 kN

Least Frequent Event: Survivals

Load, L_i, (kN)	i	N_i	iN_i	i^2N_i
0.729	-	0	-	-
0.702	2	1	2	4
0.675	1	6	6	6
0.648	0	5	0	0
Sum		12	8	10

Table 4.9: Single nugget Staircase results.

Mean:

$$\mu = 0.648 + 0.027\left(\frac{8}{12} + \frac{1}{2}\right)$$

μ = 0.6795 kN

Convergence Factor:

$$\left(\frac{(10 \times 12) - 8^2}{12^2}\right) = 0.3889$$

Standard Deviation:

$$s = 1.620 \times 0.027\left(\frac{(10 \times 12) - 8^2}{12^2} + 0.029\right)$$

s = 0.0183 kN

216

Standard Deviation on the Mean:

$$S_m = \frac{1.06 \times 0.0183}{\sqrt{25}}$$

$$S_m = 0.0039 \ kN$$

Upper and Lower 95% Confidence on the Mean:

$$0.6795 \pm 1.96 \times 0.0039$$

$$0.6795 \pm 0.0076 \ kN$$

Standard Error on the Standard Deviation:

$$S_s = \frac{1.27 \times 0.0183}{\sqrt{25}}$$

$$S_s = 0.0046 \ kN$$

Upper and Lower 95% Confidence on the Standard Deviation:

$$0.0183 \pm 1.96 \times 0.0046$$

$$0.0183 \pm 0.0091 \ kN$$

4.4.2: Probit Testing of Single Nugget Joints.

The results for the Probit testing of single nugget joints are presented below in Table 4.10. The table details each load range that was used in the process, the number of specimens tested at each load range, and the amount surviving as a number, a percentage, and a transformed Y value.

Load Range (kN)	No. Tested	No. Surviving	% Surviving	Transformed Y Value
0.639	40	37	92.50	-1.44
0.657	20	9	45.00	0.13
0.666	20	9	45.00	0.13
0.675	20	9	45.00	0.13
0.684	30	4	13.33	1.11

Table 4.10: Single nugget Probit results.

The transformed Y values achieved at each of the load ranges used where then plotted as data points on the graph below.
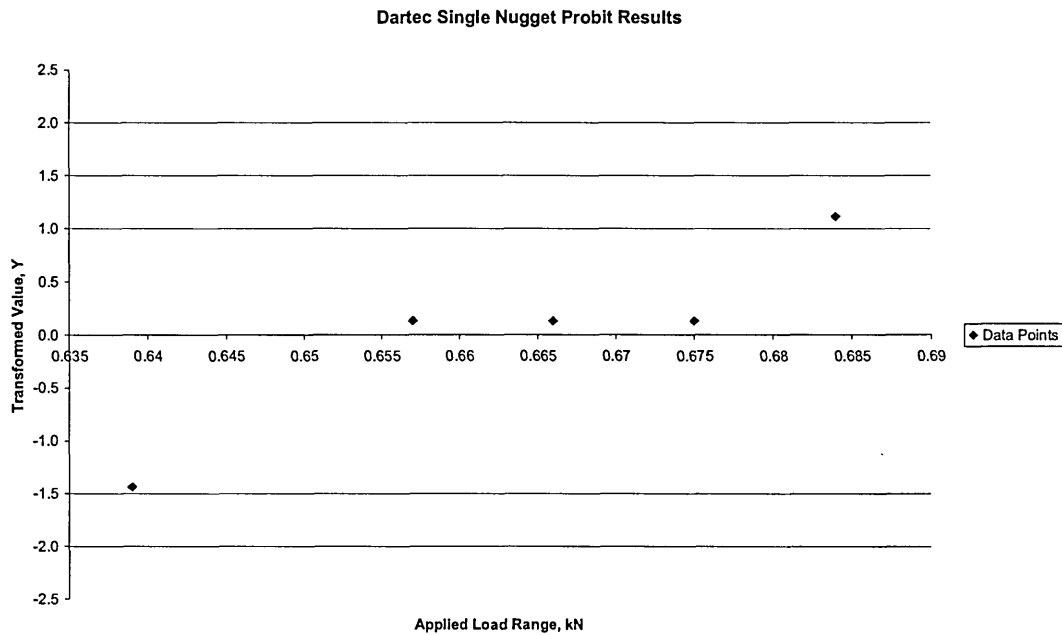
Fig 4.85: Single nugget Probit results.

4.4.2.1: Calculation of Response Curve.

The data gathered in the single nugget Probit test was analysed in the manner discussed in Section 3.1.3.3 so that a response curve could be determined that would fit the data points. The analysis and calculations for the response curve are shown below and the resulting line is shown in Fig 4.86.

Applied Load Range, X (kN)	X^2	Observed Per Cent Survival, p	Observed Transformed Values, Y	XY	Fitted Values	
					Y_f	p_f
0.639	0.408	92.5	-1.4	-0.920	-1.23	89.07
0.657	0.432	45	0.1	0.083	-0.34	63.31
0.666	0.444	45	0.1	0.084	0.10	46.02
0.675	0.456	45	0.1	0.085	0.54	29.46
0.684	0.468	13.3	1.1	0.760	0.98	16.35

Sum	3.321	2.207		0.048	0.091
Average	$\overline{X} = 0.664$			$\overline{Y} = 0.010$	

Table 4.11: Single nugget Probit response curve calculations.

Number of groups tested, k = 5

Fitted line intercept, a:

Intercept, a = $\overline{Y}$

a = -0.010

Slope of fitted line, b:

$$\text{Slope, } b = \frac{\sum (XY) - k\overline{X}\,\overline{Y}}{\sum X^2 - k\overline{X}^2} \qquad b = \frac{0.091 - 5 \times 0.664 \times 0.01}{2.207 - 5 \times 0.664^2}$$

b = 49.173
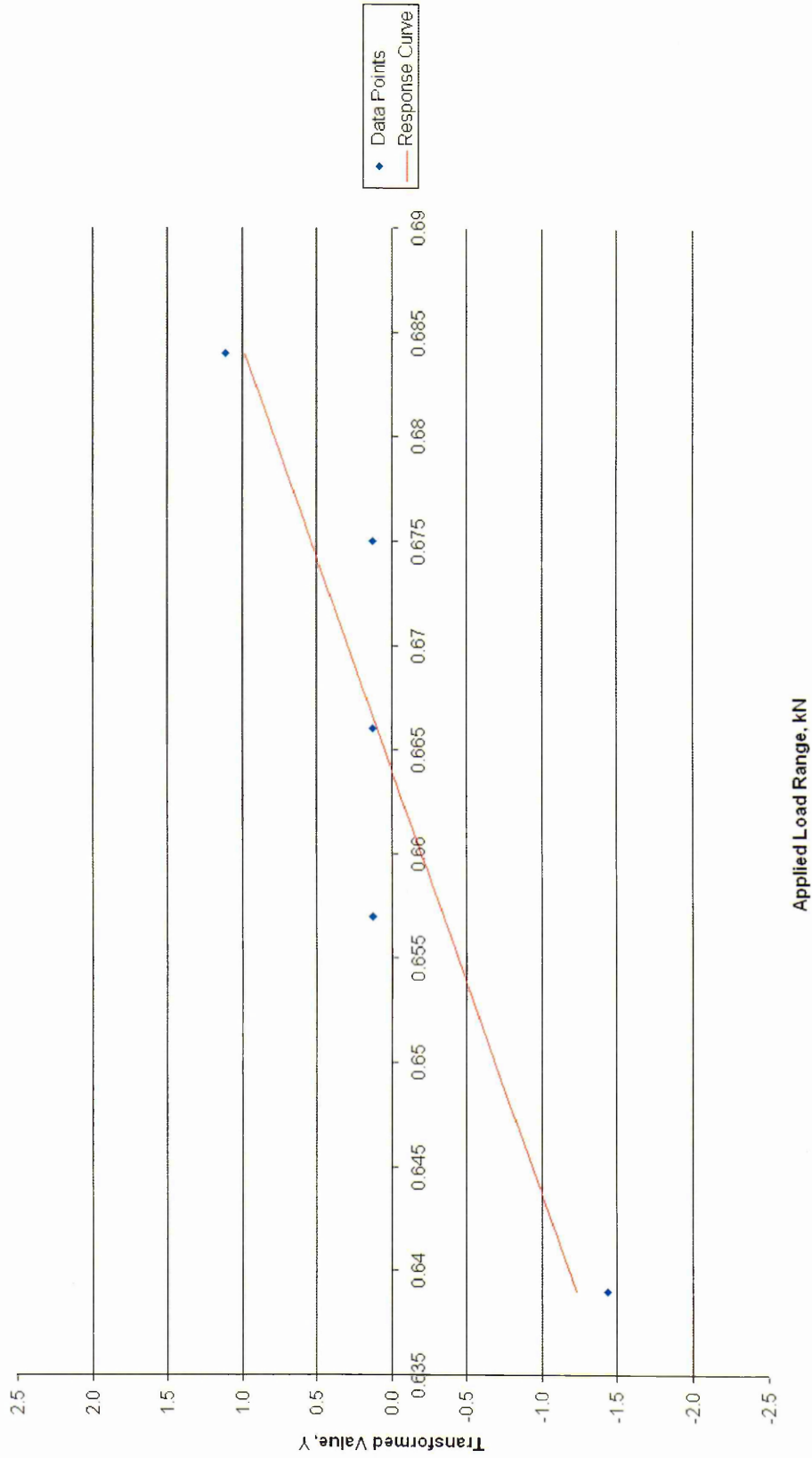
Fig 4.86: Single nugget Probit response curve.

4.4.2.2: Calculations for the Derived Estimates.

The response curve data was analysed using the Derived Estimate process described in Section 3.1.3.5 so that values for the mean fatigue strength and the standard deviation of the fatigue strength distribution could be determined.

$$X(Y) = \overline{X} + \frac{Y - a}{b}$$

$b = 49.173$

$a = -0.010$

$\overline{X} = 0.664$

Stated Per Cent Survival	Transformed Value, Y	Derived Estimate, X(Y), (kN)
84.13	-1.000	0.644
50	0.000	0.664

Table 4.12: Derived estimates based on single nugget Probit response curve.

4.4.3: Multi-Spot Weld Fatigue Testing.

The following sections detail the results that were obtained through the Staircase fatigue testing of all multi-spot welded joints. Each section contains the tabulated results for the Staircase process, as well as the mathematical analysis and calculations carried out on these results in order to determine values for the mean fatigue strength per spot weld, and the standard deviation per spot weld, of the fatigue strength distribution. Values for the upper and lower 95% confidence limits, for the derived values of the mean fatigue strength per spot weld, and standard deviation per spot weld, are also presented.

4.4.3.1: Double Nugget Staircase Results.

Load Range, kN	Step No. i	1	2	3	4	5	6	7	8	9	10	11	12	13	14	15	16	17	18	19	20	21	22	23	24	25	26	27	28	29	30	Survivals, r	Failures, f
1.413	2				X		X																		X		X					0	4
1.377	1			O		O		X		X				X		X						X		O		O		X		X		4	7
1.341	0		O						O		X		O		O		X		X		O		O						O		X	7	4
1.305		O										O						O		O												4	0
																																Σr	Σf
																																15	15

Number of

Test Number

Fig 4.87: Double nugget Staircase results.

Step divide used: 0.036 kN

Least Frequent Event: Even occurrences

Load, L_i, (kN)	i	N_i	iN_i	i^2N_i
1.413	2	4	8	16
1.377	1	7	7	7
1.341	0	4	0	0
1.305	-	-	-	-
Sum		15	15	23

Table 4.13: Double nugget Staircase results.

Mean per Spot Weld:

$$\mu = 1.341 + 0.036\left(\frac{15}{15} - \frac{1}{2}\right)$$

μ = 1.359 kN

μ = 0.6795 kN per spot weld

Convergence Factor:

$$\left(\frac{(23 \times 15) - 15^2}{15^2}\right) = 0.5333$$

Standard Deviation per Spot Weld:

$$s = 1.620 \times 0.036\left(\frac{(23 \times 15) - 15^2}{15^2} + 0.029\right)$$

s = 0.0328 kN

s = 0.0164 kN per spot weld

224

Standard Deviation on the Mean per spot Weld:

$$S_m = \frac{1.01 \times 0.0164}{\sqrt{30}}$$

S_m = 0.0059 kN per spot weld

Upper and Lower 95% Confidence on the Mean per Spot Weld:

$$0.6795 \pm 1.96 \times 0.0059$$

0.6795 ± 0.0059 kN per spot weld

Standard Error on the Standard Deviation per Spot Weld:

$$S_s = \frac{1.34 \times 0.0164}{\sqrt{30}}$$

S_s = 0.0040 kN per spot weld

Upper and Lower 95% Confidence on the Standard Deviation per Spot Weld:

$$0.0164 \pm 1.96 \times 0.0040$$

0.0164 ± 0.0079 kN per spot weld

Example Double Nugget Video Monitor Screen Grabs.
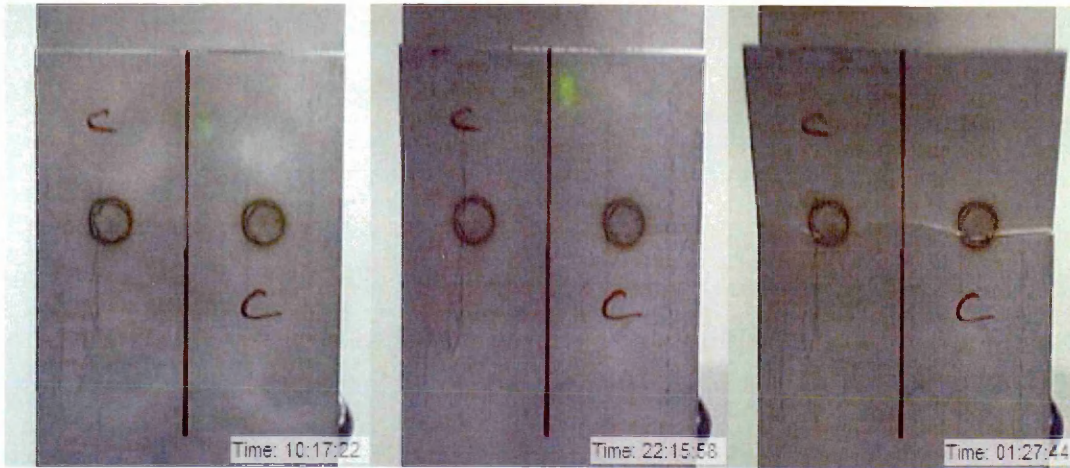
Fig 4.88: Example double nugget video monitor screen grabs from side 1 of a specimen. From left to right: test start, failure conditions met, complete failure.
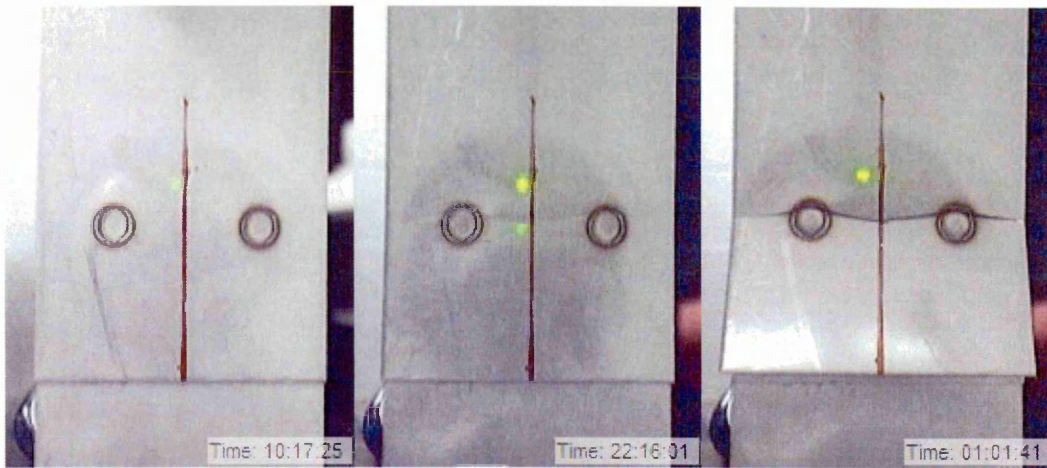
Fig 4.89: Example double nugget video monitor screen grabs from side 2 of a specimen. From left to right: test start, failure conditions met, complete failure.

226

4.4.3.2: Four Nugget Staircase Results.

Load Range, kN	Step No. i	1	2	3	4	5	6	7	8	9	10	11	12	13	14	15	16	17	18	19	20	21	22	23	24	25	26	27	28	29	30	Survivals, r	Failures, f
2.852	3																			X				X								0	1
2.898	2										X		X						O		X		O		X				X			2	5
2.844	1			X		X		X		O		O		X		X		O				O				X		O		X		5	7
2.790	0		O		O		O		O						O		O										O				X	7	1
2.736		O																														1	0
																																Σr 15	Σf 15

Fig 4.90: Four nugget Staircase results.

Step divide used: 0.054 kN

Least Frequent Event: Even occurrences

Load, L_i, (kN)	i	N_i	iN_i	i^2N_i
2.952	3	2	6	18
2.898	2	5	10	20
2.844	1	7	7	7
2.790	0	1	1	0
2.736	-	-	-	-
Sum		15	24	45

Table 4.14: Four nugget Staircase results.

Mean per Spot Weld:

$$\mu = 2.790 + 0.054\left(\frac{24}{15} - \frac{1}{2}\right)$$

μ = 2.8494 kN

μ = 0.7115 kN per spot weld

Convergence Factor:

$$\left(\frac{(45 \times 15) - 24^2}{15^2}\right) = 0.4400$$

Standard Deviation:

$$s = 1.620 \times 0.054\left(\frac{(45 \times 15) - 24^2}{15^2} + 0.029\right)$$

s = 0.0410 kN

s = 0.0148 kN per spot weld

Standard Deviation on the Mean per Spot Weld:

$$S_m = \frac{1 \times 0.0148}{\sqrt{30}}$$

S_m = 0.0027 kN per spot weld

Upper and Lower 95% Confidence on the Mean per Spot Weld:

$$0.7115 \pm 1.96 \times 0.0027$$

0.7115 ± 0.0053 kN per spot weld

Standard Error on the Standard Deviation per Spot Weld:

$$S_s = \frac{1.41 \times 0.0148}{\sqrt{30}}$$

S_m = 0.0038 kN per spot weld

Upper and Lower 95% Confidence on the Standard Deviation per Spot Weld:

$$0.0148 \pm 1.96 \times 0.0038$$

0.0148 ± 0.0075 kN per spot weld
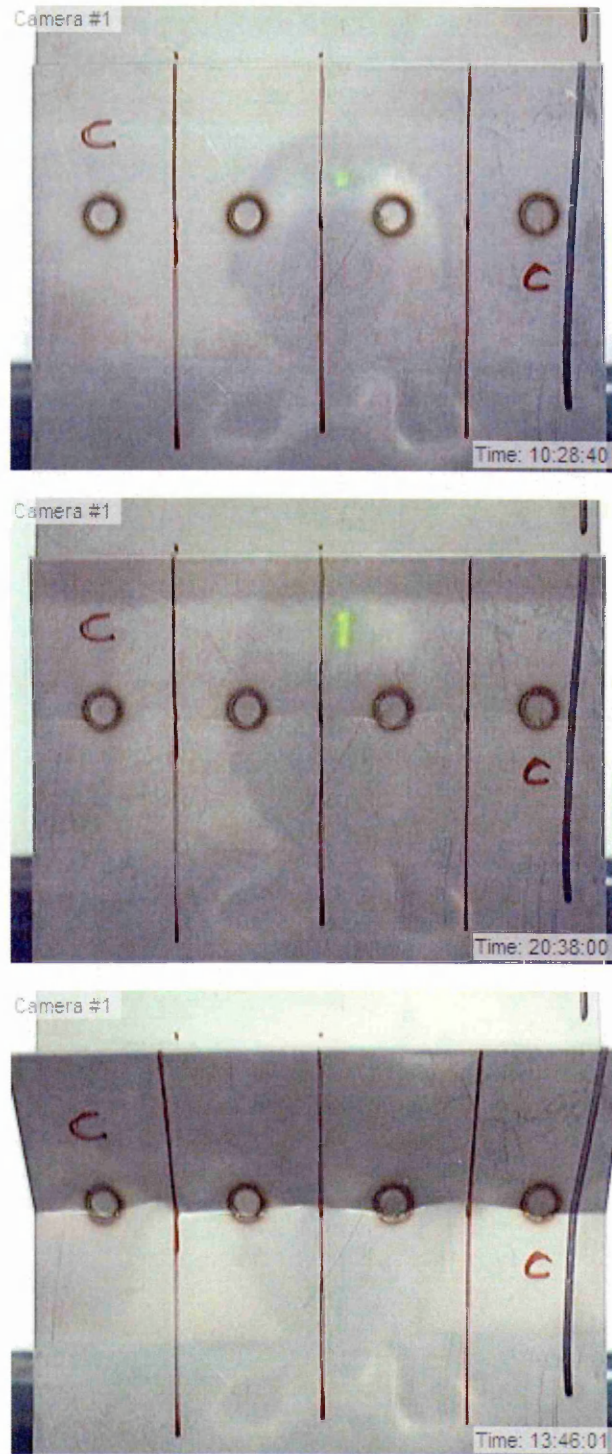
Fig 4.91: Example four nugget video monitor screen grabs from side 1 of a specimen. From top to bottom: test start, failure conditions met, complete failure.
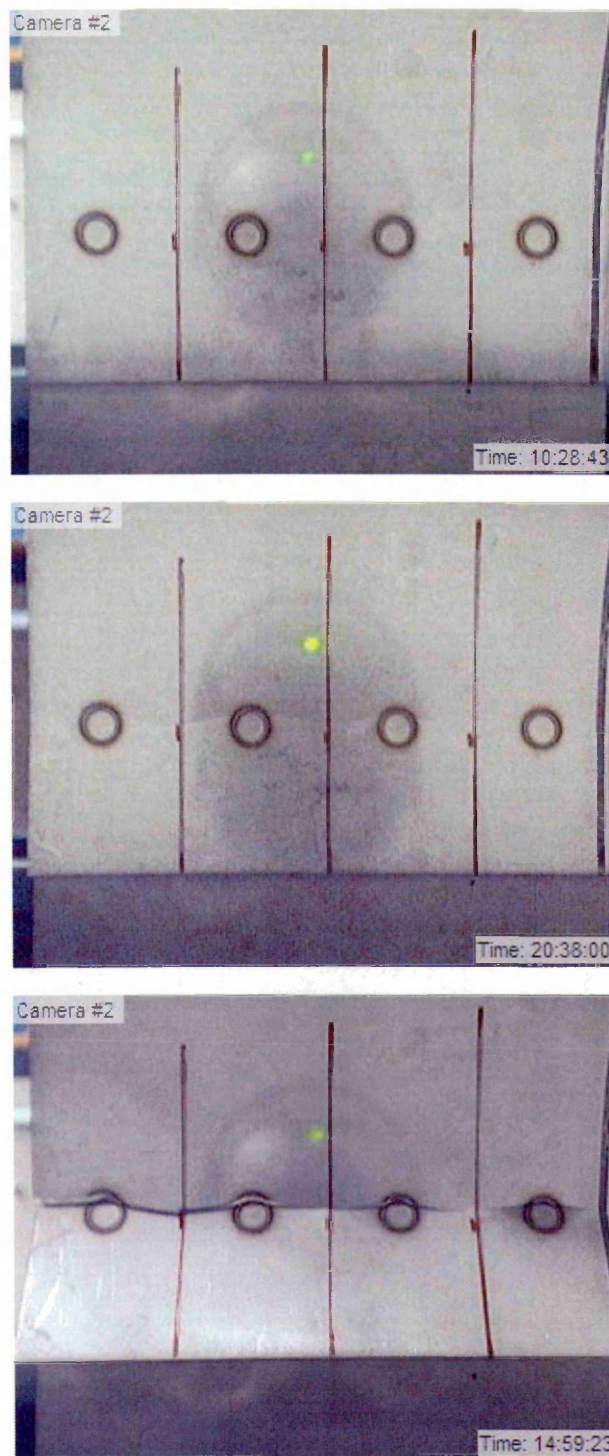
Fig 4.92: Example four nugget video monitor screen grabs from side 2 of a specimen. From top to bottom: test start, failure conditions met, complete failure.

4.4.3.3: Eight Nugget Staircase Results.

Load Range, kN	Step No. i	1	2	3	4	5	6	7	8	9	10	11	12	13	14	15	16	17	18	19	20	21	22	23	24	25	26	27	28	29	30	Survivals, r	Failures, f
5.679	2						X				X																					0	2
5.580	1					O		X		O		X				X				X				X		X		X		X		2	8
5.481	0		X		O				O				X		O		X		O		X		O		O		O		O		X	8	5
5.382		O		O										O				O				O										5	0
																															Σr	Σf
																															15	15

Fig 4.93: Eight nugget Staircase results.

Step divide used: 0.099 kN

Least Frequent Event: Even occurrences

Load, L_i, (kN)	i	N_i	iN_i	i^2N_i
5.679	2	2	4	8
5.580	1	8	8	8
5.481	0	5	0	0
5.382	-	-	-	
Sum		15	12	16

Table 4.15: Eight nugget Staircase results.

Mean per Spot Weld:

$$\mu = 5.481 + 0.099\left(\frac{12}{15} - \frac{1}{2}\right)$$

μ = 5.5107 kN

μ = 0.6888 kN per spot weld

Convergence Factor:

$$\left(\frac{(16 \times 15) - 12^2}{15^2}\right) = 0.4267$$

Standard Deviation per Spot Weld:

$$s = 1.620 \times 0.099\left(\frac{(16 \times 15) - 12^2}{15^2} + 0.029\right)$$

s = 0.0731 kN

s = 0.0091 kN per spot weld

233

Standard Deviation on the Mean per Spot Weld:

$$S_m = \frac{1.04 \times 0.0091}{\sqrt{30}}$$

S_m = 0.0017 kN per spot weld

Upper and Lower 95% Confidence on the Mean per Spot Weld:

$$0.6889 \pm 1.96 \times 0.0017$$

0.6889 ± 0.0034 kN per spot weld

Standard Error on the Standard Deviation per Spot Weld:

$$S_s = \frac{1.3 \times 0.0091}{\sqrt{30}}$$

S_s = 0.0022 kN per spot weld

Upper and Lower 95% Confidence on the Standard Deviation per Spot Weld:

$$0.0091 \pm 1.96 \times 0.0022$$

0.0091 ± 0.0043 kN per spot weld
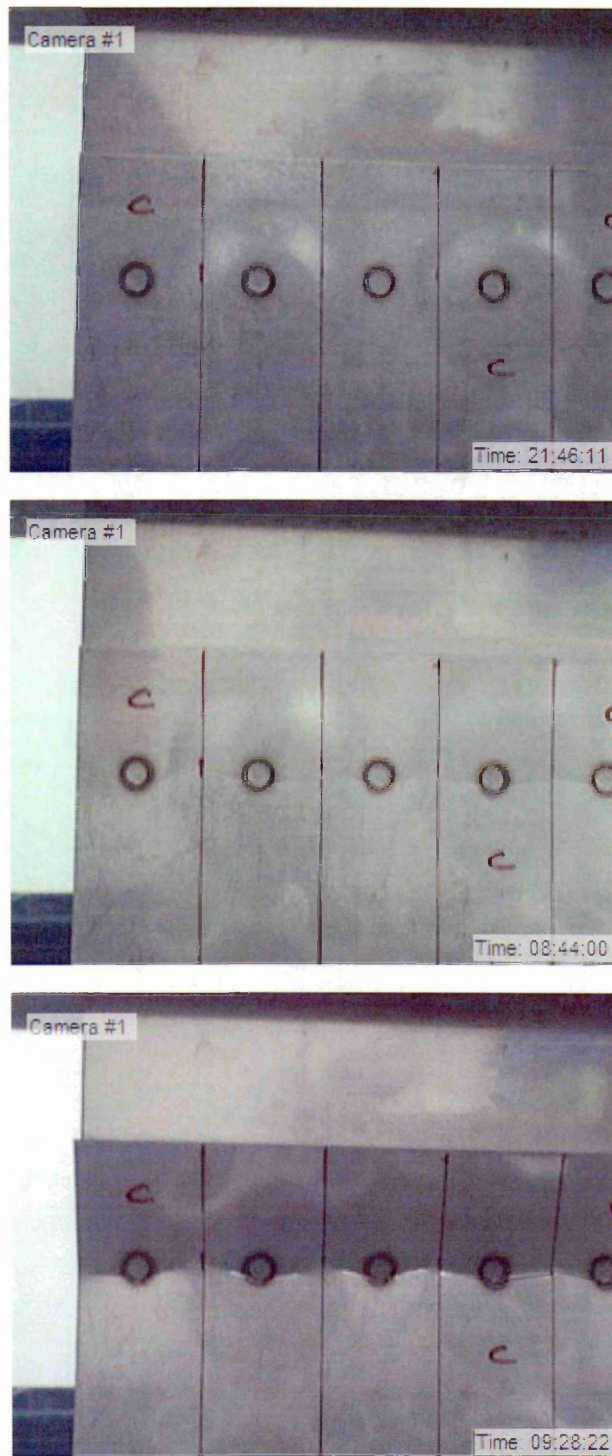
Fig 4.94: Example eight nugget video monitor screen grabs from one half of side 1 of a specimen. From top to bottom: test start, failure conditions met, complete failure.
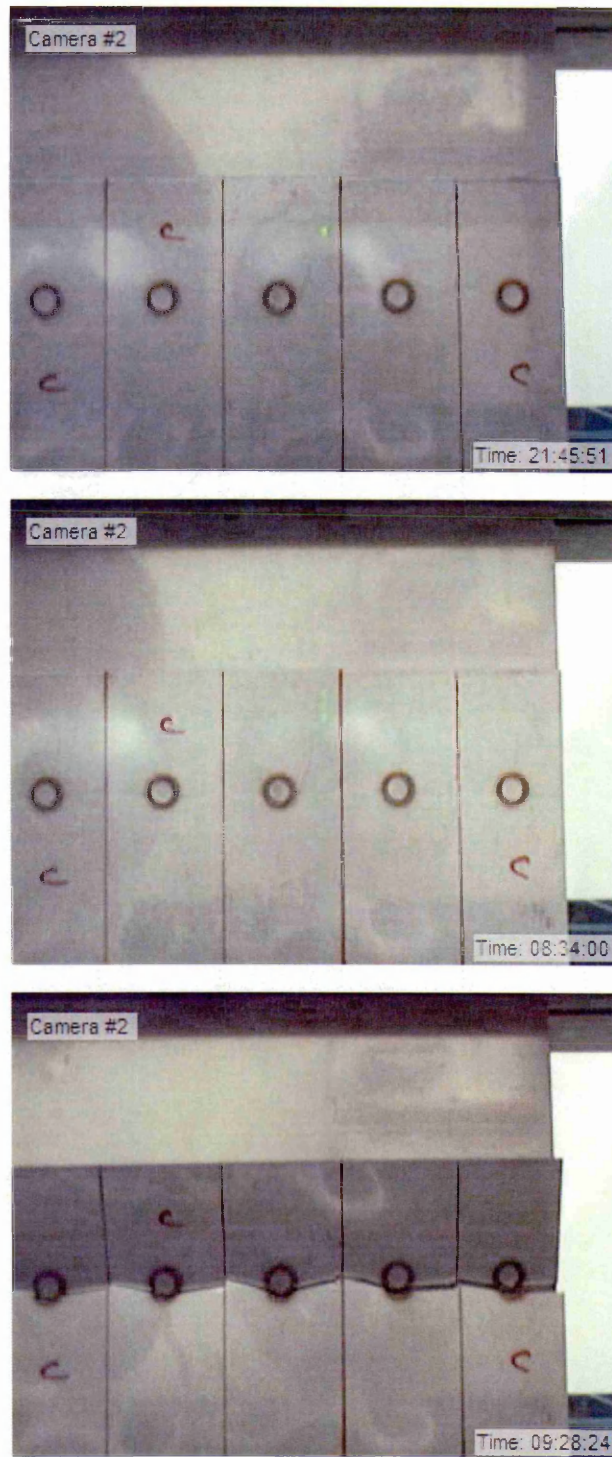
Fig 4.95: Example eight nugget video monitor screen grabs from second half of side 1 of a specimen. From top to bottom: test start, failure conditions met, complete failure.
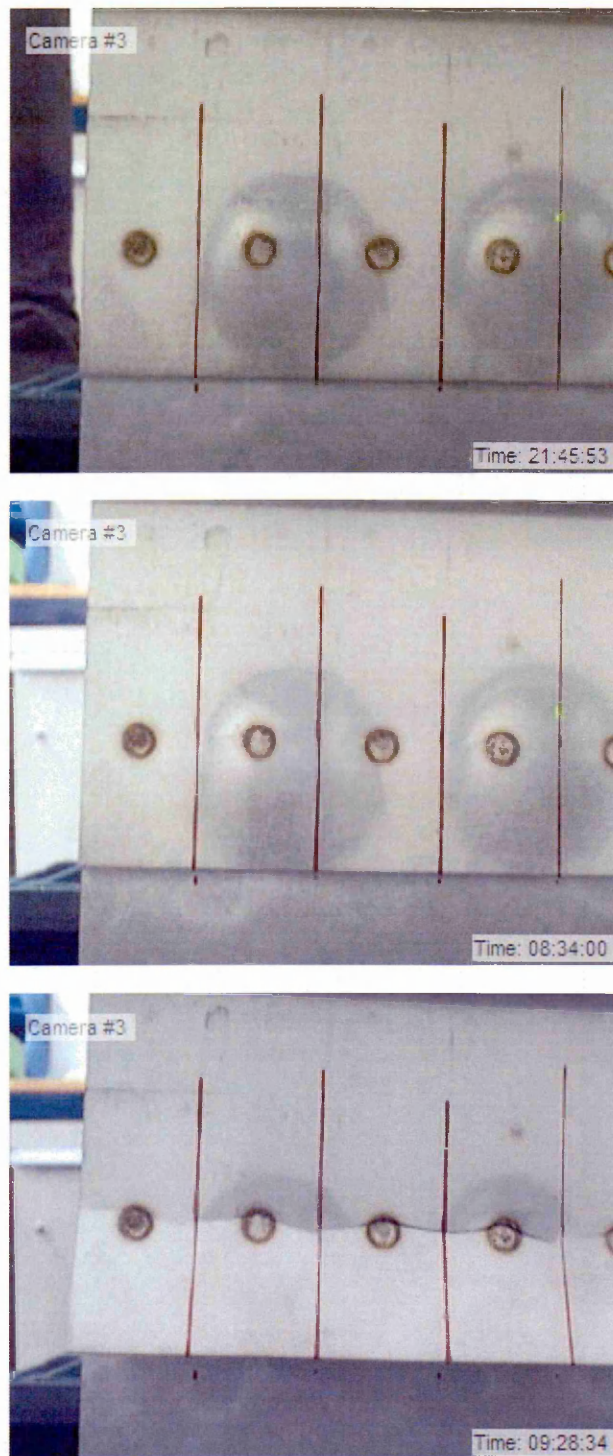
Fig 4.96: Example eight nugget video monitor screen grabs from one half of side 2 of a specimen. From top to bottom: test start, failure conditions met, complete failure.
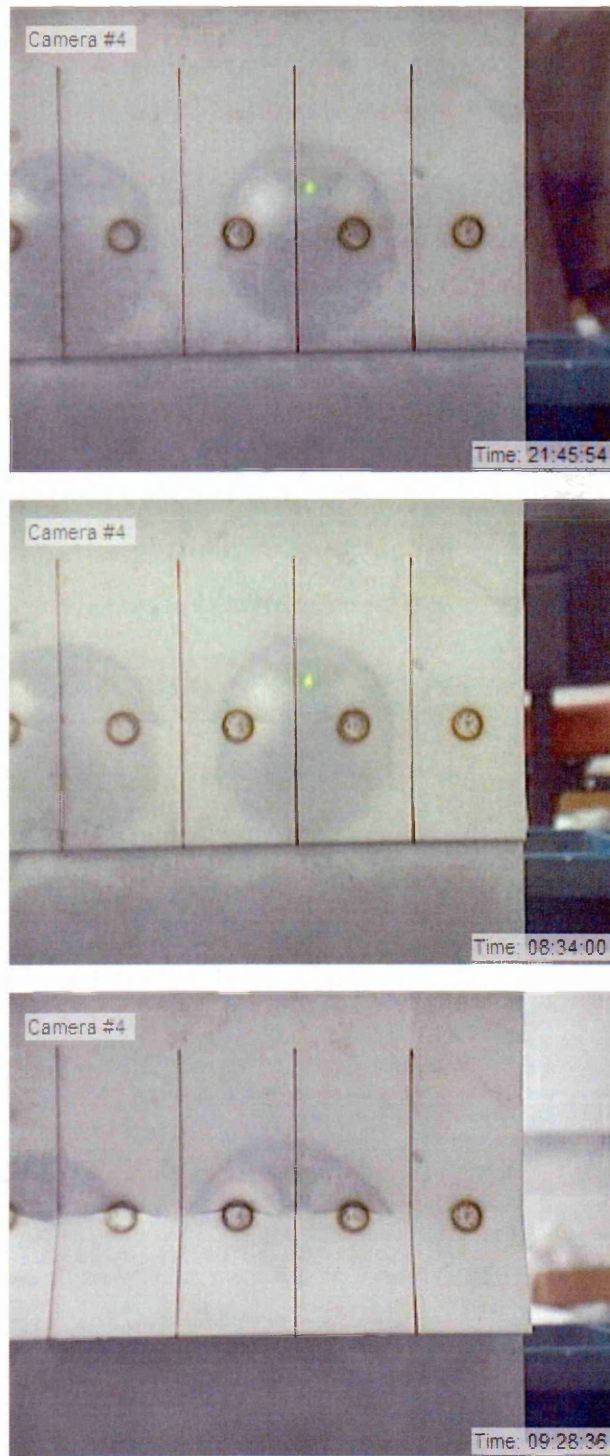
Fig 4.97: Example eight nugget video monitor screen grabs from second half of side 2 of a specimen. From top to bottom: test start, failure conditions met, complete failure.

4.4.3.4: Sixteen Nugget Staircase Results.

Load Range, kN	Step No. i	1	2	3	4	5	6	7	8	9	10	11	12	13	14	15	16	17	18	19	20	21	22	23	24	25	26	27	28	29	30	Survivals, r	Failures, f
11.390	2																										X				X	0	2
11.200	1			X				X		X						X		X				X				O		X		O		2	7
11.010	0		O		X		O		O		X		X		O		O		X		O		X		O				O			8	5
10.820		O				O						O		O						O				O								6	0
Σ																																Σr = 16	Σf = 14

Fig 4.98: Sixteen nugget Staircase results.

Step divide used: 0.190 kN

Least Frequent Event: Failures

Load, L_i, (kN)	i	N_i	iN_i	i^2N_i
11.390	2	2	4	8
11.200	1	7	7	7
11.010	0	5	0	0
10.820	-	-	-	-
Sum		14	11	15

Table 4.16: Sixteen nugget Staircase results.

Mean per Spot Weld:

$$\mu = 11.010 + 0.19\left(\frac{11}{14} - \frac{1}{2}\right)$$

μ = 11.0643 kN

μ = 0.6193 kN per spot weld

Convergence Factor:

$$\left(\frac{(15 \times 14) - 11^2}{14^2}\right) = 0.4541$$

Standard Deviation per Spot Weld:

$$s = 1.620 \times 0.19\left(\frac{(15 \times 14) - 11^2}{14^2} + 0.029\right)$$

s = 0.1487 kN

s = 0.0093 kN per spot weld

Standard Deviation on the Mean per Spot Weld:

$$S_m = \frac{1.13 \times 0.0093}{\sqrt{30}}$$

S_m = 0.0019 kN per spot weld

Upper and Lower 95% Confidence on the Mean per Spot Weld:

$$0.6913 \pm 1.96 \times 0.0019$$

0.6913 ± 0.0038 kN per spot weld

Standard Error on the Standard Deviation per Spot Weld:

$$S_s = \frac{1.29 \times 0.0093}{\sqrt{30}}$$

S_s = 0.0022 kN per spot weld

Upper and Lower 95% Confidence on the Standard Deviation per Spot Weld:

$$0.0093 \pm 1.96 \times 0.0022$$

0.0093 ± 0.0043 kN per spot weld
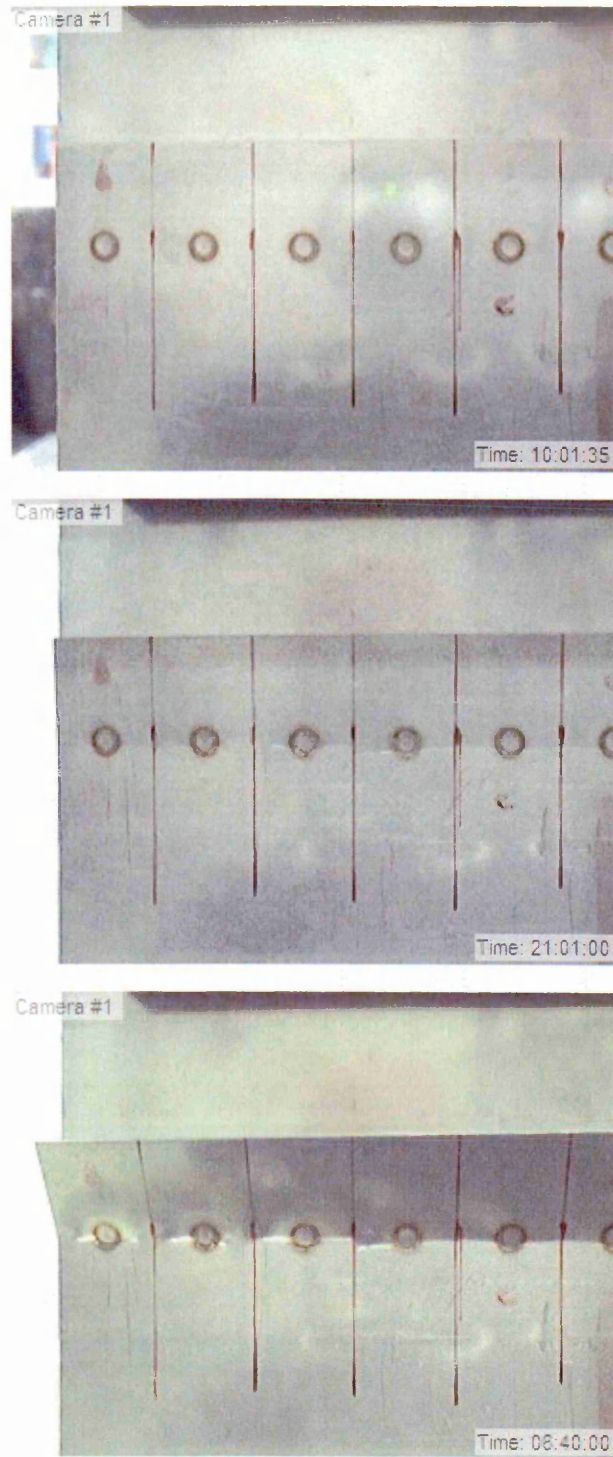
Fig 4.99: Example sixteen nugget video monitor screen grabs from the outside edge of side 1 of a specimen. From top to bottom: test start, failure conditions met, complete failure.
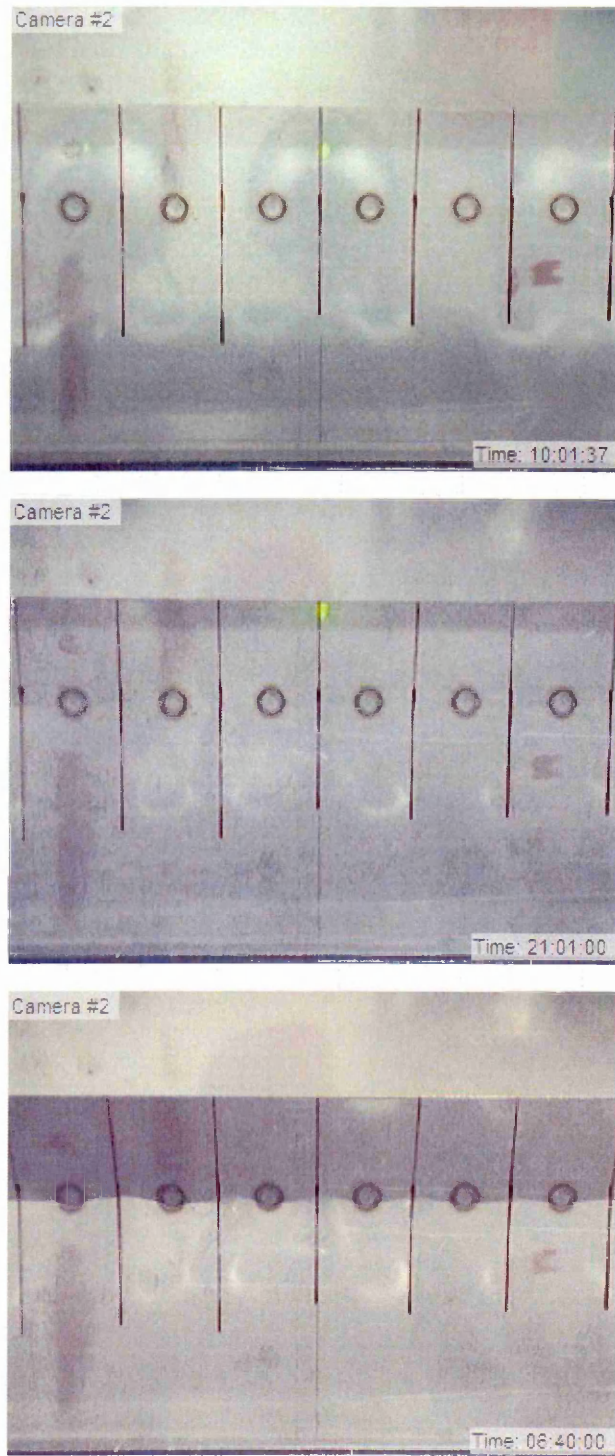
Fig 4.100: Example sixteen nugget video monitor screen grabs from the middle of side 1 of a specimen. From top to bottom: test start, failure conditions met, complete failure.
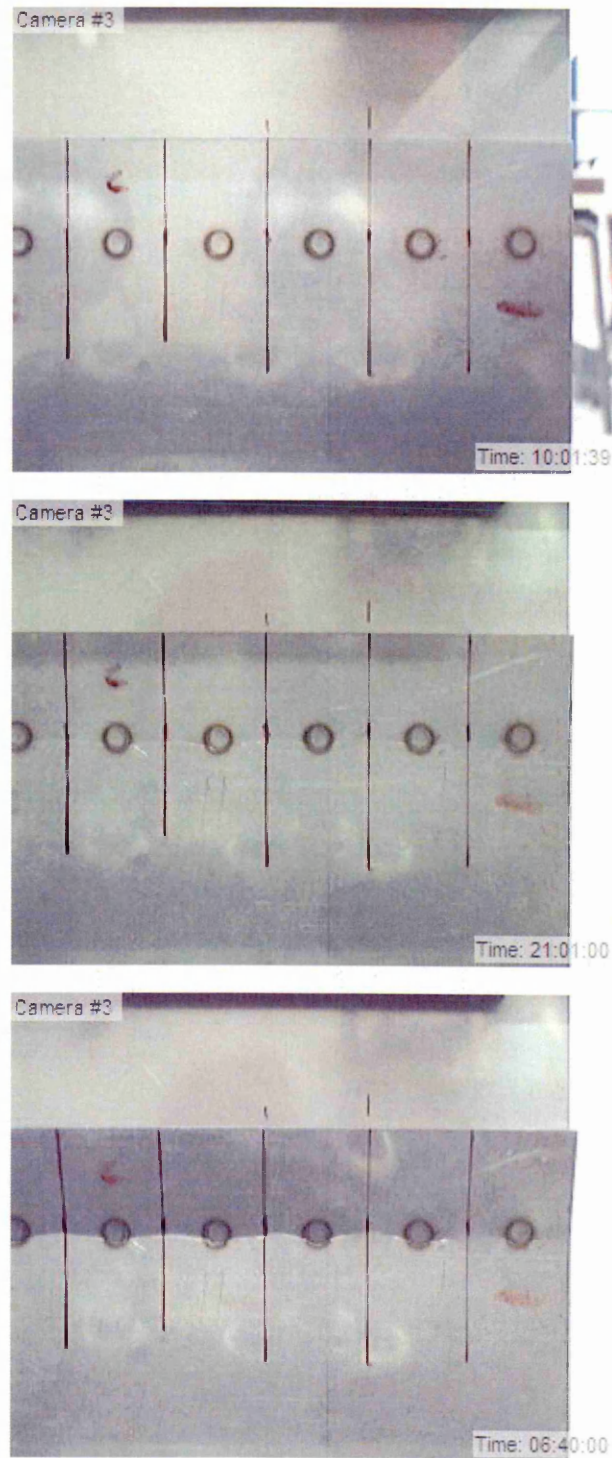
Fig 4.101: Example sixteen nugget video monitor screen grabs from the inside edge of side 1 of a specimen. From top to bottom: test start, failure conditions met, complete failure.
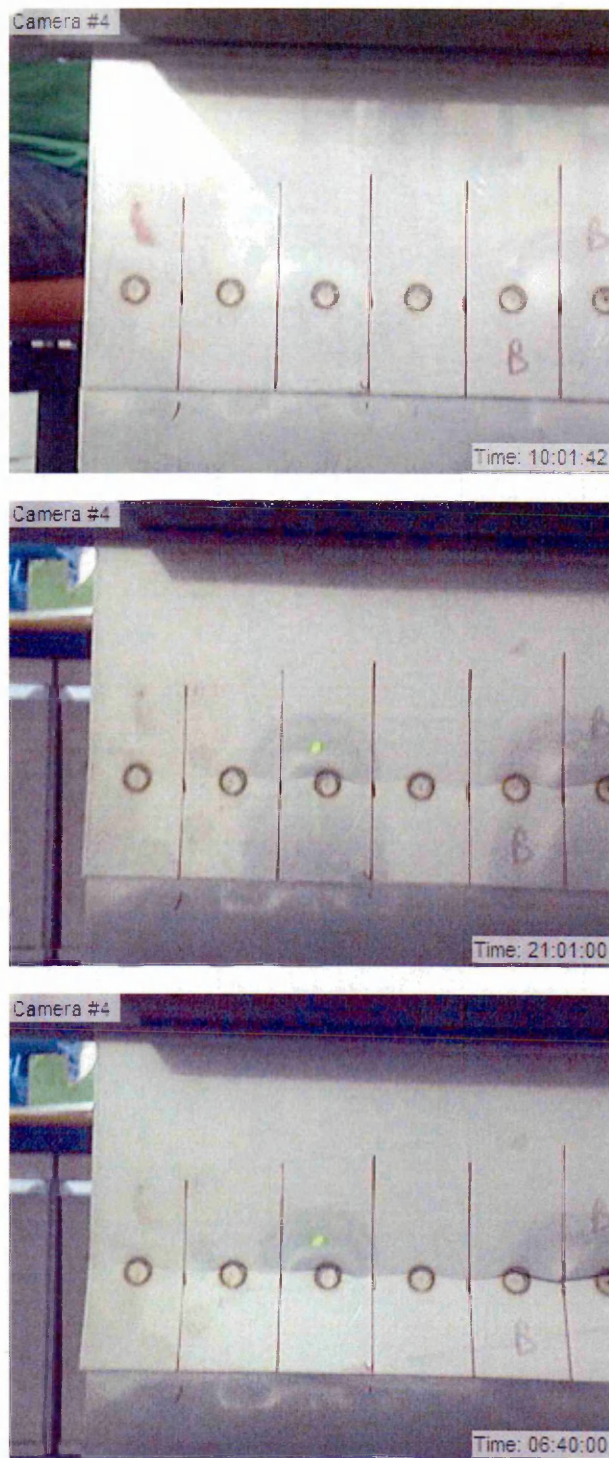
Fig 4.102: Example sixteen nugget video monitor screen grabs from the outside edge of side 2

of a specimen. From top to bottom: test start, failure conditions met, complete failure.
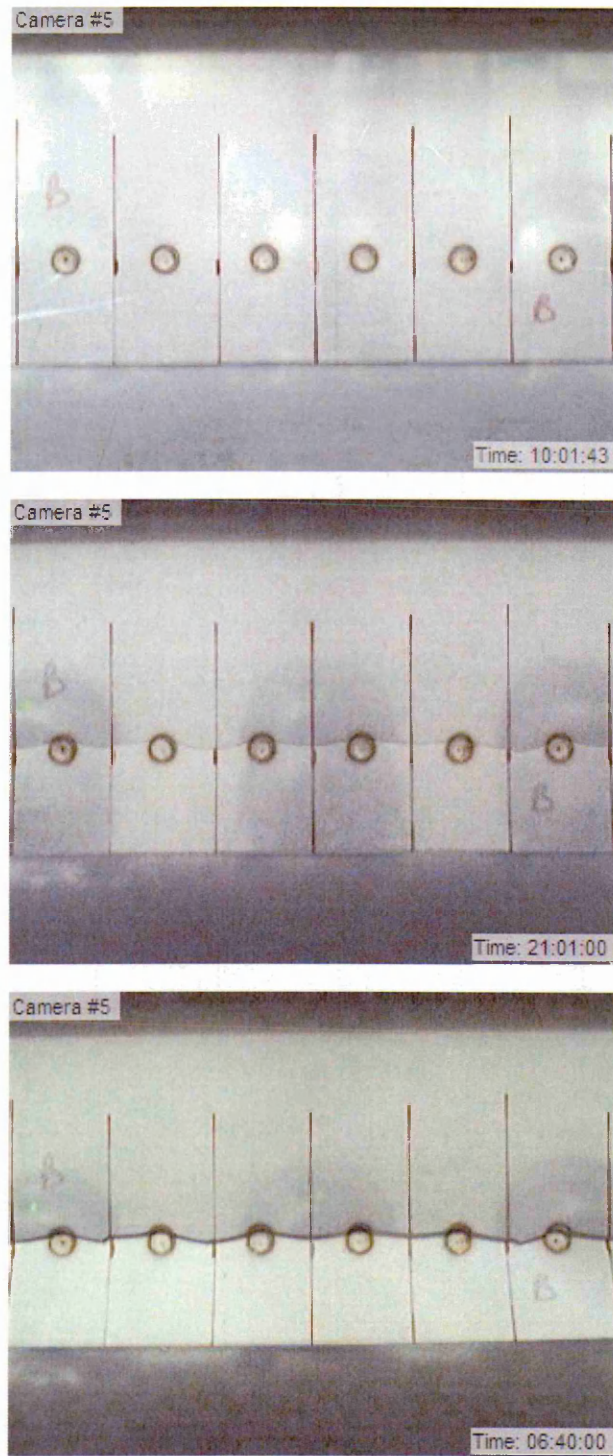
Fig 4.103: Example sixteen nugget video monitor screen grabs from the middle of side 2 of a specimen. From top to bottom: test start, failure conditions met, complete failure.
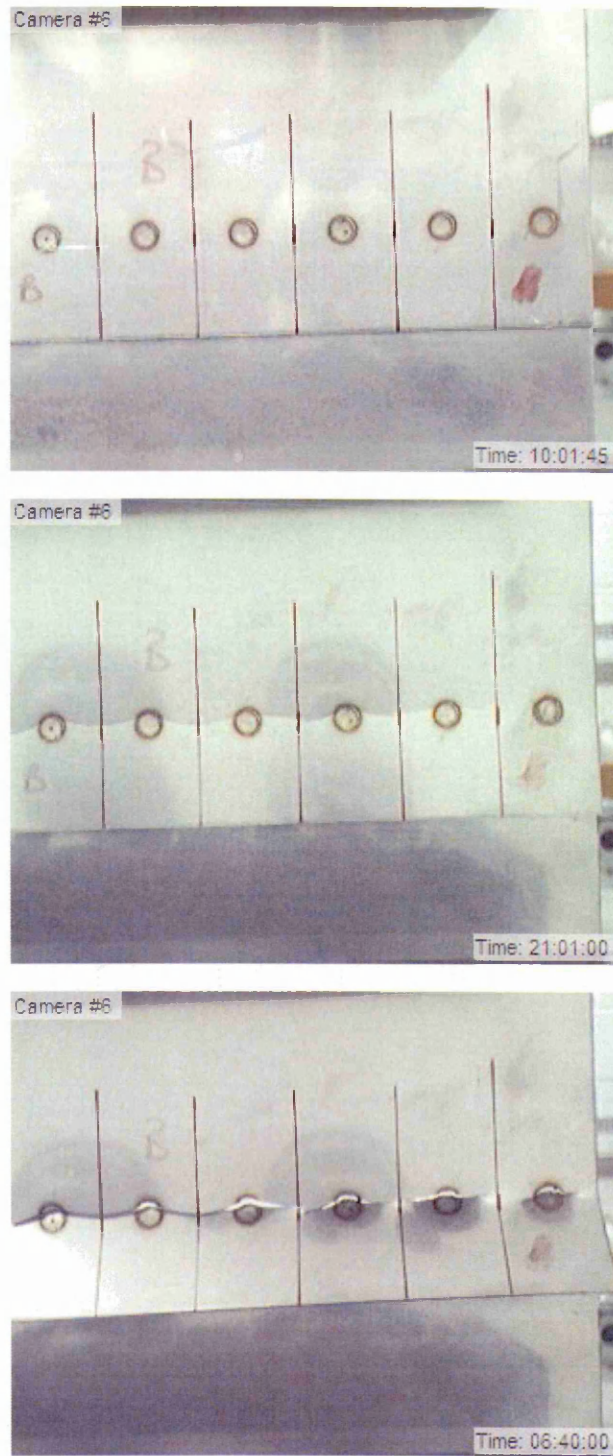
Fig 4.104: Example sixteen nugget video monitor screen grabs from the inside edge of side 2 of

a specimen. From top to bottom: test start, failure conditions met, complete failure.

4.4.4: Correlation between Predicted and Experimental Multi-Spot Weld Fatigue Properties.
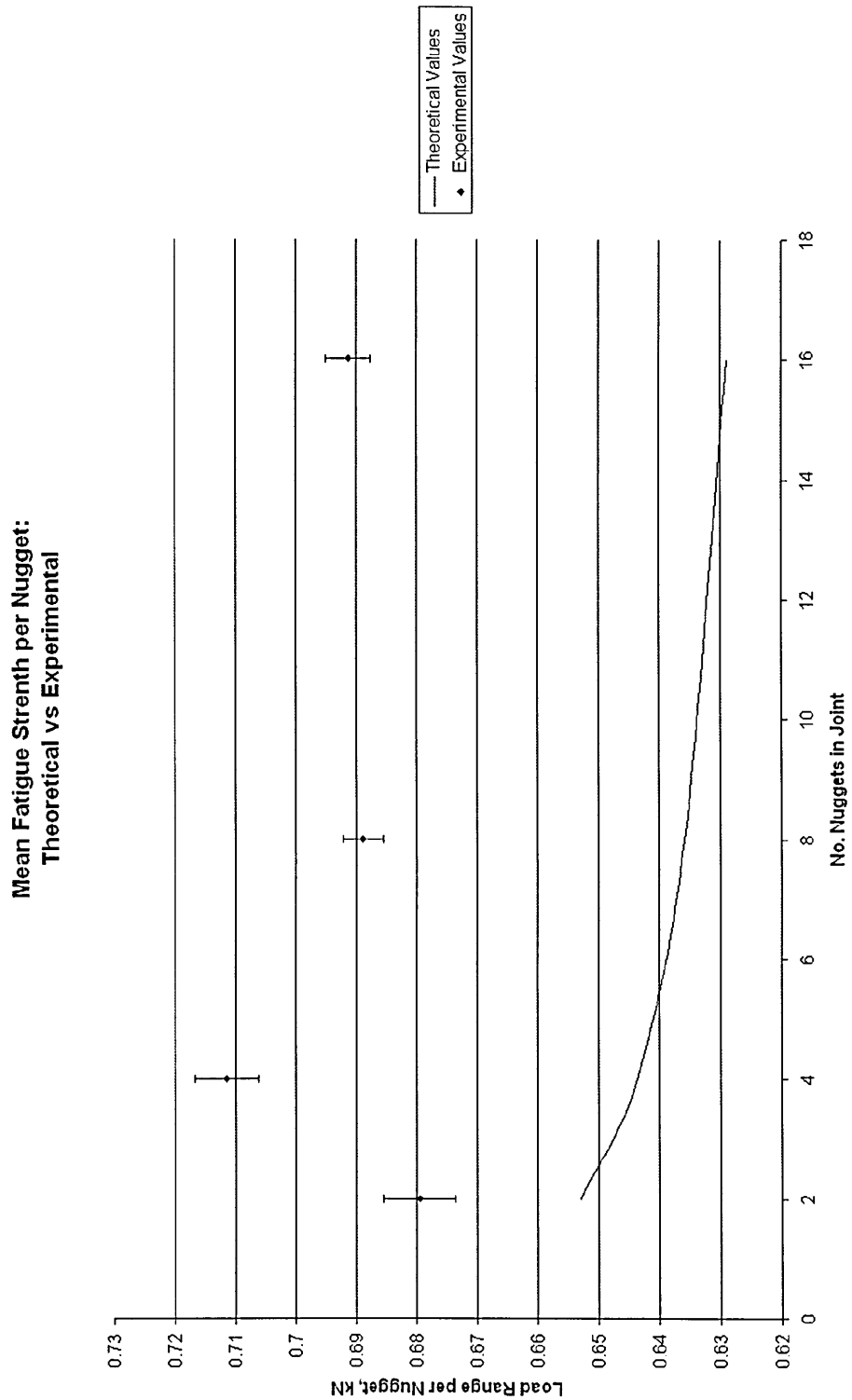
Fig 4.105: Correlation between predicted and experimental multi-spot weld mean fatigue strength.
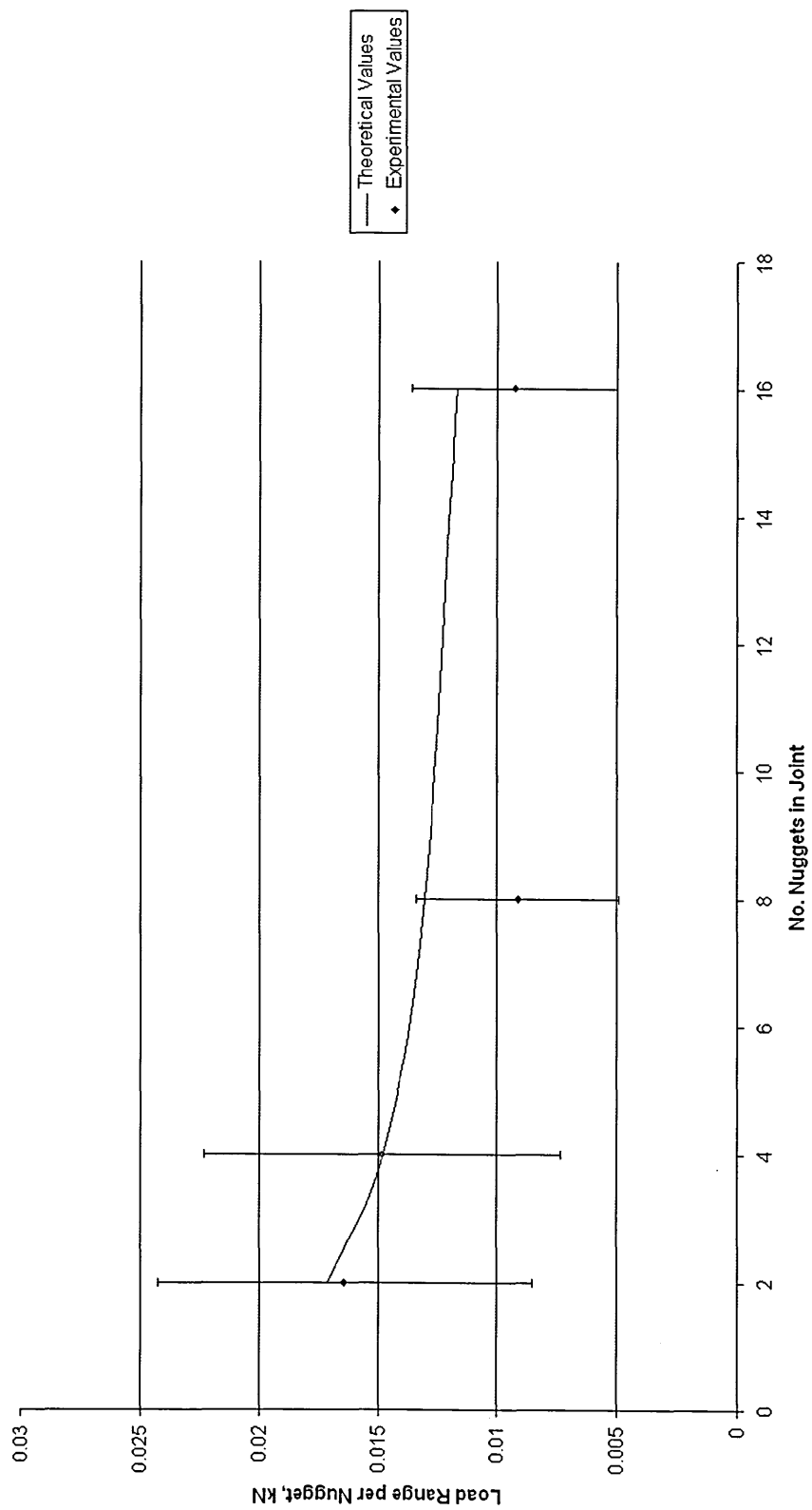
Fig 4.106: Correlation between predicted and experimental multi-spot weld standard deviation.

4.5: Thermoelastic Stress Analysis.

The following images are those that were recorded by the thermoelastic stress analysis camera during the second of the three eight nugget fatigue tests monitored by this equipment. An image was recorded every 100K cycles up until 1000K cycles when the specimen started to fail. After this point two further images were recorded, one at 1050K and one at 1075K cycles, before the specimen failed completely. Only the one set of images are shown as the images from the remaining two tests show very similar results to these.
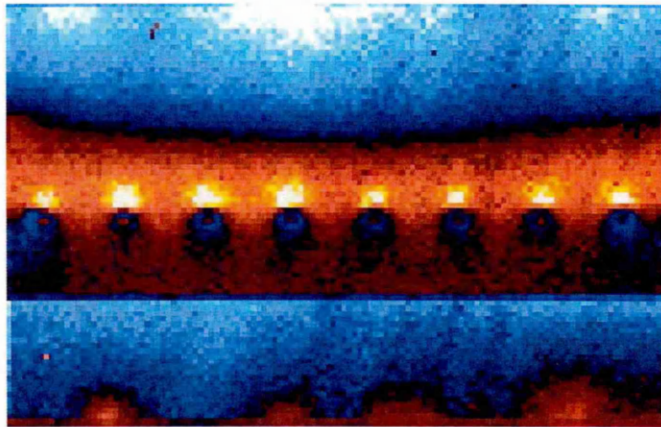
Fig 4.107: Test two 100K cycles.
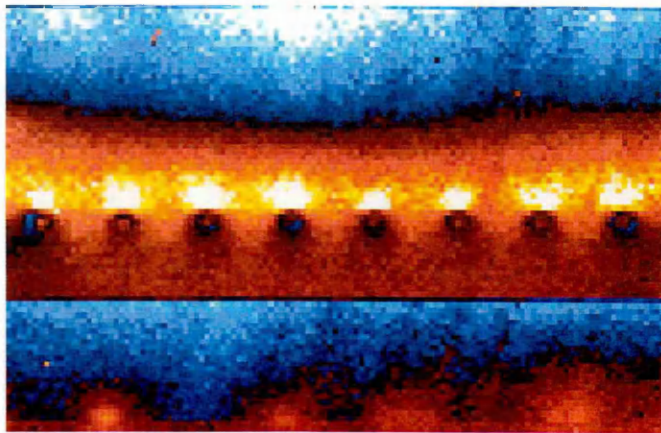
Fig 4.108: Test two 200K cycles.
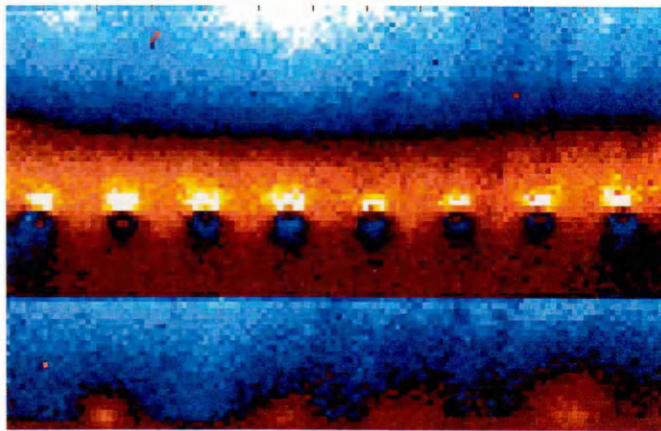
Fig 4.109: Test two 300K cycles.
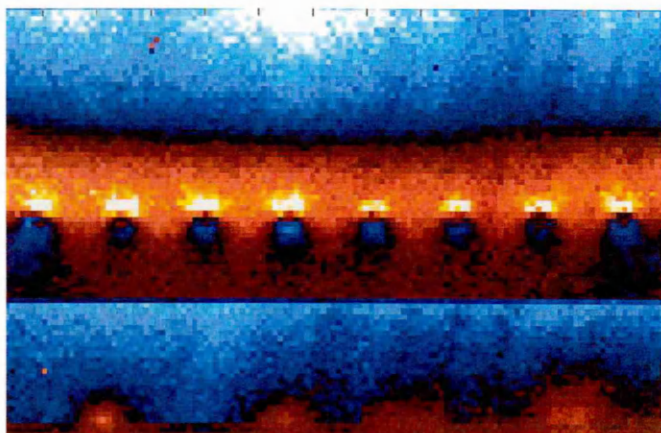
Fig 4.110: Test two 400K cycles.

251
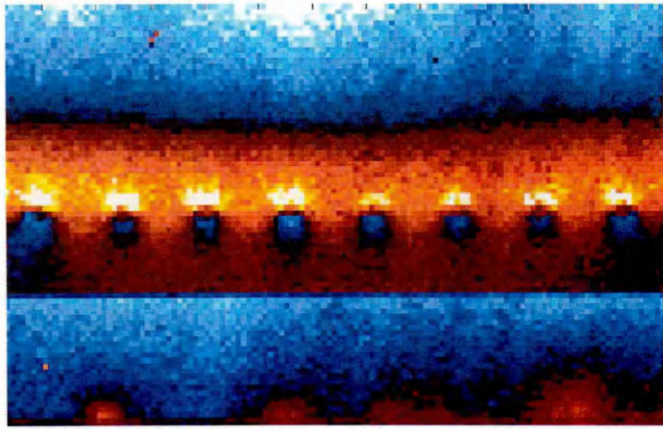
Fig 4.111: Test two 500K cycles.
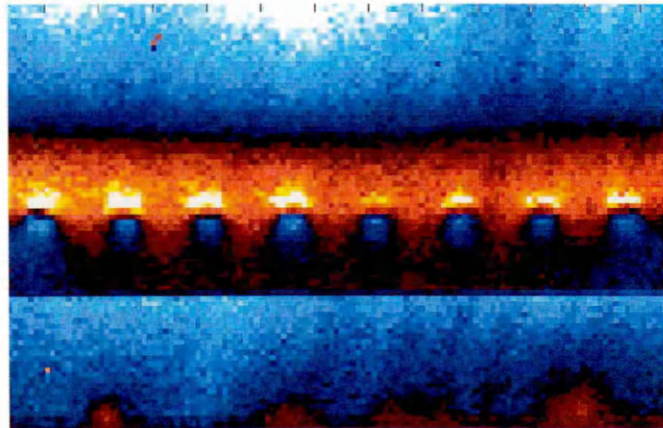
Fig 4.112: Test two 600K cycles.
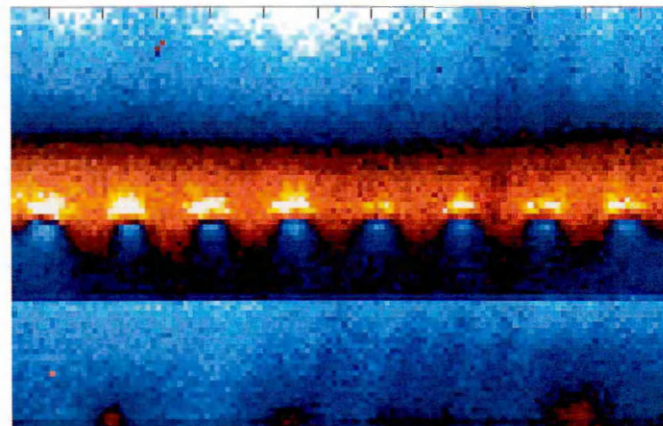
Fig 4.113: Test two 700K cycles.
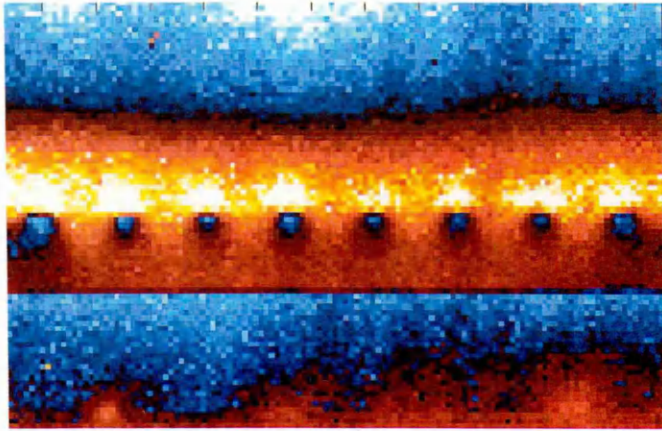
Fig 4.114: Test two 800K cycles.
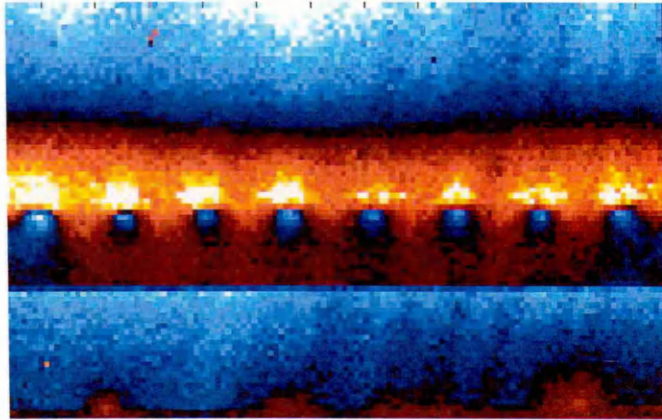
Fig 4.115: Test two 900K cycles.
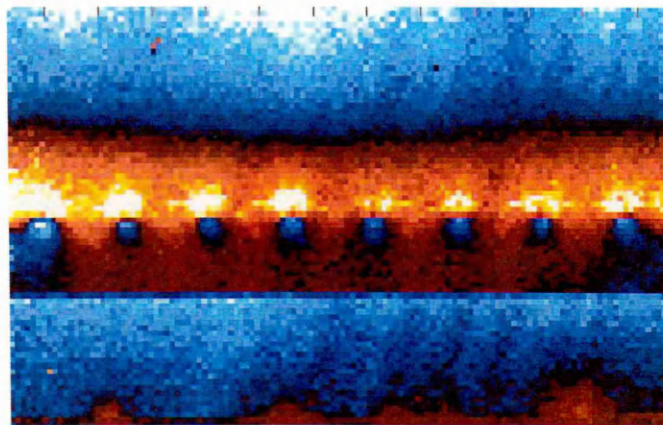
Fig 4.116: Test two 1000K cycles.

253
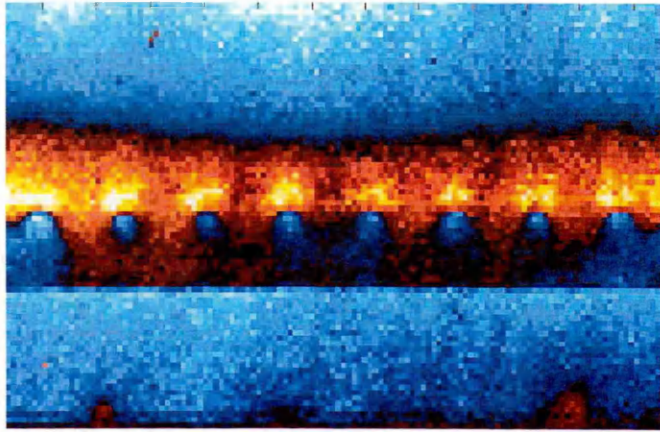
Fig 4.117: Test two 1050K cycles.
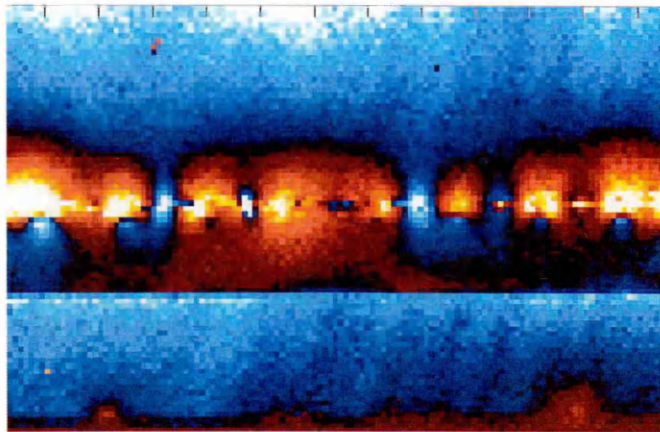
Fig 4.118: Test two 1075K cycles.

254

5: Discussion.

5.1: Base Material Characterisation.

The results for both the tensile and hardness testing were slightly above the values quoted in the mill certificate of the supplied material, but they were well within the tolerances given for this grade and finish of AISI 301. The difference can be attributed to the inherent variations during manufacture and the different testing techniques and equipment.

5.2: Optimum Welding Parameter Investigation.

All the specimens produced in the weldability study failed by interface shearing of the weld nugget when lap-shear tested. Generally it is preferred that spot welded joints fail by weld pull-out, since this implies that the weld nugget is stronger than the surrounding parent plate and is therefore of an acceptably high quality. This preferred failure mode stems from high production industry were qualitative testing of spot welds is the dominant method for quality assurance. The qualitative testing employed usually comprises of a simple chisel test, which is where a chisel, or wedge, is forced between the sheets joined by the spot weld until they are separated. If the separation is caused by shearing of the weld nugget, the join is classed as inadequate and the specimen fails, if they are separated by failure in the parent plate, the join is considered to be sufficient and the specimen passes.

However, AISI 301 is not a standard material typically used in these areas and this type of failure mode is typical for spot welded AISI 301 sheets that undergo lap-shear tests. The cause of this particular failure mode being dominant is due to the high strength and hardness of AISI 301, which offers a considerable amount of restraint. The large amount of restraint will minimise the amount of joint rotation occurring and therefore help to maintain shear as the dominant mode of loading on the nugget [25, 45].

This can be avoided by producing a bigger weld, however, this requires the application of excessively large amounts of force to ensure an intimate bond in the area of the weld between the faying surfaces. Such levels of force are difficult to produce without powerful and expensive spot welding equipment and even then the amount of energy and time required to generate a sufficient amount of force to ensure intimate bonding would make the process uneconomical. Therefore, the dominance of the interfacial shearing as a failure mode is not considered detrimental to the results.

It is clear from Fig 4.1 that the strongest welds are being achieved at a welding current of 4.6 kAmps and a welding time of 15 cycles. It can also be seen that there is a general trend of increasing lap-shear strength with increasing welding current. This was to be expected as the increased current generally ensures the production of a more uniform nugget, with fewer imperfections.

However, the graph also indicates that the lap-shear strength has a tendency to decrease with increasing weld times in excess of 15 cycles. This is unusual as the amount of welding time is a controlling factor in the magnitude of heat generated when producing a weld and, generally, the more heat produced, the better the quality and stronger the weld nugget. Normally the weld strength will increase with welding time until such a time is reached where the heat is being dissipated through the electrodes and surrounding base material at the same rate at which it is being generated. At this point the amount of heat being generated and the weld strength achieved will plateau [5], not decrease as is being seen here. A brief examination of the welds produced using the same welding current and electrode force, but different weld times, has shown a definite change in microstructure. It is possible that this change in microstructure is the cause of this reduction in weld strength seen with increasing weld time and that it is possibly caused by a difference in the temperature gradients. However the cause of this reduction in strength with weld time is of little significance since it dos not appear to be affecting the consistency of the welds produced.

Looking at the results for the consistency of the welds made at each of the parameter sets shows that the repeatability is generally good. However, problems seem to occur when using a welding time of less than 15 cycles, particularly for high welding currents. Welds produced using welding times of less than 15 cycles also had a tendency to exhibit expulsion during their production. When this occurred the specimen was rejected, as welds that had been subjected to expulsion would almost certainly have poor consistency when compared to welds that had not. It is likely that welding times below 15 cycles do not provide sufficient time to ensure that a homogenous weld pool is created, which leads to imperfections and an increased risk of expulsion. This would explain the greater tendency of the welds produced using a welding time of 10 cycles to exhibit expulsion and also the greater amount of inconsistency and lower mechanical properties of these welds when compared to others produced using longer welding times.

Since consistency was the most important factor when choosing the welding parameter values to use in this project, it was decided to ignore all parameter sets that produced a range of lap-shear strength results in excess of 0.4 kN. Since strength was also an important issue to consider, the parameter set that produced the strongest welds within these limits of range was chosen as the first set to use in this project. This was a parameter set comprising of a welding current of 4.6 kAmps and a welding time of 15 cycles

However, there was some concern about the tendency for expulsion and electrode sticking to occur when welding currents in excess of 4.6 kAmps were used. Since any weld that was subjected to expulsion during its manufacture would be rejected, resulting in lost material and time, it was decided to lower the welding current chosen for this study to 4.5 kAmps. This would reduce the risk of expulsion occurring, whilst still maintaining strong consistent welds.

257

5.3: Optimum Pitch Distance Investigation.

5.3.1: Variation in weld strength.

During the lap-shear tests three types of failure were observed. In the specimens taken from the samples made with pitch distances above 17.5 mm, failure occurred by interface shearing of the weld nugget, similar to the joints made in the weldability study. Therefore, the load at failure of these specimens gave a representative indication of the strength of the individual nugget.

In the single weld specimens taken from the multi-spot welded samples made with pitch distances below 17.5 mm, the vast majority of failures occurred in the base material, either by weld pull-out or by excessive rotation and plastic deformation of the base metal. These types of failure were not representative of the strength of the individual weld nuggets and where therefore excluded from the analysis.

The reason these types of failures occurred was due to the very narrow single weld TSSW specimens that resulted from separating narrow pitched multi-spot welded samples into single nugget specimens. As the specimens were so narrow, the distance from the centre of the weld nugget to the edge of the specimen (edge distance) was very small in comparison to the actual nugget size. This small ratio of edge distance to nugget size meant that there was not enough supporting edge material to give appropriate levels of joint stiffness, this lead to excessive amounts of joint rotation, resulting in failure in the base material. The overall effect of this means that the results obtained from the 12.5 mm and 15 mm pitch samples could not be used to measure variation in weld nugget strength as the loads recorded were a measure of the strength of the single specimen joints as a whole, rather than just the nuggets.

When it came to testing the 17.5 mm pitch samples, a cross over was noted between parent plate failure and weld nugget failure. On two of the three samples tested, the first weld failed in the parent plate, by weld pull-out, while the remaining four welds all failed by interface failure.

This would suggest that the ratio of the edge distance to nugget size is increasing between the first and second welds. This would mean that either the specimen width is increasing or the weld nugget diameter is decreasing. Since the specimens from any group of pitch distance samples were all cut to the same width, it is reasonable to assume that the nugget diameter is decreasing. This would be expected in a multi-spot welded joint where current shunting was occurring, since the first weld in any row of welds would be expected to be larger than the subsequent welds, due to it not experiencing any current leakage.

The single weld specimens from the remaining samples produced using pitch distances of 20, 30, 40 and 50 mm all failed by interface shearing of the weld nugget, meaning the magnitudes for failure load recorded during the lap-shear tests were indicative of the mechanical strength of the nugget. The effect of specimen width on joint stiffness can also be seen clearly in the images in Figs 4.3 through 4.29, with the amount of plastic deformation caused by the degree of joint rotation visibly decreasing as the specimen width increases.

The results for the 20 mm, 30 mm, and 40 mm pitch distance samples show a steady decrease in the variation in failure load between welds made in the same series. This follows the theory that as the pitch distance is increased, less and less current is lost through shunting, as the distance between welds becomes too great and therefore offers too much resistance. This therefore allows for consistent sized and, consequently, consistent strength welds to be produced.

The results would suggest that if the first two welds from a row of welds made using a pitch distance of 20 mm were removed, then the remaining welds would all have similar mechanical properties. A row of welds made using a pitch distance of 30 mm would only require the first weld to be removed and a row of welds made using a pitch distance of 40 mm would not require the removal of any welds.

The results from the samples welded with a pitch distance of 50 mm indicate a stronger first weld compared to the other welds in the series, which all have consistent strength properties. This is most likely due to an unseen anomaly, perhaps an effect of inductance caused by welding such large samples [11], or possibly the results are just representative of the degree of inherent variation caused by the testing of very wide specimens.

5.3.2: Variation in Nugget Diameter.

On examination of the nugget diameter measurements, taken from welds produced at each of the pitch distances under investigation, it is difficult to ascertain whether current shunting is affecting the size of the nuggets produced.

If current shunting was occurring then one would expect the first weld produced in any sequence to display the largest diameter, with all subsequent welds being of similar sizes, with any variation being attributed to inconsistencies in the process or equipment.

In the results to the experiments carried out in this study only the sequence welded at a pitch distance of 12.5 mm displays this characteristic and even then the difference in size between the first weld and all subsequent welds is negligible. It could be argued that the results are not representative of the true nugget diameter of welds produced at the specified pitch distances, since only one sample from each arrangement was tested. However, it is far more likely that the electrical resistance of the material is so high, that even at small pitch distances, such as those below 20 mm, the resulting amount of current shunting is too small to reliably detect using the present methods of sample preparation and measurement. In this case further testing would be futile and would not produce sufficiently accurate, nor representative, results.

The likelihood of this was realised at the start of the project, which is the reason why only one group of specimens were tested. However, since the results from the Variation in Weld Strength Study indicate that there is an effect of current shunting on weld strength, and that the effect is likely to be caused by a reduction in the nugget diameter of welds, subsequent to the first, then it is important that the effect of current shunting on nugget diameter be fully investigated.

5.4: Variation in Nugget Diameter at Extremely Close Pitch Distances.

Examination of the change in nugget diameter between the first and second welds produced in each specimen showed that three of the five specimens exhibited the expected decrease in nugget diameter between the first and second weld. However, it also showed that the first and second welds in one of the specimens both had identical diameters and that one of the specimens exhibited an increase in nugget size when comparing the diameter of the first nugget to that of the second.

Overall the results of the five specimens used as part of this study displayed very little change between the diameters of the first and second nuggets. The average change in diameter was a decrease of 0.085 mm, which is what would be expected if current shunting was occurring. However, if this is the case at very small pitch distances it would suggest that any variation found between the nugget diameters of the welds produced in the Variation in Nugget Diameter Study will likely be the result of the inherent variability of the welding equipment and/or the sectioning and examining process, and not the result of current shunting.

Based on the evidence found here and in the Variation in Nugget Strength study, and taking into account that smaller specimens would be easier to produce and handle, a protocol of using a pitch distance of 20 mm and removing the first and second welds produced in any series was chosen as being the best approach for manufacturing consistent specimens for the purposes of fatigue testing in this project.

5.5: Fatigue Testing.

5.5.1: Staircase Fatigue Testing of Single Nugget Joints.

The initial estimate of a mean fatigue load range of 0.756 kN for the single nugget joints, was slightly higher than the final calculated value. This was expected since the chosen value was an estimate based on results gathered from testing similar, but considerably wider joints. As explained in Section 3.1.2, situations such as this dictate that testing continues until a turnaround point has been defined. The results obtained before this turnaround point have been omitted from the results sections and investigation, since they were not used in the evaluation process.

The final calculated value for the standard deviation of 0.0183 kN is reasonably close to the estimated value of 0.027 kN. The close proximity of this initial estimate to its final calculated value directly influences the accuracy of the results produced by the Staircase process, since the ratio of the estimated standard deviation to the final calculated standard deviation *(d/s)* affects the correction factors *G* and *H* used to determine the 95% confidence limits on the final calculated mean fatigue strength and standard deviation values. The bigger the difference between the estimate and the final calculated value for the standard deviation, the more the values for *G* and *H* begin to diverge away from a normalised level. This increases the upper and lower bands on the 95% confidence limits, as shown in Equations 3.6 and 3.9 in Section 3.1.2.2. The values calculated in this Staircase study, for both the mean fatigue strength and the standard deviation, can therefore be considered to be accurate measurements.

On examination of different specimens at various stages of fracture it can be seen that cracks initiated on both sides of the specimen at the notches present at the edge of the diffusion bonded zone at the sheet interface. The cracks then grew through the thickness of both sheets, towards the surface. Once the cracks had penetrated the surface they began to grow laterally across the specimen width.

Generally the cracks on each side of the specimen grew at the same rate, resulting in the classic 'tick' bend on failure, associated with lap joints.
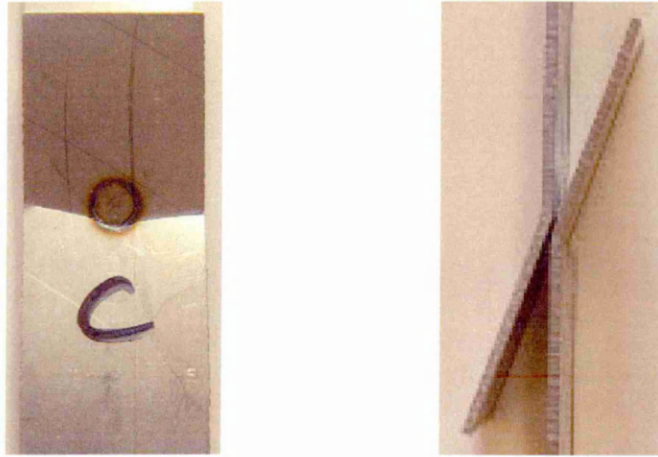
Fig 5.1: Even fatigue cracking in single spot welded joints.

On some specimens the crack on one side of the joint took dominance and managed to traverse the entire width of the specimen faster than the crack on the opposite side. This resulted in complete fracture on one side of the specimen, but left the crack on the opposite side in an earlier stage of lateral growth. The occurrence of these dominant cracks always happened in the very late stages of the cycle life of a specimen. During this time crack growth would accelerate on both sides of the specimen resulting in either two even cracks, as seen above, or a dominant crack, as seen below. Since the portion of the total cycle life taken up in this final stage of the fatigue test was so small, the effect of uneven cracking on the results was not significant enough to warrant concern.

Fig 5.2: Uneven fatigue cracking in single spot welded joints.

263

5.5.2: Probit Fatigue Testing of Single Nugget Joints.

The response curve fitted to the Probit data points correlates well with the estimate PDF that can be produced from the Staircase data. The main inconsistency between the two plots is in the positioning of the mean fatigue strength value, which can be found at the point where the transformed value, Y, equals zero.

Comparison of Staricase PDF and Probit Response Curve
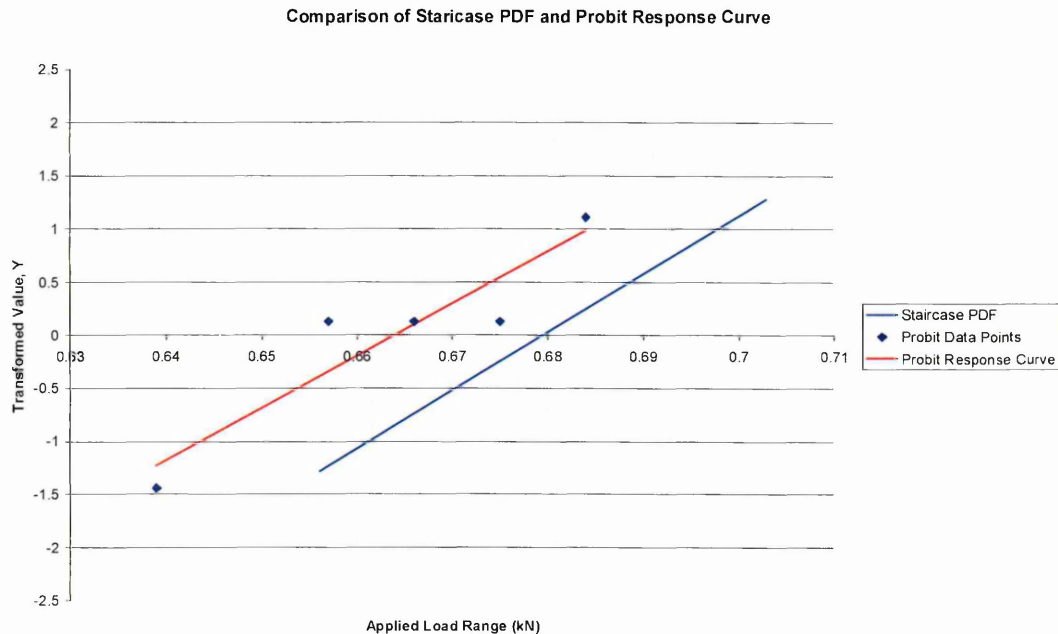
Fig 5.3: Comparison of Staircase PDF estimate and Probit response curve.

The similarities between the gradients of the two lines indicate that the values for the individual standard deviations, displayed by the two distributions, vary very little from one another. This is confirmed in the results, which show standard deviations of 0.0183 kN and 0.0203 kN for the Staircase and Probit results respectively.

This is reassuring, since it removes a considerably amount of doubt in the ability of the Staircase testing process to produce reliable values for standard deviation. This would suggest that the standard deviation values for the multi-spot welded joints generated by the Staircase process will be comparable in accuracy to those that could be generated using the more time consuming, but generally more accurate, Probit process.

264

By indicating such a small standard deviation, these results suggest that the capability of the equipment, and author, to produce welds with consistent fatigue properties, was significantly underestimated. While this is a good thing, since the production of consistent welds was a primary condition for this investigation, it also means that there needs to be a very high degree of accuracy and repeatability in the testing process. By having a fatigue strength distribution with such a small standard deviation, it means that even very minor changes in the applied load range can result in significant changes in the probability of survival. Therefore, if the equipment is not able to accurately produce the loads requested of it, then it could cause a significant change in the outcome of the test.

The minor discrepancy between the mean fatigue strength values calculated by the Staircase and Probit distributions is a case in point. If the individual data points plotted from the Probit results are considered, it can be seen that there is a degree of ambiguity around the mean level, with three different load levels each purporting to produce a 45% probability of survival. As explained, these inaccuracies are an understandable problem from having such a small standard deviation, since small standard deviations mean that if the equipment deviates, even slightly from the requested load, then there will be a significant difference between the predicted and actual survival probability. It is therefore likely that since these three load levels were so close to one another the equipment had trouble accurately and consistently producing the individually requested loads for the three data points, without some degree of overlap. This resulted in the survival probability of the three data points being equal.

Since the Probit study was carried out using a significantly larger number of specimens, the value it calculates as being the mean fatigue strength will be a more accurate representation of the actual value when compared to the one predicted by the Staircase process, it was therefore still used to predict the values required to Staircase test the multi-spot welded joints. Fortunately, the problem explained above does not indicate that the values predicted by the Staircase process for the multi-spot welded joints will be inaccurate. This is because the load range levels used in the multi-spot welded tests are larger and more spread out. This makes it much easier for the fatigue equipment to accurately and consistently produce the required load levels.

5.5.3: Multi-Spot Weld Staircase Testing Process.

For each of the different multi-spot welded specimen configurations tested, it was clear early on that the values for the mean fatigue strength, predicted by the proposed theory and the collected Probit data, would be lower than the ones determined experimentally, since the first group of results from each multi-spot welded joint configuration tested were all survivals. These early results were omitted from the results and analysis stages, since they did not form part of the active levels.

Once the first turnaround point had been found, and data for the active levels was being collected, it became apparent that the predicted values for standard deviation were reasonably accurate, as the spread of active load levels was at an acceptable level.

The various stages of fatigue crack growth occurring in all the multi-spot welded joints were the same as those predicted and seen in single nugget joints. The fatigue cracks occurring in the double and four nugget multi-spot weld tests were very similar to the single nugget specimens, with cracks on a given side of the specimen propagating at a similar rate for all spot welds, resulting in complete fracture occurring very shortly after any one crack reached the critical failure length. The tendency for cracks on one side of the double welded specimens to propagate faster than the ones on the other side was similar to that of the single nugget specimens, however this tendency increased with the four nugget specimens, with the majority showing more advanced cracking on one side when compared to the other.

As with the single nugget specimens, this uneven cracking always manifested itself in the very last stages of the fatigue life of the specimen. Since the portion of the overall fatigue life taken up by this stage of crack growth was so small, the effect of this uneven cracking on the results was not considered to be significant.

With the eight nugget specimens, the stage of crack development for each of the cracks at failure became more uneven. Some of the specimens that completed the designated 10^6 cycles without meeting the conditions for failure were removed from the test equipment while the cracks were still in the early stages of lateral growth. When these specimens were examined, it revealed that all the cracks on both sides of the specimens were of an equal length. When the specimens that had continued to be tested until the test was stopped by the displacement trips where examined, the majority showed groups of three to five welds that had more advanced cracking on one side of the specimen. The location of these groups of heavily cracked welds varied, some occurred in the middle of the specimen (Fig 5.4), some occurred on the edge (Fig 5.5).
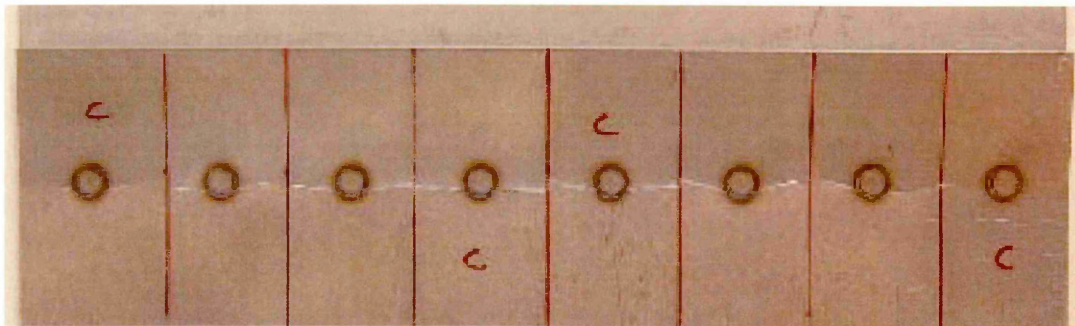
Fig 5.4: Group of cracked welds occurring in the middle of an eight weld specimen.
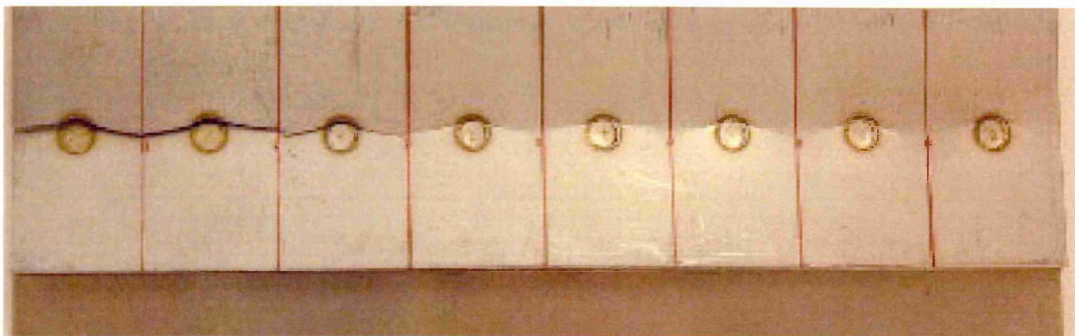
Fig 5.5: Group of cracked welds occurring at the edge of an eight weld specimen.

When larger groups of welds developed these more advanced cracks at the edge of a specimen, it sometimes caused the specimen to lose rigidity in one half. This would cause the actuator of the fatigue equipment to rotate around its axis of operation, which would result in additional torsional stresses being applied to the specimen through rotation of the upper jaw.
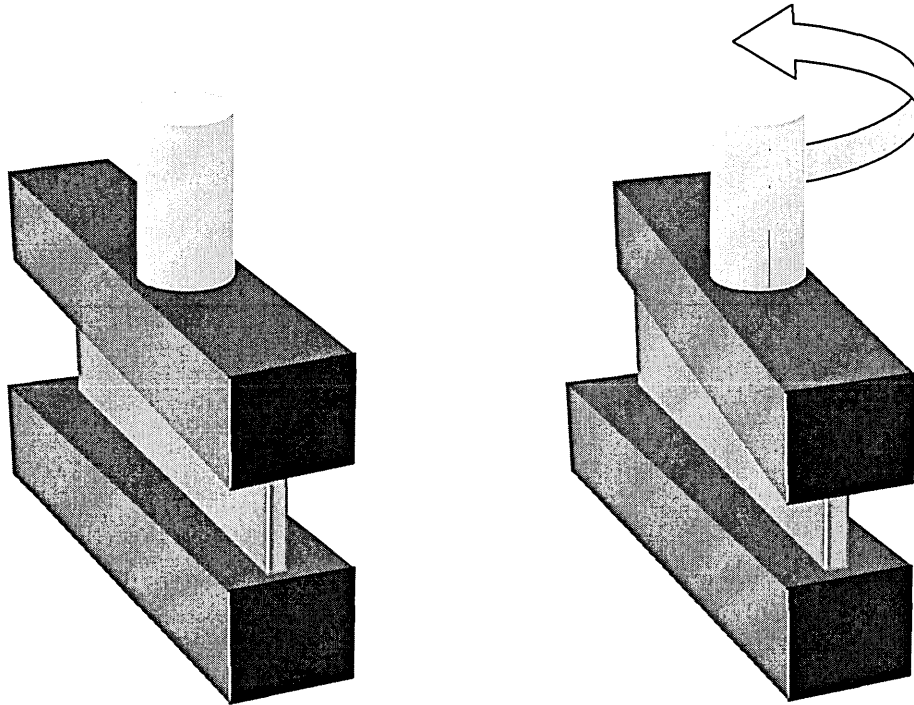
Fig 5.6: Rotation of upper jaw and actuator.

Fortunately this did not affect the results, since the rotation of the actuator always occurred after the conditions for failure, stipulated by this study, had been met, and so the test had effectively already ended.

A similar situation, where groups of welds would develop into failure cracks at an advanced rate, occurred with the sixteen nugget specimens, except the groups of welds consisted of between four to ten welds. As before, these groups appeared on both halves and both sides of the specimen, with no preference to any particular location. As with the eight nugget specimens, if these groups congregated on the edge of the specimen it caused an imbalance in the load, resulting in the actuator rotating and imparting additional torsional stresses on the specimen. Again, this was not considered to be significant, since it always occurred after the conditions for failure had been met.

The monitoring system devised for the multi-spot welded fatigue tests operated within expected levels. There were some instances where it was difficult to determine the length of the fatigue cracks, due to a shadow or reflection obscuring the image. These instances were rare but when they did occur a thorough analysis of a still image taken at the point where 10^6 cycles would have been completed was carried out to identify the size of any fatigue cracks present as best as possible.

A discrepancy of up to 5000 cycles could be found when comparing the number of cycles recorded by the monitoring equipment and the number calculated using the time indexing on the video footage. This was to be expected as the cycle counter on the fatigue equipment is not 100% accurate and the 5000 cycle discrepancy accounts for only a 0.5% variation, which is well within accepted tolerances.

5.6: Correlation between Theoretical and Experimental Mean Fatigue Strength Data.

The results for the mean fatigue strength, determined for each of the multi-spot welded joints tested, were all higher than the theoretical values predicted from the single nugget Probit results.

Mean Fatigue Strenth per Nugget:
Theoretical vs Experimental
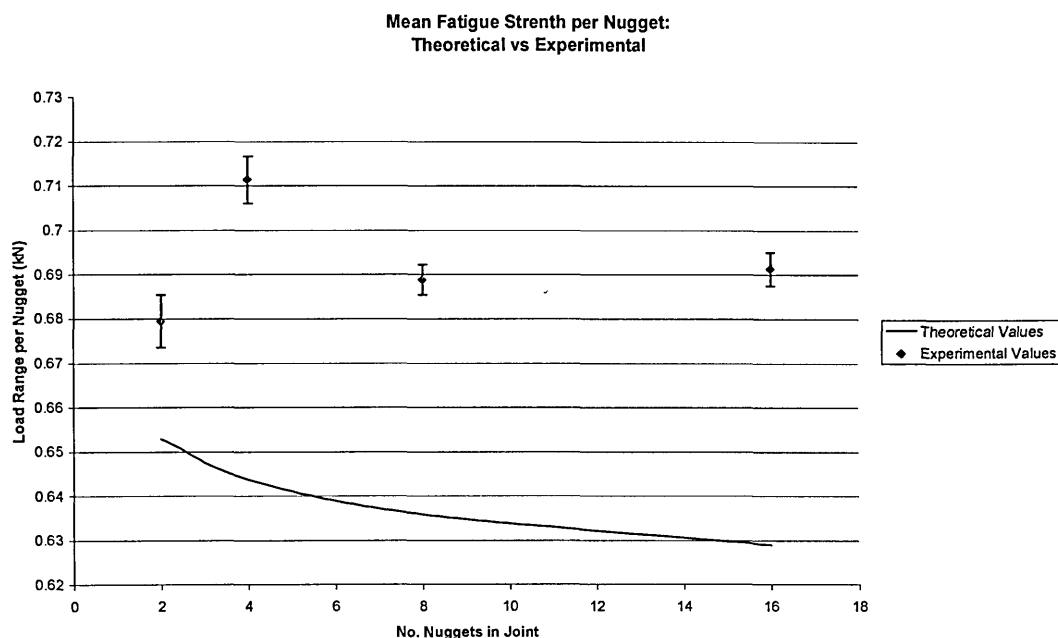
Fig 5.7: Correlation between theoretical and experimental mean fatigue strength data.

The difference between the corresponding theoretically proposed values and experimental values is small in terms of an absolute scale, however, in terms of the distributions they represent, they are all at least 1 standard deviation higher than expected. This would suggest that the correlation between the estimated magnitudes and the actual magnitudes is fairly poor.

It can also be determined from Fig 4.91 (repeated above as Fig 5.7) that the general trend shown by the experimental results is different to that which was predicted by the theoretical model. This indicates that in addition to the magnitudes of the theoretically predicted results being different to those determined experimentally, the variation in mean fatigue strength as the number of nuggets increase, is also different to that predicted by the proposed theory.

The general trend shown by the experimental results indicates a constant mean fatigue strength per nugget, which is very similar in magnitude to that which was derived for the single nugget joints in the Staircase study. It can determined from the multiplication rule of probability, explained in Section 1.1, that every time a weld is added to a multi-spot welded joint, the mean fatigue strength of that joint, as a whole, will increases, since there is more available contact area to transmit load. However, the increment by which the mean fatigue strength of the whole joint increases, reduces with every additional spot weld.

This is because the survival criteria of a multi-spot welded joint is defined as the survival of 100% of the constituent welds, therefore, every time a weld is added, the probability of the joint surviving at a given fatigue load per spot weld decreases, since the addition of every spot weld will cause an increase in the number of conditions that need to be met in order for the joint to survive. For example, consider two ostensibly identical multi-spot welded joints, each with a mean fatigue strength of X. If these two joints were tested individually at an applied fatigue load of X, each one would have a 0.5 probability of surviving. If however, these two individual joints were combined into a single joint and tested at an applied fatigue load of X per spot weld, i.e. $2X$, then the probability of the joint surviving will drop to 0.25. This is because, while the probability of each individual weld surviving this applied load is still 0.5, in order for the whole joint to survive, both of the welds must remain intact. Therefore, the probability of the whole joint surviving is defined by the multiplication rule of probability and is calculated as the product of the two individual probabilities [1].
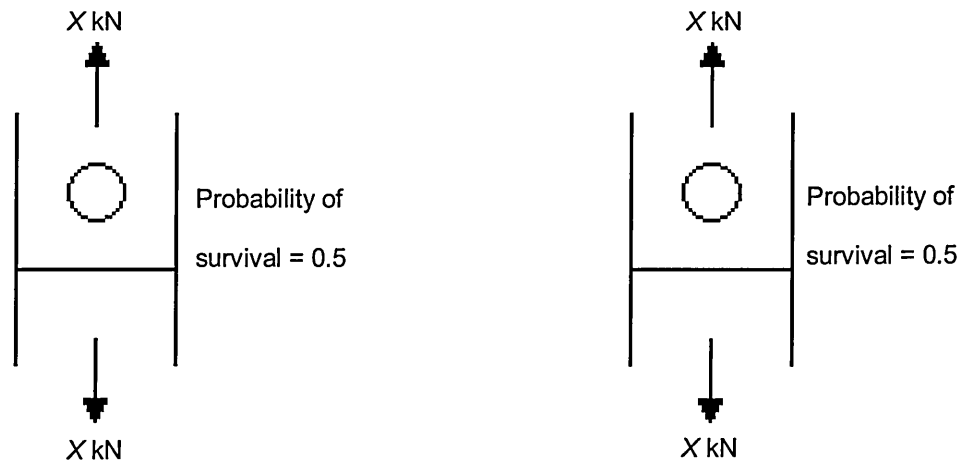
Fig 5.8a: Probability of two identical spot welds surviving two individual fatigue tests using an applied load equal to their mean fatigue strength.
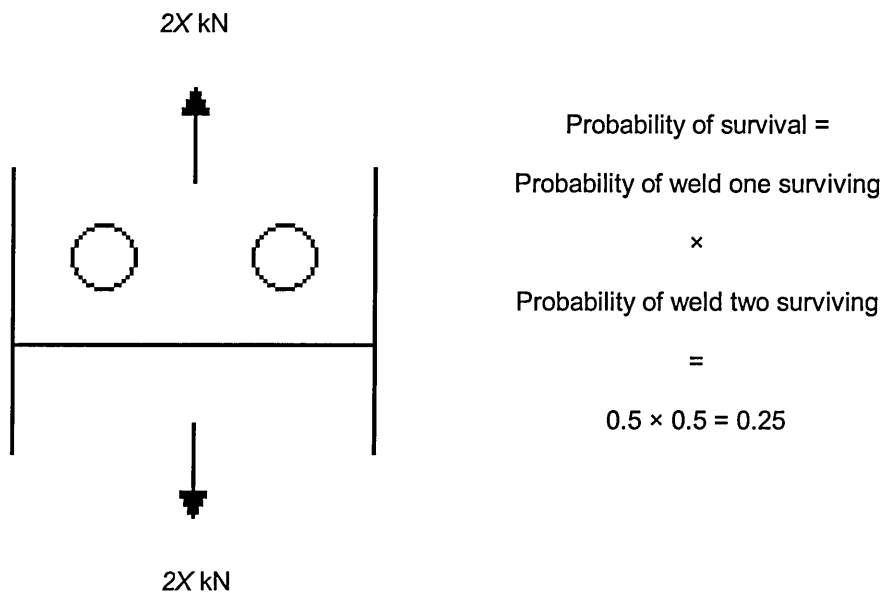
Fig 5.8b: Probability of double weld joint surviving a fatigue test using a proportionally identical load.

272

For the whole joint to have a probability of survival of 0.5, the joint must be tested at a fatigue load per spot weld, which is equal to the load that would result in a probability of survival in the individual welds of 0.707, since 0.707 × 0.707 = 0.5. This is why the proposed theoretical model predicts a steady decline in the mean fatigue strength per spot weld as the number of welds increases.

However, the trend shown here by the experimental results suggests that increasing the number of nuggets present in a joint does not alter their respective mean fatigue strength values when considering them as part of a whole joint. Since the statement made concerning basic statistics still applies, the trend indicates that increasing the number of nuggets present in a joint has a strengthening effect on the fatigue properties of the joint as a whole, such that the mean fatigue strength per spot weld remains at a constant level. Since the predicted trend is downward this would indicate that the addition of each weld must strengthen the joint by an amount that is larger than the amount caused by the addition of the previous weld.

The cause for this difference in trend and magnitude patterns must therefore be linked to a change in a parameter that affects fatigue properties. In addition, the change in this parameter must vary such that the difference between the experimental value and the predicted value increases with each additional spot weld. It has already been shown in Section 2.3.8 that joint stiffness is the dominant factor when determining the fatigue properties of a spot welded joint and that joint stiffness is itself controlled, primarily, by joint geometry. It is therefore reasonable to suggest that there is an unaccounted affect on joint stiffness, which is having an increasingly pronounced affect every time the number of nuggets in the joint increases and that this unaccounted affect is itself caused by a change in geometry each time a weld is added.

As explained, the manufacturing process of all the welded joints used in this project involved producing a nineteen nugget multi-spot welded joint and then dividing it into the single and various multi-spot welded joints that needed to be tested. This approach was adopted since it was considered to be a good way to ensure that all the joints contained welds made at different positions in a given weld series, therefore making the different joint configurations more comparable. However, this process meant that, in order to obtain each test specimen, a dividing cut had to be made, and every time this cut was made a very small portion of material would be lost from the specimen width. This causes a problem in that each of the different specimen configurations are divided from the nineteen nugget joint using only one or two cuts, depending on the specimens position in the nineteen nugget joint.

This means that the amount of material lost from the width of each configuration of either the single or the multi-spot welded joints, remains at an approximately constant level. Since every spot weld added to a joint adds an additional 20 mm of total specimen width, the constant amount of material lost by the dividing cut will mean that for every weld added to the joint, the width per spot weld will increase slightly.

If the width of each of the specimens tested is measured, it can be seen that the average width per spot weld does indeed increase with the number of spot welds present in the joint.

Number of Spot Welds in Joint	Average Width per Spot Weld (mm)
1	19.18
2	19.71
4	19.86
8	19.96
16	20.03

Table 5.1: Average width per spot weld (mm) for each of the multi-spot welded joints tested.

274

From this table it can be seen that not only is the width per spot weld more for the multi-spot welded joints than it is for the single spot welded joints used to predict their fatigue properties, but the difference in the width per spot weld between the single and multi-spot welded joints increases every time more welds are added.

Davidson [25] and Orts [54] both proved that the width of a spot welded specimen has a measurable effect on the joint stiffness, with wider specimens displaying a higher resistance to joint rotation. This has also been shown visually in this project in the Variation in Nugget Strength Study.

The degree to which an increase in the width of a TSSW joint will increase the joints fatigue strength characteristics will be unique to each specific joint configuration, since it will depend on the extent to which the fatigue strength characteristics of that joint are influenced by increases in joint stiffness, and whether the stiffness of the joint can be sufficiently increased through increases in joint width. It is therefore very difficult to determine the extent to which the increases in joint width per spot weld, seen in the multi-spot welded joints, will affect the mean fatigue strength, since the geometry of the joints tested in Davidson's and Orts' work differs from those tested in this project.

However, while it is not possible to use the data from the Davidson [25] and Orts [54] studies to show, conclusively, the extent to which this variation in width per spot weld would affect the mean fatigue strength values per spot weld of the multi-spot welded joints used in this study, the effect of specimen width on mean fatigue strength can be approximated using the information presented in Section 2.3.6, regarding the fatigue behaviour of TSSW joints.

Since the manner in which increases in joint width effect fatigue strength characteristics is through increases in joint stiffness, only joints that fail through sheet cracking will benefit from an increase in joint width. This is because joint stiffness only has an influential affect on joints that fail through sheet cracking. Once the joint stiffness gets to a certain level, shear cracking will supersede sheet cracking as the dominant failure mode, meaning that increasing joint stiffness further will have a limited affect. This would also indicate that, even if the TSSW joint in question does normally fail through sheet cracking, it will only benefit from width increases up to a threshold value, defined as the point when shear cracking supersedes sheet cracking as the dominant failure mode.

Past this value any increase in joint stiffness brought about through increases in joint width will not affect the fatigue strength characteristics, since joint stiffness is no longer influencing the fatigue properties of the joint. This can be seen in Fig 2.38 (repeated below as Fig 5.8) which shows that increasing the width of the particular joints tested in the Orts study, from 50 mm to 70 mm, does not appear to affect the maximum fatigue strength of the joints tested at a given cycle life, whereas an increase in the width from 25 mm to 50 mm appears to increase the maximum fatigue strength of these particular joints by approximately 63% [54].
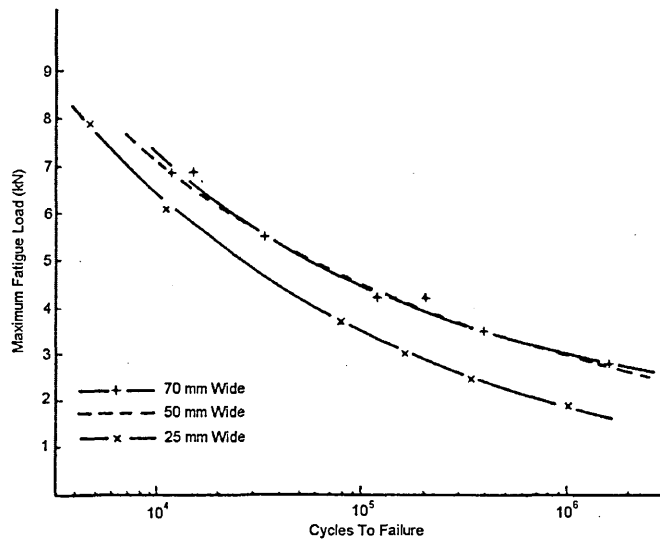
Fig 5.9: Effect of sample width on fatigue strength [54].

Based on the TSSW fatigue behaviour data, increases in the width of TSSW joints that have low levels of joint stiffness, or that are susceptible to joint rotation, such as the joints used in this project, will result in a proportional increase in the fatigue strength characteristics of the TSSW joint, which will be brought about by increases in joint stiffness. This behaviour will continue until such a point is reached where shear cracking starts to supersede sheet cracking as the dominant failure mode. At this point the affect of increases in joint width on fatigue strength characteristics will begin to diminish, until shear cracking completely replaces sheet cracking as the dominant failure mode. At this stage any further increases in joint width will have little to no affect on the fatigue strength characteristics of the joint.

In order to assess the extent to which the changes in the width per nugget appears to have affected the mean fatigue strength per nugget values in the multi-spot welded joints, values need to be calculated for the mean fatigue strength of the equivalent single nugget joints, needed to produce the mean fatigue strength per spot weld seen in the results. These values then need to be compared to the mean fatigue strength of the single nugget joints that were used in this project so as to provide an indication of the extent to which the mean fatigue strength has been affected.

No. of nuggets present in joint	Experimentally Calculated Mean Fatigue Strength per spot weld (kN)	Corresponding single nugget mean fatigue strength (kN)	Percentage increase in mean fatigue strength compared to single nugget joints.
2	0.6795	0.690563	2.656253
4	0.7115	0.732612	6.86124
8	0.6888	0.716957	5.2957
16	0.6193	0.726506	6.250639

Table 5.2: Increase in the mean fatigue strength of the corresponding multi-spot welded joint - single nugget joint compared to the single nugget joints tested.

Once the mean fatigue strength values are calculated, the widths per spot weld determined for each of the four different multi-spot welded joint configurations need to be compared to the width of the single nugget joints that were actually tested in this project. This will produce an indication as to the degree to which the joint width was increased.

Number of Spot Welds in Joint	Average Width per Spot Weld (mm)	Percentage increase in width per spot weld compared to single nugget joints.
2	19.71	2.76
4	19.86	3.55
8	19.96	4.07
16	20.03	4.43

Table 5.3: Increase in joint width of corresponding multi-spot welded joint - single nugget joint compared to single nugget joints tested.

Plotting both sets of these data produces the graph shown in Fig 5.8, which depicts the increase in mean fatigue strength that appears to be achieved through increases in joint width.
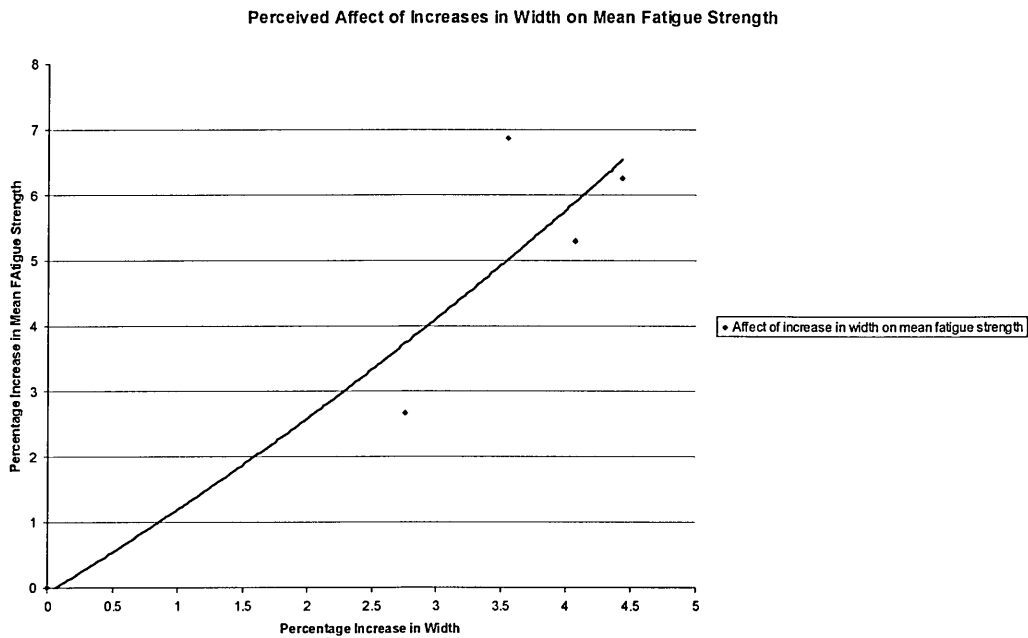
Fig 5.10: Perceived affect of increases in width on mean fatigue strength.

As mentioned, a direct comparison of these values to the existing data is not possible due to the differences between the joints tested. However, the trend indicated in Fig 5.9 does correspond to what would be expected based on knowledge of the fatigue behaviour of TSSW joints.

Based on this information, it would be reasonable to conclude that the extra width per spot weld, which occurs as the number of spot welds present in the joint increases, was adding to the joint stiffness and therefore causing an increase in the fatigue properties, per spot weld. This would cause the increase in the mean fatigue strength per spot weld seen when the experimental values for the multi-spot welded joints tested here are compared to the theoretical values. The possible problems caused by this loss of material during specimen production was considered at the start of the project, but it was thought that since the variation in width per spot weld caused by the specimen production process was so small, it would be insignificant when compared to the inherent variation of the welding process. However, as mentioned previously, the significant underestimation of the capability for producing consistent spot welds has resulted in a very small standard deviation, which means that even minor variations, such as this, will have a measurable effect on the experimental results.

5.7: Correlation between Theoretical and Experimental Standard Deviation Data.

The correlation between the experimental and theoretically proposed results, for the standard deviation per nugget, is extremely good, especially considering the very small changes that occur as the number of nuggets increase.

**Standard Deviaiton per Nugget
Theoretical vs Experimental**
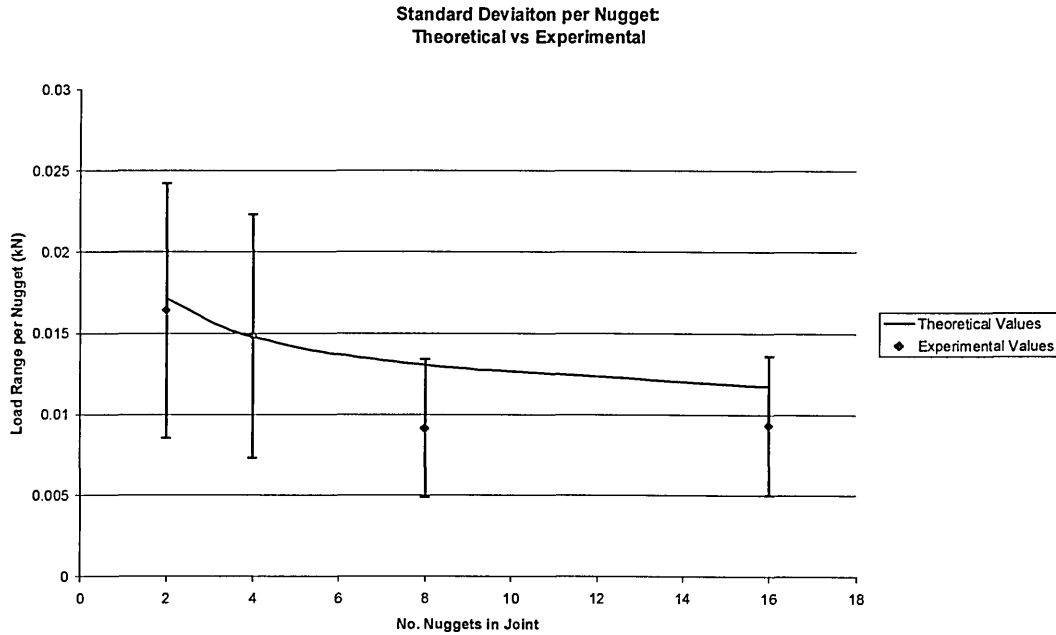
Fig 5.11: Correlation between theoretical and experimental standard deviation data.

The fact that the experimental results for standard deviation per nugget correlate well to the already small values proposed by the theory, indicates that the cause of the discrepancy between the theoretical and experimental mean fatigue strength values is only affecting the 'positioning' of the distribution and not the underlying shape. This would suggest that the cause of this affect is consistent for a given joint configuration and would therefore support the theory that the cause is down to an unaccounted increase in joint stiffness caused by an increase in the width per spot weld.

5.8: Thermoelastic Stress Analysis.

A comparison of the images taken during the TSA at adjacent cycle lives should have revealed only small amounts of variation, however, some of the results show large changes in the brightness and colour intensity of the entire image when compared to the previous recording. This is not an indication of a sudden change in the loading of the specimen and is therefore not indicative of the occurrence of load redistribution. The cause of this abrupt image change is due to subtly changes in the ambient temperature of the laboratory where the tests where carried out. Due to the sensitivity of the equipment, even slight changes in ambient temperature affect the data that is collected.

The results also display small stress field at the bottom of each specimen, these stress fields are caused by the bolts that tighten the grips that clamp the lower half of the specimen into the fatigue equipment.

The images taken at the start of each test, and at 100,000 cycles, give little indication of an unbalanced load. There are some minor differences between the stress fields present above each of the spot welds, but due to the poor resolution of the images, the ability of the equipment to only measure stress fields on the surface of the specimen, and the tendency of the readings to be heavily influenced by minor changes in ambient temperature, these variations are considered to be too small to suggest that there was a significant degree of unbalanced loading occurring at the start of the fatigue tests.

The recorded images also show little evidence that suggests that the load was being redistributed at any point during the fatigue test. Examining the shape and size of the stress field of each individual nugget and the shape and size of the two adjacent to it, and then comparing them with the shape and size they are after another 100,000 cycles, reveals very little in terms of a change in supported load. The only time that the DeltaTherm equipment appears to distinguish any change in the loading of the individual spot weld nuggets is the instant before complete fracture occurs. By this point the conditions for fatigue failure, set out in Section 2.3.9, have already been met. This indicates that load redistribution does not occur until the very late stages of fatigue cracking, in which case, the criteria for failure used in this project is adequate to ensure uniform loading of each nugget in a multi-spot welded specimen for the duration of a fatigue test and therefore supports the required condition of statistically independent survival probabilities for each nugget.

5.9: Proposed Model.

Based on the data collected, the values for the mean fatigue strength and the standard deviation of the fatigue strength distribution, predicted by the model proposed at the start of this project, correlate well with the actual fatigue behaviour of multi-spot welded joints, in relation to geometrically proportional single spot welded joints. Even though the mean fatigue strength values do not correlate exactly with the predicted values, there is strong evidence to suggest that the minor increase in actual values is caused by an equally minor increase in the width per spot weld as the number of nuggets present in the joint increases. Further support for the model is found in the excellent correlation between the theoretical and experimental standard deviation results.

It can therefore be stated that:

$$X_m = X_s - (m_n \times S) \qquad Eq.\ 5.1$$

Where:

X_m = *Mean fatigue strength of the multi-spot welded joint.*

X_s = *Mean fatigue strength of a proportionally size single nugget joint.*

m_n = *Relationship factor equal to the Z value read from the standard normal distribution tables for a probability equal to $\sqrt[n]{0.5}$.*

S = *Standard deviation of a proportionally size single nugget joint.*

And:

$$S_m = d_n \times S \qquad Eq.\ 5.2$$

Where:

S_m = *The standard deviation of the multi-spot welded joint.*

d_n = *Relationship factor equal to the Z value read from the standard normal distribution tables for a probability equal to $\sqrt[n]{0.8413} - \sqrt[n]{0.5}$.*

S = *The standard deviation of a proportionally sized single nugget joint.*

6: Conclusions.

6.1: Weldability Study.

- For the resistance spot welding equipment used in this project, the optimum welding parameters for resistance spot welding 1 mm thick sheets of quarter hardened AISI 301 were found to be:

Welding Current:	4.5 kAmps
Welding Time:	15 Cycles
Welding Force:	3.25 kN

- These parameters produced welds with good mechanical properties with a high degree of consistency and repeatability.

6.2: Optimum Pitch Distance Study.

- Multi-spot welded joints with consistent welds can be produced in AISI 301 by using a pitch distance of 20 mm and removing the first and second welds made in a series. This process was shown to produce individual welds that were consistent and also kept the width of the multi-spot welded joints to an acceptable size.

- The amount of rotation occurring in a joint can be visually observed to decrease as the width of the specimen increases.

- An effect of current shunting on nugget strength can be seen at pitch distances below 30 mm. Above this value any variation in strength between nuggets can be account for by the inherent variation of the test equipment used.

- Even though there is an apparent effect of current shunting on nugget strength, there appears to be a negligible effect of current shunting on the nugget diameter of spot welds made in quarter hardened AISI 301, even at extremely close pitch distances.

6.3: Single Nugget Fatigue Investigation.

- Values for mean fatigue strength and the standard deviation of the fatigue strength distribution, for single nugget joints, can be determined using a Staircase fatigue testing approach.

- A Probit fatigue testing process can be used to determine the whole probability density function for the fatigue strength distribution of single welded joints. This will produce more accurate, but comparable, values for the mean fatigue strength and the standard deviation to those found in a Staircase testing process.

- Single spot welded joints can be produced with an extremely high degree of consistency in terms of fatigue properties. This is illustrated by the very small standard deviation for the fatigue strength distribution found for single nugget joints.

- Crack propagation on both sides of single nugget spot welds is not always equal. Instances can occur in the latter stages of lateral fatigue crack growth, where the crack on one of the sides takes dominance and propagates at a faster rate than the crack on the other side.

- Statistical fatigue studies of this nature should be carried out on a single piece of test equipment to maintain consistency. Minor differences between test equipment can result in different results for the same test, which will have a significant affect if the standard deviation of the fatigue strength distribution is small, as was the case here.

6.4: Multi-Spot Weld Fatigue Investigation.

- Values for the mean fatigue strength and the standard deviation of the fatigue strength distribution of multi-spot welded joints, can be determined using a Staircase fatigue testing approach.

- As with single nugget specimens, the propagation of cracks on both sides of the specimens is not always equal. In addition, groups of cracks present on one side of the specimen can develop at different rates to the other cracks on the same side of the specimen, leading to areas of nuggets with more advanced cracks than other areas.

- A video surveillance system can be used to monitor the size and growth of cracks occurring in a multi-spot welded joint. Linking this system to the fatigue equipment can allow it to be used to define the instant when failure conditions, based on crack size, have been met.

6.5: Thermoelastic Stress Analysis.

- The positioning and size of any stress fields present in a multi-spot welded joint, during the application of a fatigue load, can be detected and identified using TSA equipment.

- The loading of the individual spot welds of a multi-spot welded joint, of the configuration used in this study, appears to be balanced at the start of a fatigue test.

- The loading of the individual spot welds during the fatigue testing of multi-spot welded joints, of the configuration used in this study, appears to be balanced throughout the duration of the fatigue test, up to the point were failure is deemed to have occurred.

- The balanced loading conditions of the multi-spot welded joints during the fatigue tests, witnessed during the TSA study, indicates that the survival probabilities of the individual spot welds that make up the multi-spot welded joints used in this study, are statistically independent.

6.6: Accuracy of Proposed Theoretical Model.

- The proposed model can be considered to accurately predict the mean fatigue strength per nugget of a multi-spot welded joint. The minor discrepancy found in the results presented in this study is caused by a minor variation in specimen width per spot weld.

- The proposed model predicts the standard deviation per nugget with an excellent degree of accuracy. This indicates that the discrepancy between the predicted and experimental mean fatigue strength values is consistent for a given specimen size and therefore supports the hypothesis suggested above.

- At present the model will only work for joints that are made up entirely of spot welds geometrically identical to the single nugget specimen used to predict the values. The model could be extended to include specimens that contain a range of differently spaced and positioned nuggets, although this would require a significant amount of further work.

7: Further Work.

The ultimate goal of this project was to be able to develop a statistical model that would enable designers to predict the fatigue strength properties of any multi-spot welded joint from data on the fatigue properties of single spot welded joints.

What this project has shown is that a model can be defined that will predict the fatigue behaviour of a multi-spot welded joint from experimental data on representative single spot welded joints for a simplified approach, where the individual component spot welds in the multi-spot welded joint are all effectively geometrically identical, and all support an equal portion of the overall load.

This suggests that a similar approach can be used for complex multi-spot welded joints, provided that the single spot welded joints, used to predict the behaviour, accurately represent the geometry and loading conditions of the individual component spot welds that make up the multi-spot welded joint.

Support for this can be found by using the same testing methodology developed in this study to predict and test the fatigue strength behaviour of multi-spot welded joints of differing complexity. This data could then also be used to test the effect on accuracy of combining this model with some of the existing ones to predict fatigue strength behaviour in complex multi-spot welded joints, as opposed to using the existing models on their own. Further testing should also be carried out to determine if the joints have to be split down into single spot welded joints or can they be split down in other ways.

8: References.

[1]   Attwood, G., Skipworth, G., 1994. *Statistics 1*. Heinemann Educational Publishers.

[2]   *A Guide for Fatigue Testing and the Statistical Analysis of Fatigue Data*, 1963. ASTM STP 91-A.

[3]   Weibull, W., 1961. *Fatigue Testing and the Analysis of Results*. Pergamon Press. Pages 15 - 17.

[4]   Weibull, W., 1961. *Fatigue Testing and the Analysis of Results*. Pergamon Press. Pages 225 – 247.

[5]   Kearns, W.H., 1980. *Resistance and Solid-State Welding and Other Joining Processes*. Welding Handbook Volume 3. 7th Edition. Macmillan Press. Pages 2 – 11.

[6]   *Resistance Spot Welding* – Basic Information, TWI Paper.

[7]   *Resistance Welding Overview*. KVA.
        Available From: www.kvawelding.com/ResistanceWeldingOverview.html
        [Accessed in May 2004].

[8]   *Robot Welding*.
        Available From: www.robot-welding.com/spot_welding.htm
        [Accessed in March 2006].

[9]   Kearns, W.H., 1980. *Resistance and Solid-State Welding and Other Joining Processes*. Welding Handbook Volume 3. 7th Edition. Macmillan Press. Pages 16 – 19.

[10]   Hilton, B.R., 1950. *Welding Design and Processes*. Chathnam: W. & J. Mackay & Co. Ltd. Pages 302 – 305.

[11]   Houldcroft, P.T., 1967. *Welding Processes.* London: Cambridge University Press. Pages 106 – 127.

[12]   Cary, H.B., Resistance Welding. *Modern Welding Technology*, Section 6-3, Pages 213 – 219.

[13]   Davies, A.C., 1993. *Resistance Welding and Flash Butt Welding.* London: Cambridge University Press. Pages 197 – 208.

[14]   Hilton, B.R., 1950. *Welding Design and Processes.* Chathnam: W. & J. Mackay & Co. Ltd. Pages 309 – 316.

[15]   Resistance Spot Welding, 1983. Welding, Brazing, and Soldering. Metals Handbook Volume 6, 9th Edition. ASM. Pages 469 – 493.

[16]   *Phylink.*

Available From: www.physlink.com/education/askexperts/ae432.cfm

[Access in March 2006].

[17]   Algor: *Centre for Mechanical Design and Technology Design.*

Available   From: http://www.algor.com/service_support/hints_tips/joule_heating.asp

[Accessed in March 2006].

[18]   Bakeley, P., 2000. Resistance Spot Welding at Maximum Speed. *Welding and Metal Fabrication.*

[19]   *Overview of Resistance Welding.*

Available From : www.livco.com/umchapter1.pdf

[Accessed in January 2004].

[20]   Centre Line, 2004.*Centre Line Technical Brief, CL-TD-P-1102.*

[21]   Wray, T., 2004. *Resistance Spot Welding of Duplex Stainless Steel*. PhD Thesis. Sheffield Hallam University.

[22]   *Hyperphysics.*

Available   From: http://hyperphysics.phy-astr.gsu.edu/hbase/electric/elecur.html [Accessed in March 2006].

[23]   Giachino, Weeks, Johnson, 1973. *Welding Technology*. 2nd Edition. American Technical Society. Pages 109 – 118.

[24]   Davidson, J.A., 1983. A Review of the Fatigue Properties of Spot Welded Sheet Steels. *SAE Technical Paper Series*. United States Steel Corp.

[25]   Davidson, J.A., 1983. Design-Related Methodology to Determine the Fatigue Life and Related Failure Mode of Spot-Welded Sheet Steels. *HSLA Steels Technology & Applications*. 8306-022. Pages 539 – 551.

[26]   McMahon, J.C., Smith, G.A., Lawrence, F.V., 1990. Fatigue Crack Initiation and Growth in Tensile Shear Spot Weldments. *Fatigue and Fracture Testing of Weldments*, ASTM STP 1058. Pages 47 – 77.

[27]   BS 1140:1993. *Resistance Spot Welding of Uncoated and Coated Low Carbon Steel*. British Standards Institute.

[28]   BS EN ISO 14273:2001. *Specimen Dimensions and Procedure for Shear Testing Resistance Spot, Seam and Embossed Projection Welds*. British Standards Institute.

[29]   Swanson, S.R., 1974. *Handbook of Fatigue Testing*. American Society for Testing and Materials. Pages 19 – 27.

[30]   Gere, Timoshenko, 1995. *Mechanics of Materials*. 3rd SI Edition. London: Chapman & Hall. Pages 116 – 125.

References.

[31]   Roylance, D., 2001. *Fatigue*. Department Of Materials Science and Engineering. Massachusetts Institute of Technology.

[32]   Benham, P.P., Crawford, R.J., Armstrong, C.G., 1999. *Mechanics of Engineering Materials*. 2nd Edition. Essex: Longman.

[33]   Ncode: Managing Durability.
        Available From: http://www.ncode.com/page.asp?section=00010001000100130022 [Accessed in March 2006].

[34]   Weibull, W., 1961. *Fatigue Testing and the Analysis of Results*. Pergamon Press.

[35]   Ashby, M.F., Jones, D.R.H., 1998. *Engineering Materials 1*. 2nd Edition. Oxford: Butterworth-Heinemann.

[36]   *NDT Resource Centre*.
        Available Form : http://www.ndt-ed.org/EducationResources/CommunityCollege/Materials/Structure/fatigue.htm [Accessed in March 2006].

[37]   Mann, J.Y., 1967. *Fatigue of Materials, an Introductory Text*. Melbourne University Press. Page 54.

[38]   Mann, J.Y., 1967. *Fatigue of Materials, an Introductory Text*. Melbourne University Press. Pages 61-71.

[39]   Linder, J., Melander, A., Larsson, M., Bergengren, Y., *Fatigue Strength of Spot Welded Austenitic and Duplex Stainless Sheet Steels Tested in Air and in 3% NaCl Solution*. Swedish Institute for Metals Research.

[40]   Linder, J., Larsson, M., *Fatigue Properties of Spot Welded Sheet Steels*. Swedish Institute for Metals Research.

References.

[41]   Sperle, J.O., Fatigue *Strength of Spot Welded High Strength Steel Sheet*. Swedish
         Symposium on Classical Fatigue.

[42]   Linder, J., Larsson, M., *Fatigue Design of Spot and Plug Welded Stainless   Steel*.
         Swedish Institute for Metals Research.

[43]   Middleton, J.C., Turner, A.F., 1991. *Mechanical Properties of Electric Resistance Spot
         Welds in Stainless Steels*. Rotherham: British Steel Technical.

[44]   Nordberg, H., 2005. *Fatigue Properties of Stainless Steel Lap Joints*. Outokumpu
         Stainless Research Foundation.

[45]   Sperle, J.O., *Fatigue Strength of Spot Welded High Strength Steel Sheet*. Sweden:
         Central Research and Development. Pages 333 – 356.

[46]   BS EN ISO 14273:2001. *Specimen Dimensions and Procedure for Shear Testing
         Resistance Spot, Seam and Embossed Projection Welds*. British Standards Institute.

[47]   Linder, J., Larsson, M., *Fatigue Properties of Sheet Steels*. Swedish Institute for Metals
         Research.

[48]   Efunda: Engineering Fundamentals.
         Available From:
         http://www.efunda.com/formulae/solid_mechanics/fracture_mechanics/fm_lefm_K.cfm
         [Accessed in March 2006].

[49]   Key-to-Steel.com: Knowledge Article.
         Available From: www.key-to-steel.com/ViewArticle.asp?ID=49
         [Accessed in March 2005].

[50]   Giachino, Weeks, Johnson, 1973. *Welding Technology*. 2nd Edition. American Technical
         Society. Pages 212.

293

[51]   Parker, A. P., 1981. *The Mechanics of Fracture and Fatigue.* London: E. & F. N. Spon Ltd. Pages 124-127.

[52]   Davidson, J. A., 1983. *A Review of the Fatigue Properties of Spot-Welded Sheet Steels.* SAE Technical Paper Series, 830033.

[53]   Linder, J., Melander, A., Larsson, M., Bergengren, Y., *Fatigue Strength of Spot Welded Austenitic and Duplex Stainless Sheet Steels Tested in Air and in 3% NaCl Solution.* Swedish Institute for Metals Research.

[54]   Orts, D. H., 1981. *Fatigue Strength of Spot Welded Joints in a HSLA Steel.* SAE Technical Papers Series.

[55]   Davidson, J. A., Imhof Jr, E.J., 1984. *The effect of Tensile Strength on the Fatigue Life of Spot-Welded Sheet Steels.* United States Steel Corp.

[56]   Sperle, J. O., Lundh, H., *Strength and Crash Resistance of Structural Members in High Strength Dual-Phase Steel Sheet.* Central Research and Development. Pages 343 – 352.

[57]   *Stainless Steel - Grade 301.*
Available from: www.azom.com/details.asp?ArticleID=960
[Accessed in March 2006].

[58]   *301 Stainless Steel Material Properties Data Sheet.*
Available from: www.suppliersonline.com/propertypages/301.asp
[Accessed in March 2006].

[59]   *Stainless Steel.*
Available from: www.techsavvy.com/industry/file/national/09dvn/psw06.html
[Accessed in March 2006].

[60]   Kearns, W.H., 1980. *Resistance and Solid-State Welding and Other Joining Processes.* Welding Handbook Volume 3. 7th Edition. Macmillan Press. Pages 40.

[61]   Kearns, W.H., 1984. *Metals and their Weldability.* AWS Welding Handbook, 7th Edition. The Macmillan Press. Pages 119 - 121.

[62]   Kearns, W.H., 1984. *Metals and their Weldability.* AWS Welding Handbook, 7th Edition. The Macmillan Press. Page 124.

[63]   Song, J., Mourelatos, Z.P., Gu, R.J., 2005. *Sensitivity Study of Staircase Fatigue Tests Using Monte Carlo Simulation.* SAE 2005-01-0803.

[64]   Hans Nordeberg. *Om Utvarderingsmetoder Vid Utmattning.* Inatitutet for Metaliforskning.

[65]   Dixon, W.J., Mood, A.M., *Method for Obtaining [and] Analyzing Sensitivity Data.* American Statistical Association. Pages 109 – 126.

[66]   DeltaTherm Instruction Manual.

[67]   Private communications with Volvo trucks.